

**TITANIUM-GRAPHITE COMPOSITES FOR  
BIOMEDICAL APPLICATIONS:  
A STUDY ON MECHANICAL PROPERTIES AND  
BIOCOMPATIBILITY**

**KAMAL BIN YACOB**

**NATIONAL UNIVERSITY OF SINGAPORE**

**2005**

## **Acknowledgements**

This undertaking would not have been possible without the guidance, patience and support from the many, many individuals, who have touched my life in ways words could barely describe. I am eternally indebted to my research supervisor, Prof Teoh Swee Hin, for his wisdom and leadership. It has been an honour and privilege to be part of Prof Teoh's research team, during which time I have learnt numerous invaluable lessons.

I would also like to express my heart-felt gratitude to Dr Masae Sumita from Japan. His vast experience in titanium properties and boundless enthusiasm have contributed enormously to this project. I would also like extend my appreciation to Dr Junzo Tanaka, Prof Takao Hanawa, Dr Norio Maruyama, Dr Akiko Yamamoto, Dr Sachiko Hiromoto , Dr Daisuke Kuroda and all staff of the Reconstitution Materials Groups, Biomaterials Centre, National Institute for Materials Science, Japan, for going out of their way to assist me with this research project and making my stay in Japan a memorable experience.

I am also fortunate to have worked alongside highly motivated and intelligent staff and students at BIOMAT Centre. Although we were working on separate projects, their insightful feedback and assistance have helped this undertaking in no small way.

To all staff at the Materials Science Lab, Department of Mechanical Engineering, in particular Mr Thomas Tan, Mdm. Zhong Xiang Li, Mr. Abdul Khalim Bin Abdul, Mr. Juraimi Bin Madon, Mr. Maung Aye Thein and Mr. Ng Hong Wei, I would like to show

my sincere appreciation for their kind assistance and expertise in materials characterization.

I would also like to thank all staff and students of the Division of Bioengineering, in particular, Dr Kazutoshi Fujihara and Mr Zhang Yanzhong for their patience and invaluable assistance.

Finally, to a very special person, Miss Dinah Tan, “Thank you for your patience, guidance and support.”

# CONTENTS

Acknowledgements	ii
Table of Contents	iv
Summary	ix
List of Tables	xi
List of Figures	xii
List of Symbols	xvi
Chapter 1. Introduction	1
1.1 Purpose	1
1.2 Motivation	2
1.3 Objectives and Scope	5
Chapter 2. Literature Survey	7
2.1 History of Titanium	7
2.1.1 Fatigue Properties of Titanium	9
2.1.2 In-vitro Studies on the Biocompatibility of Titanium	13
2.2 History of Graphite	14
2.2.1 Lubrication Properties of Graphite	15
2.3 Powder Metallurgy	16
2.4 Total Hip Replacement (THR)	19
2.5 Biological Response to Implants	23

2.5.1	Mechanism of Cellular Response to Bulk Implant Material	23
2.5.2	Wear Particle Induced Osteolysis	25
Chapter 3.	Experimental Procedure	28
3.1	Materials	28
3.2	Particle Analysis	29
3.3	Compaction Technique	29
3.4	Sintering and Hot Isostatic Pressing of Compacts	30
3.5	Microstructure of Compacts	33
3.6	Tensile Properties of Compacts	34
3.7	Fatigue Properties of Compact	36
3.8	Cell Culture	37
3.9	Biocompatibility of Raw Powder	39
3.9.1	Preparation of Raw Powder for Cell Culture	39
3.9.2	Cell Culture with Raw Powder	40
3.10	Biocompatibility of Wear Debris	40
3.10.1	Generation of Wear Debris	41
3.10.2	Wear Debris Preparation for Cell Culture	41
3.10.3	Cell Culture with Wear Debris	42
3.11	Biocompatibility of Compacts	42
3.11.1	Water Contact Angle Measurements	43
3.11.2	Compact Preparation for Cell Seeding	44
3.11.3	Cell Seeding on Surfaces of Compacts	45

3.12	alamarBlue™ Reduction	45
3.13	Fluorescence Microscopy	48
Chapter 4. Characterization of Particles and Sintered Compacts		52
4.1	Raw Powder Characteristics	52
4.1.1	Particle Size Distribution of Raw Powder	52
4.1.2	Raw Powder Morphology	55
4.2	Sintered Titanium and Titanium-Graphite Compact Characteristics	57
4.2.1	Microstructure	57
4.2.2	Porosity of Compacts	63
Chapter 5. Hardness, Tensile Properties and Fatigue Strength of Compacts		66
5.1	Hardness of Compacts	66
5.2	Tensile Properties of Compacts	69
5.2.1	Tensile Strength and Stiffness of compacts	69
5.2.2	Tensile Fracture Surfaces of Compacts	71
5.2.3	Discussion on Tensile Properties of Compacts	75
5.3	Fatigue Performance	77
5.3.1	Fatigue Strength of Compacts	78
5.3.2	Fatigue Fracture Surfaces of Compacts	80
5.3.3	Discussion on fatigue Performance of Compacts	82

Chapter 6. Characterization of Wear Debris	84
6.1 Morphology of Wear Debris	84
6.2 Particle Size Distribution of Wear Debris	86
6.2.1 Particle Size Distribution Based on Total Particle Number	86
6.2.2 Particle Size Distribution Based on Total Particle Volume	90
6.3 Pros and Cons of Using CTAn for Particle Size Analysis	94
Chapter 7. Biocompatibility Studies	97
7.1 Biocompatibility of Raw Powder	97
7.1.1 alamarBlue™ Reduction of Cells Cultured with Raw Powder	97
7.1.2 Statistical Significance of Cell Proliferation Assay Involving Raw Powder	99
7.1.3 Fluorescence Microscopy of Cells Cultured with Raw Powder	100
7.1.4 Discussion on Biocompatibility of Raw Powder	105
7.2 Biocompatibility of Wear Debris	108
7.2.1 alamarBlue™ Reduction of Cells Cultured with Wear Debris	108
7.2.2 Statistical Significance of Cell Proliferation Assay Involving Wear Debris	110
7.2.3 Fluorescence Microscopy of Cells Cultured with Wear Debris	111
7.2.4 Discussion on Biocompatibility of Wear Debris	115
7.3 Biocompatibility of Sintered Compacts	117
7.3.1 Water Contact Angle Measurements	117
7.3.2 Statistical Significance of Water Contact Angle Tests on Sintered Compacts	120

7.3.3	alamarBlue™ Reduction of Cells seeded on Sintered Compacts	121
7.3.4	Statistical Significance of Cell Proliferation Assay Involving Sintered Compacts	123
7.3.5	Fluorescence Microscopy of Cells seeded on Sintered Compacts	124
7.3.6	Discussion on Biocompatibility of Sintered Compacts	128
Chapter 8. Conclusions and Recommendations		129
8.1	Conclusions	129
8.2	Recommendations	133
References		135
Appendices		
Appendix 1	Engineering Drawing of Tensile and Fatigue Tests Specimens	A1-1
Appendix 2	Engineering Drawing of Tensile and Fatigue Tests Specimen Grip	A2-1
Appendix 3	Tutorial on Using CTAn Software to Determine Particle Size Distribution	A3-1
Appendix 4	Calculations for the Students T-Test on the Cell Proliferation Assay Involving Raw Powder	A4-1
Appendix 5	Calculations for the Students T-Test on the Cell Proliferation Assay Involving Wear Debris	A5-1
Appendix 6	Calculations for the Students T-Test on the Water Contact Angle Test on Sintered Compacts	A6-1
Appendix 7	Calculations for the Students T-Test on the Cell Proliferation Assay Involving Sintered Compacts	A7-1



## Summary

Fracture and cell cytotoxicity are major problems associated with implant loosening, postoperative infection and ultimate implant failure. This project aims to characterize the tensile properties, fatigue performance and biocompatibility of a novel Titanium Graphite composite. This metal matrix composite, patented by SH Teoh et al, has the potential to deliver high wear resistance, superior durability and good biocompatibility.

Titanium-graphite composites with 5-wt% and 10-wt% graphite were fabricated using powder metallurgy. Commercial purity titanium was thoroughly mixed with high purity graphite powder, compacted via the blended elemental method and hot isostatically pressed to form metal matrix composites. The fabricated had generally low porosities of below 2% and exhibited a triphasic microstructure comprising equiaxed titanium grains, titanium carbide and unreacted graphite.

The tensile properties of the composites were investigated using a universal testing machine. The composites displayed good tensile stiffness, but relatively poor tensile strengths. The fatigue performance of the composites was also evaluated by applying a sinusoidal uniaxial tensile load of frequency 20 Hz and Stress Ratio 0.1, under laboratory conditions. The Endurance Limit of the composites under cyclic tensile loads was found to be lower than that of pure titanium. Post-testing measurements of the oxide content of the composites revealed that the composites had a relatively high oxide content of 0.5%, which resulted in embrittlement, and hence poor fatigue and tensile performance.

Biocompatibility studies were conducted on the composites, their wear debris, as well as the raw powder used to fabricate the composites. The 3T3 fibroblast cell line and primary rat osteoblast cells were used in these experiments. The cells were either cultured with the wear debris or raw powder particles, or were seeded on the polished surfaces of the composites. Cell proliferation was evaluated using the alamarBlue™ assay, while cellular viability was determined by observation under a fluorescence microscope, after the cells have been stained with a mixture of Calcein AM and Ethidium homodimer-1. The results indicated that the titanium graphite composites, and their wear debris, did not adversely affect cellular proliferation nor viability, and hence display good biocompatibility.

## LIST OF TABLES

<b>TABLE</b>		<b>PAGE</b>
Table 3.1	: Elemental constituents of pure HDH titanium powder	28
Table 3.2	: Elemental constituents of pure graphite powder	29
Table 3.3	: Specimen nomenclature.	32
Table 4.1	: Raw powder size distribution statistics	55
Table 4.2	: Average pore size of sintered and HIPped specimens	62
Table 4.3	: Porosity of compact	64
Table 5.1	: Mean tensile properties of compacts.	70
Table 6.1	: Statistical information on particle size distribution of wear debris (based on particle frequency)	89
Table 6.2	: Statistical information on particle size distribution of wear debris (based on particle volume percentage)	94

## LIST OF FIGURES

<b>FIGURE</b>		<b>PAGE</b>
Figure 1.1	: Triphasic Titanium-Graphite 5-wt% composite	5
Figure 2.1	: S-N Curve of Ti-6Al-4V	12
Figure 2.2	: Crystal structure of graphite.	15
Figure 2.3	: X-ray images of hip joint of a 37-year old patient.	20
Figure 2.4	: Schematic of a hip prosthesis	21
Figure 2.5	: AP Radiograph of a cementless hip arthroplasty.	27
Figure 3.1	: Four stage heating cycle of the sintering process	32
Figure 3.2	: Tensile and fatigue tests specimens	35
Figure 3.3	: Secondary grips for tensile tests	36
Figure 3.4	: Water contact angle measurement of 10-10 specimen.	44
Figure 4.1	: Particle size distribution of raw powders used to fabricate compacts	53
Figure 4.2	: Morphology of raw powders used to fabricate compacts	56
Figure 4.3	: Photo-micrographs of sintered, HIPed compacts	58
Figure 4.4	: Scanning electron microscopy images of sintered, HIPped compacts	61
Figure 5.1	: Different orientations of compact surfaces	66
Figure 5.2	: Vickers hardness of compacts	67
Figure 5.3	: Micro-Vickers hardness of titanium and titanium Carbide regions of compacts	68

Figure 5.4	: Stress-Strain Curves: a) 0-0; b) 10-5; c) 10-10; and d) all specimens.	70
Figure 5.5	: 0-0 tensile fracture surface, showing presence of dimples with local cleavage facets.	71
Figure 5.6	: 0-0 tensile fracture surface, showing micro-void coalescence	72
Figure 5.7	: 10-5 tensile fracture surface, showing the interface the titanium carbide regions and the titanium matrix.	72
Figure 5.8	: 10-5 tensile fracture surface. Shown is a transgranular crack in the titanium matrix.	73
Figure 5.9	: 10-10 tensile fracture surface, showing the TiC and Ti Matrix Interface	73
Figure 5.10	: 10-10 tensile fracture surface, showing the formation of dimples, as well as local cleavage facets near the TiC region, in the Ti Matrix.	74
Figure 5.11	: Effect of Graphite Content on Tensile Strength of Compacts	76
Figure 5.12	: Effect of Graphite Content on Young's Modulus of Compacts	77
Figure 5.13	: S-N curve of 0-0 specimens obtained during fatigue testing	79
Figure 5.14	: S-N curve of 10-5 specimens obtained during fatigue testing	79
Figure 5.15	: 0-0 fatigue fracture surface, showing presence of fatigue striations.	80
Figure 5.16	: 0-0 fatigue fracture surface, showing chevron patterns.	81
Figure 5.17	: 10-5 fatigue fracture surface, showing transgranular cleavage facets of titanium matrix surrounding TiC.	81
Figure 6.1	: 0-0 Wear Debris	84
Figure 6.2	: 10-5 Wear Debris	85
Figure 6.3	: 10-10 Wear Debris	85

Figure 6.4	: Particle size distribution of 0-0 wear debris based on particle frequency.	87
Figure 6.5	: Particle size distribution of 10-5 wear debris based on particle frequency.	88
Figure 6.6	: Particle size distribution of 10-10 wear debris based on particle frequency.	88
Figure 6.7	: Particle size distribution of 0-0 wear debris (volume percentage)	92
Figure 6.8	: Particle size distribution of 10-5 wear debris (volume percentage)	92
Figure 6.9	: Particle size distribution of 10-10 wear debris (volume percentage)	93
Figure 7.1	: alamarBlue™ Reduction of 3T3 Cells Cultured with Raw Powder	98
Figure 7.2	: alamarBlue™ Reduction of Rat Osteoblast Cultured with Raw Powder	98
Figure 7.3	: Fluorescence Microscopy of Interaction of 3T3 Cells with Raw Powder	101
Figure 7.4	: Fluorescence Microscopy of Interaction of Rat Osteoblast with Raw Powder	103
Figure 7.5a	: alamarBlue™ Reduction of 3T3 Cells Cultured with Wear Debris	109
Figure 7.5b	: alamarBlue™ Reduction of Rat Osteoblast Cultured with Wear Debris	109
Figure 7.6	: Fluorescence Microscopy of Interaction of 3T3 Cells with Wear Debris	112
Figure 7.7	: Fluorescence Microscopy of Interaction of Rat Osteoblast with Wear Debris	113
Figure 7.8	: Water Contact Angle Measurements of Compact Surfaces	118
Figure 7.9	: alamarBlue™ Reduction of 3T3 Cells Seeded on Compact Surfaces	122

Figure 7.10	: alamarBlue™ Reduction of Rat Osteoblast Seeded on Compact Surfaces	122
Figure 7.11	: Fluorescence Microcopy of 3T3 Cells 1 Week After Seeding on Compact Surfaces	125
Figure 7.12	: Fluorescence Microcopy of Rat Osteoblast 1 Week After Seeding on Compact Surfaces	126

## LIST OF SYMBOLS

### SYMBOL

S	: Applied cyclical stress amplitude in fatigue testing
N	: Number of cycles to failure in fatigue testing
$\sigma_{\max}$	: Maximum applied stress
$\sigma_{\min}$	: Minimum applied stress
$\Delta\sigma$	: Stress range
$\sigma_u$	: Stress amplitude
$\sigma_m$	: Mean stress
R	: Stress ratio
d <sub>90</sub>	: 90 <sup>th</sup> Percentile size
0-0	: Specimens of commercial purity titanium
10-5	: Composite specimens sintered from powder comprising 5% by weight 10 $\mu$ m graphite and 95% by weight commercial purity titanium
10-10	: Composite specimens sintered from powder comprising 10% by weight 10 $\mu$ m graphite and 90% by weight commercial purity titanium
T75	: Tissue culture flask with 75 cm <sup>2</sup> available for cell culture
AO <sub>595</sub>	: The spectrophotometric absorbance of cell culture medium alone subtracted from the absorbance of medium plus alamarBlue <sup>TM</sup> at the wavelength of 595 nm



$AO_{560}$	: The spectrophotometric absorbance of cell culture medium alone subtracted from the absorbance of medium plus alamarBlue™ at the wavelength of 560 nm
$R_0$	: Correction factor, computed as $AO_{560}/AO_{595}$ .
$A_{560}$	: Spectrophotometric absorbance of alamarBlue™–cell culture medium mixture of experimental specimens at wavelength of 560 nm
$A_{595}$	: Spectrophotometric absorbance of alamarBlue™– cell culture medium mixture of experimental specimens at wavelength of 595 nm
$V_c$	: Theoretical volume of compacts
$Q_g$	: Weight percent of graphite powder
$Q_{Ti}$	: Weight percent of titanium powder
$W_{total}$	: Total weight of powders
$\rho_g$	: Density of graphite (2.21 g/cm <sup>3</sup> )
$\rho_{Ti}$	: Density of titanium (4.54 g/cm <sup>3</sup> )
$\rho_{th}$	: Theoretical density of compacts
$\rho_{act}$	: Actual density of compacts
$W_{act}$	: Actual weight of compacts
$V_{act}$	: Actual volume of compacts
$\rho_{rel}$	: Relative density of compacts
$P$	: Porosity of compacts
HRV	: Vickers Hardness
$V_{debris}$	: Volume of wear debris particle.
$d$	: Linear dimension of the particle.

$p$	: Probability that observed data is due purely to random chance (Students T-Test)
$n$	: Number of replicates
$\bar{x}$	: Mean value of a set of data
$\Sigma x$	: Sum of all the replicate values in a data sampling
$\Sigma x^2$	: Sum of squares of each replicate value
$(\Sigma x)^2$	: Square of the sum of all the replicate values in a data sampling
$\sigma_d^2$	: The variance of the difference between the means of the two sets of data used in the Students T-Test
$\sigma_d$	: The standard deviation of the difference between the means of the two sets of data used in the Students T-Test
$t$	: Value of $t$ statistic obtained from the Students T-Test

# **Chapter One**

## **Introduction**

### **1.1 Purpose**

In designing long-lasting and functional joint prosthetic implants, engineers and clinicians face two major obstacles, namely biocompatibility and durability. Wear and fatigue fracture account for most implant failures. Wear, apart from weakening and roughening the surface of the implant, also generates debris, which cause adverse tissue reactions, eventually leading to substantial loss of bone around the implant and consequently loosening of the fixation.

Titanium and its alloys have been extensively studied and is the most widely used biometal for its relatively low modulus, high strength to weight ratio, excellent corrosion resistance and biocompatibility. Titanium, however, exhibits poor wear resistance. In an effort to improve on the wear resistance of titanium, a titanium-graphite metal matrix composite was developed and patented by NUS [1]. In 2002, NUS signed a Memorandum of Understanding with the National Institute for Materials Science, Japan, to further improve on the patented material, as well as to characterize its properties. The main aim of this project was the study of the feasibility of the improved titanium-graphite composite for use as an orthopedic biomaterial. The microstructure of the said composite would be extensively characterized. The tensile mechanical properties and long term durability, in terms

of resistance to fatigue would be examined. In addition, the biocompatibility of the material, both in bulk form as well as the wear debris generated, would be investigated.

### 1.2 Motivation

In the industrialized world, advances in medical care have increased the average life-span of the population. These advances, however, represent a doubled edged sword. The human body has not been able to evolve to the extent necessary to function optimally in our twilight years. As a result, debilitating diseases such as osteoarthritis, bone cancer and avascular necrosis plague the elderly. In America, for instance, 165 000 hip replacements and 326 000 knee replacements are performed in 2001 [2]. Total joint replacements with metallic alloys and synthetic polymers have revolutionized the treatment of end-stage arthritis over the past three decades. Total joint arthroplasty provides dramatic pain relief and vast improvement in joint function for patients with a variety of end-stage joint diseases, and approximately half a million such operations are performed worldwide, at a cost exceeding five billion dollars annually. There is therefore an enormous economic potential to be reaped in the field of biomaterials. There are currently thousands of medical devices available and the global medical devices market is estimated to be worth US\$169 billion. [3].

Of even greater significance is the impact of biomaterials in improving the quality of life of patients. Ever since the first hip prosthesis was fabricated by Charnley in

November 1962, [4] a wide variety of hip prosthesis have been developed and clinically tested. The more successful prostheses include metal-on-metal (comprising 316 stainless steel, cobalt-chromium alloys, titanium), metal-on-polymer (comprising metal femoral heads and ultra high molecular weight polyethylene (UHMWPE) acetabular cups), ceramic-on-ceramic (consisting of alumina and zirconia heads and cups), and ceramic-on-polymer (comprising ceramic heads and UHMWPE cups). Whilst these prostheses have achieved commendable success in relieving pain and improving mobility of the patients, problems of poor long-term durability abound. Few of these prostheses survive beyond 25 years [5].

The major long term complications of total joint arthroplasty are aseptic loosening and periprosthetic osteolysis, resulting in implant failure, bone stock deficiency, periprosthetic fractures, and subsequent revision surgery. Revision surgery in such cases is particularly difficult and often requires the use of special components and massive bone grafts. In some cases the extent of bone loss is so massive as to preclude revision surgery altogether. One of the theories put forward to explain the occurrence of aseptic loosening and periprosthetic bone loss postulates that these related processes reflect an adverse cellular response to degradation products of implant materials [6]. The degradation products are produced by corrosion and wear, which generates millions of particles annually in the preprosthetic space [7, 8]. Improving on the wear resistance of the prostheses is thus fundamental to their long-term performance. It is with these concerns in

## Chapter 1: Introduction

---

mind that a novel titanium-graphite biomaterial was developed by Teoh et al [SH Teoh, R Thampuran, WKH Seah and JCH Goh. Sintered titanium - graphic composite having improved wear resistance and low frictional characteristics. U.S. Patent 5,758,253, May 26, 1998.]. The main desirable mechanical characteristics of an ideal hip implant are as follows:

- 1) good biocompatibility;
- 2) excellent corrosion resistance in body fluids;
- 3) an elastic modulus close to that of bone, such that stresses are transferred effectively to the surrounding bone, thus encouraging bone ingrowth;
- 4) has a surface capable of allowing stable attachment to bone;
- 5) has a low coefficient of friction; and
- 6) has high wear resistance.

The triphasic sintered and hot isostatically pressed titanium-graphite composite (Figure 1.1) developed by powder metallurgy could potentially meet these requirements. It has a lubricating phase made up of free graphite, a hard wear resistant phase made up of titanium carbide and a biocompatible base of pure titanium.

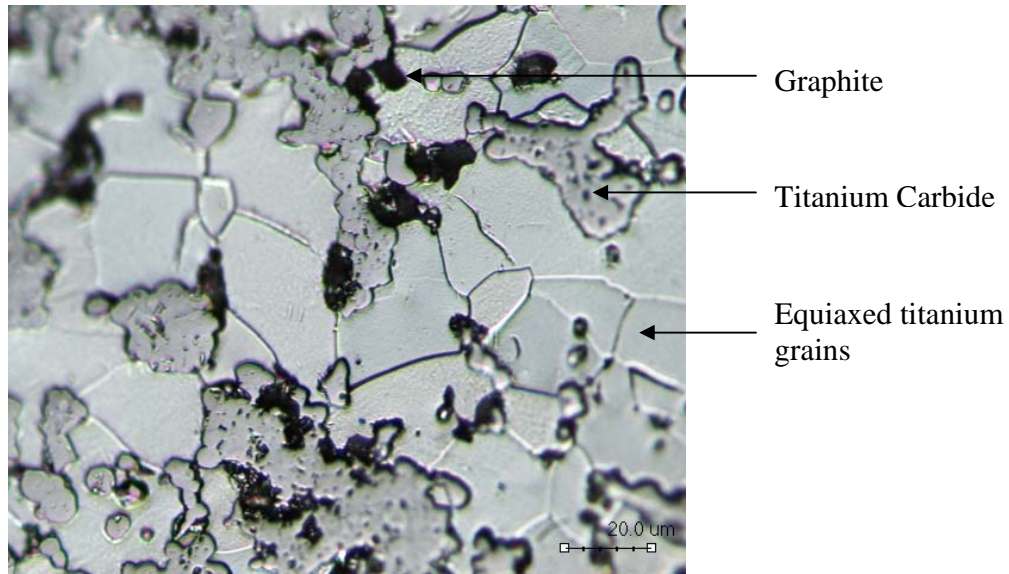


Figure 1.1: Triphasic Titanium-Graphite 5-wt% composite

### 1.3 Objectives and Scope

Previous work involving the titanium-graphite composite have focused on the tribological characteristics and performance of the said composite in a hip wear simulator. This study aims to fully characterize the metallographic, mechanical and cytotoxic properties of the composite and the wear debris generated.

Specifically, the objectives and scope of this project are:

- 1) To characterize in depth the microstructure and porosity of the composites;
- 2) To determine the tensile strength and modulus of the composites;
- 3) To determine the fatigue performance of the composites;
- 4) To generate and characterize the wear debris;
- 5) To study the cytotoxicity of the raw powder and wear debris towards the

## **Chapter 1: Introduction**

---

3T3 fibroblast cell line and primary rat osteoblast culture;

- 6) To determine if the polished surfaces of the sintered compacts promote adhesion of 3T3 fibroblast cell line and primary rat osteoblast culture; and
- 7) To study the cytotoxicity of the polished surfaces of the sintered compacts towards the 3T3 fibroblast cell line and primary rat osteoblast culture.



## Chapter Two

### Literature Survey

#### 2.1 History of Titanium

Titanium is the ninth most abundant element in the earth's crust. Titanium was discovered in England by Reverend William Gregor in 1791. He recognized the presence of a new element in ilmenite, and named it *menachite*. At around the same time, Franz Joseph Muller also produced a similar substance, but could not identify it. The element was independently rediscovered several years later by German chemist Martin Heinrich Klaproth in rutile ore. Klaproth confirmed it as a new element and in 1795 he named it for the Latin word for Earth (also the name for the Titans of Greek mythology).

Titanium has always been difficult to extract from its various ores. Pure metallic titanium (99.9%) was first prepared in 1910 by Matthew A. Hunter by heating  $\text{TiCl}_4$  with sodium in a steel bomb at 700-800°C in the Hunter process. Titanium metal was not used outside the laboratory until 1946 when William Justin Kroll proved that titanium could be commercially produced by reducing titanium tetrachloride with magnesium in the Kroll process which is the method still used today.

Titanium has a density of  $4.54 \text{ g/cm}^3$  and exists in two forms;  $\alpha$ -titanium, which has a hexagonally closed-packed (HCP) crystalline structure and  $\beta$ -titanium, which has a body centred cubic (BCC) crystalline structure. At room temperature, the  $\alpha$ -titanium predominates, unless the metal is alloyed with other metals known as  $\beta$ -stabilizers. However, when titanium is heated to  $880 \text{ }^\circ\text{C}$ , which is below its melting point of  $1660 \text{ }^\circ\text{C}$ , the HCP  $\alpha$ -phase transforms into the BCC  $\beta$ -phase. This temperature is known as the  $\alpha$ -to- $\beta$  transition temperature.

The large scale use of titanium and its alloys for orthopaedic applications began in the early 1970s. This was spurred, in large part, by the poor performance of cast and CoCr femoral stems, which displayed poor fatigue performance and high degree of proximal bone resorption, due to the excessive stiffness of the material. Interest in titanium and its alloys grew rapidly in Europe and North America in the second half of the 1970s. Titanium and its alloys offered several advantages over other metals for use as orthopaedic implants. Firstly, they are less stiff and have higher strength than the CoCr implants. Their relatively low stiffness enabled a more physiological transmission of loads to the femur, which, according to Wolfe's Law, would avoid proximal stress shielding and thus prevent bone resorption in the proximal femur. Secondly, they are biocompatible and are suitable for use as endoprostheses intended to remain permanently inside the human body [9]. Thirdly, due to the formation of a protective oxide film on the surface, titanium and its alloys display good corrosion resistance in the body fluid. This is essential in maintaining the long term stability of the implant. Lastly,

titanium and its alloys have high strength-to-weight ratios. Titanium is as strong as steel, but 45% lighter; it is 60% heavier than aluminum, but twice as strong. This results in less hindrance to patient mobility when used as orthopaedic implants.

### 2.1.1 Fatigue Properties of Titanium

Fatigue is a process by which a material is weakened by cyclic loading. The amplitude of the applied stress may be lower than the ultimate tensile stress, or even the yield stress of the material concerned, yet catastrophic failure occurs. The process begins at an initiation site within the material such as microscopic crack or surface imperfections, such as notches. These are regions of high stress concentration. As the cyclic stress is applied to the material, the crack widens and propagates throughout the material, causing eventual failure.

Analysis of the fatigue performance of a material involves investigating its S-N characteristics, whereby S is the applied cyclical stress amplitude, and N, the number of cycles to failure. The S-N curve of a material could be determined by mounting the test specimen on a universal testing machine, and applying a sinusoidal stress on the specimen. The number of cycles to failure of the test specimen is then determined for each test amplitude. The test usually begins with a relatively high amplitude of cyclical stress, for instance, 80% of the ultimate tensile stress of the material, until the material fails. The process is repeated for a lower applied stress amplitude and proceeds until a stress amplitude low enough

## Chapter 2: Literature Survey

---

not to cause failure after more than  $10^6$  cycles. This stress amplitude is known as the Endurance Limit of the material. The existence of the Endurance Limit is due to the presence of interstitial elements, such as pin dislocations, which prevent slip from occurring [10].

Fatigue was first observed in the failure of iron mine-hoist chains arising from repeated small loadings by William Albert in 1829 [11]. The first systematic study on fatigue was conducted by Sir William Fairbairn and August Wöhler in 1860. Wöhler studied the performance of railroad axles, and proposed the use of S-N curves in mechanical design. The origin of fatigue failure in microscopic cracks was demonstrated by Sir James Alfred Ewing in 1903 [11].

Some variables pertinent in fatigue testing are listed below:

$$\Delta\sigma = \sigma_{\max} - \sigma_{\min}$$

$$\sigma_u = \frac{\Delta\sigma}{2}$$

$$\sigma_m = \frac{\sigma_{\max} + \sigma_{\min}}{2}$$

$$R = \frac{\sigma_{\min}}{\sigma_{\max}}$$

where:

$\sigma_{\max}$  = Maximum applied stress

$\sigma_{\min}$  = Minimum applied stress

$\Delta\sigma$  = Stress range

## Chapter 2: Literature Survey

---

$\sigma_u$  = Stress amplitude

$\sigma_m$  = Mean stress

R = Stress ratio

Some of the factors which influence fatigue life of a material are:

- 1) The magnitude of the applied stress, including stress concentrations caused by part geometry.
- 2) The surface defect geometry and location.
- 3) The quality of the surface finish. Surface roughness, scratches and the presence of notches act as local stress concentrators and crack nucleation sites.
- 4) Size, frequency and location of internal defects.
- 5) Grain size. Most metals, whose microstructure consist of fine grains, exhibit longer fatigue life than coarse-grained metals.
- 6) Uneven cooling of the material may result in uneven distribution of the different phases, and lead to heterogeneous materials properties.
- 7) Direction of the applied stress may affect fatigue life of non-isotropic materials.
- 8) Exposure to harsh environmental conditions may cause corrosion, erosion or gas-phase embrittlement of the material, thus reducing fatigue life.

Titanium and its alloys generally exhibit good high cycle fatigue strengths as compared with their tensile strengths. The S-N curves of most titanium alloys tend to flatten out at  $10^7$  cycles, and the fatigue limit is generally between 40%

and 60% of the tensile strength [12]. The endurance limit of titanium depends on a number of factors such as the alloy composition, heat treatment, type of metal working done, as well as the testing conditions. For commercial purity titanium, the endurance limit ranges from 130 MPa to 300 MPa [13, 14].

Nakazawa et al [15] have conducted fatigue tests on Ti-6Al-4V. The tests were carried under tension-tension mode at a stress ratio of 0.1. A sinusoidal wave frequency of 20 Hz was used for the test, and all tests were performed in laboratory air of humidity 40% to 70%. From their investigations, the endurance limit of the titanium alloy was found to be 250 MPa. The S-N curve of the Ti-6Al-4V determined in their investigation is shown in Figure 2.1 below.

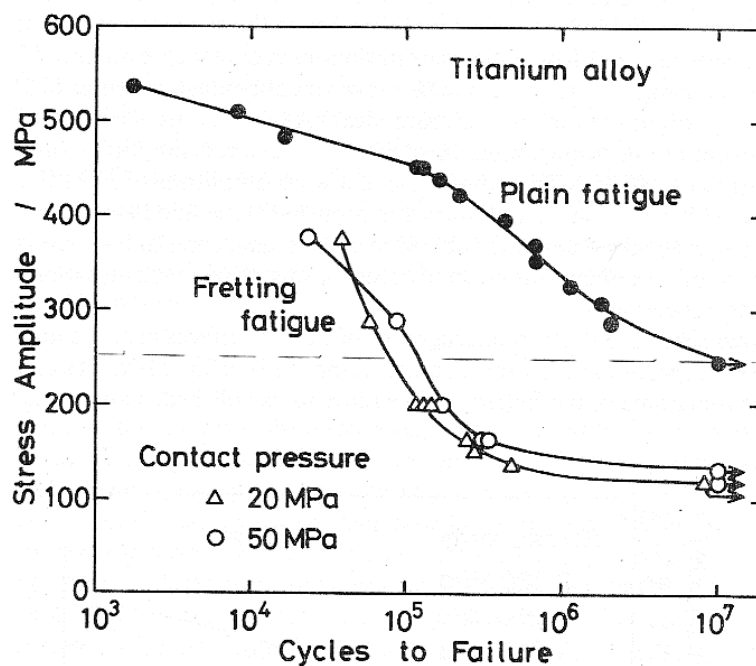


Figure 2.1: S-N curve of the Ti-6Al-4V [15]

### 2.1.2 In-vitro Studies on the Biocompatibility of Titanium

The biocompatibility of titanium has been extensively studied. Titanium displays high corrosion resistance, high specific strength and good osteointegration properties. Many studies involving the cytotoxicity of titanium and its alloys have used the Balb/C 3T3 cell line [16, 17, 18, 19]. The 3T3 cell line is a continuous, immortalized but not transformed cell line which is commonly used in cytotoxicity analysis. The cells are sensitive to contact inhibition and are suitable for cytotoxicity tests. In addition, the 3T3 fibroblast cell lines were chosen also due to the predominance in connective tissue, robust cell growth and the distinct morphology change upon adhesion to surfaces. The in-vitro studies have found that titanium and its alloys display good biocompatibility towards the 3T3 cell line. There was no significant reduction in cellular proliferation and cell morphology, as compared to the respective control cultures [19].

The biocompatibility of titanium has also been assessed with osteoblast cells [16, 18, 20, 21, 22] since most biomedical applications of titanium involve contact with bone tissue (for example in orthopaedics and dentistry). Harris et al have assessed the cytocompatibility of different coated titanium surfaces with both 3T3 cells and osteoblast [16]. The study has concluded that the nitrogen ion implanted unalloyed titanium surface was one of the best surfaces for osteoblast and fibroblast proliferation. Overall, titanium was found to be not cytotoxic to both cell types.

## 2.2 History of Graphite

Graphite is an allotrope of carbon with a density of  $2.21 \text{ g/cm}^3$ . It has a lamellar structure with weak van der Waals interplanar forces that enables it to be a remarkable lubricant. Natural deposits of graphite have been called black lead, silver lead, and plumbago, which is another name for the lead ore galena. The structure of graphite consists of layers of carbon atoms joined in regular hexagons by strong bonds. The layers are held together by long-range, relatively weak attractive forces called Van der Waals forces. The layers can slide over each other easily, which accounts in part for the lubricating property of graphite.

Graphite is generally greyish-black, opaque and has a lustrous black sheen. It is unique in that it has a combination of both metallic and non-metallic properties of both a metal and a non-metal. It is flexible but not elastic, has a high thermal and electrical conductivity, and is highly refractory and chemically inert.

The unusual combination of properties is due its crystal structure, shown in Figure 2.2 [23]. The carbon atoms are arranged hexagonally in a planar condensed ring system. The layers are stacked parallel to each other. The atoms within the rings are bonded covalently, whilst the layers are loosely bonded together by van der Waals forces. The high degree of anisotropy in graphite results from the two types of bonding acting in different crystallographic directions. World production of graphite was estimated to be about 602,000 tons in 2000, with China being the biggest producer followed by India, Brazil, Mexico and then the Czech Republic.



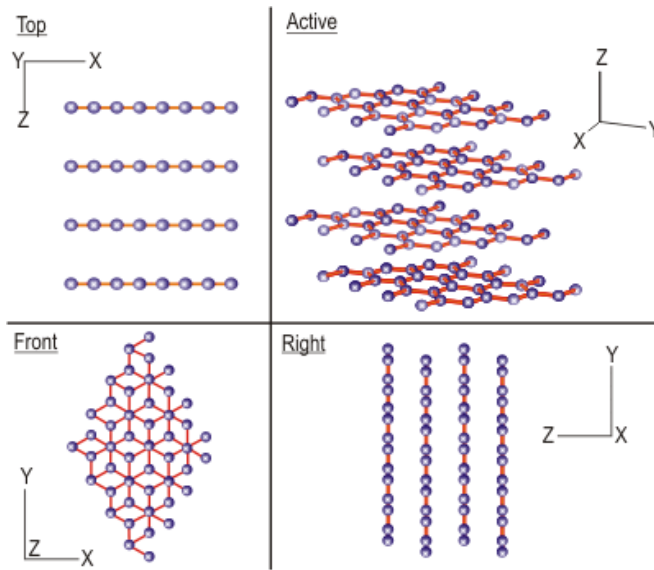


Figure 2.2: Crystal structure of graphite [23].

### 2.2.1 Lubrication Properties of Graphite

Graphite is a lamellar solid and has the ability to reduce friction when applied between two contacting surfaces. Graphite's ability to form a solid film lubricant arises from the fact that weak Van der Waals forces govern the bonding between individual layers, which permits the layers to slide over one another and making it an ideal lubricant. Hence, the presence of a graphite on the articulating surfaces of biomaterials could help reduce wear of the prosthesis.

The tribological properties of metal-graphite composites is characterized by two stages. When sufficient wear of the metal matrix at the articulating surfaces has taken place, the graphite particles are released onto the sliding surfaces. In the first stage, known as the transient stage, graphite film starts to form on the surface.

There is significant asperity interaction in this stage. In the second stage, known as the steady state, a stable graphite film has formed on the surface and prevent direct contact between the articulating surfaces. The constant replenishment of graphite particles as the articulating surface is removed due to wear is crucial in maintaining the steady state, and hence it is necessary to design metal-graphite composites with sufficient unreacted graphite particles throughout the entire volume of the composite.

### **2.3 Powder Metallurgy**

Powder Metallurgy was first described by C.G. Goetzel in 1949 [24]. This technique enables the production of metal matrix composites, such as the titanium-graphite composites used in this study. This processing technique offers good microstructural control of the various phases formed, such as the titanium, titanium carbide and graphite phases formed in the titanium-graphite composites. Secondly, this approach employs lower processing temperatures, and hence, theoretically, would offer better control over interface kinetics of particles used. Lastly, this technique allows the matrix alloy compositions and microstructure refinements that are only available through the use of rapidly solidified powders to be employed [25].

The basic processes involved in powder metallurgy include mixing, compacting and sintering of the powder mixture. Proper mixing of the raw powder is essential in ensuring uniform distribution of particles, which eventually results in the

formation of a uniform microstructure and porosity of the composite. These factors, in turn play a critical role in the mechanical and tribological behaviour of the material. In general, the larger the size of the powder particle, the higher the degree of distribution uniformity within the mixture.

Once the raw powder has been thoroughly mixed, the next stage involves compaction of the powder mixture. There are two types of compaction techniques that are commonly used, namely the blended elemental method and hydrostatic pressing method. In the first method, consolidation of the powders is achieved by applying a uniaxial load to create the required compaction pressure. In the second method, the required pressure is achieved by applying hydrostatic forces to the powders. In this study, compaction was first done in a punch-die assembly, which applies a uniaxial compressive force on the powder particles. The compaction process in the blended elemental approach has been described in detail by R.M. German [26]. Briefly, this process comprises three stages. The first stage involves particle rearrangement during initial pressurization. During this stage, the number of contacts between particles increases as rearrangement and sliding takes place. Upon further pressurization, particle deformation takes place and the area of contact between particles enlarge. New contacts are also formed in this stage. It is crucial that the compaction pressure is not further increased excessively, lest a third stage of strain hardening may occur. Strain hardening may result in the fracture of the powder particles and should be avoided.

The next step in powder metallurgy involves sintering of the green compacts. This is a heat treatment process, which takes place below the melting point of the raw powder, increases the thermal energy and enhances the diffusion of the particles. This process enhances strength and greatly reduces the porosity of the compacts.

Documented literature [27, 28] has postulated that there are three stages in sintering, namely the initial, intermediary and final stages. These stages are characterized in terms of the changes in the pore morphology where necking between particles can eventually lead to pore closure and full densification. The changes in the pore morphology are caused by atomic migration, which has been found to be initiated by three mechanisms namely viscous flow, evaporation-condensation and self-diffusion.

Several parameters play an important role in the densification process, namely particle size, sintering time and temperature. It has been concluded that sintering temperature is the most important variable [26, 29]. Control of the environmental conditions during sintering is also crucial, especially when sintering titanium-containing composites. The presence of oxygen at an elevated temperature would result in surface oxide formation, which would greatly hinder diffusional bonding, and weaken the compact. For this reason, sintering of titanium-graphite composites in this study was performed in a vacuum.

Hot isostatic pressing (HIP) is the application of heat and pressure simultaneously to a part, causing it to shrink and densify uniformly. It can be used directly to consolidate a powder or supplementary to further densify a cold pressed, sintered, or cast part. The pressure medium is typically a gas (argon or nitrogen) but can be a liquid (glass) or molten metal. Heating is done in an electric furnace. By heating the material and simultaneously applying high isostatic pressure, it is possible to achieve yielding of the material particles, thus uniformly eliminating porosity. To densify a powder directly requires a can to transmit the pressure to the powder. Applications of HIP include the densifying of high performance ceramics, ferrites and cemented carbides, net-shape forming of nickel-base superalloy and titanium powders, compacting of high-speed tool steel, diffusion bonding of similar and dissimilar materials, and eliminating voids in aerospace castings or creep damaged blades [30, 31]. Hot isostatic pressing results in a very uniform grain structure, greatly reduced porosity and exceptional properties. Dissimilar materials could be bonded together through the application of HIP. Fatigue life is often better than achieved by any other processing method [32]. It also is used to diffusion bond same and dissimilar materials that could not otherwise be bonded.

### **2.4 Total Hip Replacement (THR)**

Total hip replacement surgery is a treatment option for patients with severely damaged hip joints, usually associated with conditions such as osteoarthritis, rheumatoid arthritis and conditions of deficient bone quality like Paget's disease. THR creates an artificial joint that will replace the diseased joint.

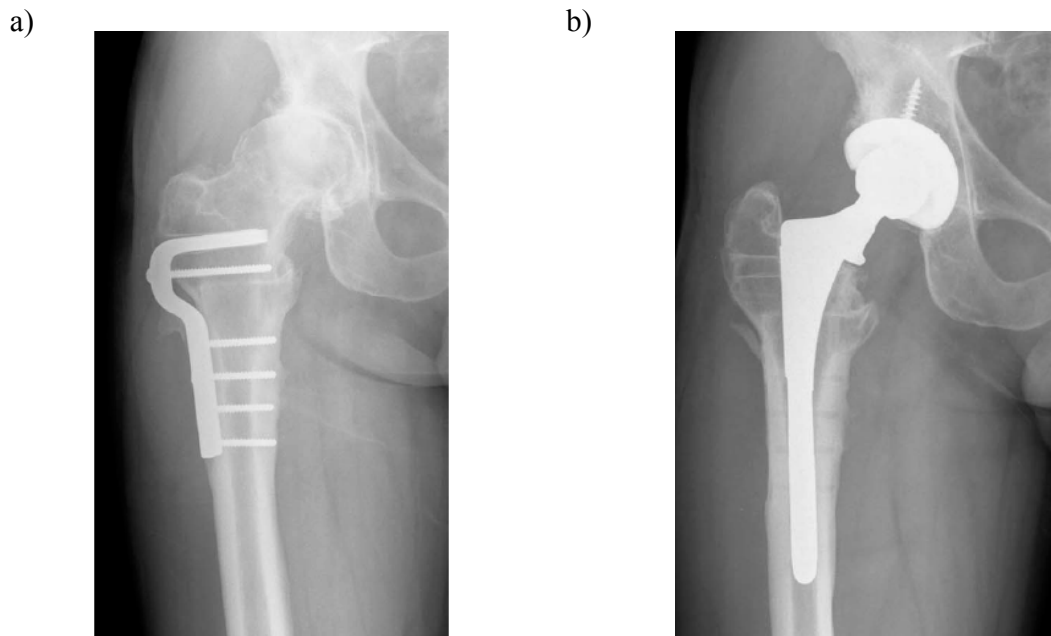


Figure 2.3: X-ray images of Hip Joint of a 37-year Old Patient [33]. a) Early onset of osteoarthritis, treated by medial displacement osteotomy. b) Total Hip Replacement

Figure 2.3 [33] shows an osteoarthritic joint before and after THR. Some of the key features of a well designed hip prosthesis are:

- 1) relieve joint pain;
- 2) restore mobility;
- 3) restore normal leg length;
- 4) be able to support the body weight of the patient;
- 5) be anchored securely in bone for long term fixation and durability; and
- 6) be biocompatible and stable in vivo.

A schematic drawing of a hip prosthesis is shown in Figure 2.4 [34].

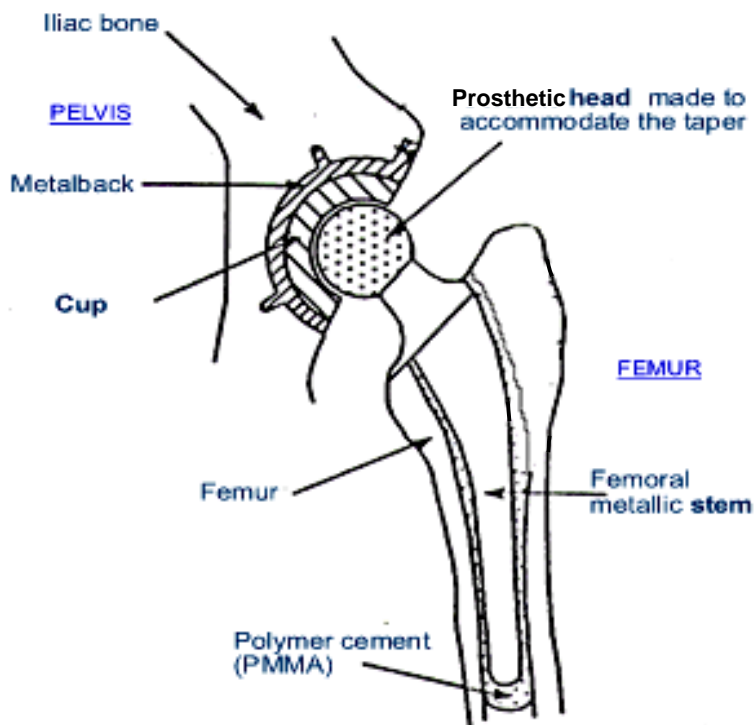


Figure 2.4: Schematic of a Hip Prosthesis [34].

THR surgery is the most commonly performed joint-replacement procedure. Each year, over 200,000 Americans undergo THR surgery [35]. A typical THR consists of a cup type acetabular component and a femoral component whose head is designed to fit into the acetabular cup and thus enabling joint articulations. The femoral stem is tapered so that it can be fixed into a reamed medullary canal of the femur. During THR surgery, the ball and socket arthritic joint is first removed. The top part of the femur is removed, and the tapered stem of the femoral component of the prosthesis is fitted within the central (medullary) canal of the patient's femur. Any remaining cartilage and some bone is removed from

the patient's acetabulum, and a prosthetic acetabular cup is fitted in its place.

There exists several different types of prostheses for THR, and these are discussed below.

The metal-on-plastic implant consists of a metal femoral head and acetabular cup, and a plastic spacer is placed in between. The metals used include titanium, stainless steel, and cobalt chrome. The plastic spacer is fabricated from polyethylene. Implant fixation is achieved by either of two methods: it is either press-fit or cemented into place. In the press-fit method, the implant is fit snugly into the bone, and new bone forms around the implant to secure it in position.

When an implant is cemented, a special bone cement, known as polymethyl methacrylate (PMMA) is used to secure the prosthesis in position. This type of implant is the most commonly used hip replacement prosthesis. Unlike the metal-on-plastic implant, the metal-on-metal prosthesis, which uses similar materials, does not have a plastic spacer in between. Metal-on-metal implants do not wear out as quickly as the metal and plastic materials. The metal and plastic implants wear at a rate of about 0.1 millimeters each year. Metal-on-metal implants wear at a rate of about 0.01 millimeters each year, about 20 to 100 times less than metal-on-plastic [36, 37]. Despite the low wear rates, it is not known whether metal-on-metal implants will last longer. The wear debris that is generated from the metal-on-metal implants contain metal ions, which are released into the blood, and these metal ions can be detected throughout the body. The concentration of these metal ions increases over time. Ceramic-on-ceramic implants are designed to be the



most resistant to wear of all available hip replacement implants. They wear even less than the metal-on-metal implants and are corrosion resistant. Ceramics are more scratch resistant and smoother than any of these other implant materials. However, ceramics are very brittle material, and display poor impact strength. Data on the long term durability of the ceramic-on-ceramic implants, as well as possible complications, are unavailable.

### **2.5 Biological Response to Implants**

The cellular response towards implant materials depends largely on the dimensions of the implants. Many implants are relatively inert in bulk form, but particles of these materials may bring about detrimental cellular reactions in the surrounding bone [16]. An understanding of the different mechanisms involved is thus imperative in any study involving biocompatibility of implant materials.

#### **2.5.1 Mechanism of Cellular Response to Bulk Implant Material**

Implant surfaces are generally designed to promote soft and hard tissue adherence, eventually resulting in integration with bone and the surrounding soft tissue [16]. Upon implantation, the surface of the implant is coated immediately with host plasma constituents, including protein components of the extracellular matrix (ECM). The amount of cell adhesion to a surface plays a pivotal role in the response of the cells to the surface. There are two types of cell adhesion, namely cell–substrate and cell–cell. In cell–substrate adhesion, the cells attach to the ECM proteins adsorbed onto the substrate surface. Fibroblast and osteoblast are

anchorage-dependant cells the formation of such adhesion sites is vital to their survival.

Cell adhesion is mediated by several types of transmembrane receptor proteins, associated with the cell cytoskeleton. One mechanism of cell adhesion involves their adhesion to adsorbed ECM proteins using small highly organized complexes, known as focal contacts. Initially, the adhesion sites do not associate with the actin cytoskeleton of the cells, and is known as ‘dot’ adhesions. Upon maturity, the adhesion sites associate with the actin stress fibres to form ‘dash’ adhesions [38]. The formation of cell adhesion sites results in the positioning of the actin filaments responsible for the contractile mechanism of the cell [39], which has an effect on cellular behaviour and morphology [40, 41].

If cells are not adequately adhered, a fibrous capsule, with a liquid-filled void, may form between the soft tissue and implant [42, 43]. This may result in further implant destabilization, inhibition of tissue regeneration and repair, and increased possibility of infection, due to poor vascularization around the implant and fibrous tissue [42, 44, 45].

Cells respond in a different, and often, more detrimental manner to wear debris.

### 2.5.2 Wear Particle Induced Osteolysis

Total Hip Replacement is a major surgery, and several potential complications may occur. These include implant failure, deep vein thrombosis, dislocation of the prosthetic hip joint, infection and periprosthetic osteolysis. Complications as a result of osteolysis are the most common causes for revision surgery [46]. The extent of foreign body response depends on size, type, number and surface area of the particles. Larger particles, over 50  $\mu\text{m}$ , induce fibrous encapsulation, while smaller particles, below 7  $\mu\text{m}$ , are phagocytosed. Phagocytosis of smaller particles is detrimental and results in macrophage activation and release of a variety of cytokines like interleukins, tumour necrosis factor  $\alpha$  (TNF- $\alpha$ ), PGE2 and metalloproteases [46].

Particles generated in THRs are much finer, due to abrasion and adhesion types of wear. Scanning electron microscopy of the wear debris has revealed that the mean size of the particulate debris is 0.5  $\mu\text{m}$ , and nearly 90 % of the particles are less than 1  $\mu\text{m}$ . In cases of failed hip arthroplasties involving metal prostheses, studies have shown that there is a 7- to 21-fold increase in metal levels adjacent to the loose implant. It has also been documented that a granulomatous soft tissue membrane, known as the interfacial membrane (IFM), forms at the bone-failed-prosthesis interface [47, 48, 49]. Histological examination of this membrane has shown that it is composed predominantly of macrophages, foreign body giant cells, which contain or are in close proximity to the implant particles. In the periprosthetic space in vivo, the cells interact with the particles, and in the case of

smaller particles, phagocytosis also occurs. The presence of non-degradable particles results in a constant state of activation of all cell types in the periprosthetic space. Other studies involving commercially pure titanium particles have concluded that titanium particles of between 1.5  $\mu\text{m}$  to 4.0  $\mu\text{m}$  had the greatest impact on cell vitality and proliferation [20].

Different types of particles induce different responses in vivo. Titanium particles, affects osteoblast viability in-vitro [21], but has been shown to enhance fibroblast proliferation (at particle concentration of 0.0083 and below, volume/volume) [50]. The effect of carbon particles on cell viability depends on the particle size, aspect ratio and crystallinity [51, 52, 53]. It has been shown that carbon fibres of nanophase diameters increased osteoblast adhesion (by up to 33 %), proliferation (by up to 150%), alkaline phosphatase activity (by up to 300%), and calcium deposition (by up to 100%) while at the same time decreased competitive cell adhesion compared to their larger diameter counterparts [54, 55]. These findings suggest that nanophase diameter carbon fibres may have potential applications in improving osteo-integration and minimizing fibrous-tissue encapsulation.

Particles of larger, amorphous hydrogenated carbon coating ( $d_{90} = 37 \mu\text{m}$ ) were found to be relatively inert to primary rat bone marrow cell cultures [51]. Other researchers have also found that single carbon fibres of lower crystallinity and of a more basic chemical composition were more biocompatible and contributed to the regeneration of both soft and hard tissues [56].

The detrimental effect of osteolysis is clearly seen in Figure 2.5 [46].



Figure 2.5: AP radiograph of a cementless hip arthroplasty. arrows indicate extent of femoral osteolysis. [46]

Osteolysis is the most significant complication arising from THR. Most long-term follow-up studies have attributed the incidence of osteolysis as the predominant cause of prosthesis failure [57]. The direct correlation between osteolysis and wear has been well established. It is thus imperative for manufacturers of hip prostheses and clinicians to give due consideration to the incidence of osteolysis in prosthesis design, method of fixation to bone, and the choice of bearing surfaces in hip arthroplasty.

## Chapter Three

### Experimental Procedure

#### 3.1 Materials

Pure grade Hydride-DeHydride (HDH) titanium powder from Toho Titanium, Japan, was used to fabricate the sintered compacts. HDH Titanium is also known as ELCL titanium (Extra Low Chlorine) for improved biocompatibility. The purity of the titanium powder is 99.7 % and the mean particle size of the titanium powder is 40  $\mu\text{m}$ . The particles exhibit an angular morphology, as compared to gas-atomized titanium powder, which is spherical. The composition of the titanium powder used is shown in Table 3.1.

Table 3.1: Elemental constituents of pure HDH titanium powder

Impurity Constituent	Cl	Mg	Fe	Mn	Si	N	C	H	O
Maximum Quantity (% Weight)	0.003	0.001	0.05	0.01	0.02	0.03	0.02	0.06	0.35

High purity graphite powder (99.5%), Mesh -325, purchased from Cerac Incorporated, USA, was used in the fabrication of titanium graphite composites. The elemental constituents of the graphite powder is shown in table 3.2.

Table 3.2: Elemental constituents of pure graphite powder

Impurity Constituent	Ca	Mg	Si
Maximum Quantity (% Weight)	0.01	0.01	0.01

### 3.2 Particle Analysis

The morphology of the titanium and graphite particles were determined by Scanning Electron Microscopy (Jeol, Japan). The nomenclature used to describe the particle morphology was derived from ASTM F1877-98(2003)e1.

### 3.3 Compaction Technique

The binary powder mixtures, comprising titanium and graphite powders, were thoroughly mixed in two steps. Firstly, the powders were mixed for 1 hour in a V-shaped blender. Thereafter, the powders were thoroughly mixed using a mechanofusion system for 20 minutes. Mechanofusion is a technique of stressing the powders at a high level of energy. The simultaneous generation of compression and shear forces causes mechanical energy to be applied to the powder mixtures resulting in stable, homogeneous blends of the powder mixtures. The blended powders were poured in a rectangular punch-die set, of cross-sectional dimensions (10mm X 55mm). The main function of the punch-die set, is to transmit loads symmetrically to form a compact of homogeneous density. The set is made of hardened steel so that it is able to withstand the high pressure used.

A hydraulic press was used to uni-axially compress the powder at a pressure of 6 tons/cm<sup>2</sup> (0.6 GPa). The thickness of the compacts formed were about 7mm. Zinc Stearic Acid was used as a lubricant.

The compaction pressure affects the density and porosity of the compact. A higher compaction pressure results in higher compact density and lower percentage porosity. A compaction pressure of 0.6 GPa was selected for this work as previous studies on the material have shown that an increase in compaction pressure yielded diminishing returns in increasing compact density while reducing the percentage porosity.

#### **3.4 Sintering and Hot Isostatic Pressing of Compacts**

Sintering was performed at the Biomat Laboratory in a Carbolite (C1000) heater, which is capable of heating up to 1500 °C in a vacuum-sintering atmosphere at 10<sup>-5</sup> mbars. High vacuum was achieved in a 2-stage process. The initial roughing phase, performed by a rotary pump lowers and sustains the furnace pressure to 10<sup>-2</sup> mbars. The second stage involves a diffusion pump where pressures of 10<sup>-5</sup> mbars were reached.

The compacts were then inserted into a high temperature ceramic tube. Both ends of the tube were covered with stainless steel foil to ensure even heating and



### Chapter 3: Experimental Procedure

---

prevent contamination of the oven by the highly reactive titanium. The ceramic tube containing the green compacts was then placed in the oven.

Sintering would only start once the pressure in the vacuum has been lowered to, and sustained at,  $10^{-5}$  mbars. The various stages of the heating cycle is described below and shown schematically in Figure 3.1:

- 1) The oven was heated at a rate of  $10\text{ }^{\circ}\text{C}/\text{min}$  to  $500\text{ }^{\circ}\text{C}$ . The temperature was sustained at  $500\text{ }^{\circ}\text{C}$  for 1 hour to vapourize and remove all the zinc stearic acid lubricant.
- 2) The oven was further heated at a rate of  $5\text{ }^{\circ}\text{C}/\text{min}$  to a temperature of  $1250\text{ }^{\circ}\text{C}$ . This temperature was sustained for 2 hours. In this stage, neck growth between the powder particles occur, as well formation of titanium carbide in the binary powder compacts. The heating duration of 2 hours was selected as previous work has shown appreciable titanium carbide formation and good sintered compact mechanical properties. An increase in heating period produced diminishing returns in terms of improvements in mechanical properties.
- 3) The final stage involves cooling of the sintered compacts in the oven, at a controlled cooling rate of  $10\text{ }^{\circ}\text{C}/\text{min}$ , to room temperature.

The nomenclature used to describe the various specimens in this thesis consist of two numbers, which correspond to the particle size of the graphite used in the raw powder and the graphite content. For example, 10-5 is used to describe the

### Chapter 3: Experimental Procedure

---

specimens, whose raw powder contained graphite particles of  $10\ \mu\text{m}$  in size, and whose graphite content is 5%. Table 3.3 describes the nomenclature of the specimens used in this study.

Table 3.3: Specimen Nomenclature.

Specimen	0-0	10-5	10-10
Graphite Particle Size	N.A.	$10\ \mu\text{m}$	$10\ \mu\text{m}$
Graphite Content (% weight)	0	5%	10%

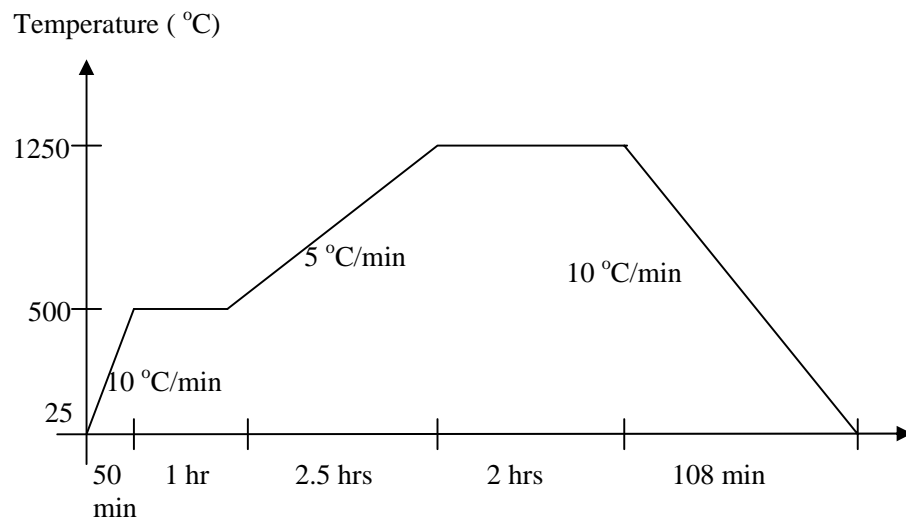


Figure 3.1: Four stage heating cycle of the sintering process

Following sintering, the compacts were sent to Japan for Hot Isostatic Pressing (HIP) at  $1000\ \text{°C}$ , for 1 hour, at a pressure of 200 MPa. HIP would further

increase the density of the compacts, and reduce the porosity uniformly throughout the compact volume, for enhanced mechanical properties.

### 3.5 Microstructure of Compacts

The microstructure of the surface of the sintered and HIPped compacts were grinded with SiC sandpaper of varying grades, polished with diamond suspension and SiO<sub>2</sub>. Finally, the surface of the polished specimen was etched for 15 s with Kroll's Etchant, which was prepared by mixing 2 ml of 40 % hydrofluoric acid, 6 ml of 65 % nitric acid and 92 ml of de-ionized water. The detailed protocol employed for the metallographic examination of the compact surface is described below:

1. The surfaces of the specimens were grinded with SiC sandpaper of grade 320 to obtain a flat surface. A force of 3 lbs/specimen was applied, and the rotation speed was 120 rpm.
2. Next, the surfaces of the specimens were grinded with SiC sandpaper of grade 600 for 1 minute to obtain a smooth surface. A force of 3 lbs/specimen was applied, and the rotation speed was 120 rpm.
3. The specimens were washed thoroughly to remove any residual SiC.
4. The surfaces of the specimens were then polished with diamond suspension of particle size 6  $\mu\text{m}$  for 4 minutes. A force of 5 lbs/specimen was applied, and the rotation speed was 120 rpm.

### **Chapter 3: Experimental Procedure**

---

5. Thereafter the surfaces of the specimens were polished with diamond suspension of particle size 1  $\mu\text{m}$  for 3 minutes. A force of 5 lbs/specimen was applied, and the rotation speed was 120 rpm.
6. The final polishing step involves polishing the specimens with  $\text{SiO}_2$  suspension for 4 minutes. A force of 3 lbs/specimen was applied, and the rotation speed was 120 rpm.
7. Finally the polished specimens were etched with Kroll microetchant (92 ml distilled water, 6 ml nitric acid of 65% concentration and 2 ml hydrofluoric acid of 40% concentration).
8. The microstructures of the specimens were observed under an optical microscope.

Photomicrographs of the micro-structures observed would be shown and discussed in Chapter 4, section 4.2.

### **3.6 Tensile Properties of Compacts**

Tensile tests were conducted in the High Temperature Synthesis Laboratory of the National Institute for Materials Science, Tsukuba, Japan. A Shimadzu AG-I Autograph Precision Universal Tester was used for the tensile tests. The test specimens used are shown in Figure 3.2 below. Refer to Appendix 1 for the engineering drawing detailing the precise dimensions. Prior to testing, all surfaces of the test specimen were grinded with sand paper of successively larger grit size, up to grit 600, to remove any visible surface cracks and stress concentrators.

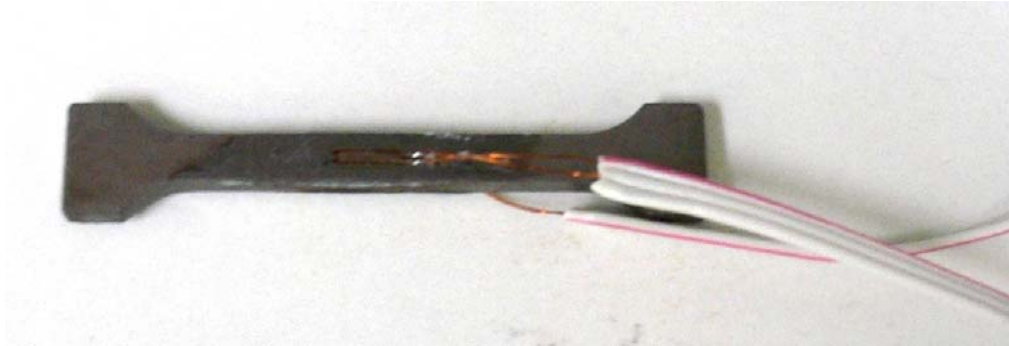


Figure 3.2: Tensile and fatigue tests specimens

There was insufficient surface area of contact, at the tips of the specimen for direct mounting between the grips of the universal testing machine, without damaging the test specimens. To ensure that the test specimens are fixed firmly in place throughout the duration of the tensile and fatigue tests, a secondary grip, shown in Figure 3.3, was designed and fabricated. Refer to Appendix 2 for the detailed engineering drawings of the secondary grips.

Tensile tests were performed on a total of 5 test pieces apiece for the 0-0 and 10-5 specimens, while for the 10-10 specimens, the tensile tests were performed on a total of 3 test pieces.

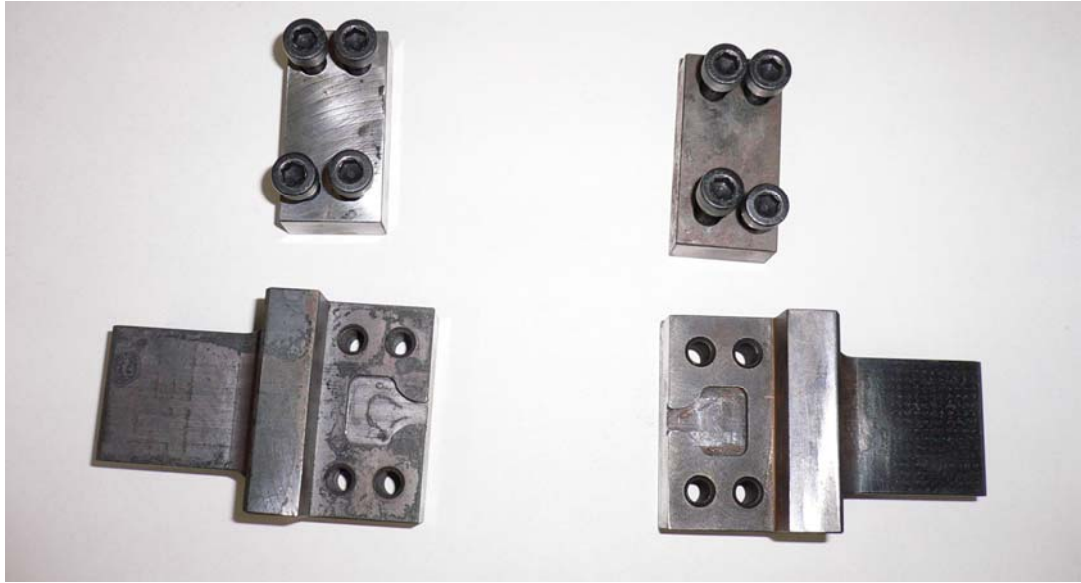


Figure 3.3: Secondary grips for tensile tests

### 3.7 Fatigue Properties of Compact

The fatigue tests were performed on an MTS 858 Tabletop System, a 100kN capacity closed-loop electrohydraulic fatigue testing machine. The fatigue tests were conducted in the High Temperature Synthesis Laboratory of the National Institute for Materials Science, Tsukuba, Japan. The specimens used were identical to the ones used in the tensile tests. The same secondary grips used in the tensile tests were used in the fatigue tests, to securely mount the specimens to the tester. The testing conditions employed were as follows:

- a) Test Medium: Air;
- b) Frequency of Cyclic Loading: 20 Hz;
- c) Ratio of minimum to maximum applied stress: 0.1

### 3.8 Cell Culture

Biocompatibility of the raw powder, wear debris and bulk compacts was determined using Balb/C 3T3 cell line and primary rat osteoblast cell cultures. The 3T3 cell line was obtained from American Type Culture Collection (ATCC). The 3T3 cell line is a continuous, immortalized but not transformed cell line which is commonly used in cytotoxicity analysis. The cells are sensitive to contact inhibition and are suitable for cytotoxicity tests. In addition, the 3T3 fibroblast cell lines were chosen also due to the predominance in connective tissue, robust cell growth and the distinct morphology change upon adhesion to surfaces.

Cytotoxicity studies were also conducted on rat osteoblast in-vitro as future application of these composites as joint replacement prosthesis would necessitate their implantation in the respective patients' bone. The in-vitro studies provide an insight on the effect on cell proliferation of fibroblasts and osteoblasts, when in contact with the titanium-graphite composites. All cell work was conducted in a tissue culture hood in a sterile clean room. Every possible step was taken to maintain the sterility of the culture.

Both 3T3 cells and rat osteoblast were cultured in T75 tissue culture flasks and sub-cultured to Passage 5 to obtain sufficient cell number for the biocompatibility tests. The tissue culture medium used was Dulbecco's Modified Eagle's Medium (DMEM), fomented with 10% Fetal Bovine Serum (FBS) and 1% Penicillin/

### **Chapter 3: Experimental Procedure**

---

Streptomycin solution. The cell cultures were placed in a cell culture incubator (Sanyo), which maintained a temperature of 37 °C and a CO<sub>2</sub> content of 5%. The 3T3 cells were obtained from American Type Culture Collection (ATCC). The cells were thawed, placed in tissue culture solution and centrifuged at 1000 rpm for 10 minutes. The supernatant solution was removed and the cell pellet sub-cultured in the tissue culture flasks, and incubated. The cells were sub-cultured every three days at confluency.

The rat osteoblast was obtained from a primary culture from a section of the femur of a rat. The bone section was placed in tissue culture flask. Tissue culture medium was added and the flask incubated for 24 hrs to allow the osteoblast to migrate from the bone chip to the flask. After 24 hrs, the remaining bone chip was removed. The tissue culture medium was removed and the flask rinsed with Phosphate Buffered Solution (PBS) three times. The PBS was removed and 5 ml of 0.05 % of Trypsin/ 0.02 % EDTA solution was added to the cell culture. After incubation for 5 minutes, the cell suspension was transferred to a centrifuge tube and 10 ml of tissue culture medium was added to the cell suspension. 15 ml of tissue culture medium was added to the tissue culture flask, which was then incubated. The cell suspension was centrifuged at 1000 rpm for 10 minutes, after which the supernatant fluid was removed. The remaining cell pellet was sub-cultured in two tissue culture flasks, with 15 ml of tissue culture medium added to each flask. The cell culture was then incubated. The cells were sub-cultured at



confluency once every week, and the tissue culture medium changed twice weekly.

### 3.9 Biocompatibility of Raw Powder

The cytotoxic effect of titanium particles has been investigated by several researchers [20, 21, 58]. The studies have indicated that the presence of titanium particles, in particular particles below 10  $\mu\text{m}$  in sufficiently high concentration, have an impact on the proliferation of osteoblast [20]. That study also indicated that particles below 10  $\mu\text{m}$  were phagocytosed by the osteoblast, which, it was postulated, had an effect on reducing the proliferation rate of the cells.

The purpose of the current study was threefold:

- a) to determine if the binary powder mixture of titanium and graphite is cytotoxic to the cells;
- b) to determine if the presence of the binary powder mixture had an effect on cellular morphology; and
- c) to determine if the raw powder particles are phagocytosed by the cells, and the effects thereof.

#### 3.9.1 Preparation of Raw Powder for Cell Culture

The separated powder was first thoroughly cleaned in separate acetone baths and placed in a sonicator for five minutes. The acetone was subsequently removed carefully. The powder was then sonicated for another five minutes in a bath of de-

## **Chapter 3: Experimental Procedure**

---

ionized water. Thereafter, the powder was sterilized in an autoclave, prior to cell culture, and kept in a sterile tissue culture hood.

Finally, a powder suspension was prepared. The suspension comprised of PBS, 1% Penicillin/Streptomycin and 5% separated powder. The suspension was placed on an orbital shaker to form a uniform suspension. The concentration of the powder suspension was 1.0% (weight/weight).

### **3.9.2 Cell Culture with Raw Powder**

Cell culture with the separated powder was performed on the 3T3 cells and rat osteoblasts in Passage 5. The cells were seeded on 48-well plates, at a density of 1000 cells/well for 3T3 cells and 10000 cells/well for rat osteoblast. 50  $\mu$ l of powder suspension was added to 450  $\mu$ l of tissue culture medium, to obtain 0.1% (weight/weight) separated powder suspension per well. This concentration was selected as it was reported to be representative of the particle concentration found in the surrounding tissue of loose implant in biopsy study [59]. The tissue culture medium was changed every three days. Care was taken to ensure that no powder particle was removed during the medium change.

### **3.10 Biocompatibility of Wear Debris**

The biocompatibility of the wear debris of the titanium and titanium-graphite composites was evaluated by determining the cell proliferation rate of the 3T3

## **Chapter 3: Experimental Procedure**

---

cells and rat osteoblast, seeded at 10000 cells/well in a 48-well plate, with wear debris added to the cell culture in each well at a concentration of 1%.

### **3.10.1 Generation of Wear Debris**

Wear debris from the sintered, post-HIPed titanium-graphite composites were generated for cytotoxicity analysis. The stages involved were as follows:

1. the surfaces of the specimens, cutting tools and all grips and fixtures were cleaned with acetone;
2. plane-milling of all surfaces of the specimens to remove the oxide layer;
3. milling of the specimen to obtain large debris;
4. the debris collected were placed in an agate pestle and ground with an agate mortar;
5. the wear debris obtained was cleaned in an acetone bath and sonicated.

### **3.10.2 Wear Debris Preparation for Cell Culture**

The wear debris generated was first thoroughly cleaned in separate acetone baths and placed in a sonicator for five minutes. The acetone was subsequently removed carefully. The debris was then sonicated for another five minutes in a bath of de-ionized water. Thereafter, the debris was sterilized in an autoclave, prior to cell culture.

Finally, a wear debris suspension was prepared. The suspension comprised of PBS, 1% Penicillin/Streptomycin and 5% wear debris. The suspension was placed on an orbital shaker to form a uniform suspension.

### **3.10.3 Cell Culture with Wear Debris**

The protocol for passaging the 3T3 cells and rat osteoblast has been described in Section 4.8.1. After Passage 5, the cells were seeded on 48-well plates, at a density of 1000 cells/well for 3T3 cells and 10000 cells/well for rat osteoblast. 50  $\mu$ l of wear debris suspension was added to 450  $\mu$ l of tissue culture medium, to obtain 0.1% (weight/weight) wear debris suspension per well. This concentration was selected as it was reported to be representative of the particle concentration found in the surrounding tissue of loose implant in biopsy study [59]. The tissue culture medium was changed every three days. Care was taken to ensure that no wear debris was removed during the medium change.

### **3.11 Biocompatibility of Compacts**

The biocompatibility of the sintered post-HIPed was determined by the proliferation rate of cells seeded on the polished surface of the compacts. The morphology of the adherent cells was also studied.

### 3.11.1 Water Contact Angle measurements of Surface of Compacts

The wetting behaviour of the surfaces of the compacts, both polished and unpolished, were determined by performing the water contact angle test. The wetting behaviour gives an indication of the degree of hydrophilicity of the compact surfaces. The equipment used to evaluate the water contact angle was the VCA – Optima Surface Analysis System. A detailed account of the method of performing the water contact angle test is described below:

- 1) The specimen to be evaluated is placed beneath the syringe;
- 2) A water droplet, of volume 50  $\mu\text{l}$  was released from the computer controlled syringe onto the specimen surface;
- 3) An image of the water droplet was taken at the precise moment contact is made with the specimen surface (time = 0s);
- 4) Images of the water droplet are taken at 10s intervals, to study the shape of the water droplet with time, up to 150s (from time = 10s to time = 150s);
- 5) The angle between the tangent to the surface of the water droplet, at the point of contact, and the surface of the specimen is measured from time = 0s to time = 150s. This angle is known as the water contact angle;
- 6) The procedure was performed on five different specimens for each specimen type (0-0, 10-5, 10-10, polished and unpolished).

Figure 3.4 shows a typical image of the water drop on the specimen surface, and the water contact angle measured.

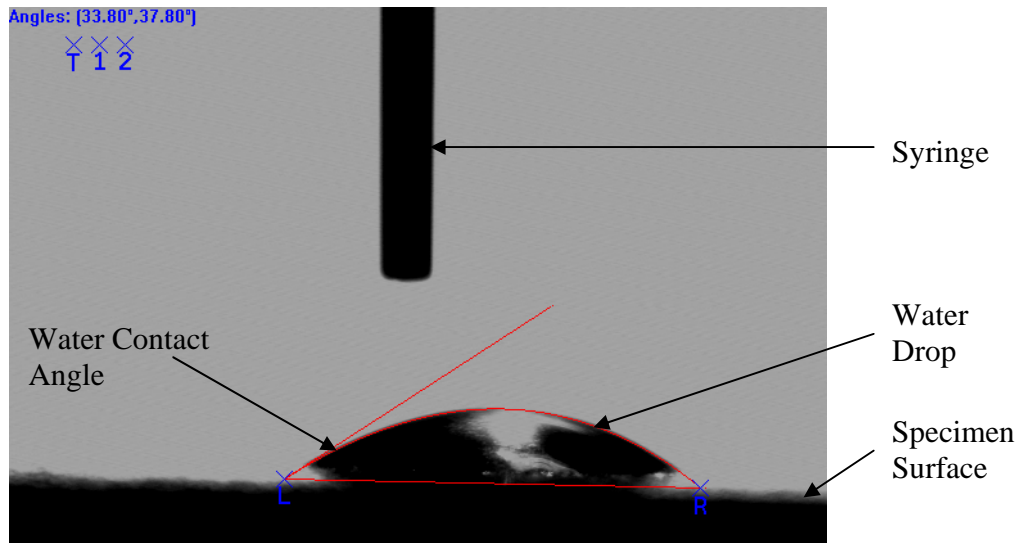


Figure 3.4: Water contact angle measurement of 10-10 specimen.

### 3.11.2 Compact Preparation for Cell Seeding

Prior to the cell cytotoxicity studies, the specimens used were prepared as follows. Firstly, all the surfaces of the sintered, post-HIPed compacts were grinded with sand paper of grit size 400, to remove the oxide layer. Next, the compacts were cut to a height of 3 mm using a diamond cutter (Isomet® Low Speed Saw, Buehler Ltd.). The specimens were placed in an acetone bath in a sonicator for 5 minutes. Next, the specimens were dried, mounted on a specimen holder and grinded and polished, as described in Section 4.5 above. Thereafter, the specimens were once again placed in an acetone bath and sonicated for 5 minutes, followed by sonication in a bath of de-ionized water, and sonicated for another 5 minutes. Finally the specimens were dried and autoclaved.

### 3.11.2 Cell Seeding on Surfaces of Compacts

The autoclaved titanium-graphite composite compacts were placed in 48-well plates, one, in each well, with the polished surface facing up. 20 µl of cell suspension (containing 1000 3T3 cells and 10000 rat osteoblast cells) was added on the surface of each specimen. Care was taken to ensure that the cell suspension did not spill over to the bottom of the plate. Cells were allowed to adhere to the polished surface of the compacts for 3 hours, after which 500 µl of tissue culture medium was gently added to each well. Optical microscopy of the surface of each well revealed that an insignificant number of cells had spilled over and adhered to the surface of the plate. Most of the cells had indeed attached to the surface of the *compacts*. The cell cultures were placed in the incubator, and the tissue culture medium changed every three days.

### 3.12 alamarBlue™ Reduction

The alamarBlue™ assay incorporates a fluorometric/colorimetric growth indicator based on detection of metabolic activity. Specifically, the system incorporates an oxidation-reduction (redox) indicator that both fluoresces and changes colour in response to chemical reduction of growth medium resulting from cell growth. alamarBlue™ is soluble, stable in culture medium and is non-toxic. The continuous monitoring of cells in culture is therefore permitted [60]. Cells grown in the presence of alamarBlue™ and subsequently analyzed by flow cytometry for CD44, CD45RB, CD4, and heat stable antigen are found to produce similar numbers of viable cells and antigen expressing cells as non-

### Chapter 3: Experimental Procedure

---

AlamarBlue™ exposed cells. In addition, AlamarBlue™ does not interfere with the ability of hybridomas to secrete antibody [61]. Because AlamarBlue™ is nontoxic, the cells under study can be returned to culture or used for other purposes including histological studies. Proliferation measurements with AlamarBlue™ may be made either spectrophotometrically by monitoring the absorption of AlamarBlue™ supplemented cell culture media at two wavelengths, or alternatively, proliferation measurements with AlamarBlue™ may be made fluorometrically. Proliferation may therefore be monitored with AlamarBlue™ using either a standard spectrophotometer, a standard spectrofluorometer, a spectrophotometric microtiter well plate reader, or spectrofluorometric. The protocol for monitoring of cell proliferation using AlamarBlue™ is described below:

1. Work was done in a darkened clean room.
2. The cell culture medium was removed from the wells of the 48-well plates.
3. All specimens were rinsed with PBS.
4. A mixture of 10% AlamarBlue™ stock solution and 90% DMEM without serum was prepared. The mixture was placed in an opaque container to prevent degradation of the AlamarBlue™ when exposed to light.
5. 0.5 ml of the AlamarBlue™ –DMEM mixture was added to each well.
6. The control for this experiment consisted of 3T3 and rat osteoblast cells cultured in the well of the 48-well plate.
7. All the samples were placed in the incubator and incubated for 4 hours.



### Chapter 3: Experimental Procedure

---

8. Thereafter, the mixture from each well was transferred in triplicates of 100  $\mu\text{l}$  to each well of a 96-well plate.
9. The spectrophotometric absorbance for a wavelength of 560 nm of the alamarBlue<sup>TM</sup>-DMEM mixture was measured in a microplate reader, against a reference wavelength of 595 nm. Shaking of the samples was done in the microplate reader, for a duration of 3.0 s and a settle time of 1.0 s, prior to absorbance measurement.

The alamarBlue<sup>TM</sup> reduction was determined as follows. Firstly, the absorbance of the medium alone was subtracted from the absorbance of medium plus alamarBlue<sup>TM</sup> at the wavelength of 595 nm. This value is called  $AO_{595}$ . The absorbance of the medium alone was then subtracted from the absorbance of medium plus alamarBlue<sup>TM</sup> at the wavelength of 560 nm. This value is called  $AO_{560}$ .

A correction factor  $R_0$  was calculated from  $AO_{595}$  and  $AO_{560}$ , where

$$R_0 = \frac{AO_{560}}{AO_{595}}$$

The percentage of alamarBlue<sup>TM</sup> reduced was then obtained as follows:

$$\% \text{ Reduction} = A_{560} - (A_{595} \times R_0) \times 100$$

where:

$A_{560}$ : Spectrophotometric absorbance of alamarBlue<sup>TM</sup>-DMEM mixture of experimental specimens at wavelength of 560 nm.

$A_{595}$ : Spectrophotometric absorbance of alamarBlue<sup>TM</sup>-DMEM mixture of experimental specimens at wavelength of 595 nm.

### 3.13 Fluorescence Microscopy

The morphology and distribution of live/dead cells was analyzed by fluorescence microscopy. Two different combinations of dyes were used to stain the cells seeded on the compacts as well as cells cultured with wear debris. Initially, a combination of fluorescein diacetate (FDA) and propidium iodide (PI) obtained from Molecular Probes, USA. FDA is converted to the fluorescent compound fluorescein in living cells and stains the cells green. PI, on the other hand, is membrane impermeant and is excluded from viable cells. It stains dead cells red. The protocol for staining the cells with FDA and PI is described below:

1. Work was done in a darkened clean room.
2. A stock solution of 1mg/ml FDA was prepared by dissolving 1g of FDA in 1l of acetone. The solution was stored in an opaque container at 4°C.
3. The FDA solution was diluted 500-fold in PBS to obtain a concentration of 2µg/ml and stored in an opaque container.
4. The stock PI of concentration 1mg/ml was diluted 10-fold in PBS to obtain a final concentration of 0.1mg/ml and stored in an opaque container.
5. The tissue culture medium was removed and the experimental samples rinsed thrice with PBS.
6. 0.5 ml of the 2µg/ml FDA solution was added to each well. The 48-well plates were then wrapped completely in aluminum foil and incubated for 30 minutes.
7. The FDA solution was then removed and the samples rinsed thrice with PBS.

### Chapter 3: Experimental Procedure

---

8. 0.5 ml of the 0.1mg/ml PI solution was then added to each well. The 48-well plates were then wrapped completely in aluminum foil and kept at room temperature for 2 minutes.
9. The PI solution was removed and the samples rinsed.
10. The samples were viewed under a fluorescence microscope.

More accurate results were obtained with the LIVE/DEAD® Viability/Cytotoxicity Assay Kit (L-3224) from Molecular Probes, USA. The kit consists of 4 mM in anhydrous DMSO of Calcein AM and 2 mM in DMSO/H<sub>2</sub>O 1:4 (v/v) of Ethidium homodimer-1(EthD-1). The Calcein AM produces an intense green fluorescence in live cells while EthD-1 produces a bright red fluorescence in dead cells. Observation of the viability of the cells under a fluorescence microscope was done in two steps. Firstly, the optimal dye concentration was determined, as outlined below:

1. 3T3 and rat osteoblast were cultured in separate wells of separate 48-well plates, at a density of 10000 cells/well.
2. LIVE/DEAD® Viability/ Cytotoxicity Assay Kit was removed from the freezer and allowed to warm to room temperature.
3. After 3 days, dead cells were obtained by adding 0.1% saponin for 10 minutes, at room temperature.
4. Serial dilution of the LIVE/DEAD® Viability/ Cytotoxicity Assay Kit was performed. 6 different concentrations of calcein AM and EthD-1 (0.1, 0.2, 0.4, 0.6, 0.8 and 1.0  $\mu$ M) were obtained.

### Chapter 3: Experimental Procedure

---

5. Each EthD-1 concentration was added to a different well containing dead cells. The cell culture plates were wrapped with aluminum foil and kept at room temperature for 40 minutes.
6. The dead cells were observed under a fluorescence microscope.
7. The EthD-1 concentration which stained the dead nuclei bright red without staining the cytoplasm significantly was selected.
8. Each calcein AM concentration was then a different well containing a fresh batch of dead cells. The cell culture plates were wrapped with aluminum foil and kept at room temperature for 40 minutes.
9. The dead cells were observed under a fluorescence microscope.
10. The calcein AM concentrations which did not give significant fluorescence in the dead cell cytoplasm were noted.
11. The concentrations of calcein AM selected from step number 10 were then added to the *live* cells.
12. The live cells were observed under a fluorescence microscope.
13. The concentration of calcein AM which generated sufficient green fluorescence in the live cells was selected.
14. It was determined that, for both 3T3 cells and rat osteoblast, the optimal concentration of calcein AM and EthD-1 were 2  $\mu\text{M}$  and 4  $\mu\text{M}$ , respectively.

### Chapter 3: Experimental Procedure

---

Once the optimal dye concentrations were determined, viability analysis of cells seeded on the polished surfaces of the compacts, as well as the cells cultured with wear debris, was performed, as follows:

1. The LIVE/DEAD® reagent stock solutions were removed from the freezer and allowed to warm to room temperature.
2. 20  $\mu\text{L}$  of the supplied 2 mM EthD-1 stock solution was added to 10 mL of sterile, tissue culture–grade D-PBS. The mixture was vortexed to ensure thorough mixing. The resultant solution contains approximately 4  $\mu\text{M}$  EthD-1 solution.
3. The reagents were then combined by transferring 5  $\mu\text{L}$  of the supplied 4 mM calcein AM stock solution to the 10 ml EthD-1 solution prepared in step 2. The solution was then vortexed to ensure thorough mixing.
4. The resultant solution contains approximately 2  $\mu\text{M}$  calcein AM and 4  $\mu\text{M}$  EthD-1.
5. Approximately 500  $\mu\text{L}$  of the working solution was added to each well containing either cells cultured with wear debris, cells cultured with raw powder, or cells seeded on the polished surfaces of the compacts.
6. The experimental setup was covered in aluminum foil and left to incubate for 45 minutes at room temperature in the clean room.
7. The labeled cells were observed under a fluorescence microscope through longpass and dual emission filters.

## **Chapter Four**

### **Characterization of Particles and Sintered Compacts**

#### **4.1 Raw Powder Characteristics**

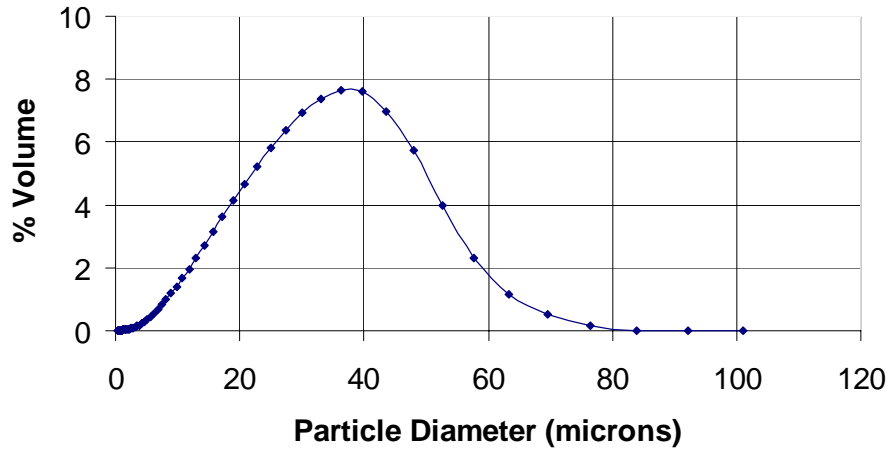
The raw powder used to fabricate the titanium-graphite composite compacts were analyzed for their particle size distribution and morphological characteristics.

##### **4.1.1 Particle Size Distribution of Raw Powder**

Particle size distribution of raw powders used to fabricate compacts: a) Pure Titanium; b) Pure Graphite; c) 10-5 Specimens; and d) 10-10 specimens as measured by laser diffraction, are shown in Figure 4.1 below. It is observed that the all raw powder mixtures exhibit a unimodal particle size distribution. The particle sizes for each powder mixture are also quite statistically dispersed, with a relatively large standard deviation ranging from 9  $\mu\text{m}$  to 15  $\mu\text{m}$  (see Table 4.1). Qualitatively, the data set for each powder mixture does not display significant degree of skewness from their respective mean.

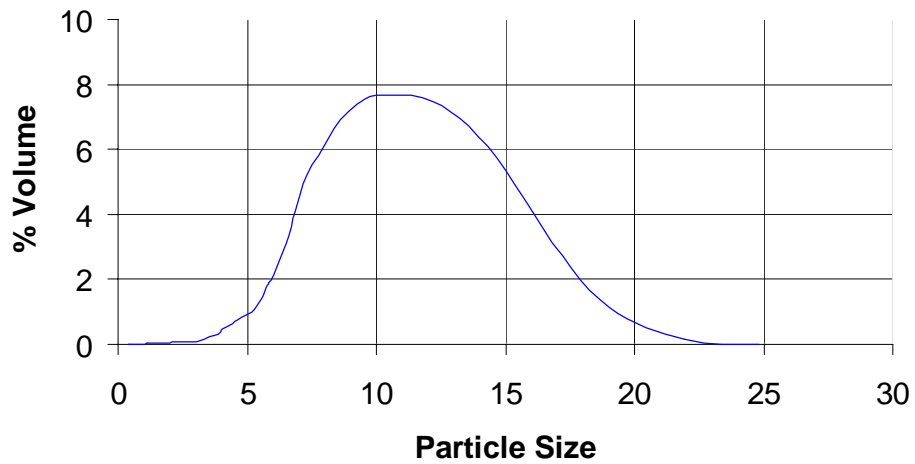
a)

**Particle Size Distribution of 0-0 Specimens**



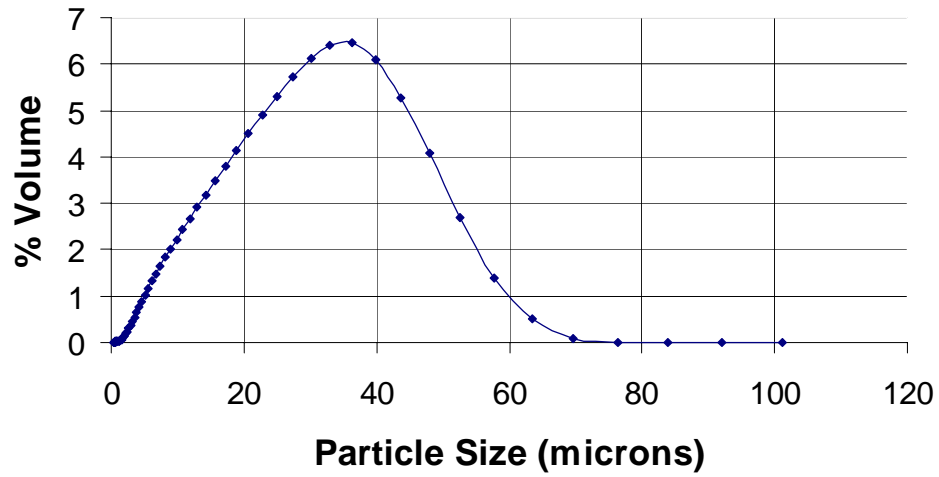
b)

**Particle Size Distribution of Graphite**



c)

**Particle Size Distribution of 10-5 Specimens**



d)

**Particle Size Distribution of 10-10 Specimens**

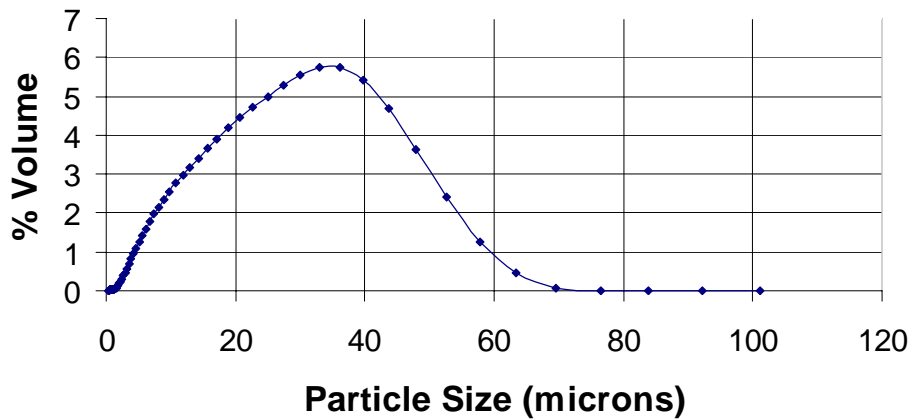


Figure 4.1: Particle size distribution of raw powders used to fabricate compacts: a) pure titanium; b) pure graphite; c) 10-5 specimens; and d) 10-10 specimens



## Chapter 4: Characterization of Particles and Sintered Compacts

---

Statistical information pertaining to the size distribution of the particles is listed in Table 4.1 below:

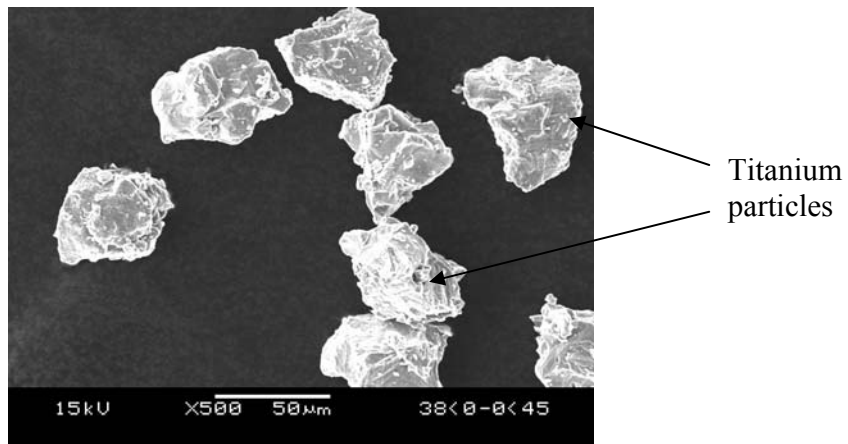
Table 4.1: Raw powder size distribution statistics

Sample	Mean ( $\mu\text{m}$ )	Std Dev ( $\mu\text{m}$ )	Median ( $\mu\text{m}$ )	Mode ( $\mu\text{m}$ )
<b>0-0</b>	31.10	14.82	30.25	37.96
<b>Graphite</b>	10.28	9.02	10.10	9.371
<b>10-5</b>	26.25	14.82	25.01	37.96
<b>10-10</b>	24.68	14.89	22.72	34.58

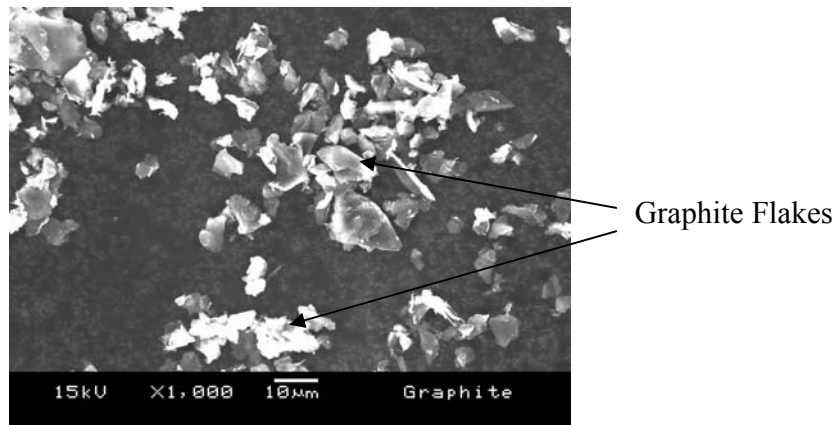
### 4.1.2 Raw Powder Morphology

The morphological characteristics of the raw powder was studied with a Scanning Electron Microscope, SEM (Jeol, Japan). The titanium particles had an irregular, angulated and granular morphology while the graphite particles had smooth flaky morphology. From the images of the 10-5 and 10-10 powder mixtures, the titanium and graphite particles were uniformly distributed. Refer to Figure 4.2 below for the Scanning Electron Microscopy images of representative samples of the raw powder mixtures.

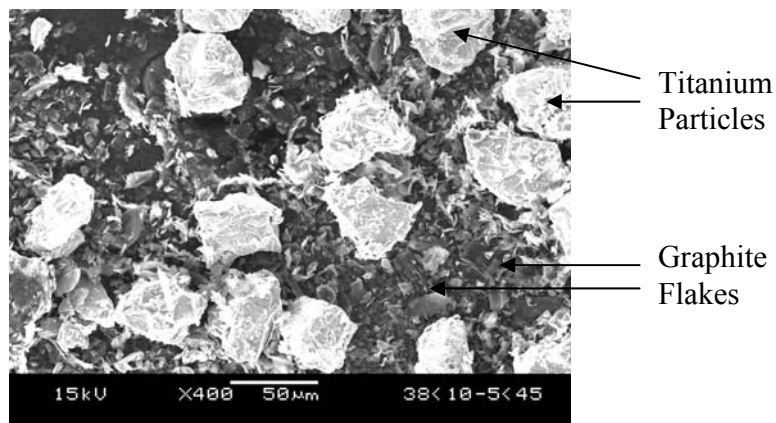
a)



b)



c)



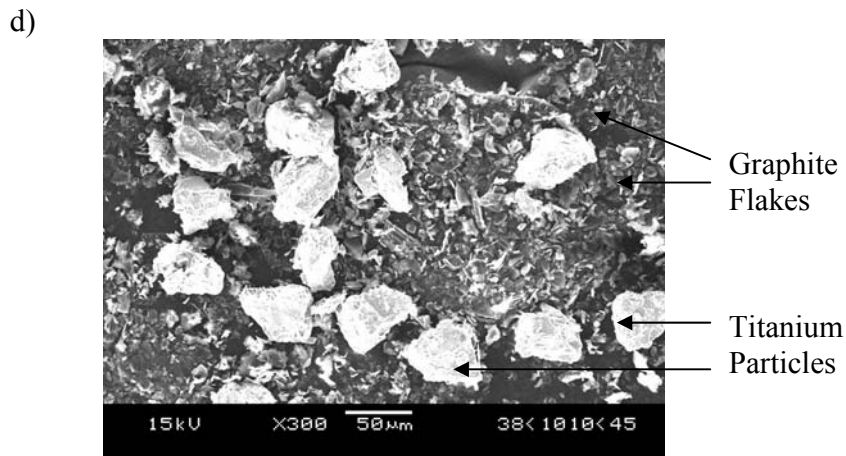


Figure 4.2: Morphology of raw powders used to fabricate compacts: a) pure titanium; b) pure graphite; c) 10-5 specimens; and d) 10-10 specimens

## 4.2 Sintered Titanium and Titanium-Graphite Compact

### Characteristics

After polishing and etching, as described in Section 3.5, the surfaces of the compacts were observed using optical and Scanning Electron Microscopy.

#### 4.2.1 Microstructure

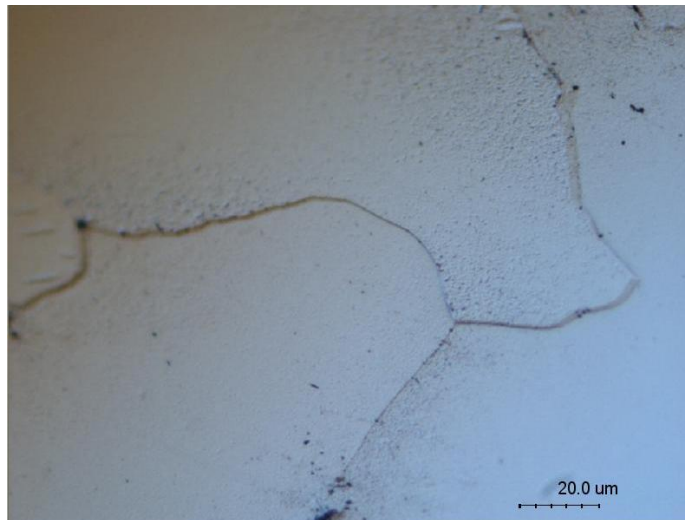
The polished surface of the compacts were observed under an optical microscope (Olympus, Japan), as shown in Figure 5.6 below. From the photomicrographs and SEM images, equiaxed primary alpha titanium was formed after the sintering and Hot Isostatic Pressing processes of the pure titanium powder. The binary powder mixtures, on the other hand, produced a tri-phasic composite of pure equiaxed primary alpha titanium (white regions with grains), titanium carbide (grey

## Chapter 4: Characterization of Particles and Sintered Compacts

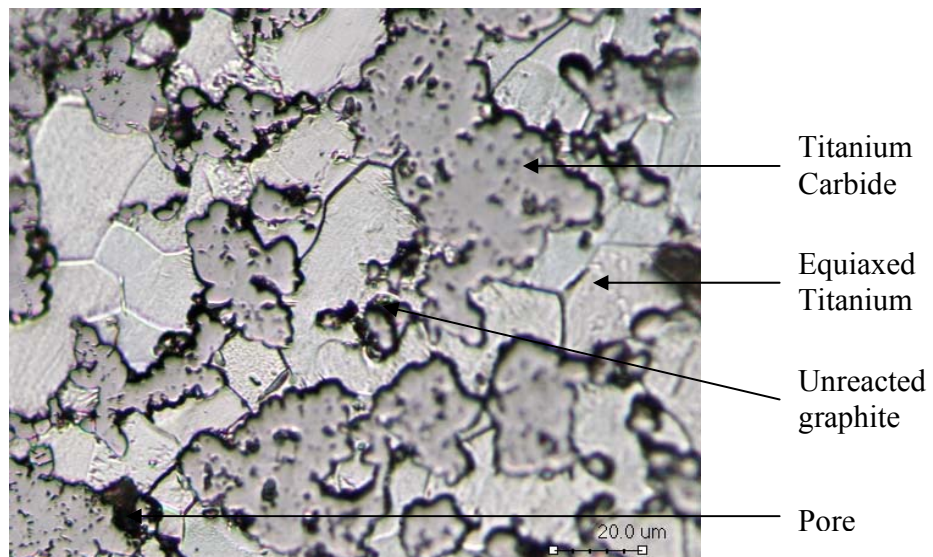
---

regions) and unreacted graphite (black regions). The titanium carbide phase was observed to form along the grain boundaries of the titanium matrix.

a)



b)



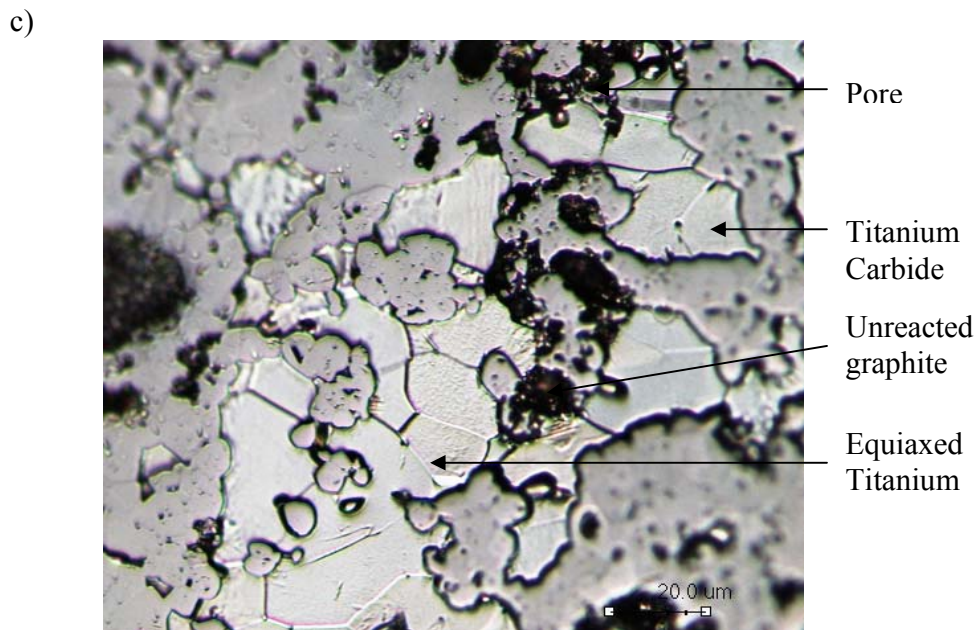


Figure 4.3: Photo-micrographs of sintered, HIPped compacts  
a) pure titanium; b) 10-5 specimens; and c) 10-10 specimens

The formation of the titanium carbide phase along the grain boundaries of the composites could be explained through an understanding of the sintering process. Studies done by Kingery and Berg (1955) [11] and Ichinose and Kuczynski (1962) [12] have reported that there are three stages in sintering. They are the initial, intermediate and final stages. These stages are characterized in terms of the changes in the pore morphology where necking between particles can eventually lead to pore closure and full densification. The changes in the pore morphology are caused by atomic migration, which has been found to be initiated by three mechanisms namely viscous flow, evaporation-condensation and self-diffusion. The first two mechanisms are bulk transport mechanisms responsible for the characteristic shrinkage of sintered compacts, while the third one is a

## Chapter 4: Characterization of Particles and Sintered Compacts

---

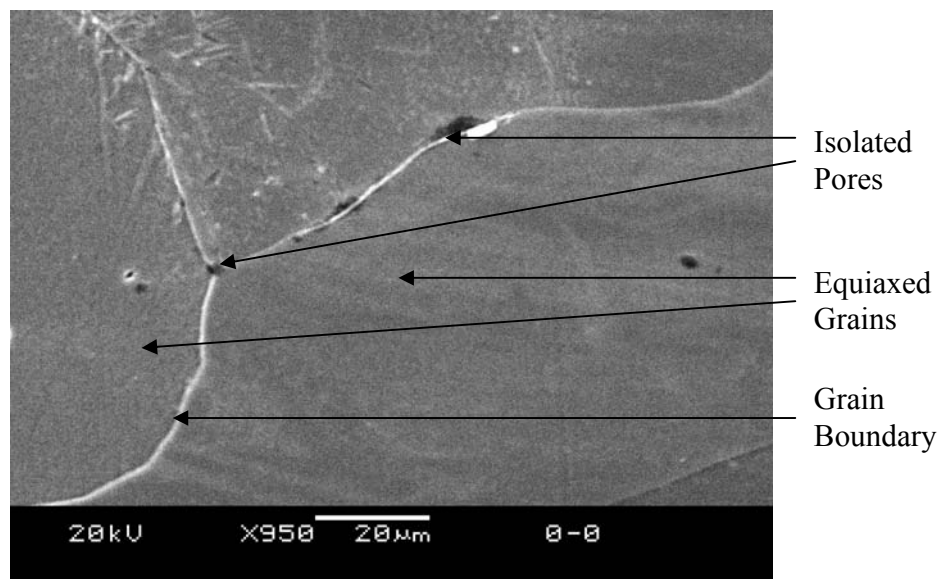
surface diffusion process. Hence the formation of TiC, due to the reaction between the titanium and graphite powder particles, which follows the mechanism described above, has to take place at the interface between the 2 particles, resulting in the formation of TiC along the grain boundaries.

The surfaces of the compacts were then observed in a scanning electron microscope (JEOL, Japan), as shown in Figure 4.4 below. The SEM images reinforced the observations made from optical microscopy. In addition, it was also observed that the size of the pores increased with increasing graphite content. The pores of the titanium graphite composites were observed to be isolated and formed at the boundary between titanium carbide and the titanium matrix. Additionally, the pores occur in regions where there is unreacted graphite. The fact that there exists unreacted graphite (which improves lubrication and hence increases wear resistance) indicates that the 2 hour sintering period did not allow complete necking between titanium and graphite particles to take place. Hence, there was insufficient pore closure and incomplete densification at the inter-facial regions.

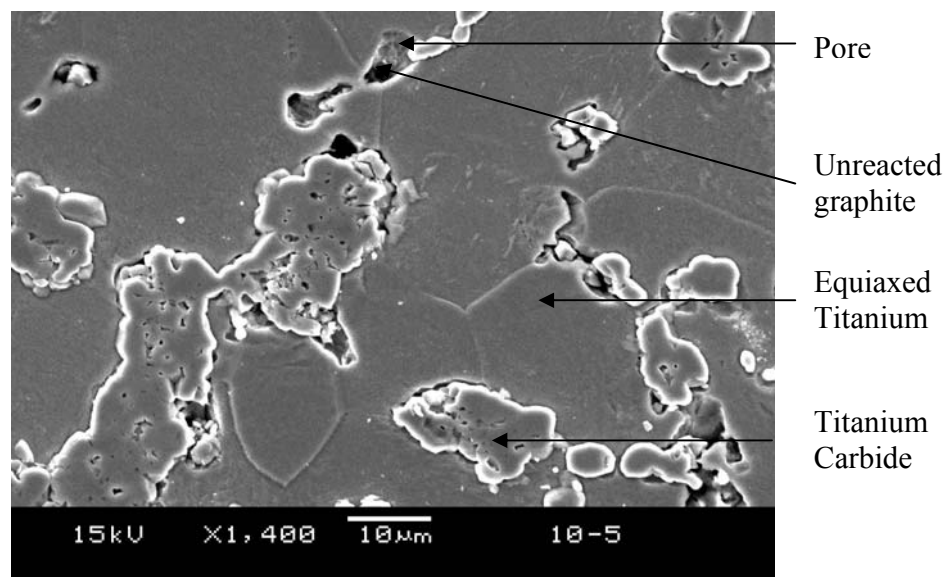
## Chapter 4: Characterization of Particles and Sintered Compacts

---

a)



b)



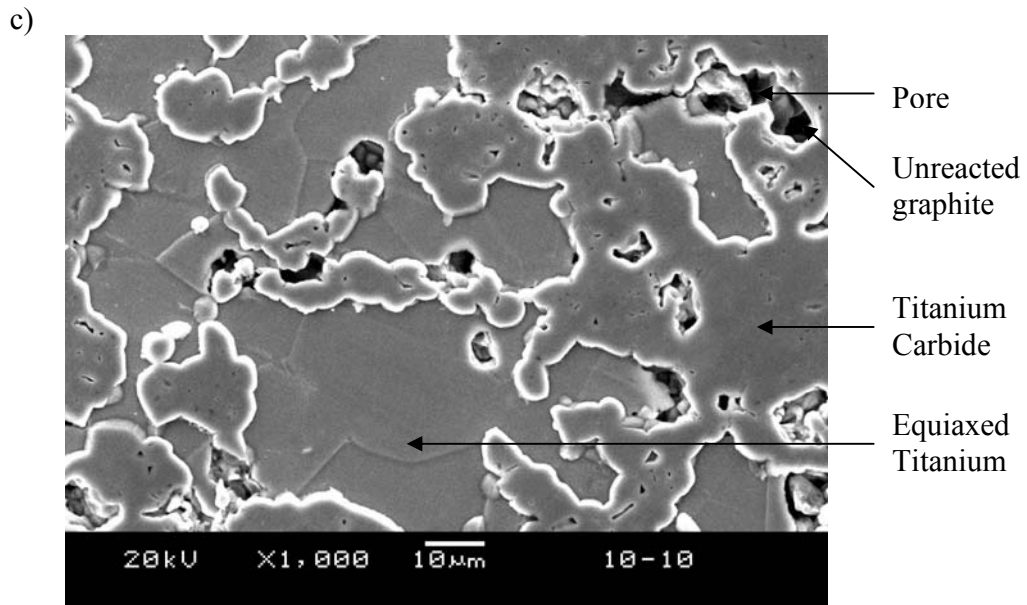


Figure 4.4: Scanning electron microscopy images of sintered, HIPped compacts: a) pure titanium; b) 10-5 specimens; and c) 10-10 specimens

The SEM images allowed for the measurement of the pore sizes of the sintered compacts. The average pores sizes of the compacts were measured and shown in Table 4.2.

Table 4.2: Average pore size of sintered and HIPped specimens

Specimen	0-0	10-5	10-10
Average Pore Size	4 $\mu\text{m}$	8 $\mu\text{m}$	11 $\mu\text{m}$



The addition of graphite resulted in decreasing grain size of the titanium matrix. The formation of titanium carbide along the grain boundaries interfered with the growth of the titanium matrix grains during the sintering process. The higher the graphite content, the smaller the size of the titanium grains. In the pure titanium specimen, the average grain size was 140  $\mu\text{m}$ , while the average grain sizes of the 10-5 and 10-10 composites were 32  $\mu\text{m}$  and 21  $\mu\text{m}$ , respectively.

### 4.2.2 Porosity of Compacts

The porosity of the compacts, before and after sintering and HIP, were determined as follows:

The rule of mixtures is used to compute the density of the titanium-graphite compacts.

Theoretical volume of compacts,  $V_c$ ,

$$V_c = \left[ \frac{Q_g W_{total}}{\rho_g} \right]_{\text{graphite}} + \left[ \frac{Q_{Ti} W_{total}}{\rho_{Ti}} \right]_{\text{Titanium}}$$

where:  $Q_g$  = weight percent of graphite powder,

$Q_{Ti}$  = weight percent of titanium powder,

$W_{total}$  = total weight of powders,

$\rho_g$  = density of graphite (2.21  $\text{g/cm}^3$ ),

$\rho_{Ti}$  = density of titanium (4.54  $\text{g/cm}^3$ )

Theoretical density of compacts,  $\rho_{th}$ ,

## Chapter 4: Characterization of Particles and Sintered Compacts

---

$$\rho_{th} = \frac{W_{total}}{V_c}$$

where:  $V_c$  = theoretical volume of compacts

Actual density of compacts,  $\rho_{act}$ ,

$$\rho_{act} = \frac{W_{act}}{V_{act}}$$

where:  $W_{act}$  = actual weight of compacts (measured on weighing machine),

$V_{act}$  = actual volume of compacts

Relative density,  $\rho_{rel}$ ,

$$\rho_{rel} = \frac{\rho_{act}}{\rho_{th}}$$

Porosity,  $P = (1 - \rho_{rel}) \times 100\%$

The calculated porosity of the compacts, before and after sintering and HIP, are shown in Table 4.3.

Table 4.3: Porosity of compact

Specimen	Fractional Porosity (%)	
	Green Compacts	After Sintering and HIP
<b>0-0</b>	10.10	0.41
<b>10-5</b>	12.22	1.24
<b>10-10</b>	13.53	1.81

## **Chapter 4: Characterization of Particles and Sintered Compacts**

---

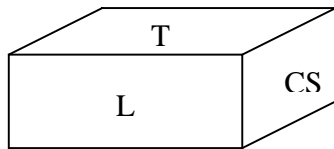
It is evident that the process of sintering and Hot Isostatic Pressing significantly reduced the porosity of the compacts, although pores were not completely removed. It was also observed that the porosity of the sintered, HIPed compacts increased with increasing graphite content. The higher graphite content resulted in increased formation of the titanium carbide phase along the titanium grain boundaries, and hence increased pore density due to incomplete densification at the interface of the different phases.

## Chapter Five

### Hardness, Tensile Properties and Fatigue Strength of Compacts

#### 5.1 Hardness of Compacts

The compacts were cut in three different planes as shown in Figure 5.1 below, and the respective Vickers Hardness measured. The reason the hardness of the compacts was measured in the three different orientations was to determine if the various phases and porosity was evenly distributed throughout the composite. The Vickers Hardness readings of the different specimens are shown in Figure 5.2.



L: Longitudinal

T: Transverse

CS: Cross-section

Figure 5.1: Different orientations of compact surfaces

The Micro-Vickers Hardness of the titanium and titanium carbide phases were measured and plotted in a bar chart (see Figure 5.3). The Vickers Hardness measurements were made with a test load of 20 kgf, for a load duration of 30s.

## Chapter 5: Hardness, Tensile Properties and Fatigue Strength of Compacts

---

Vickers Hardness measurements were made with a test load of 100 gf, for a load duration of 15s.

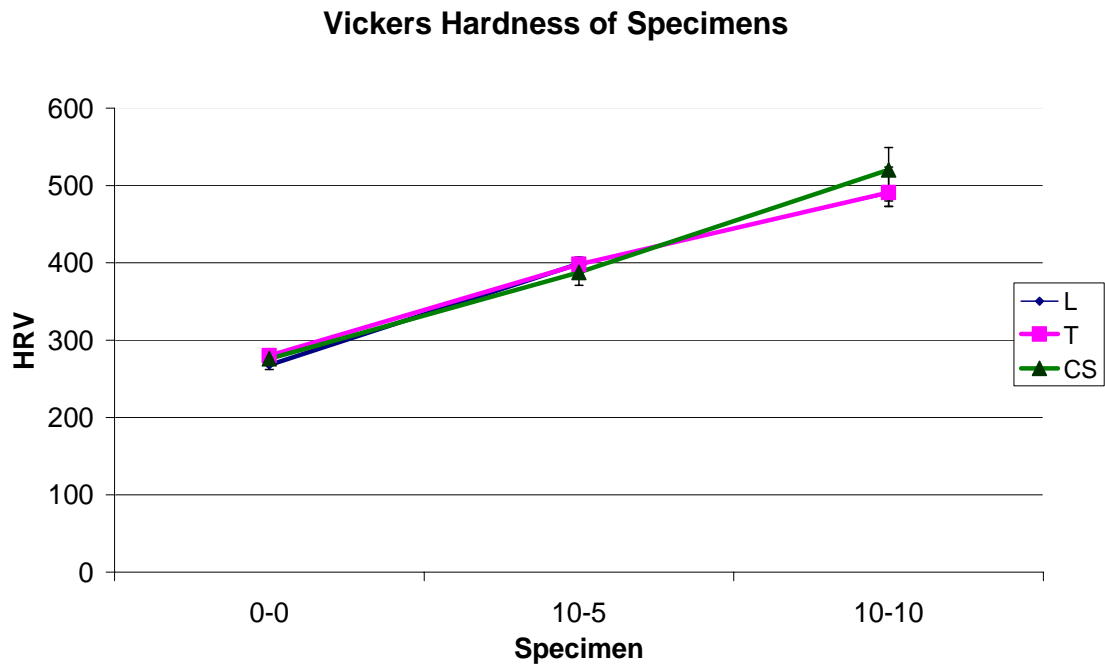


Figure 5.2: Vickers hardness of compacts

The hardness of the compacts did not vary significantly with orientation of compact surfaces, indicating that the hot isostatic pressing had further consolidated the compacts uniformly.

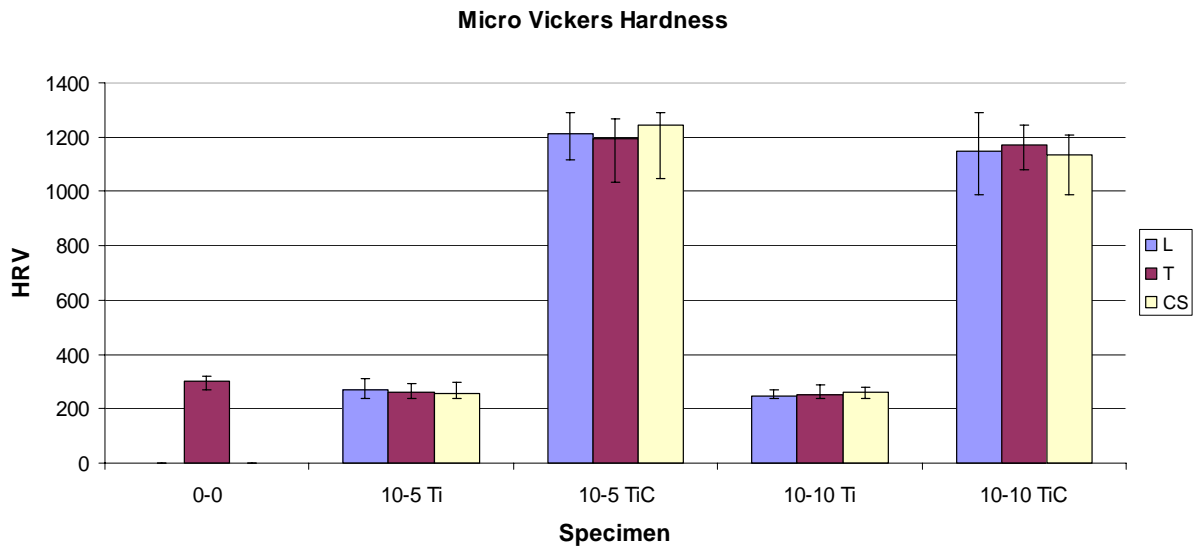


Figure 5.3: Micro-Vickers hardness of titanium and titanium carbide regions of compacts

The sintered and HIPped titanium-graphite composites, namely the 10-5 and 10-10 specimens, exhibited significantly higher hardness than the pure titanium specimens (0-0). In addition, the Vickers hardness of the compacts appeared to increase proportionally with an increase in the graphite content. Given that all the specimens had the same compacting, sintering, HIP conditions and raw materials, it is reasonable to postulate that the 10-10 specimens significantly more TiC content compared to the 10-5 specimens.

The hardness of the sintered and HIPed titanium, as well as the titanium regions of the compacts, were comparable with commercially available unalloyed titanium samples [12]. There was no significant difference in hardness between the titanium regions of the composites, and the pure titanium compacts. The

Micro-Vickers Hardness readings of the TiC regions of the composites were significantly lower than that of pure titanium carbide (3200 HRV).

### **5.2 Tensile Properties of Compacts**

The tensile strength determines the maximum uniaxial tensile force, which could be safely applied to the composites before failure occurs. The modulus of elasticity represents the amount of stress needed to elastically deform the material. It is a measure of the stiffness of the material and is closely related to the binding energy between atoms.

#### **5.2.1 Tensile Strength and Stiffness of compacts**

Following the tensile tests, the stress-strain curves for the various specimens was plotted, as shown in Figure 5.4. The sintered, HIPed pure titanium samples exhibited higher stiffness and tensile strength than commercially available unalloyed titanium. The standard deviation for both these properties was statistically low.

The titanium graphite composites, meanwhile, exhibited higher stiffness than the pure titanium samples. There was no significant difference in stiffness observed between the 10-5 and 10-10 specimens. The tensile strength of the composites, on the other hand, was lower than that of the pure titanium samples.

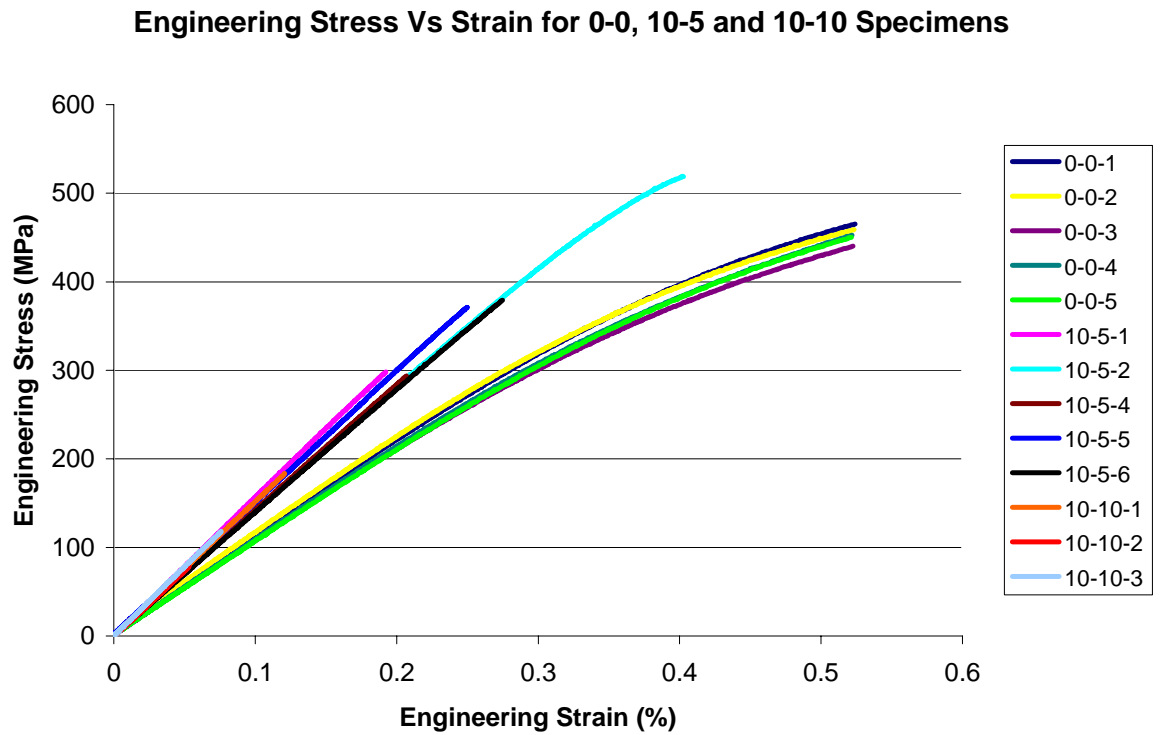


Figure 5.4: Stress-Strain Curves of sintered and HIPped Compacts.

The mean tensile properties of the compacts is summarized in Table 5.1 below.

Table 5.1: Mean Tensile Properties of Compacts.

Specimen	Young's Modulus	Std Dev	Tensile Strength	Std Dev
<b>0-0</b>	113.4 GPa	2.8 GPa	638.6 MPa	18.8 MPa
<b>10-5</b>	152.4 GPa	6.5 GPa	391.4 MPa	80.0 MPa
<b>10-10</b>	157.0 GPa	6.2 GPa	127.3 MPa	53.0 MPa



### **5.2.2 Tensile Fracture Surfaces of Compacts**

Following tensile fracture, the specimens were successively sonicated in acetone and water baths, each for a period of 5 minutes. This procedure was undertaken to remove any surface dirt and contaminants. Care was taken not to damage the fracture surfaces. Thereafter, the fracture surfaces were observed in a scanning electron microscope (SEM). The images obtained are shown below, in Figures 5.5 to 5.10.

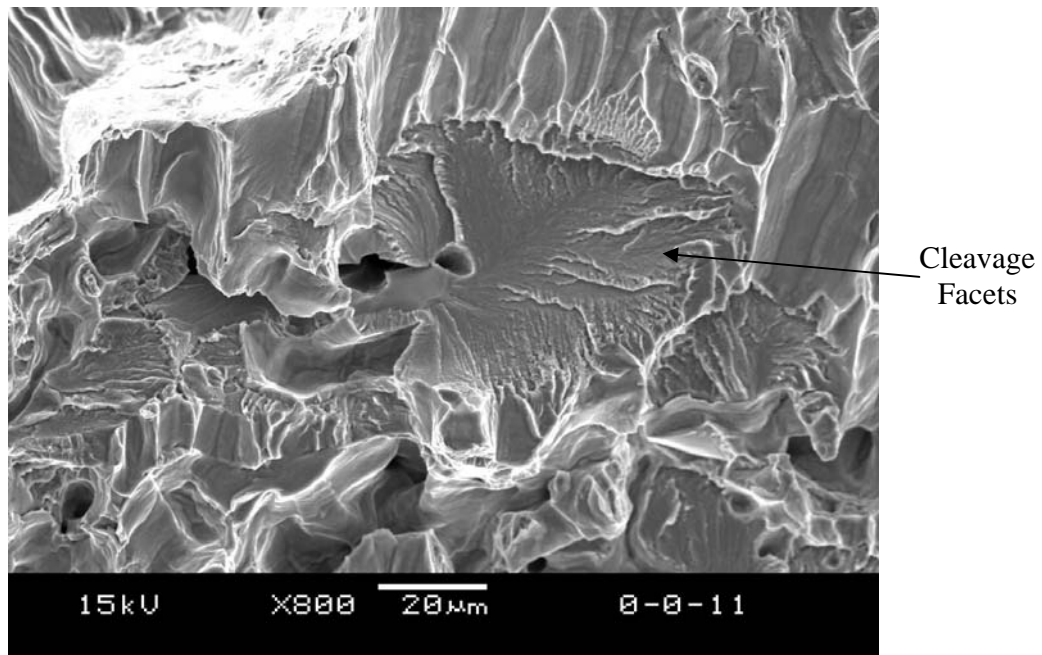


Figure 5.5: 0-0 tensile fracture surface, showing presence of dimples with local cleavage facets.

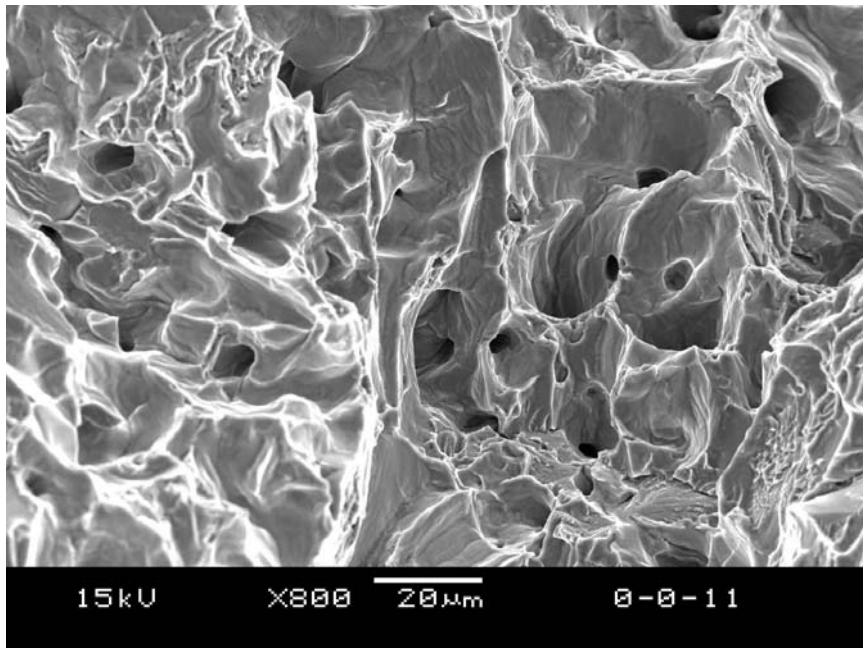


Figure 5.6: 0-0 tensile fracture surface, showing micro-void coalescence

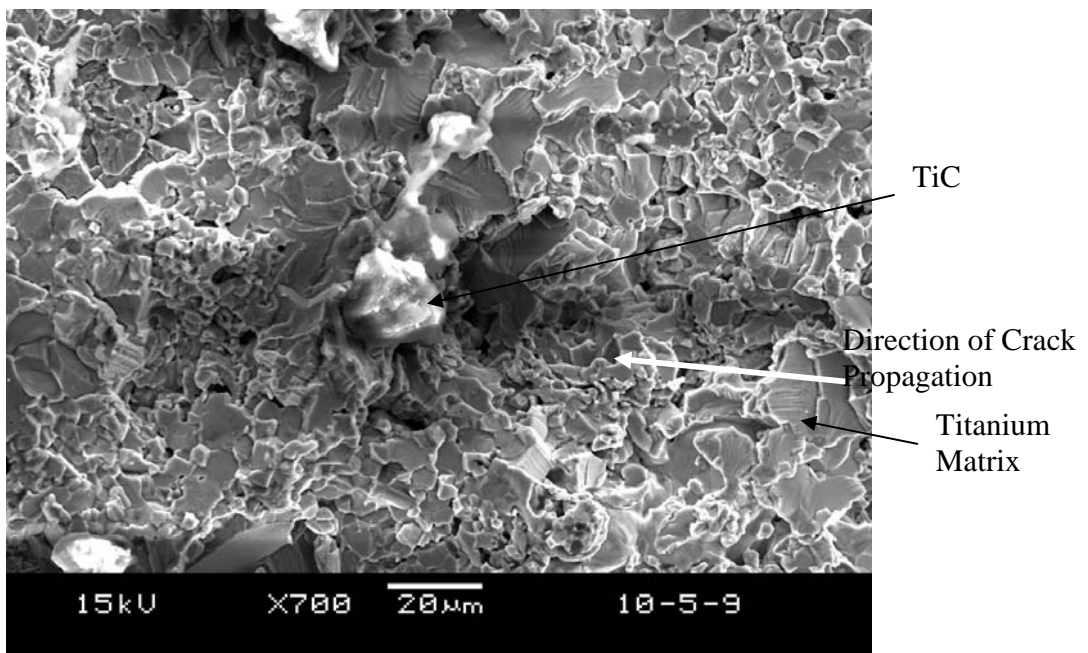


Figure 5.7: 10-5 tensile fracture surface, showing the interface the titanium carbide regions and the titanium matrix.

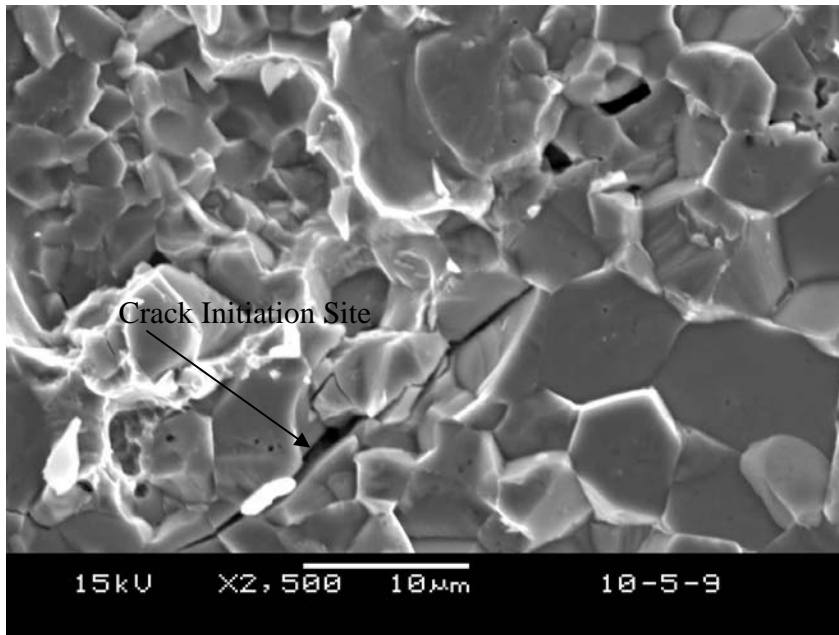


Figure 5.8: 10-5 tensile fracture surface. Shown is a transgranular crack in the titanium matrix.

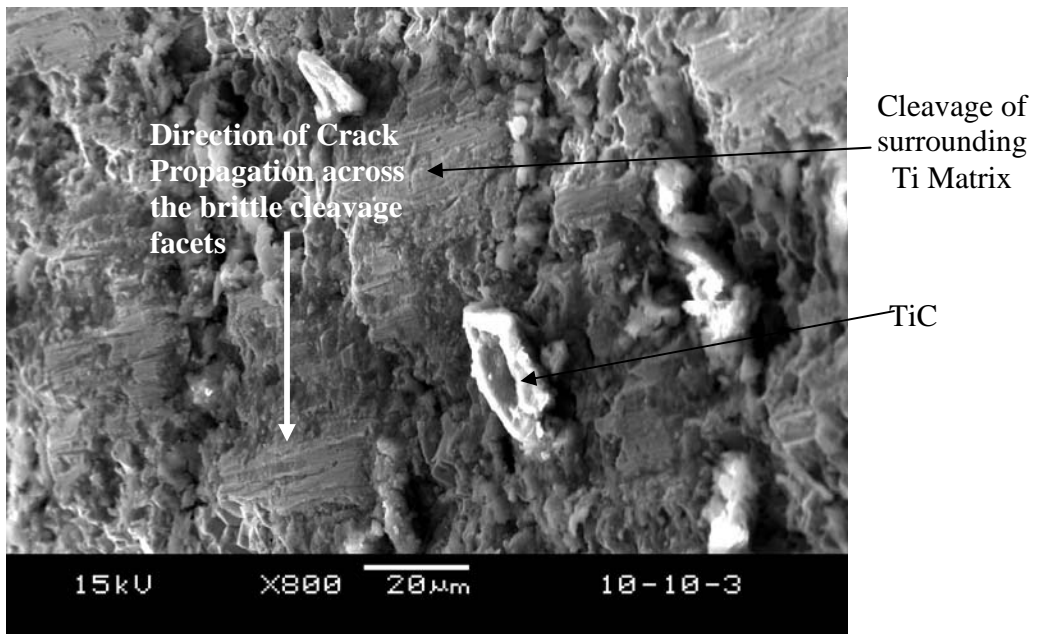


Figure 5.9: 10-10 tensile fracture surface, showing the TiC and Ti Matrix Interface

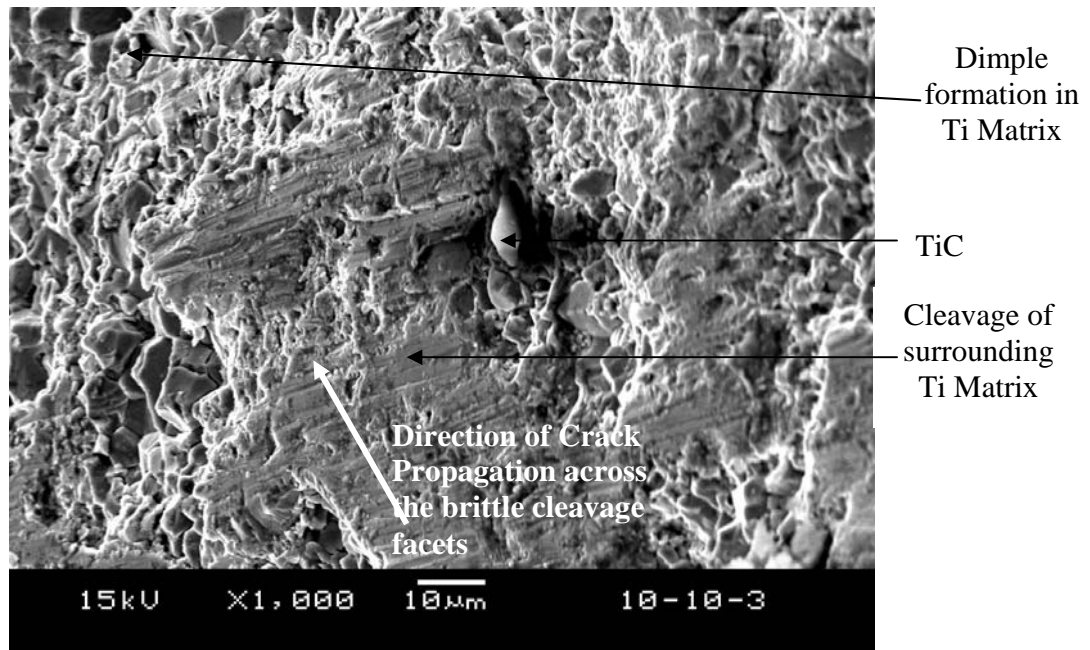


Figure 5.10: 10-10 tensile fracture surface, showing the formation of dimples, as well as local cleavage facets near the TiC region, in the Ti Matrix.

Observations of the fracture surface revealed that the surface is predominantly made up of dimples caused by micro-void coalescence resulting from ligament fracture. The dimples can be identified by the appearance of depressions on the fracture surface of approximately 2 to 10  $\mu\text{m}$  in diameter. Also observed were river patterns, indicating crack propagation along many parallel cleavage planes. The 0-0 specimens hence exhibit a mixed mode fracture mechanism involving predominantly ductile, as well as, brittle fracture. The relative brittleness of the 0-0 samples, as compared to commercially available pure titanium specimens, could be due to the higher hardness of the samples.

The titanium graphite composites, meanwhile, exhibited a more brittle mode of fracture. Cleavage facets and transgranular cracks were observed on the fracture surfaces of the composites. The cleavage facets were caused by the relatively fast propagation of cracks across the specimen, and are characterized by a relatively flat fracture region

The direction of crack propagation could be identified from observations of the fracture surface. Since the crack propagates in the path of least resistance, the cracks were most likely to have grown across the brittle cleavage facets. The surrounding ductile material was weakened as a result, and fractured through microvoid coalescence, characterized by the dimples on the fracture surface.

### 5.2.3 Discussion on Tensile Properties of Compacts

As shown in Figure 5.11, the tensile strength of the compacts is inversely proportional to the graphite content (up to 10% by weight). This correlates well with Figure 5.2, where it was observed that the Vickers hardness of the compacts were, on the other hand, *proportional* to the graphite content. Both these plots suggests that for the compacting and sintering conditions employed in this study, increasing the graphite content, up to a maximum of 10% by weight, would result in a proportionate increase in titanium carbide formation, which results in increased hardness, and hence brittleness, of the compacts.

There could be several reasons, which would account for the reduction of tensile strength with increase TiC content. Firstly, from the fractographs obtained, it was observed that there was considerable cleavage of the titanium matrix in regions surrounding the TiC formation. The TiC-titanium interface appear to provide little resistance to the propagation of cracks. Hence the higher the TiC content, the higher the number of cleavage facets on the fracture surface. Finally, as observed in the images of the polished surfaces of the compacts, the higher the graphite, and hence TiC content, the higher the porosity of the specimen. The presence of pores provides a path for the cracks to propagate, and the reduced tensile strength. The pores also act as stress concentrators, thus weakening the material.

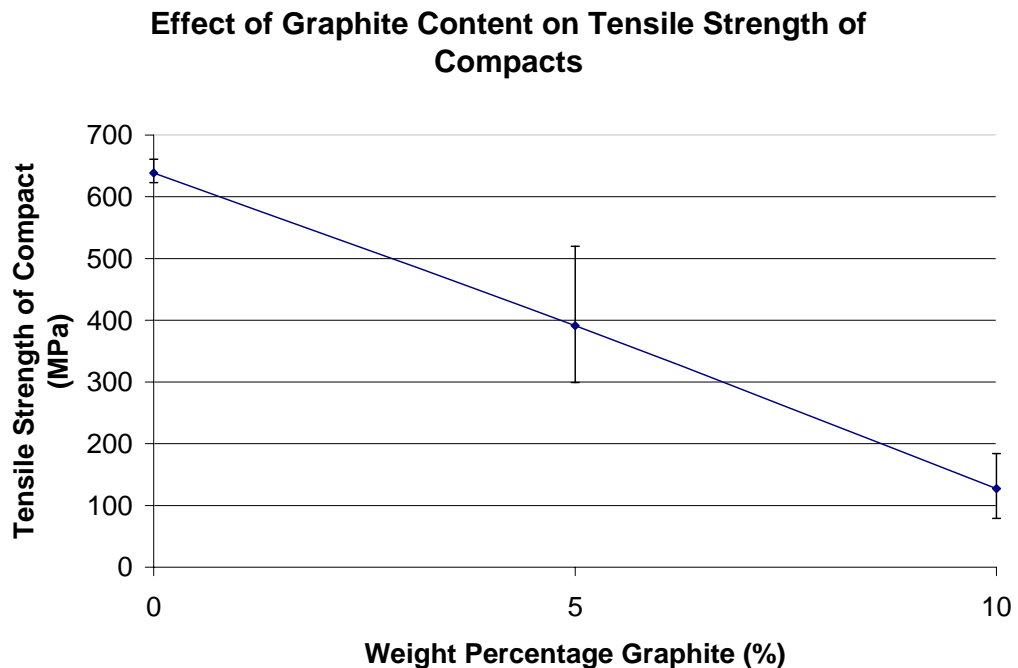


Figure 5.11: Effect of graphite content on tensile strength of compacts

As is clearly illustrated in Figure 5.12, the addition of 5% by weight of graphite greatly increases the stiffness of the compacts. Increasing the graphite content to 10% yielded no significant increase in stiffness. Thus increasing the graphite content beyond 5% yields diminishing returns in stiffness, and is indeed detrimental to the tensile strength of the composite.

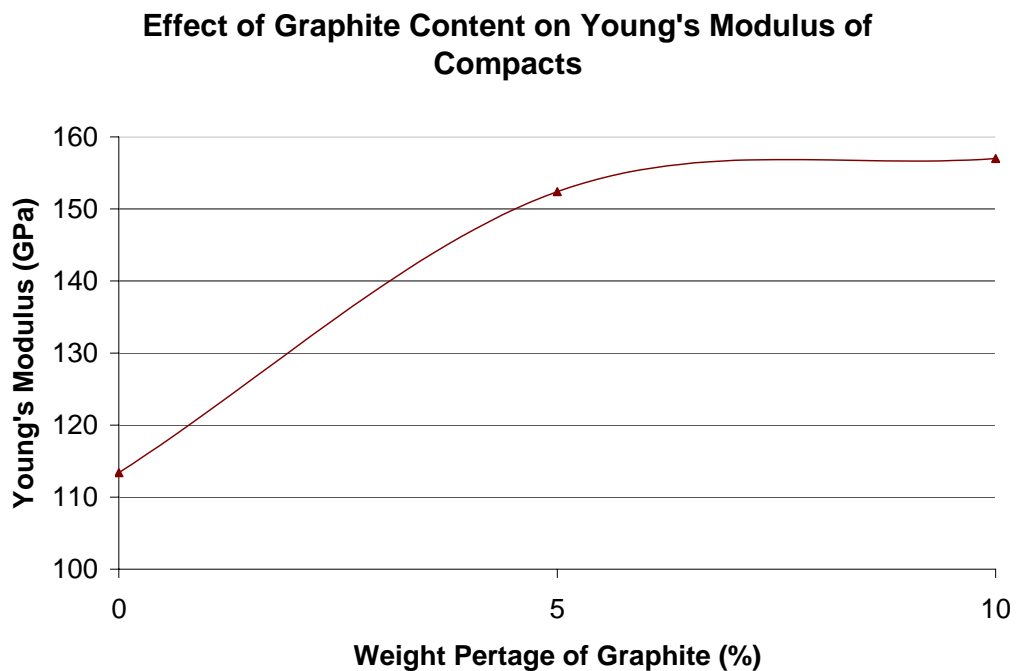


Figure 5.12: Effect of graphite content on Young's Modulus of compacts

### 5.3 Fatigue Performance

When a material is subjected to cyclic loading, even at levels below its yield strength, it may eventually fail, due to the propagation of cracks. This mode of failure is known as fatigue. Fatigue failures typically occur in three stages. Firstly,

a tiny crack initiates at the surface, often at a stress raiser such as a notch or scratch. Next, the crack propagates gradually as the cyclic loading continues. Finally sudden fracture occurs when the remaining cross-section of the material is unable to support the applied load.

### **5.3.1 Fatigue Strength of Compacts**

Fatigue tests were conducted on 0-0 and 10-5 specimens. The 10-10 specimens, which were extremely brittle, were not tested on. Persistent difficulty was faced in the machining and polishing of the 10-10 specimens, which were often damaged in the process. During the period of mechanical testing in Japan, only three 10-10 specimens were successfully machined and polished, to standards required of the mechanical tests. It was thus decided that all three specimens should be used for the tensile tests. Moreover, due to the disappointing tensile strength of those composites, the fatigue strength was also expected to be exceptionally low.

The S-N curves of the 0-0 and 10-5 specimens were plotted in Figures 5.13 and 5.14 respectively. The sintered, HIPed pure titanium samples displayed lower fatigue limit (100 MPa) than commercially available pure titanium samples (between 130 MPa and 300 MPa [13, 14]). The 10-5 composites exhibited an even lower Endurance Limit of 85 MPa. The 10-10 specimens were too brittle for High Cycle Fatigue testing to be performed. An examination of the fatigue fracture surfaces is required in order to gain an insight into the fatigue fracture mechanics of the composites.



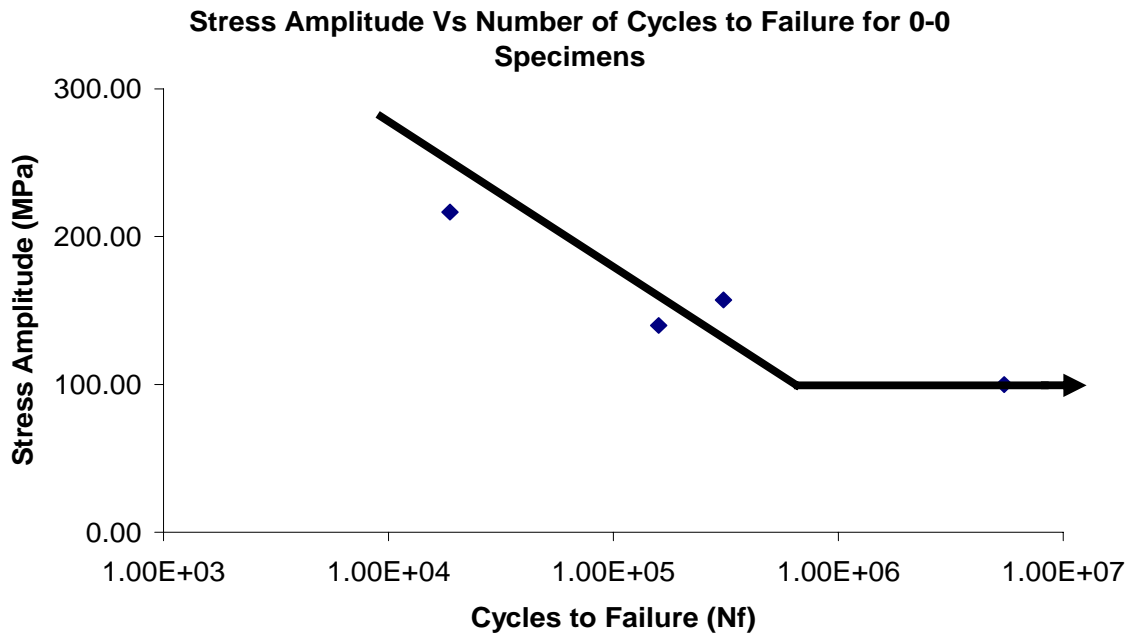


Figure 5.13: S-N curve of 0-0 specimens obtained during fatigue testing

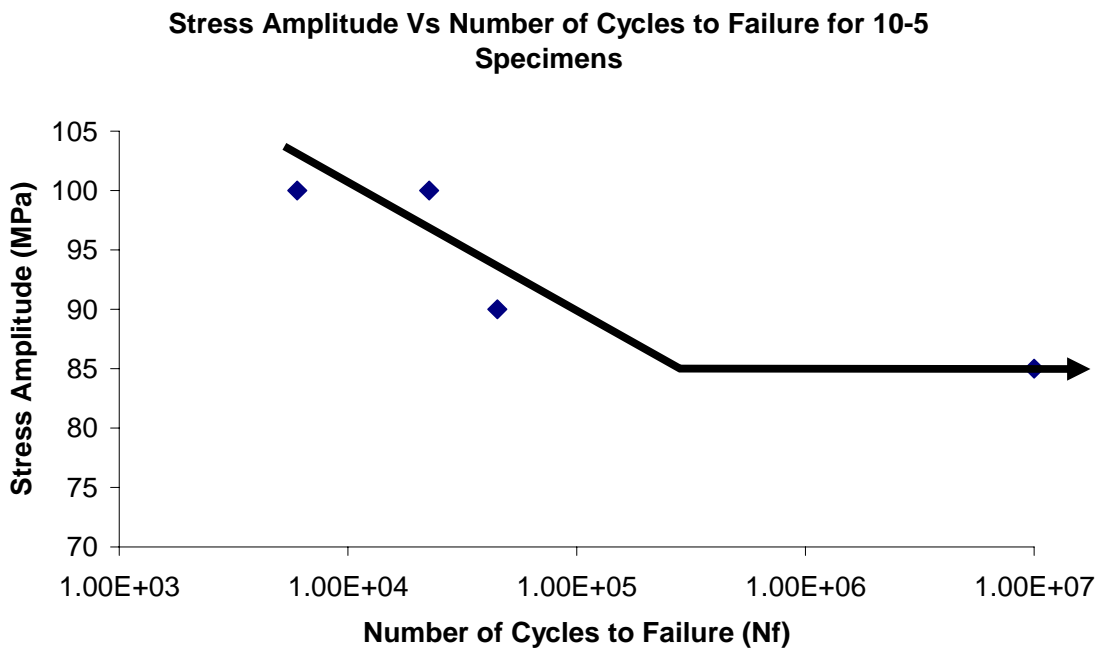


Figure 5.14: S-N curve of 10-5 specimens obtained during fatigue testing

### **5.3.2 Fatigue Fracture Surfaces of Compacts**

Following fatigue failure, the specimens were successively sonicated in acetone and water baths, each for a period of 5 minutes. This procedure was undertaken to remove any surface dirt and contaminants. Care was taken not to damage the fracture surfaces. Thereafter, the fracture surfaces were observed in a scanning electron microscope (SEM). The images obtained are shown below, in figures 5.15 to 5.17.

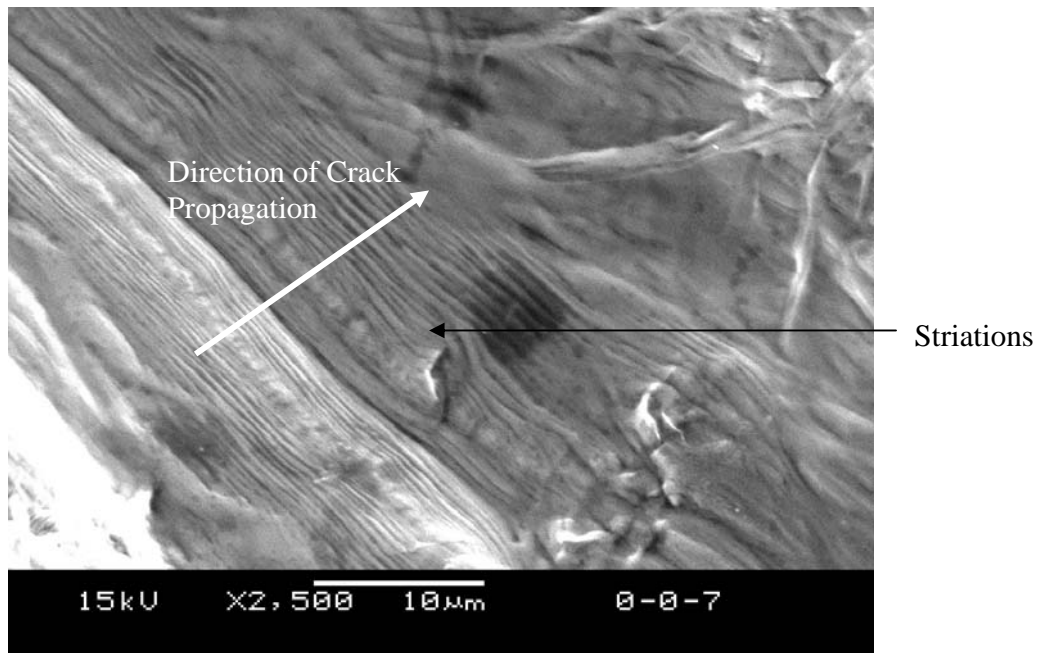


Figure 5.15: 0-0 fatigue fracture surface, showing presence of fatigue striations.

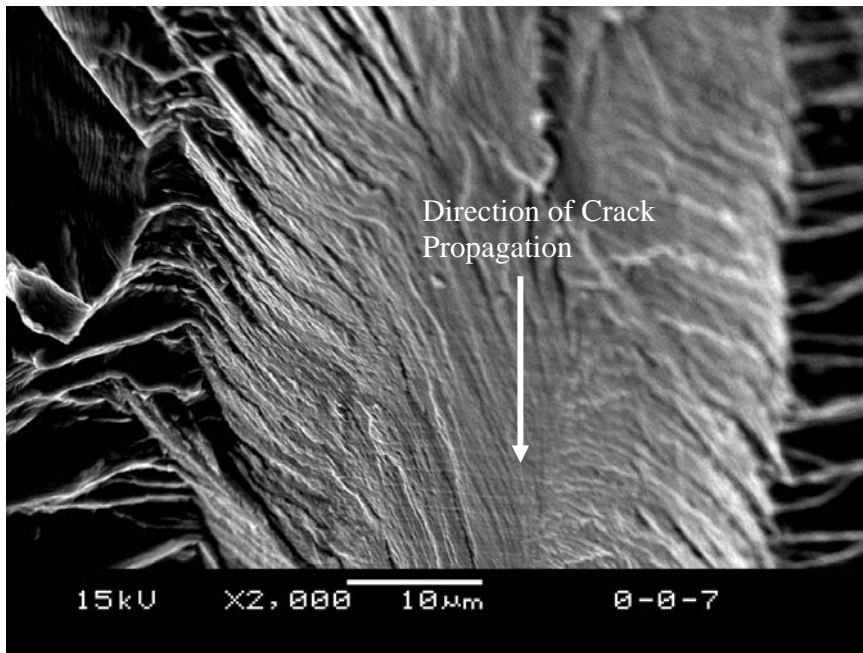


Figure 5.16: 0-0 fatigue fracture surface, showing chevron patterns.

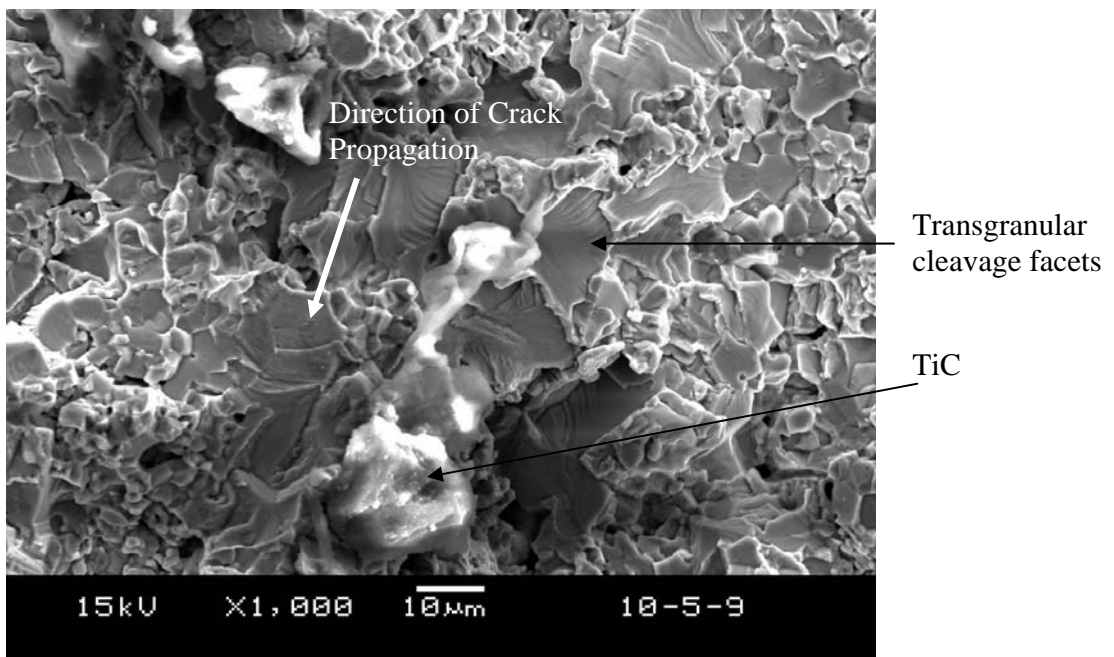


Figure 5.17: 10-5 fatigue fracture surface, showing transgranular cleavage facets of titanium matrix surrounding TiC.

The fatigue fracture surfaces of the pure titanium compacts comprised of fatigue striations as well as cleavage facets, probably caused by brittle fracture. The fracture surfaces of the 10-5 composites, meanwhile, were predominantly composed of transgranular cleavage facets. No fatigue striations were identified in fatigue fracture surfaces of the 10-5 composites, indicating that brittle, rapid fracture had taken place.

### **5.3.3 Discussion on Fatigue Performance of Compacts**

The sintered, HIPed pure titanium samples displayed lower fatigue limit (100 MPa) than commercially available pure titanium samples (between 130 MPa and 300 MPa [13, 14]). The Endurance Ratio, which is the ratio of fatigue life to tensile strength, is very low, at 0.16. This indicates that there is low resistance to crack propagation in the sintered, HIP specimens. An examination of the fatigue fracture surfaces revealed that the surfaces were made up cleavage facets, chevron patterns and fatigue striations. The striations show the position of the crack tip after each cycle. The chevron pattern is produced by separate crack fronts propagating at different levels in the material. A radiating pattern of surface markings fan away from the origin of the crack. The chevron patterns and cleavage facets indicate rapid crack propagation and the brittle nature of the material failure under cyclic loading.

The 10-5 composites exhibited even lower fatigue limit of 85 MPa than the 0-0 specimens. The Endurance Ratio, which is the ratio of fatigue life to tensile

strength, is very low, at 0.22. In similar fashion to the 0-0 specimens, the composites offered little resistance to crack propagation under a cyclic load. An examination of the fatigue fracture surface revealed the predominance of cleavage fracture surfaces. Fatigue striations were not distinct on the fracture surfaces, which indicates that the cracks propagated rapidly during the period of cyclic loading. This suggests that the bonding strength at the interface between the titanium carbide and titanium matrix was relatively low. The situation was worsened by the fact that the titanium carbide phase agglomerated, instead of small, discreet reinforcement regions. The agglomeration of the titanium carbide phase, in addition to the weak bonding strength with the titanium matrix and relatively small grain size of the titanium matrix of the composites, provide little resistance to crack propagation during cyclic loading.

The sintered, HIPped specimens hence display poor fatigue properties, and may not be suitable for applications involving uniaxial, tensile cyclic loading.

Following fatigue testing, the fractured specimens were thoroughly cleaned and sent for oxygen content analysis. It was found that the oxygen content of each test specimen was approximately 0.5%, which was significantly higher than was allowed for commercial purity titanium (of about 0.35%) [13]. One possible cause of the high oxygen content was the high temperature employed in the HIP process, which could have accelerated the diffusion of oxygen into the titanium specimens. The higher oxygen content could have embrittled the compacts, leading to poor tensile and fatigue performance.

## Chapter Six

### Characterization of Wear Debris

#### 6.1 Morphology of Wear Debris

The wear debris was generated by firstly plane milling the surfaces of the sintered compacts to produce large debris. Much finer wear debris was obtained by grinding the debris obtained with an agate pestle and mortar apparatus. This process was described in detail in section 3.10.1. The wear debris was examined by scanning electron microscopy, and the morphology analyzed. Shown below in Figures 6.1 to 6.3 are the SEM images of the debris.

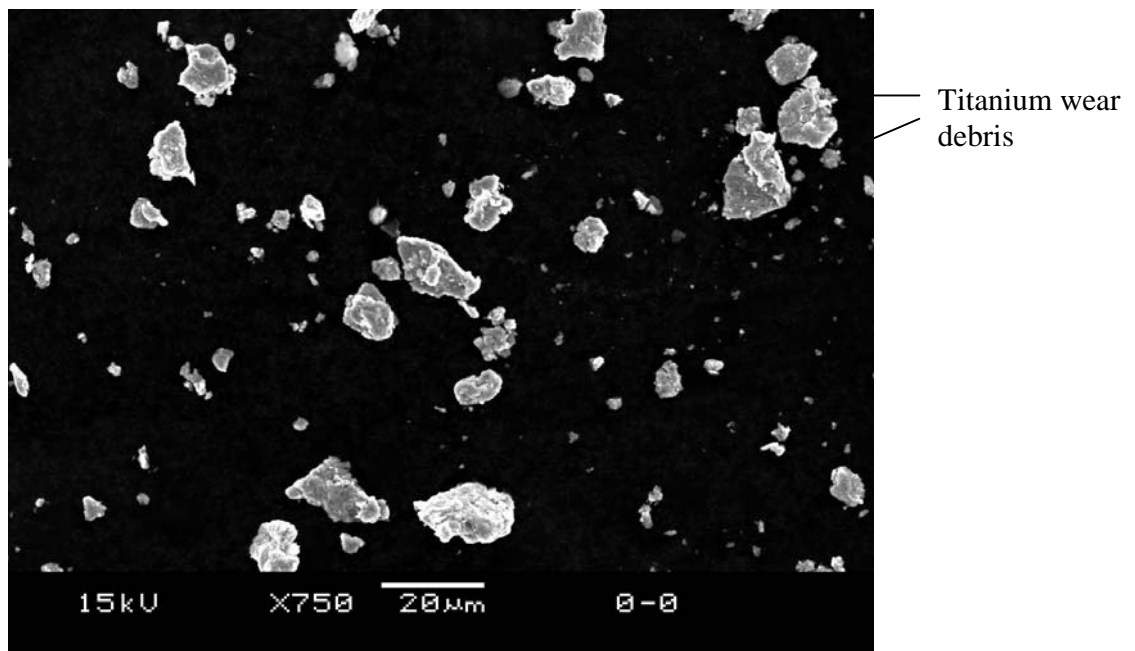


Figure 6.1: 0-0 wear debris

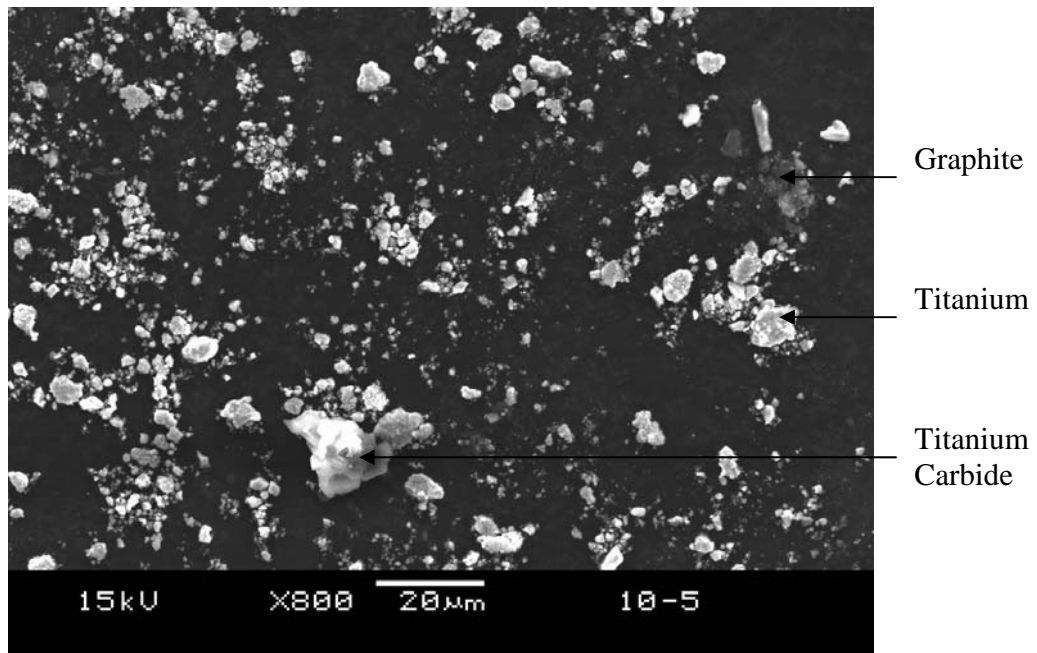


Figure 6.2: 10-5 wear debris

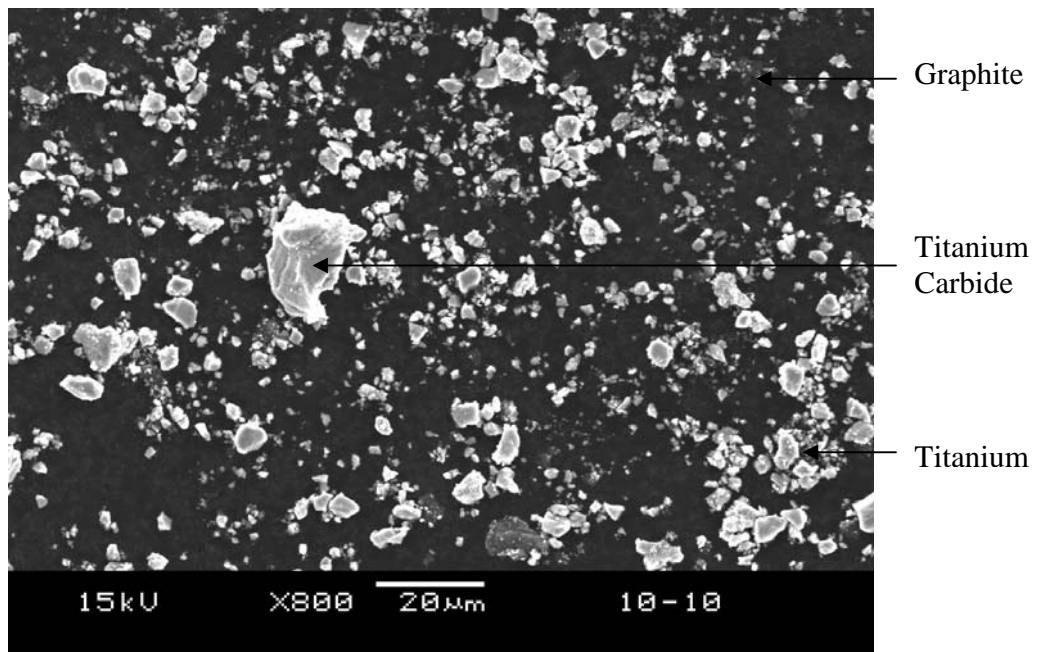


Figure 6.3: 10-10 wear debris

The composition of the various particles (Ti, TiC and graphite) in the wear debris was determined by EDX. From the SEM images, it was observed that the size of the wear debris in general were finer than the raw powders used. The morphology of the titanium and graphite particles, however, was similar. The composite wear debris had a larger percentage of particles smaller than 1.6  $\mu\text{m}$ . These sub-micron particles were probably made up of graphite as well as titanium particles, which were grinded to a greater extent due to the presence of TiC in the wear debris. The TiC particles, were larger in size than the titanium particles. The wear generation process was not very effective in reducing the size of the extremely hard TiC.

### **6.2 Particle Size Distribution of Wear Debris**

Due to the poor miscibility of the wear debris, a relatively large amount of debris is required in order to perform laser diffraction accurately. Because of the limited supply of wear debris, an alternative method was needed to determine the particle size distribution of the wear debris.

#### **6.2.1 Particle Size Distribution Based on Total Particle Number**

The particle size distribution of the wear debris at various particle size ranges, as a percentage of total particle number, was determined by analyzing the SEM images of the wear debris with a software known as CTAn (Skyscan, Belgium). By applying the appropriate level of image thresholding, the particles of the wear debris were isolated and the particle size distribution, based on particle number, determined, for different particle size ranges, as shown in Figures 6.4 to 6.6.



## Chapter 6: Characterization of Wear Debris

---

Please refer to Appendix 3 for a detailed explanation of the procedure employed in determining the particle size distribution of the wear debris.

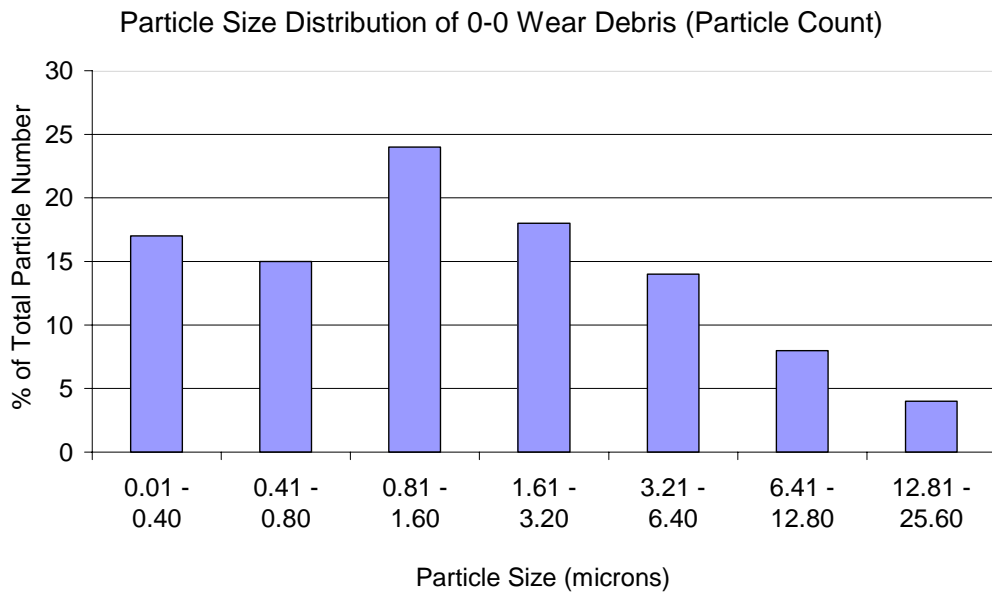


Figure 6.4: Particle size distribution of 0-0 wear debris based on particle frequency.

## Chapter 6: Characterization of Wear Debris

---

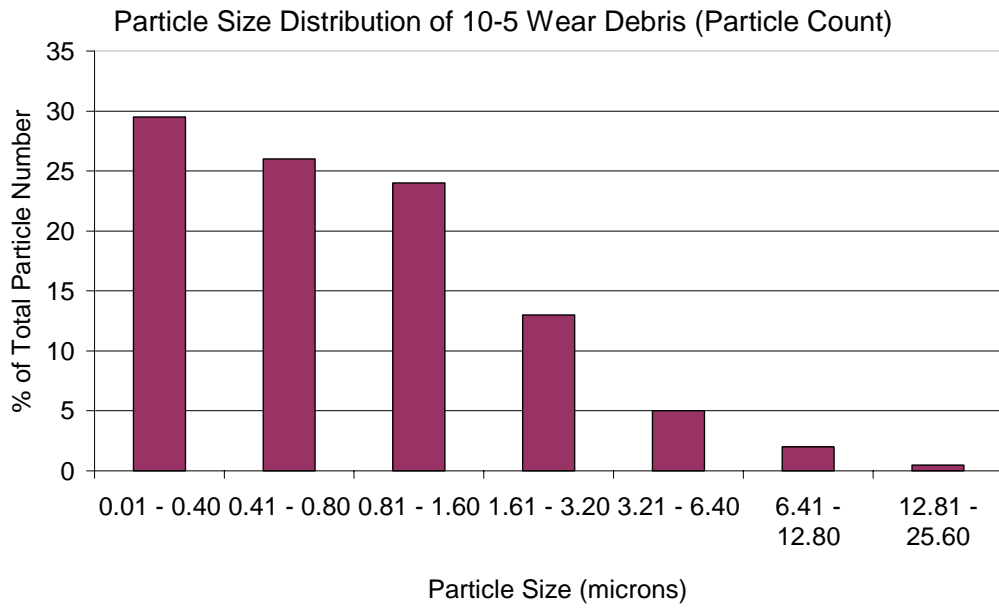


Figure 6.5: Particle size distribution of 10-5 wear debris based on particle frequency.

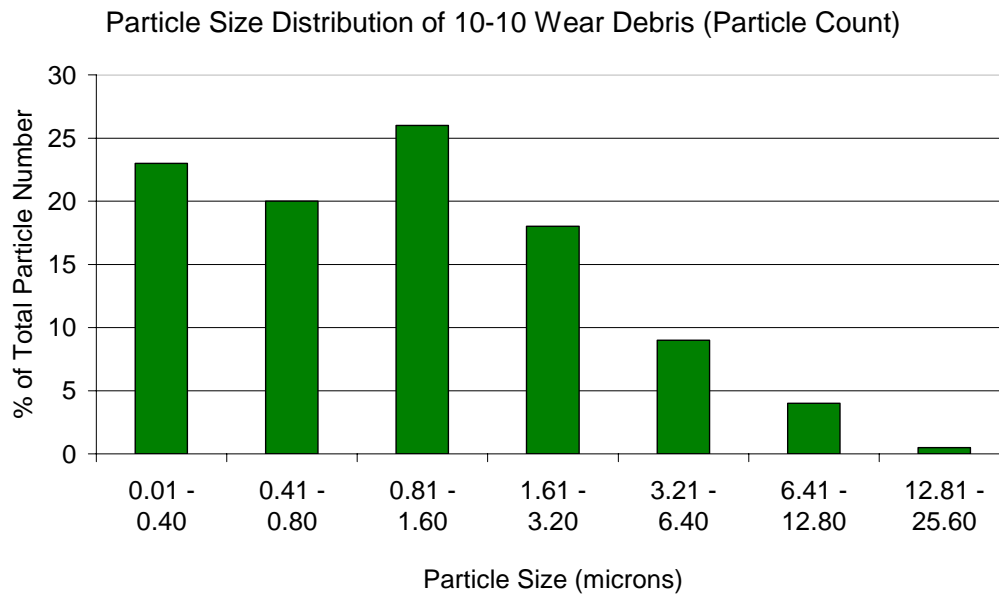


Figure 6.6: Particle Size Distribution of 10-10 Wear Debris Based on Particle Frequency.

## Chapter 6: Characterization of Wear Debris

---

The mean particle sizes for the 0-0, 10-5 and 10-10 wear debris are  $2.34 \pm 1.54$   $\mu\text{m}$ ,  $1.12 \pm 0.22$   $\mu\text{m}$  and  $1.63 \pm 0.34$   $\mu\text{m}$  respectively. The statistical details of the particle size distribution of the wear debris are summarized in Table 6.1. Most (70 %) of the titanium wear debris were smaller than 3.2  $\mu\text{m}$ , while most of the 10-5 (70 %) and 10-10 (70 %) were below 1.2  $\mu\text{m}$ . It was also observed that there was a more even spread in the size of the 0-0 wear debris particle, hence the high standard deviation value. The sizes of the 10-5 and 10-10 wear debris particles varied to a lesser degree from their respective means, as compared to the pure titanium wear debris.

Table 6.1: Statistical Information on Particle Size Distribution of Wear Debris  
(Based on Particle Frequency)

Sample	Mean ( $\mu\text{m}$ )	Std Dev ( $\mu\text{m}$ )	Median ( $\mu\text{m}$ )	Modal Range ( $\mu\text{m}$ )
<b>0-0</b>	2.34	1.54	1.2	0.81 – 1.60
<b>10-5</b>	1.12	0.22	0.6	0.01 – 0.04
<b>10-10</b>	1.63	0.34	1.2	0.81 – 1.60

The size of the wear debris generated was slightly larger than the size of predominantly polyethylene particulate debris retrieved from patients with hip prostheses, which had a mean particle size of 0.5  $\mu\text{m}$  [46]. Other studies, however, have concluded that ceramic and metallic wear debris are up to 3  $\mu\text{m}$  in size [63, 64], which compare well with the size of debris generated. In addition, the size of the wear debris obtained in the present study did not deviate much from other

studies involving biocompatibility of wear debris and titanium particles [20, 21, 50], whose results provided a basis for comparison.

### 6.2.2 Particle Size Distribution Based on Total Particle Volume

The CTAn was an invaluable tool in determining the particle size distribution of the wear debris, based on the total particle count. Earlier work involving raw powder particle size distribution, determined by laser diffraction (see Chapter 4), presented the data based on percentage of total particle volume. Hence, for consistency, it is imperative that a means of reasonably approximating the particle size distribution of the wear debris, based on percentage of total particle volume, be established.

Several studies involving biocompatibility of titanium particles have described [65, 66] means of determining particle number by approximating the mean particle shape to be a sphere. Based on the SEM images of the wear debris generated in the present study, it was observed that:

- a) the morphology of the wear debris is consistent, regardless of particle size;
- b) it is reasonable to approximate the mean particle shape of the wear debris to be spherical.

## Chapter 6: Characterization of Wear Debris

---

Hence, the linear dimensions of the particles is taken to be the diameter of the approximated sphere. The volume of each wear debris particle could then be determined by applying the following formula:

$$V_{debris} = \frac{4}{3} \pi \left( \frac{d}{2} \right)^3$$

where:

$V_{debris}$  = volume of wear debris particle.

$d$  = linear dimension of the particle.

The linear dimensions of the wear debris particles and corresponding particle count has been determined by the CTAn software, as described in Section 6.2.1. Thus, the particle size distribution of the wear debris particles, with respect to total particle volume, could be determined, and the results are plotted in Figures 6.7, 6.8 and 6.9.

**0-0 Wear Debris Size Distribution**

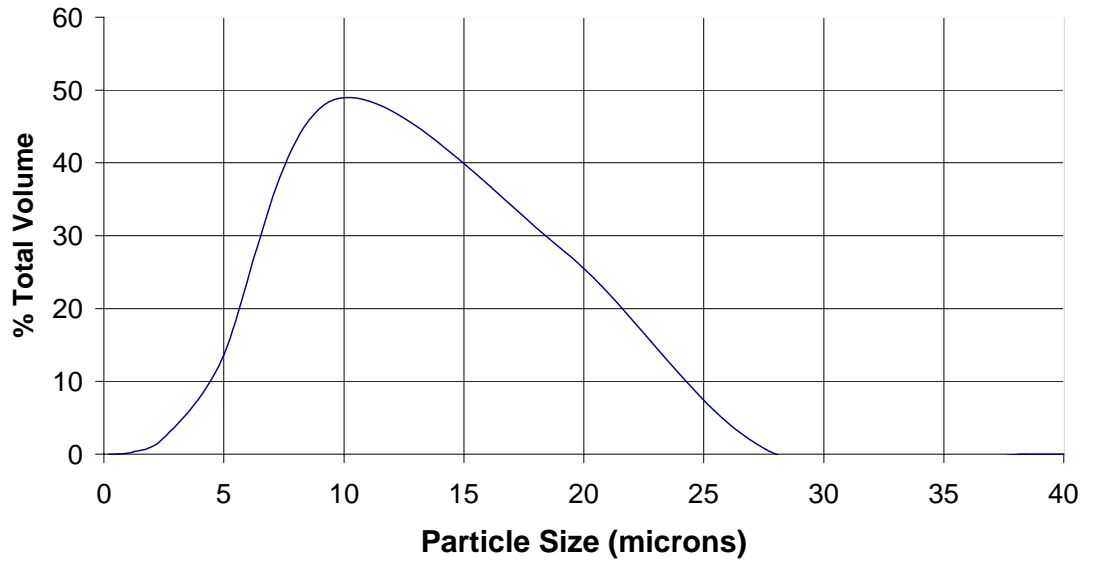


Figure 6.7: Particle size distribution of 0-0 wear debris (volume percentage).

**10-5 Wear Debris Particle Size Distribution**

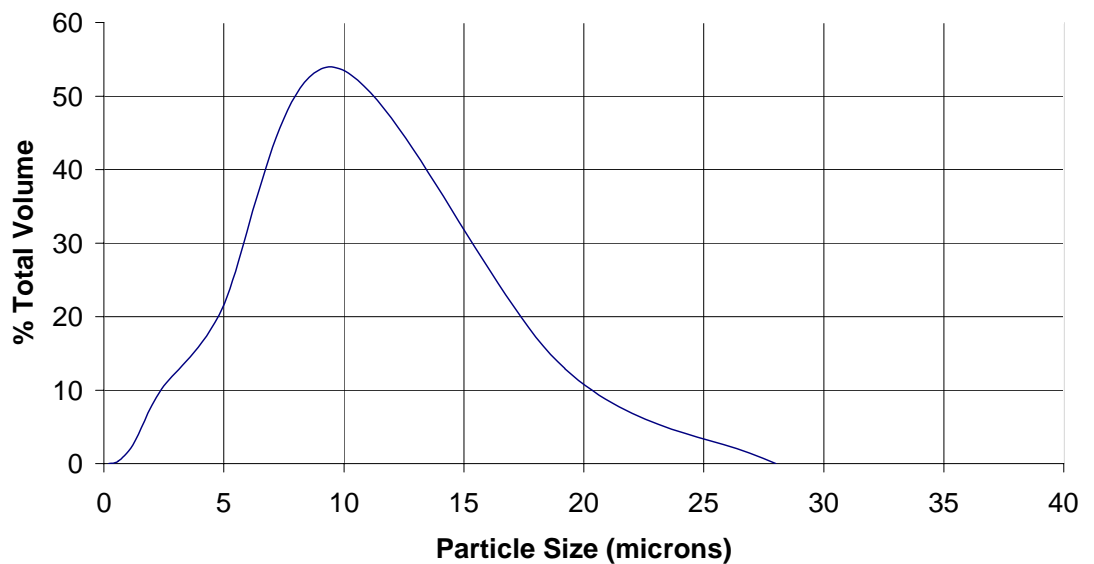


Figure 6.8: Particle size distribution of 10-5 wear debris (Volume Percentage).

**10-10 Wear Debris Particle Size Distribution**

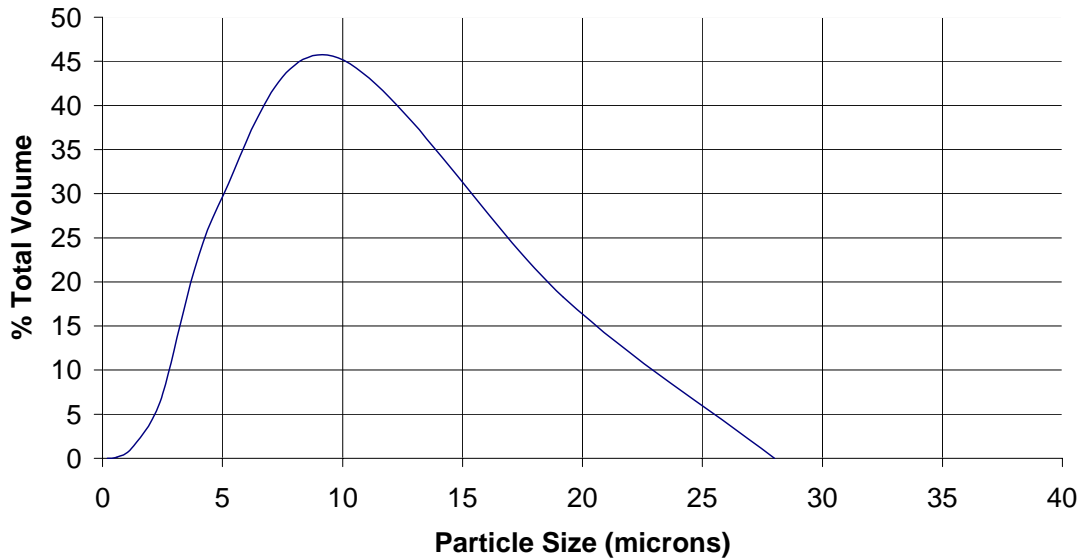


Figure 6.9: Particle size distribution of 10-10 wear debris (Volume Percentage).

The mean particle sizes for the 0-0, 10-5 and 10-10 wear debris are  $10.64 \pm 2.08$   $\mu\text{m}$ ,  $8.90 \pm 0.26$   $\mu\text{m}$  and  $9.42 \pm 0.27$   $\mu\text{m}$  respectively. The statistical details of the particle size distribution of the wear debris are summarized in Table 6.2. Most (70 %) of the titanium wear debris were smaller than 15.0  $\mu\text{m}$ , while most of the 10-5 (70 %) and 10-10 (70 %) were below 9.6  $\mu\text{m}$ . It was also observed that there was a more even spread in the size of the 0-0 wear debris particle, hence the high standard deviation value. The sizes of the 10-5 and 10-10 wear debris particles varied to a lesser degree from their respective means, as compared to the pure titanium wear debris.

## Chapter 6: Characterization of Wear Debris

---

Table 6.2: Statistical information on particle size distribution of wear debris  
(based on particle volume percentage)

Sample	Mean ( $\mu\text{m}$ )	Std Dev ( $\mu\text{m}$ )	Median ( $\mu\text{m}$ )	Modal Range ( $\mu\text{m}$ )
<b>0-0</b>	10.64	2.08	16.6	6.41 – 12.8
<b>10-5</b>	8.90	0.26	12.6	6.41 – 12.8
<b>10-10</b>	9.42	0.27	12.5	6.41 – 12.8

It is evident that when the particle size distribution is represented in terms of percentage total wear debris volume, the mean particle size increases significantly. This is due to the fact that the larger sized particles, although small in number, would make a far larger contribution to the total debris volume, than would the ubiquitous finer particles.

It is also evident that the wear debris particles generated were finer than the raw powder particles used to manufacture the specimens. The persistent grinding of the particles with the agate mortar significantly reduced the size of the wear debris. This observation was all the more evident in the composite wear debris, whereby the hard titanium carbide particles helped yield yet finer titanium wear debris.



### 6.3 Pros and Cons of Using CTAn for Particle Size Analysis

CTAn is a useful software in determining the particle size distribution in cases whereby there is insufficient particle quantity to accurately perform laser diffraction. By applying an appropriate level of thresholding, the software is able to isolate discrete particles from the image of the particles, and determine the pixel count for each individual particle. Calibration simply involves comparing the linear dimensions of the particle, measured with the scale bar in the SEM image, with the corresponding pixel count generated by the software.

The software is user friendly, and results could be obtained quickly. Only a small amount of particles is needed to obtain results. The trial version of the software, which is adequate for this purpose, is readily available from the Skyscan website [67]. This method provides a relatively clean and fuss-free alternative to laser diffraction, whereby the equipment would need to be purged and thoroughly cleaned after use. Finally, in laser diffraction the particles need to be miscible in water. Difficulties were encountered in the present work, when determining the particle size distribution of the raw powders, which were not very miscible in water, through laser diffraction (described in Chapter 4).

The disadvantages of this method are that firstly, good, clear images of the particles would first have to be obtained, preferably through Scanning Electron Microscopy. Care must be taken to ensure that there is minimal clumping of the particles. Since CTAn is only able to analyze the particle size based on the pixel

## **Chapter 6: Characterization of Wear Debris**

---

count of the image of the particle, inaccuracies could arise if the image of the particle is not properly in focus. Secondly, this method allows the measurement of particle sizes only in 2 dimensions, and hence, the accuracy of the particle size measurement of samples comprising particles which are elongated would be largely dependent on the orientation of the particles in the images. Laser diffraction eschews this problem as the actual size of the particle is being determined in 3 dimensions.

## Chapter Seven

### Biocompatibility Studies

#### 7.1 Biocompatibility of Raw Powder

The effect of the raw powders on the proliferation of 3T3 and rat osteoblast was performed as described in Section 4.8.2. The study was consisted of two parts, carried out concurrently:

- a) the alamarBlue<sup>TM</sup> Reduction at various time points, normalized to the control to determine cell proliferation; and
- b) fluorescence microscopy, to determine the distribution of live/dead cells, as well as to analyze the morphology of the cells and the range of particle sizes, which were phagocytosed by the cells.

##### 7.1.1 alamarBlue<sup>TM</sup> Reduction of Cells Cultured with Raw Powder

The proliferation rates of 3T3 cells and rat osteoblast were measured quantitatively by determining the extent of alamarBlue<sup>TM</sup> Reduction at various time points. alamarBlue<sup>TM</sup> is a redox indicator which undergoes reduction in response to metabolic activity. The alamarBlue<sup>TM</sup> reduction yields a colorimetric change, whose spectrophotometric absorbance could be measured with a micro-plate reader. Cells seeded on tissue culture plates without interaction with the raw powder, at the same seeding density, were used as controls. The alamarBlue<sup>TM</sup> reduction of the cells seeded on the compacts were measured and plotted at

## Chapter 7: Biocompatibility Studies

various time points, normalized as a fraction of the reduction measured in the control group, as shown in Figures 7.1 and 7.2 below.

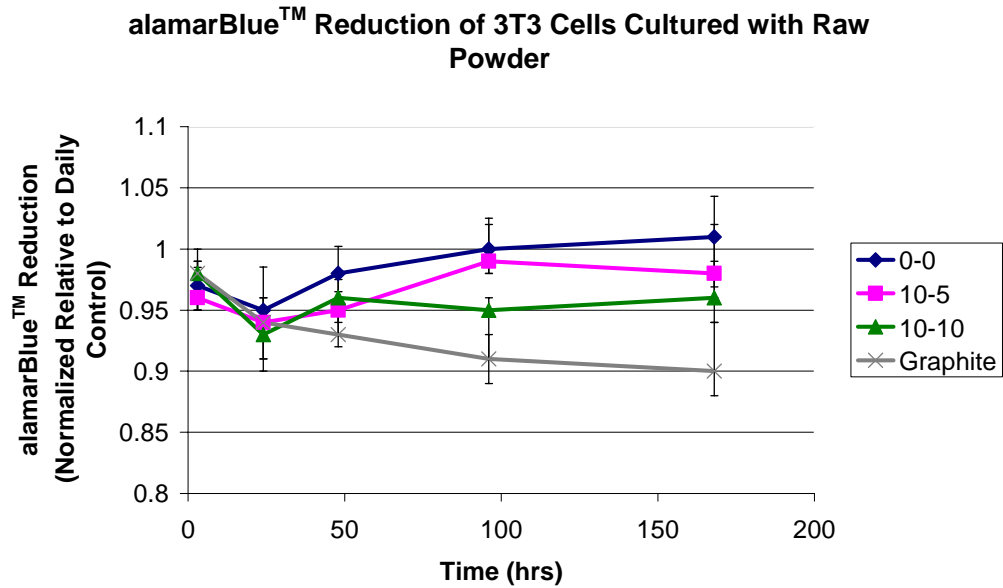


Figure 7.1: alamarBlue™ reduction of 3T3 cells cultured with raw powder

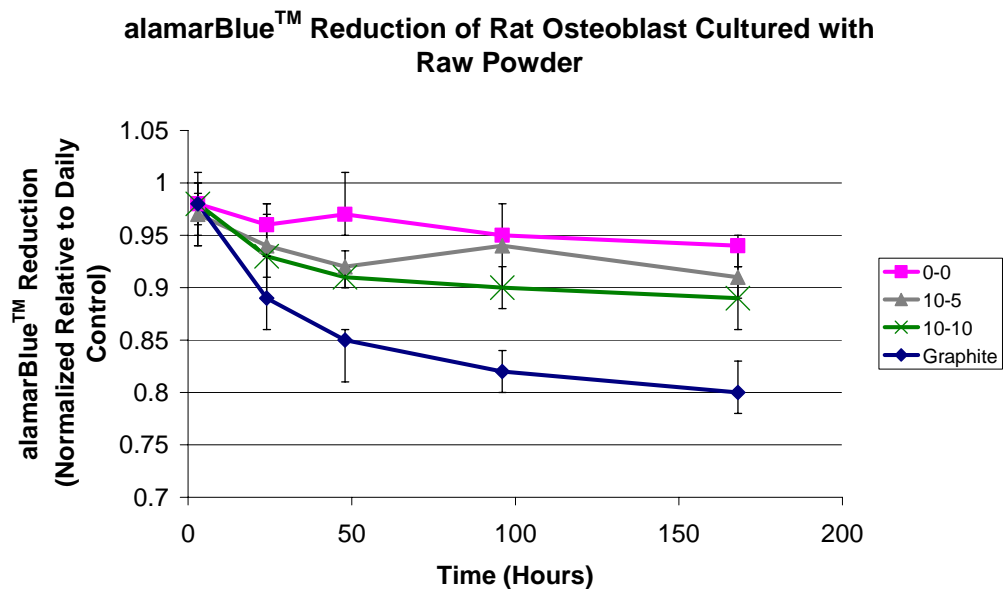


Figure 7.2: alamarBlue™ reduction of rat osteoblast cultured with raw powder

### 7.1.2 Statistical Significance of Cell Proliferation Assay Involving Raw

#### Powder

The Student's T-Test was carried out to determine the statistical significance of the cell proliferation assay involving raw powder. Five sets of results ( $n = 5$ ) were obtained for each time point and the detailed calculations are attached in Appendix 4.

In the initial stages of the 3T3 and rat osteoblast cell culture (up to 24 hours), the presence of the different types of raw powder did not result in significant difference in cellular proliferation ( $p > 0.1$ ).

After 48 hours, however, the samples containing the 10-5 powder mixture ( $p < 0.05$ ) and the pure graphite powder ( $p < 0.05$ ) caused a significant reduction in 3T3 cell proliferation, as compared to the samples containing pure titanium powder. Samples containing 10-10 powder mixture ( $p > 0.1$ ) did not cause a significant reduction in 3T3 cell proliferation at this time point. The rat osteoblast cell culture showed a similar trend, with samples containing 10-5 powder mixture ( $p < 0.05$ ) and the pure graphite powder ( $p < 0.05$ ) causing a significant reduction in rat osteoblast proliferation, as compared to the samples containing pure titanium powder. Likewise, the samples containing 10-10 powder mixture ( $p > 0.1$ ) did not cause a significant reduction in rat osteoblast proliferation

After 96 hours of cell culture, samples containing the 10-5 powder mixture continued to proliferate at a high rate and there was no significant difference in 3T3 cell and rat

osteoblast proliferation, as compared to the samples containing pure titanium powder ( $p > 0.1$ ). Samples containing 10-10 powder mixture and the pure graphite powder proliferated at a slower rate and there was significant difference in 3T3 cell and rat osteoblast proliferation, as compared to the samples containing pure titanium powder ( $p < 0.01$  and  $p < 0.001$ , respectively).

After seven days (168 hours) of cell culture, there was no significant difference in 3T3 cell and rat osteoblast proliferation in samples containing the 10-5 powder mixture, as compared to the samples containing pure titanium powder ( $p > 0.1$ ). There was, however, significant reduction in 3T3 cell and rat osteoblast proliferation in samples containing the 10-10 powder mixture ( $p < 0.05$ ), as well as the pure graphite powder ( $p < 0.001$ ).

Hence the results indicate that the presence of 10-10 powder mixture and especially graphite powder used in this experiment had a significant effect on the long-term 3T3 cell and rat osteoblast cellular proliferation. The 10-5 powder mixture, meanwhile, did not significantly impact the long term cellular proliferation.

### **7.1.3 Fluorescence Microscopy of Cells Cultured with Raw Powder**

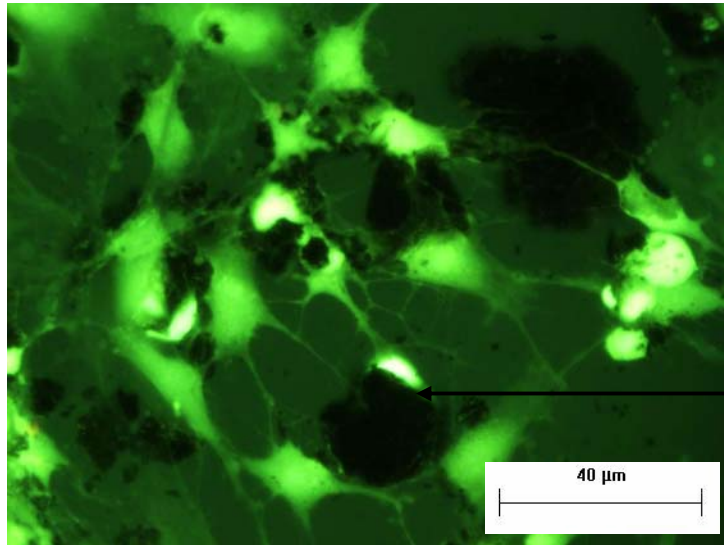
It was also important to determine if the raw powder were phagocytosed by the cells, and if the interaction with the powder brought about a change in morphology of the cells. Typical fluorescence microscopy images indicating

## Chapter 7: Biocompatibility Studies

---

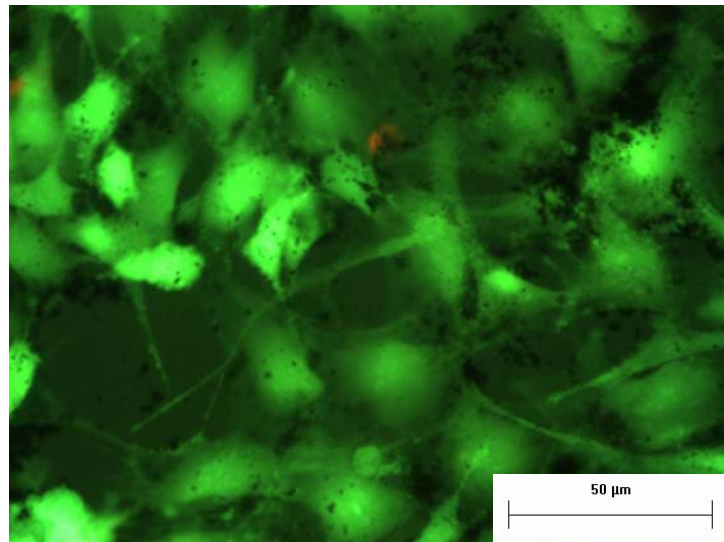
phagocytosis of powder, as well as morphology of the affected cells after 96 hours are shown in Figures 7.3 and 7.4.

a)

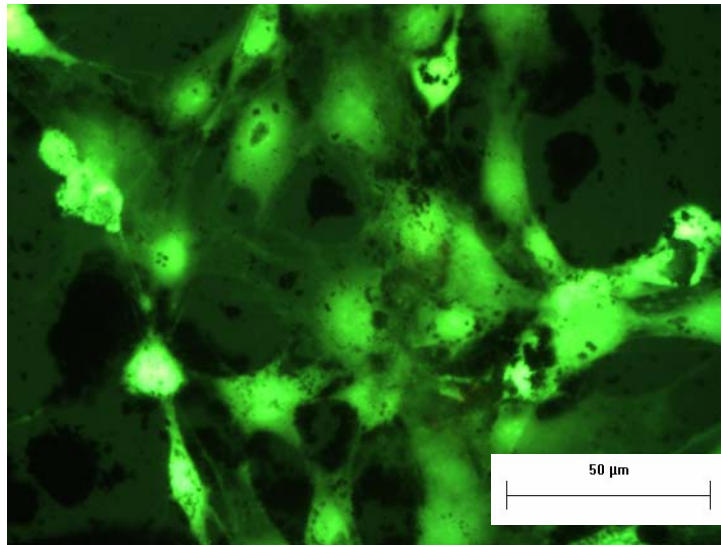


Attachment of  
plasma membrane  
of 3T3 cells onto  
powder particles

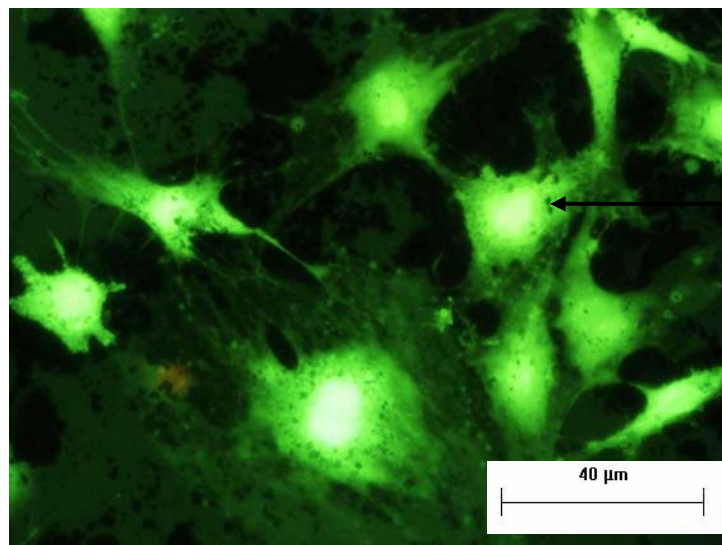
b)



c)



d)

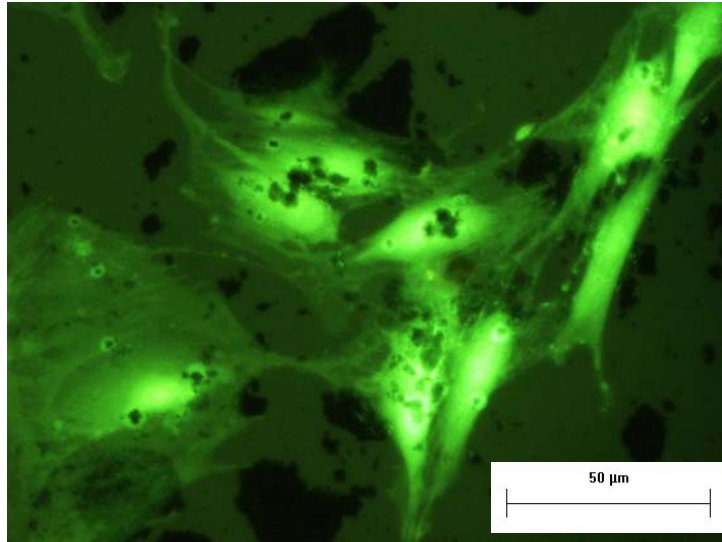


Smaller particles  
phagocytosed by  
cells

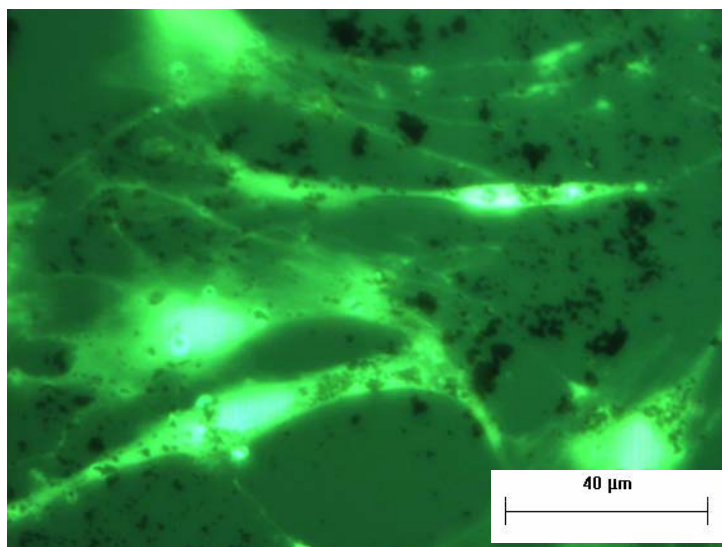
Figure 7.3: Fluorescence microscopy of interaction of 3T3 cells with raw powder: a) 3T3 cells cultured with pure titanium raw powder; b) 3T3 cells cultured with pure graphite; c) 3T3 cells cultured with 10-5 binary powder; and d) 3T3 cells cultured with 10-10 binary powder



a)



b)



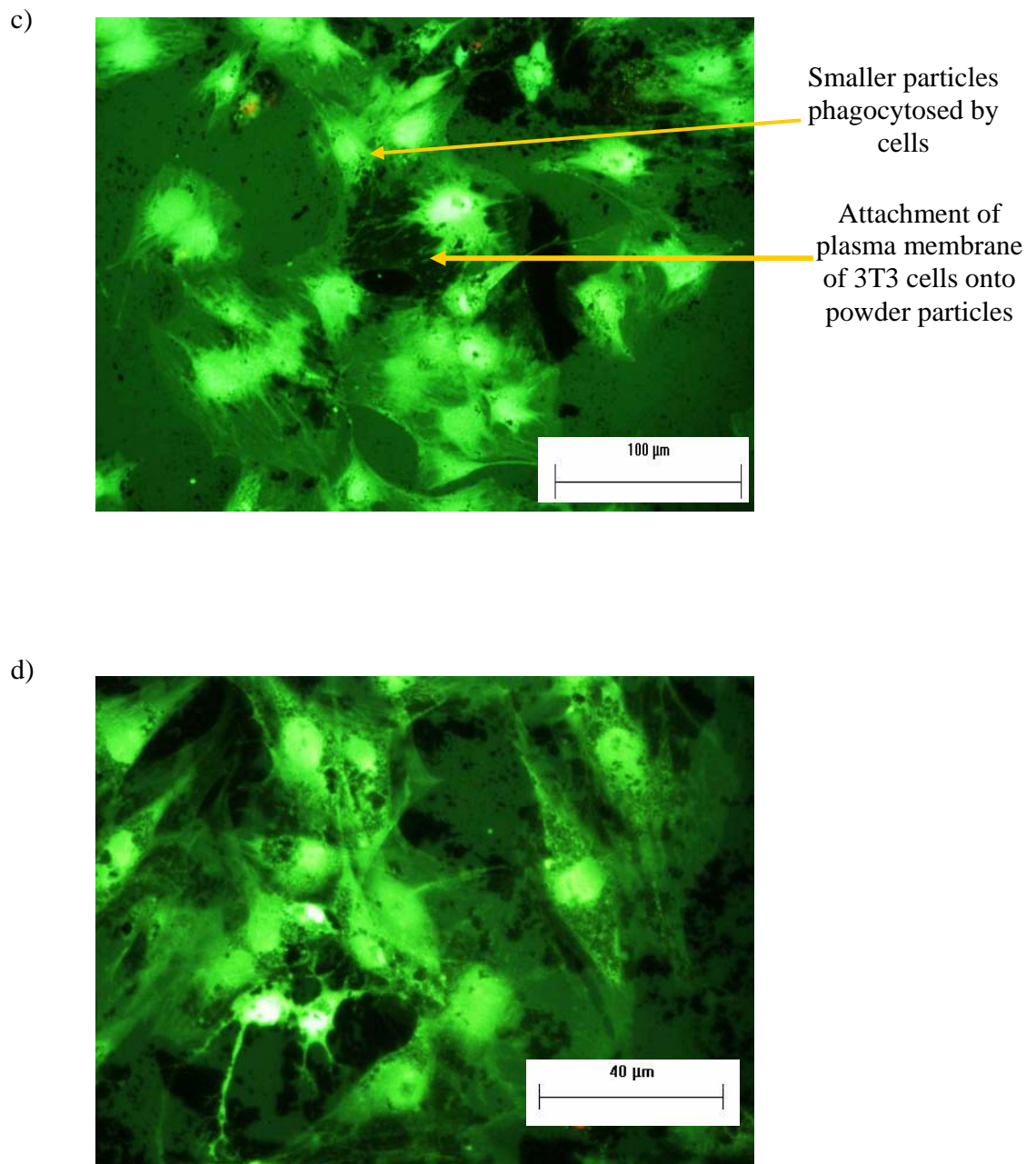


Figure 7.4: Fluorescence microscopy of interaction of rat osteoblast with raw powder: a) rat osteoblast cultured with pure titanium raw powder; b) rat osteoblast cultured with pure graphite; c) rat osteoblast cultured with 10-5 binary powder; and d) rat osteoblast cultured with 10-10 binary powder

### 7.1.4 Discussion on Biocompatibility of Raw Powder

From the micrographs obtained through fluorescence microscopy, it was observed that after 96 hours, the viable 3T3 cells and rat osteoblasts phagocytosed smaller titanium and graphite particles. Measurements of the size of the phagocytosed particles were visually made, with help from the scale bar attached to each image. It was observed that particles below 6  $\mu\text{m}$  were phagocytosed by the cells. This compared well with the results of other studies [46, 20]. The larger particles (above 10  $\mu\text{m}$ ), on the other hand, were observed to be attached to the plasma membrane of the viable cells. The cells were observed to adhere to the clusters of the larger particles.

The fact that the viable cells had internalized a large number of the smaller particles suggest that phagocytosis of smaller titanium and graphite particles, up to a certain threshold number per cell, would not affect viability. Observations of the viable cells which had phagocytosed the particles indicated that the cells growing in regions devoid of large particles (above 10  $\mu\text{m}$ ) experienced a change in morphology, as a result of the phagocytosis. Following ingestion of the particles, the cells became less elongated, as compared to the control group. The presence of larger particles also had an effect on the cellular morphology of both cell types. The cells growing in the proximity of larger particles experienced an alteration in morphology, in an attempt to attach themselves to those particles and grow around them as the cells proliferated.

Pioletti et al [21] have established that osteoblasts phagocytosed most of the particles in the first 24 hours. The results of the present study did not contradict their findings. From the normalized plots of the alamarBlue™ Reduction with time for both cell types, a steep dip in viability was observed within the first 24 hours. Subsequent to that, the proliferation of the cells resulted in a lower particle number to cell ratio, lowering the exposure level significantly. Hence there is a stabilization in the proliferation of the cells, as compared to the control group, with time.

Comparing the results of the alamarBlue™ reduction of the 3T3 celline and rat osteoblasts revealed that, in the presence of the raw powder in vitro, the fibroblasts proved more resilient. The presence of pure titanium particles did not affect fibroblast proliferation significantly. The 3T3 cells cultured with pure graphite particle experienced a significant reduction in proliferation over time, by about 10 % after 1 week. The binary powder mixtures (10-5 and 10-10), on the other hand, caused a reduction in fibroblast proliferation by between 2.5 % to 7.5 %. This reduction in proliferation could be attributed to the presence of graphite particles.

The raw powder particles, meanwhile, evoked a more cytotoxic response from the rat osteoblast. The graphite particles caused the greatest reduction in cell proliferation of up to 20 %. The pure titanium particles, meanwhile, brought about a relatively benign reduction in cell proliferation of up to 6 %. The cytotoxic

effect of the pure titanium particles was less significant than that observed in other studies involving rat osteoblasts [20, 21]. It should be noted, however, that while the concentration of titanium particles (1 mg/ml) used in the present study was similar to the study conducted by O'Connor et al, the size of the titanium particles used in that study were significantly smaller.

There have been no reported findings on the effect of fibroblast proliferation in the presence of graphite powder, but several researchers have studied the biocompatibility of carbon particles towards osteoblast proliferation. It has been reported that, while nano-scale graphite particles were relatively benign, and may indeed enhance osteoblast viability [54, 55]. In this study, it has been found that the graphite particles, of mean particle size of 10  $\mu\text{m}$ , evoked a cytotoxic response from both the 3T3 cells (by up to 10 % reduction in cell proliferation) and, to a more significant extent, the rat osteoblasts (by up to 20 % reduction in cell proliferation). The difference in biocompatibility between the nanophase carbon particles and the micron-sized graphite particles used in the present study could be attributed to the difference in particle sizes. It has been postulated that micron-sized wear debris vary significantly in size and morphology from naturally occurring components of bone, such as hydroxyapatite crystals (less than 10 nm) collagen fibres (from 100 nm to a few microns in diameter [53]).

The different viability responses of the 3T3 cells and rat osteoblasts towards the presence of the raw powder particles could be due the fact that fibroblasts are

better adapted at attaching themselves to particles. The primary function of osteoblast is to develop into bone tissue, while one of the primary functions of fibroblast in vivo is to encapsulate and isolate particulate debris.

Finally, in every case investigated in the present study, the alamarBlue™ reduction after 3 hours was lower than that of the control. Pioletti et al [68] have postulated that loading of particles in the cell culture may cause mechanical damage to the cells, and may account for the lower initial cell proliferation.

### **7.2 Biocompatibility of Wear Debris**

Wear debris was obtained from the sintered, hot isostatically pressed compacts as described in Section 4.8.3.1. The morphology and particle size distribution of the wear debris has been discussed in Chapter 6. In this section, the cell proliferation of 3T3 cells and rat osteoblast, as determined by alamarBlue™ Reduction, and the distribution of viable cells, determined from fluorescence microscopy, were examined.

#### **7.2.1 alamarBlue™ Reduction of Cells Cultured with Wear Debris**

The alamarBlue™ Reduction of 3T3 cells and rat osteoblast, cultured with wear debris, are shown in Figures 7.5a and 7.5b respectively.

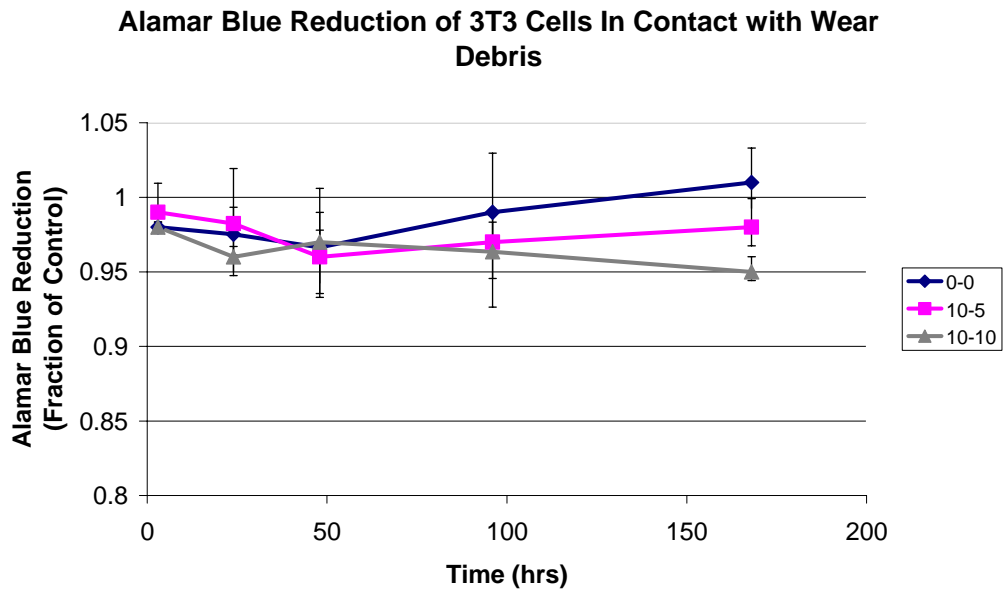


Figure 7.5a: alamarBlue™ reduction of 3T3 cells cultured with wear debris

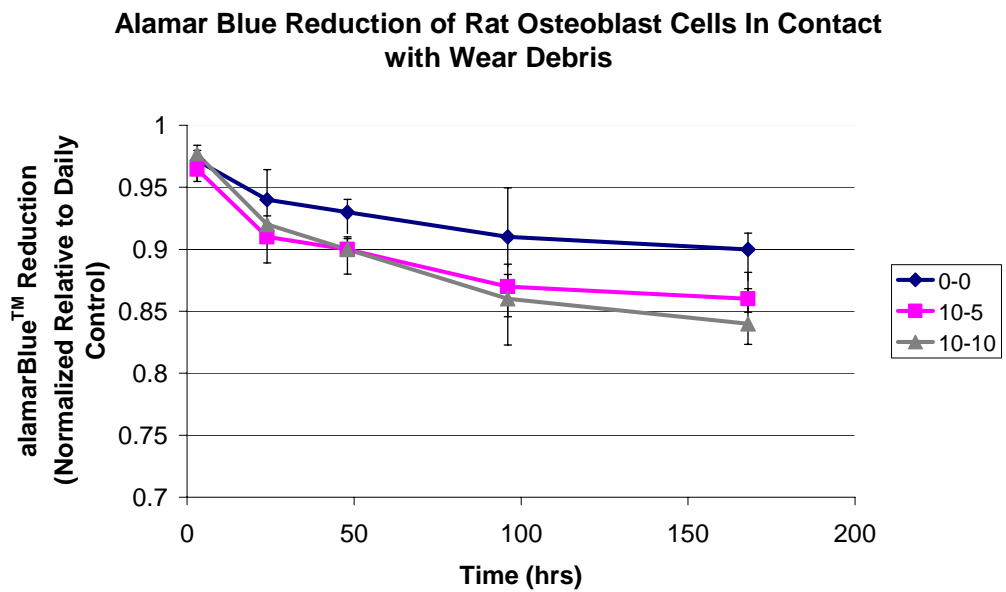


Figure 7.5b: alamarBlue™ reduction of rat osteoblast cultured with wear debris

### 7.22 Statistical Significance of Cell Proliferation Assay Involving Wear

#### Debris

The Student's T-Test was carried out to determine the statistical significance of the cell proliferation assay involving wear debris. Five sets of results ( $n = 5$ ) were obtained for each time point and the detailed calculations are attached in Appendix 5.

In the initial stages of the 3T3 cell culture (up to 48 hours), the presence of the different types of wear debris did not result in significant difference in cellular proliferation ( $p > 0.1$ ). The presence of the different types of wear debris did not result in significant difference in cellular proliferation ( $p > 0.1$ ) in the rat osteoblast cell cultures after 3 hours. However, after 24 hours, the 10-5 ( $p < 0.05$ ) and 10-10 ( $p < 0.01$ ) wear debris resulted in a significant reduction in rat osteoblast proliferation, as compared to the samples containing pure titanium wear debris. After 48 hours, there was significant reduction in rat osteoblast proliferation, as compared to the samples containing pure titanium wear debris in the samples containing 10-5 ( $p < 0.01$ ) and 10-10 ( $p < 0.01$ ) wear debris.

After 96 the samples containing the 10-10 wear debris ( $p < 0.05$ ) caused a significant reduction in 3T3 cell proliferation, as compared to the samples containing pure titanium wear debris. Samples containing 10-5 wear debris ( $0.05 < p < 0.1$ ) caused a moderate reduction in 3T3 cell proliferation at this time point. The presence of wear debris continued to have a significant impact on rat



osteoblast proliferation. There was significant reduction in rat osteoblast proliferation, as compared to the samples containing pure titanium wear debris, in samples containing the 10-5 wear debris ( $p < 0.05$ ) and the 10-10 wear debris ( $p < 0.01$ ).

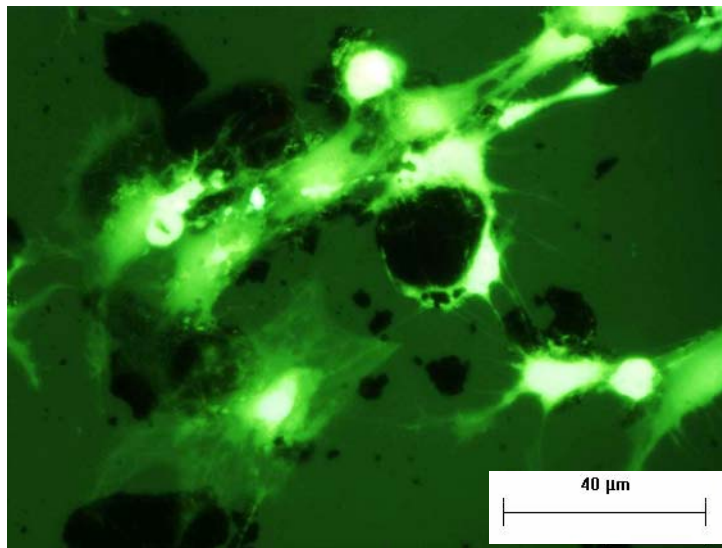
After seven days (168 hours) of cell culture, there was significant reduction in 3T3 cell proliferation in samples containing the 10-5 wear debris ( $p < 0.05$ ) and the 10-10 wear debris ( $p < 0.01$ ), as compared to the samples containing pure titanium wear debris. Likewise, the presence of the 10-5 wear debris ( $p < 0.01$ ) and the 10-10 wear debris ( $p < 0.001$ ) resulted in significant reduction in rat osteoblast proliferation, as compared to the samples containing pure titanium wear debris.

Hence the results indicate that the presence of 10-5 and 10-10 wear debris had a significant effect on the long-term 3T3 cell and rat osteoblast cellular proliferation. The presence of pure titanium wear debris did not significantly impact the long term cellular proliferation.

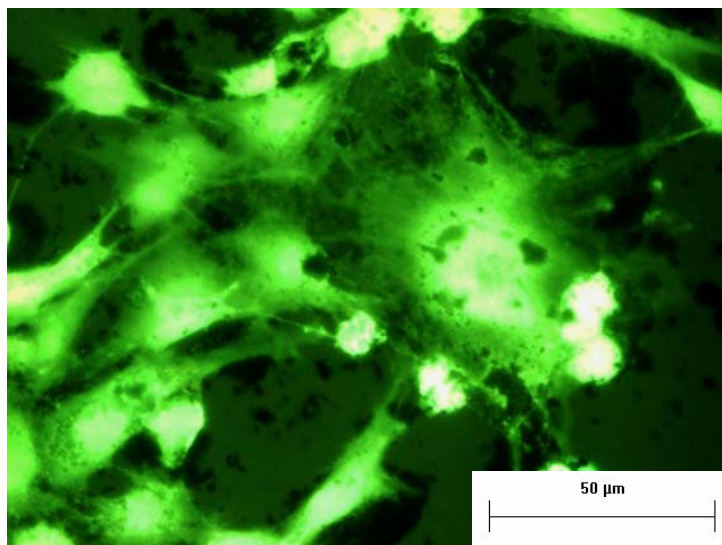
### **7.2.3 Fluorescence Microscopy of Cells Cultured with Wear Debris**

The morphology of the cells exposed to wear debris after 96 hours was studied under a fluorescence microscope, following staining with Calcein AM and Ethidium homodimer-1. The images obtained are shown in Figures 7.6 and 7.7.

a)



b)



c)

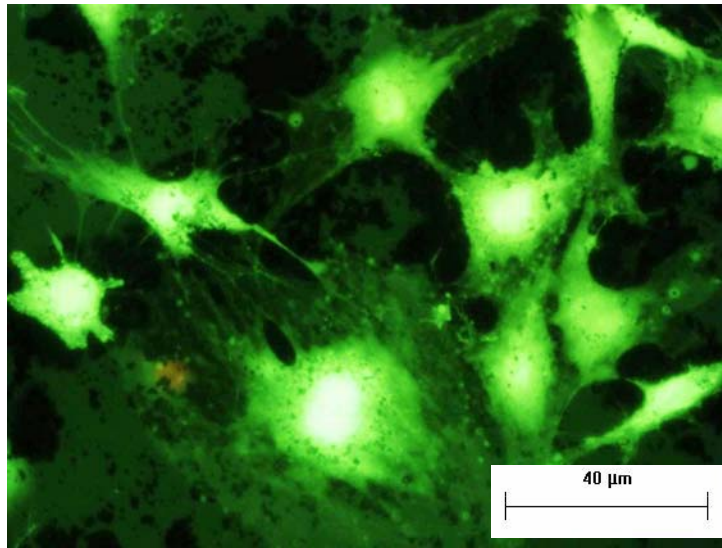
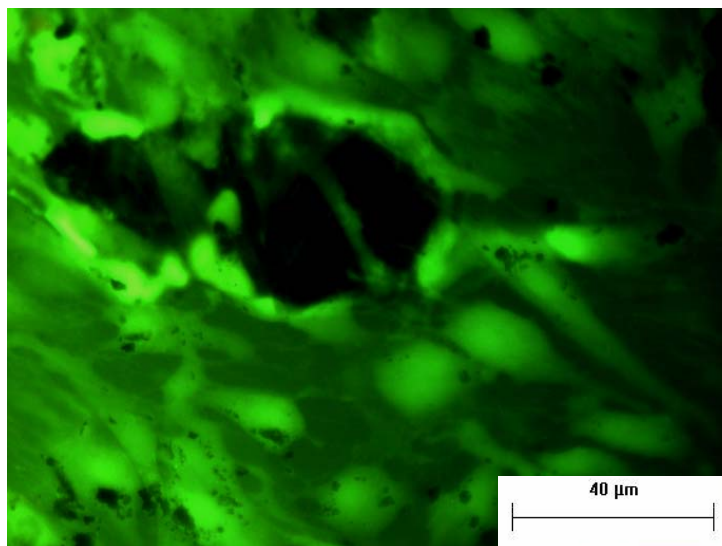
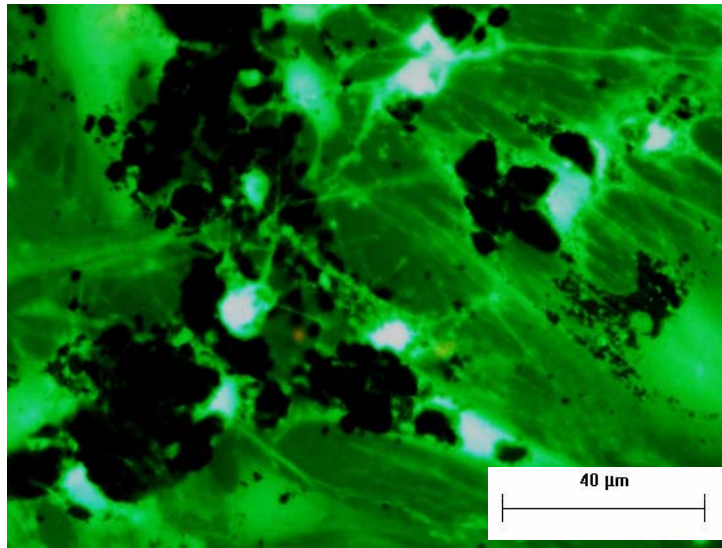


Figure 7.6: Fluorescence microscopy of interaction of 3T3 cells with wear debris: a) 3T3 cells cultured with pure titanium wear debris; b) 3T3 cells cultured with 10-5 wear debris; and c) 3T3 cells cultured with 10-10 wear debris.

a)



b)



c)

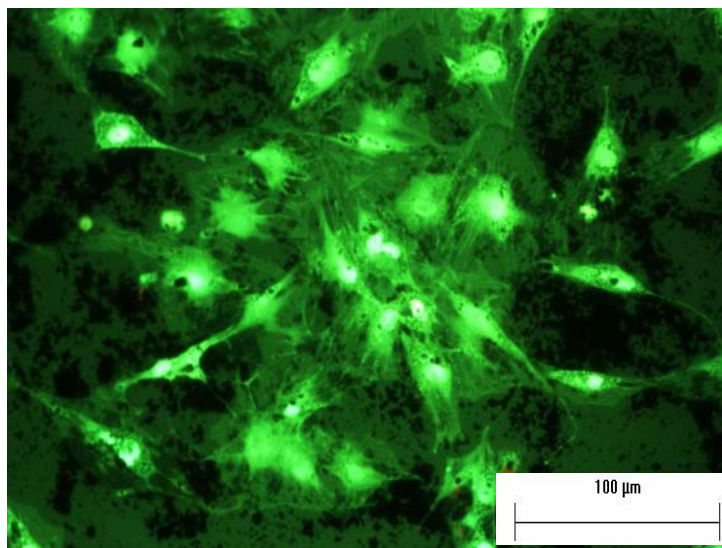


Figure 7.7: Fluorescence microscopy of interaction of rat osteoblast with wear debris: a) rat osteoblast cultured with pure titanium wear debris; b) rat osteoblast cultured with 10<sup>-5</sup> wear debris; and c) rat osteoblast cultured with 10<sup>-10</sup> wear debris.

### 7.2.4 Discussion on Biocompatibility of Wear Debris

From the micrographs obtained through fluorescence microscopy, it was observed that after 96 hours, the viable 3T3 cells and rat osteoblasts phagocytosed smaller titanium and graphite particles. From visual inspection of the images, there appeared to be more wear debris phagocytosed in each cell as compared to the number of raw powder particles internalized by the cells. This could be due to the smaller size of the wear debris, and hence, the cells were exposed to more particles below 6  $\mu\text{m}$ , as compared to the study involving raw powder.

The presence of pure titanium wear debris reduced cellular proliferation of rat osteoblast by up to 10 % after 1 week, but did not significantly affect the proliferation of the 3T3 cells. The reduction on rat osteoblast proliferation was more significant than the raw powder particles. This suggests that the smaller size of the titanium particles in the wear debris may be responsible for the reduced osteoblast proliferation. O'Connor et al [20] have determined that titanium particles of between 1.5  $\mu\text{m}$  to 4.0  $\mu\text{m}$  in size were most detrimental to rat osteoblast proliferation, and particles between 5 – 9  $\mu\text{m}$  and below were phagocytosed, and brought about a decrease in proliferation of the osteoblast, when loaded at a concentration of 1mg/ml, the same concentration used in this study.

Wear debris from the titanium-graphite composite brought about a reduction in cell proliferation of the rat osteoblasts, by up to 16 %, as well as 3T3 cells, by up

to 5 %, after 1 week of cell culture. Comparing the alamarBlue™ reduction plots with the study involving raw powder, it is apparent that the wear debris of the titanium-graphite composite was more cytotoxic than the raw powder particles.

The difference in graphite content between the 10-10 wear debris and 10-5 wear debris did not have an appreciable impact on the cell proliferation. There could be several reasons for this observation. Firstly, an increase in graphite content of the raw powder brought about an increase in the TiC formation, as observed in the photomicrographs of the polished specimen surfaces. The Vickers Hardness measurements of the specimens substantiates this point, as discussed in Section 5.1, suggesting that twice as much TiC is formed in the 10-10 specimens, as compared to the 10-5 specimens, given the sintering conditions used in this study. Hence, the amount of unreacted graphite did not increase substantially in the 10-10 specimen, as compared to the 10-5 specimen. The reduction in cell proliferation in the wear debris cell cultures, as compared to the cultures involving raw powder, was brought about predominantly by the increase in small titanium particles content, below 5 – 9  $\mu\text{m}$ , in the wear debris.

A similar trend was observed to the study involving raw powder, whereby there is a steep decline in cell proliferation between 3 hours to 24 hours after loading with particles. The cell proliferation stabilized thereafter. This could be due to the fact that most of the particles were phagocytosed within the first 24 hours, and

subsequent to that, as a result of cell proliferation, there was a reduction in the exposure level of the particles to the cell.

### **7.3 Biocompatibility of Sintered Compacts**

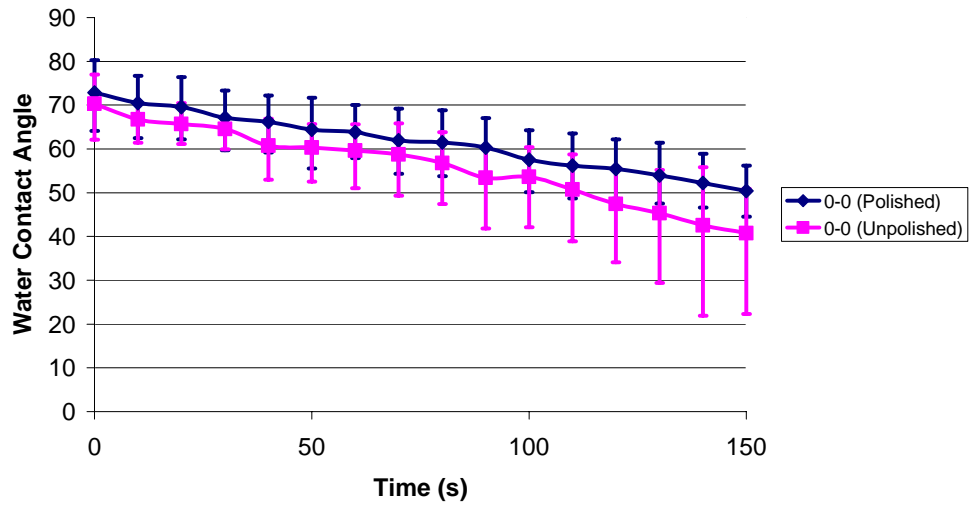
The sintered and Hot Isostatically Pressed compacts were polished and seeded with 3T3 cells and rat osteoblast, as described in section 4.9.1. The results of the cellular propagation of both cell types are described below:

#### **7.3.1 Water Contact Angle Measurements**

The wettability of a surface determines how hydrophilic the surface is. The hydrophilicity of a surface is important when seeding cells onto a surface, as it would, in theory, be easier for cells to attach themselves on more hydrophilic surfaces. The mechanism of cell attachment on bulk surfaces has been described in Section 2.5.1. The water contact angle of both the polished and unpolished compact surfaces were measured dynamically for a period of 150 s, at intervals of 10s, and are plotted as shown Figure 7.8 below.

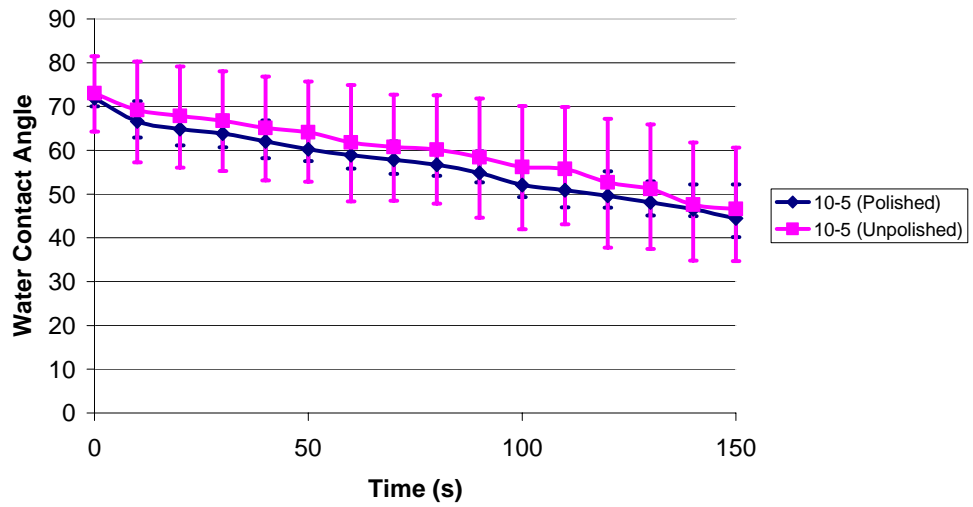
a)

Water Contact Angle of 0-0 Specimen Surfaces



b)

Water Contact Angle of 10-5 Specimen Surfaces





c)

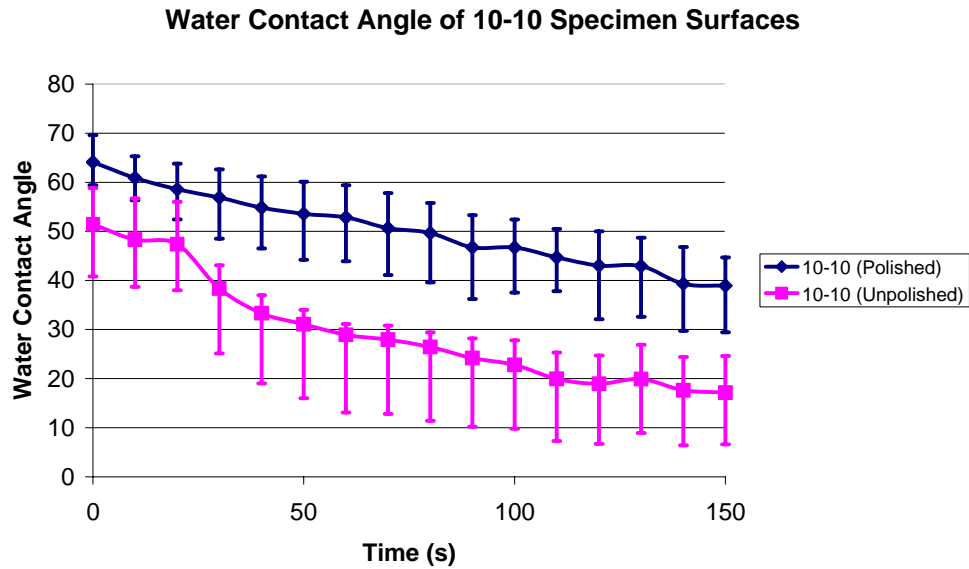


Figure 7.8: Water contact angle measurements of compact surfaces. a) 0-0 specimens; b) 10-5 specimens; and c) 10-10 specimens.

From the plots, it is evident that the water drop spreads out on the surface of the specimen being measured over a period of 150s. The initial water contact angle (at time = 0s) is relatively high for all polished specimens, at between 60 to 80 degrees. This indicates that the polished surfaces of the specimens were relatively hydrophobic. An increase in graphite content had a marginal effect in increasing the hydrophilicity of the specimen surfaces, probably by increasing the surface irregularities from increased carbide formation. Research involving titanium oxide films [69] has shown that the water contact angle on the titanium oxide films at time = 30s was approximately 33 degrees. However, the water drop on the titanium oxide surface did not spread out by much, and after 150s, the water

contact angle was approximately 32 degrees, which was not significantly lower than the angles measured on the titanium-graphite composites.

There was only marginal differences in water contact angles of the polished and unpolished specimen surfaces, for the 0-0 and 10-5 specimens. The unpolished surfaces of the 10-10 specimens were, on average, significantly more hydrophilic than the polished surfaces. It was observed, however, that the water contact angles, measured on the unpolished surfaces, varied more significantly for each sampling of the data, as compared to those measured on the polished surfaces. The large variance could be due to the unpredictability of the nature of the unpolished surfaces.

### **7.3.2 Statistical Significance of Water Contact Angle Tests on Sintered Compacts**

The Student's T-Test was carried out to determine the statistical significance of the results of the water contact angle tests on the sintered compact surfaces. Three sets of results ( $n = 3$ ) were obtained for each time point and the detailed calculations are attached in Appendix 6.

There was no significant difference in water contact angle measurements between the polished and unpolished surfaces of the pure titanium specimens ( $p > 0.1$ ), as well as the 10-5 specimens ( $p > 0.1$ ), at all time points. Polishing the surfaces of

the 10-10 specimens, however, significantly increased the water contact angle of the surfaces ( $p < 0.05$ ).

There was no significant difference in the water contact angle of the polished surfaces of the pure titanium specimen and the 10-5 specimen ( $p > 0.1$ ) and the 10-10 specimens ( $p > 0.05$ ). Additionally, there was no significant difference in water contact angle of the unpolished surfaces of the pure titanium specimens and the 10-5 specimens ( $p > 0.1$ ). There was, however, a significant difference between the water contact angle measurements on the unpolished surfaces of the pure titanium specimen and the 10-10 specimen ( $p < 0.05$ ).

### 7.3.3 alamarBlue™ Reduction of Sintered Compacts

The proliferation rates of 3T3 cells and rat osteoblast were measured quantitatively by determining the extent of alamarBlue™ Reduction at various time points. alamarBlue™ is a redox indicator which undergoes reduction in response to metabolic activity. The alamarBlue™ reduction yields a colorimetric change, whose spectrophotometric absorbance could be measured with a microplate reader. Cells seeded on a tissue culture plate, at the same density as those seeded on the compacts, were used as controls. The alamarBlue™ reduction of the cells seeded on the compacts were measured and plotted at various time points, as a fraction of the reduction measured in the control group, as shown in Figure 7.9 and 7.10 below.

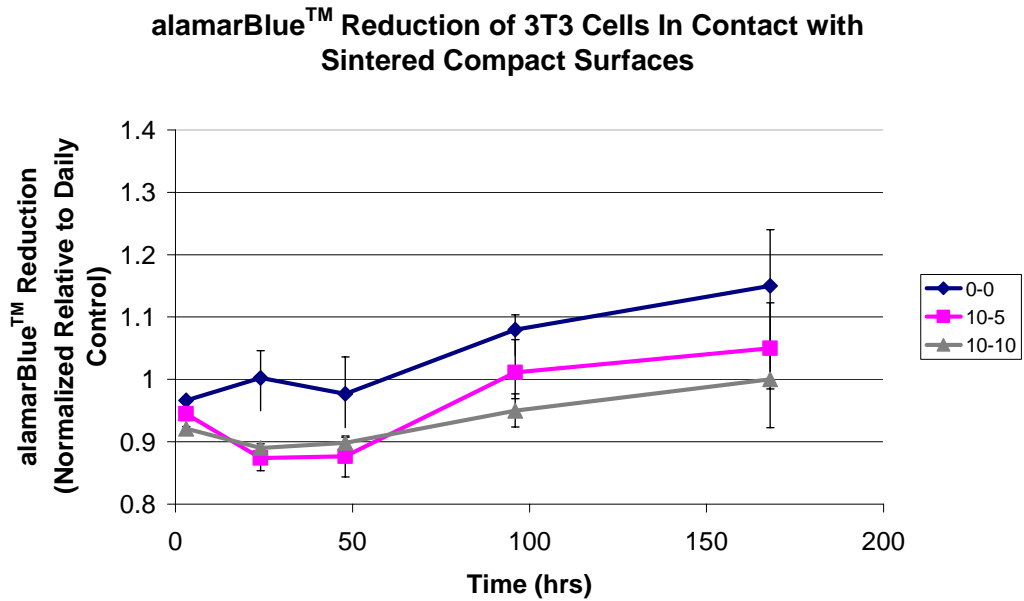


Figure 7.9: alamarBlue™ reduction of 3T3 cells seeded on compact surfaces

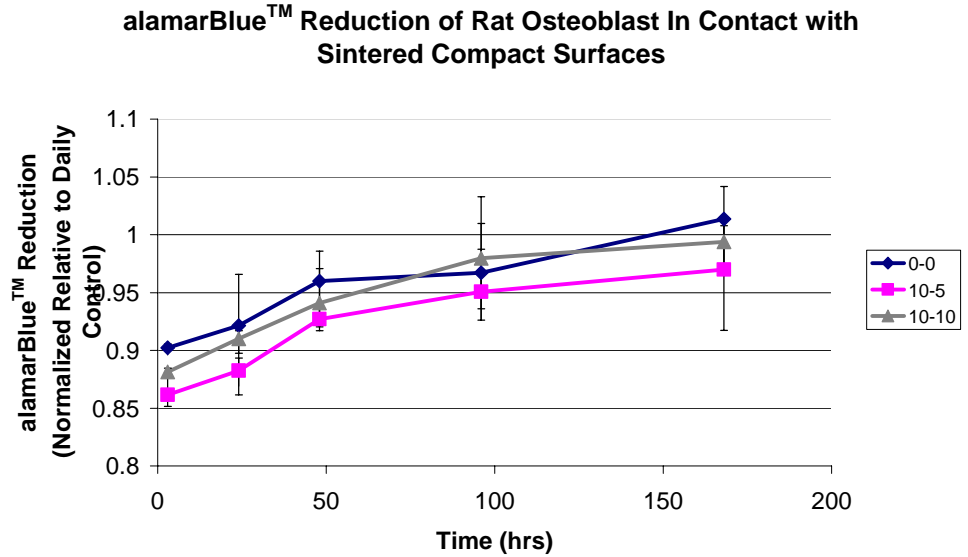


Figure 7.10: alamarBlue™ reduction of rat osteoblast seeded on compact surfaces

### **7.3.4 Statistical Significance of Cell Proliferation Assay Involving**

#### **Sintered Compacts**

The Student's T-Test was carried out to determine the statistical significance of the cell proliferation assay involving wear debris. Five sets of results ( $n = 5$ ) were obtained for each time point and the detailed calculations are attached in Appendix 7.

There was significant difference in alamarBlue™ reduction of the 3T3 cells when the cells were first seeded (3 hours) on the 10-5 ( $p < 0.05$ ) and 10-10 ( $p < 0.001$ ) specimen surfaces, as compared to the alamarBlue™ reduction of 3T3 cells seeded on pure titanium surfaces. The presence of graphite on the surfaces of the 10-5 and 10-10 specimens may have had an affect on the cellular adhesion on the specimen surfaces. Similarly, there was significant difference in alamarBlue™ reduction of the rat osteoblast when the cells were first seeded (3 hours) on the 10-5 ( $p < 0.001$ ) and 10-10 ( $p < 0.001$ ) specimen surfaces, as compared to the alamarBlue™ reduction by rat osteoblast seeded on pure titanium surfaces.

Between 24 hours to one week, there was significant difference in alamarBlue™ reduction of the 3T3 cells seeded on the 10-5 and 10-10 surfaces ( $p < 0.05$ ) as compared to the alamarBlue™ reduction of 3T3 cells seeded on pure titanium surfaces. The rat osteoblast seeded on the 10-5 specimen surface had a significant difference in alamarBlue™ reduction at between 24 hours to 48 hours after cell seeding ( $p < 0.05$ ), as compared to the alamarBlue™ reduction by rat osteoblast seeded on pure titanium

## **Chapter 7: Biocompatibility Studies**

---

surfaces. Thereafter, however, at 96 hours and 1 week after cell seeding, there was no significant difference in alamarBlue™ reduction by rat osteoblast seeded on the 10-5 surfaces, as compared to those seeded on the pure titanium surfaces ( $p > 0.1$ ).

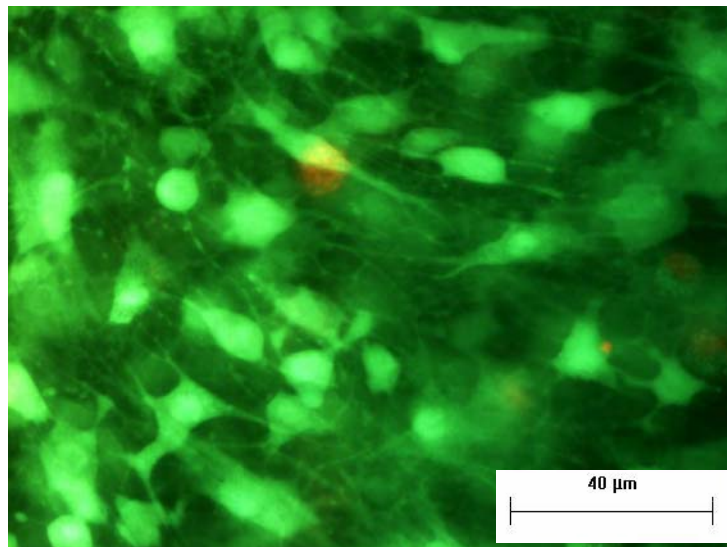
There was no significant differences in the alamarBlue™ reduction by rat osteoblast seeded on the 10-10 specimen surfaces, as compared to those seeded on the pure titanium surfaces, between 24 hours and 1 week after cell seeding was performed ( $p > 0.1$ ).

Hence the results indicate that the presence of graphite on the specimen surfaces may have an impact on cellular adhesion, but not significantly on cellular proliferation..

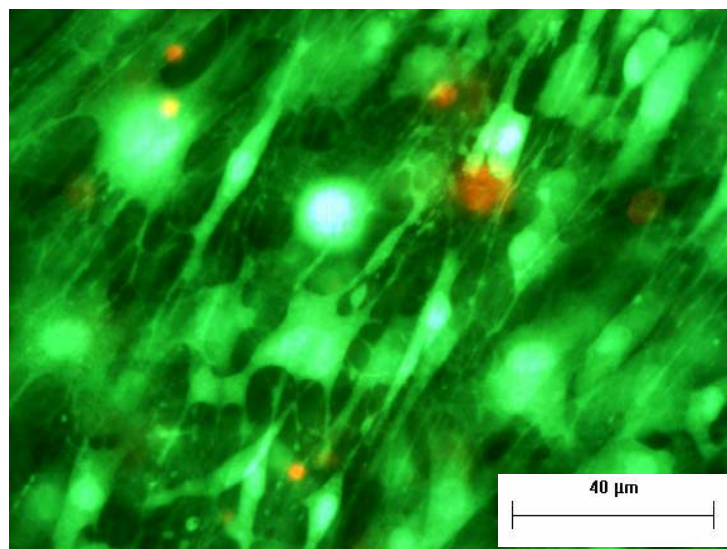
### **7.3.5 Fluorescence Microscopy of Sintered Compacts**

The distribution of viable and dead cells on the surface of the compacts was determined using the LIVE/DEAD® Viability/ Cytotoxicity Assay Kit (Molecular Probes, USA), which consists of two dyes: Calcein AM and of Ethidium homodimer-1 (EthD-1) as described in Section 4.9.4. The Calcein AM produces an intense green fluorescence in live cells while EthD-1 produces a bright red fluorescence in dead cells. The results of the fluorescence microscopy of 3T3 cells two weeks after seeding on the compact surfaces are shown in Figure 7.11 below:

a)



b)



c)

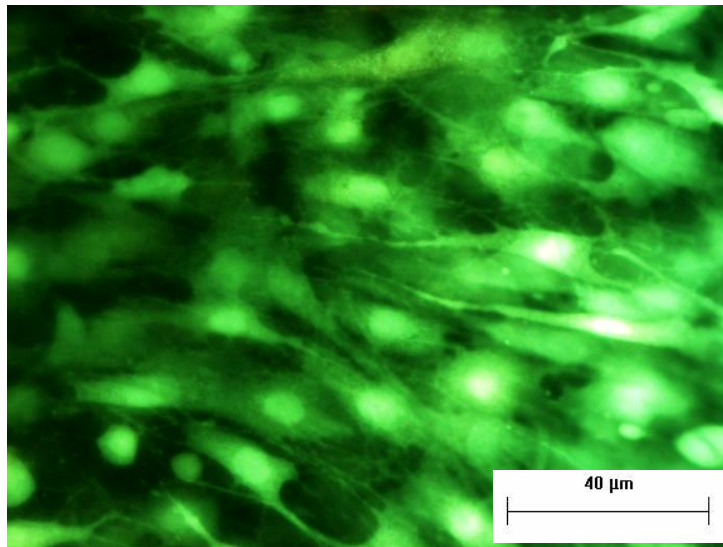
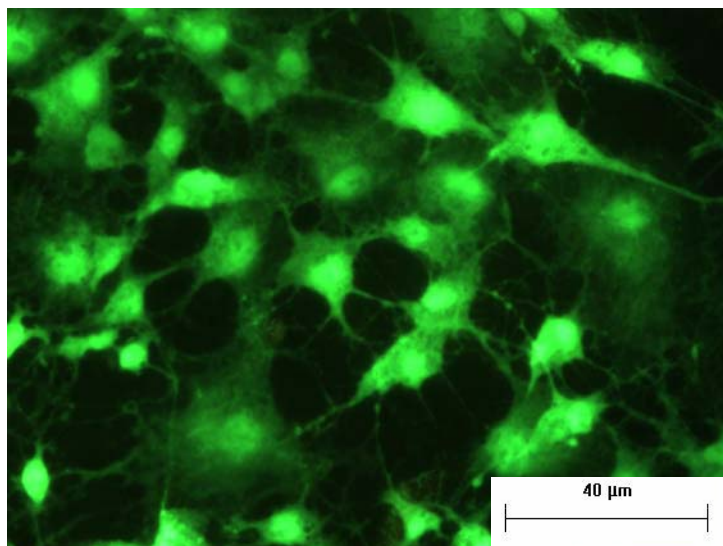


Figure 7.11: Fluorescence microcopy of 3T3 cells 1 week after seeding on compact surface: a) 0-0 surface; b) 10-5 surface; and c) 10-10 surface

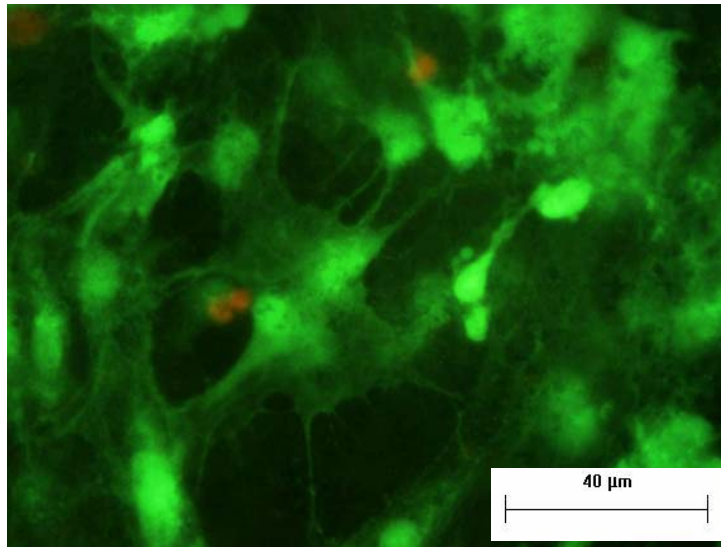
The distribution of viable cells of the rat osteoblasts were similarly studied, and the images shown in Figure 7.12 below:

a)





b)



c)

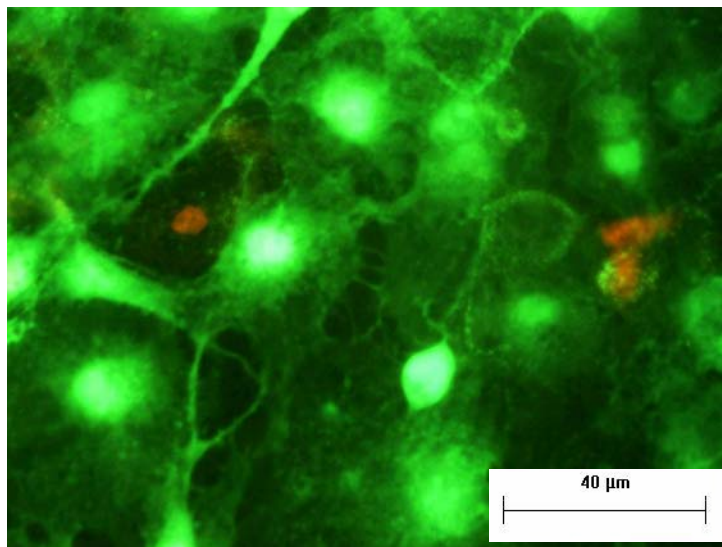


Figure 7.12: Fluorescence microcopy of rat osteoblast 1 week after seeding on compact surfaces: a) 0-0 surface; b) 10-5 surface; and c) 10-10 surface

### 7.3.6 Discussion on Biocompatibility of Sintered Compacts

From the micrographs obtained through fluorescence microscopy, it was observed that both the 3T3 cells and rat osteoblasts adhered well onto the polished surfaces of all compacts after 1 week. The surfaces of the polished compacts were not cytotoxic to the cells and there was no distinct region on each compact whereby an increased density of non-viable cells (stained red) was observed.

The cells seeded on the surfaces of the titanium-graphite composites have slightly lower proliferation, as compared to those cells seeded on the pure titanium surfaces, after one week. One possible explanation could be the presence of graphite particles on the composite specimen surfaces slightly hindered cellular adhesion.

There was a slight dip in cell proliferation, compared with the respective control, in both the 3T3 and rat osteoblast cultures 3 hours after cell seeding. This reduction in proliferation could be due to the hydrophobic nature of the compact surfaces, which could have hindered cellular adhesion. The cell proliferation stabilized for both phenotypes, with respect to the daily control, 48 hours after cell seeding. The 3T3 cells and rat osteoblast seeded on the compact surfaces did not exhibit an appreciable reduction in proliferation compared to the daily control one week after cells seeding. The 3T3 cells indeed exhibited increased proliferation on the 0-0 and 10-5 surfaces. These results indicate that the polished compact surfaces osteoblast and fibroblast adhesion and are biocompatible.

## **Chapter 7: Biocompatibility Studies**

---

There was no observable alteration in morphology of both the 3T3 cells and rat osteoblast, with respect to the control group of each phenotype (cultured on tissue culture plates).

## **Chapter Eight**

### **Conclusions and Recommendations**

#### **8.1 Conclusions**

The objectives set forth in this study have been achieved. The microstructure, mechanical properties and biocompatibility of the titanium-graphite composites has been investigated and characterized in this study.

Metal matrix composites comprising commercially pure titanium powder, of mean particle size 40  $\mu\text{m}$ , and graphite powder of mean particle size 10  $\mu\text{m}$ , were thoroughly mixed through mechanofusion system, consolidated by the blended elemental method, sintered and finally hot isostatically pressed to form compacts of porosities between 0.41% to 1.81%. The average pore size of the compacts increased with increasing graphite content and ranged from 4  $\mu\text{m}$  to 11  $\mu\text{m}$ . The pores were observed predominantly at the grain boundaries and the boundaries between titanium carbide and the titanium matrix. The microstructure of the pure titanium specimens consisted of equiaxed grains of average size 140  $\mu\text{m}$ . The microstructure of the titanium-graphite composites (10-5 and 10-10 specimens), on the other hand, consisted of three phases: equiaxed titanium matrix, titanium carbide and unreacted graphite. The average grain size of the titanium matrix in the 10-5 and 10-10 specimens were 32  $\mu\text{m}$  and 21  $\mu\text{m}$  respectively. The unreacted graphite content increased with increasing initial graphite composition and were observed to be present within the pores.

## Chapter 8: Conclusions and Recommendations

---

The Vickers hardness of the compacts was evaluated in three different orientations, namely the cross-section, longitudinal and transverse sections. The average Vickers Hardness of the 0-0, 10-5 and 10-10 specimens were 275 HRV, 395 HRV and 500 HRV respectively. The hardness of the compacts did not vary significantly with the orientation, indicating that the hot isostatic pressing had consolidated the compacts uniformly, and the distribution of the titanium, titanium carbide and graphite phases, as well as the porosity, was uniform throughout the compact.

The uniaxial tensile properties of the compacts were investigated in this study. The Modulus of Elasticity of the 0-0, 10-5 and 10-10 compacts were 113.4 GPa, 152.4 GPa and 157.0 GPa, respectively. The formation of the titanium carbide phase increased the stiffness of the composites, with respect to the pure titanium specimens. Increasing the graphite content of the raw powder mixture from 5% to 10% yielded diminishing returns in increased stiffness of the composite. The increase in graphite content, however, brought about a decrease in tensile strength of the composites. The fatigue performance of the compacts was also evaluated in the present study. The fatigue limits of the 0-0 and 10-5 specimens were 100 MPa and 85 MPa. These figures represent low tensile fatigue strengths. The Endurance Ratio of both specimens, is also very low, at 0.16 and 0.22 respectively. This indicates that there is low resistance to crack propagation. An examination of the fatigue fracture surfaces of the 10-5 specimens provided ample evidence of rapid crack propagation. It was anticipated that the fatigue performance of the 10-10

## Chapter 8: Conclusions and Recommendations

---

specimens would be very poor and hence all available 10-10 specimens were used in the tensile tests. The sintered, HIPped specimens hence display poor fatigue resistance, and may not be suitable for applications involving uniaxial, tensile and cyclic loading.

The biocompatibility of the raw powder, wear debris and bulk compacts were investigated. Two different phenotypes of cells were used in this study: NIH 3T3 ECACC cell line and primary rat osteoblast cell cultures. The cell proliferation rate was determined from the alamarBlue<sup>TM</sup> reduction at various time points, normalized to the daily control. The distribution of viable cells, on the other hand, was determined through fluorescence microscopy.

The in vitro biocompatibility study of raw powder has revealed that the presence of pure titanium particles did not affect fibroblast proliferation significantly. The pure graphite particles, on the other hand, brought about a 10% reduction in proliferation fibroblast after 1 week. The binary powder mixtures (10-5 and 10-10) caused a reduction in fibroblast proliferation by between 2.5 % to 7.5 %. This reduction in proliferation could be attributed to the presence of graphite particles. The impact of the raw powder on the proliferation of rat osteoblasts was more significant. The graphite particles caused the greatest reduction in cell proliferation of up to 20 %. The pure titanium particles, meanwhile, brought about a reduction in cell proliferation of up to 6 % after 1 week. The 10-5 and 10-10 powder particle evoked an intermediate cytotoxic response, reducing rat

## Chapter 8: Conclusions and Recommendations

---

osteoblast proliferation by about 10%. There was evidence of phagocytocys of particles below 6  $\mu\text{m}$  by viable cells of both phenotypes. Internalization of particles, up to a certain threshold level, would not cause apoptosis of the cells, but did cause the cells to elongate. Larger particles, above 10  $\mu\text{m}$ , meanwhile, were not phagocytosed, but were observed to be attached to the plasma membrane of the viable cells.

The wear debris proved to be more cytotoxic than the raw powder particles, especially to the rat osteoblasts. The pure titanium wear reduced cellular proliferation of rat osteoblast by up to 10 % after 1 week, but did not significantly affect the proliferation of the 3T3 cells. Wear debris from the titanium-graphite composite brought about a reduction in cell proliferation of the rat osteoblasts and 3T3 cells, by up to 16 % and 5 %, respectively after 1 week. The increased cytotoxicity of the wear debris could be attributed to the smaller particle size of the wear debris.

The 3T3 cells and rat osteoblasts were observed to adhere to the polished surfaces of the compacts. The cells seeded on the surfaces of the titanium-graphite composites slightly lower proliferation, as compared to those cells seeded on the pure titanium surfaces, after one week. This observation could be attributed to the presence of graphite particles on the composite specimen surfaces slightly hindered cellular adhesion. There was no observable change in morphology of the cells seeded on the compact surfaces, as compared to the control group, which

were seeded on tissue culture plates. These results indicate that the polished compact surfaces promoted osteoblast and fibroblast adhesion and are biocompatible.

### 8.2 Recommendations

While the present study has been successful in characterizing the microstructure, mechanical properties and biocompatibility of the titanium-graphite composites, there are yet several ways in which the research could be improved upon.

Firstly, the mixing of the powder mixture could be further improved to yield discreet regions of titanium carbide, distributed evenly throughout the titanium matrix, with a concurrent increase in grain size of the titanium matrix, upon sintering. This would produce compacts of higher tensile and fatigue strength.

Secondly, while the composites performed poorly in uniaxial tensile and fatigue test due to their inherent brittleness, this would not preclude their use in applications involving compressive forces. Hence, experiments should be conducted to determine their compressive strengths and fatigue properties under cyclic compressive loads.

Thirdly, the fretting fatigue performance of the composites could be evaluated. The presence of lubricating graphite film on the surface of the composites may yield superior fretting fatigue performance, as compared to pure titanium specimens.



## **Chapter 8: Conclusions and Recommendations**

---

Lastly, while the in vitro studies provided an insight on the biocompatibility of the titanium-graphite raw powder, wear debris and bulk compacts, it is necessary to perform in vivo experiments to determine the full extent of biocompatibility of the material.

## References

- [1] Teoh, S.H., Thampuran, R., Seah, W.K.H. and Goh, J.C.H. Sintered titanium - graphite composite having improved wear resistance and low frictional characteristics. Singapore, 24 June 1997. (Singapore Patent, Application No. 9501510-3, Filed 17 November 1996; Japanese Patent, Application No. 8-264937, Filed 24 June 1997; German Patent, Application No. 196 41023.1, Filed 10 April 1997)
- [2] <http://www.mamashealth.com/bodyparts/jointrep.asp>
- [3] <http://www.investincanada.gc.ca/en/942/Markets.html>
- [4] <http://rheumatology.oxfordjournals.org/cgi/content/full/41/7/824>
- [5] Savarino, L., Granchi, D., Ciapetti, G., Cenni, E., Nardi Pantoli, A., Rotini, R., Veronesi, C.A., Baldini, N., Giunti, A. Ion Release in Patients with Metal-on-Metal Hip Bearings in Total Joint Replacement: A Comparison with Metal-on-Polyethylene Bearings J Biomed Mater Res (Appl Biomater) 63: 467–474, 2002
- [6] Vermes, C., Glant, T.T., Hallab, N.J., Fritz, E.A., Roebuck, K.A. and Jacobs, J.J. The Potential Role of the Osteoblast in the Development of Periprosthetic Osteolysis. Review of In Vitro Osteoblast Responses to Wear Debris, Corrosion Products, and Cytokines and Growth Factors. The Journal of Arthroplasty Vol. 16 No. 8 Suppl. 1 2001
- [7] Jacobs J.J., Shanbhag A., Glant T.T., et al Wear debris in total joint replacements. J Am Acad Orthop Surgery 2:212, 1994
- [8] Shanbhag A.S., Jacobs J.J., Glant T.T., et al: Composition and morphology of wear debris in failed uncemented total hip replacement arthroplasty. J Bone Joint Surgery Br 76:60, 1994
- [9] Brunette, D.M., Tengvall, P., Textor, M., Thomsen, P. Titanium in Medicine. Materials Science, Surface Science, Engineering, Biological Responses and Medical Applications.
- [10] Suresh, S. Fatigue of Materials, 2<sup>nd</sup> Edition. Cambridge University Press
- [11] [http://en.wikipedia.org/wiki/Metal\\_fatigue#The\\_S-N\\_curve](http://en.wikipedia.org/wiki/Metal_fatigue#The_S-N_curve)

- [12] <http://www.azom.com/details.asp?ArticleID=1341>
- [13] <http://www.matweb.com/>
- [14] <http://www.azom.com/details.asp?ArticleID=1341>
- [15] Nakazawa, K., Sumita, M., Maruyama, N. Effect of Contact Pressure on Fretting Fatigue of High Strength Steel and Titanium Alloy. ASTM STP 1159, (1992), 115 – 125
- [16] Harris, L.G., Patterson, L.M., Bacon, C., ap Gwynn, I., Richards, R.G. Assessment of the cytocompatibility of different coated titanium surfaces to fibroblasts and osteoblasts J Biomed Mater Res 73A: 12–20, 2005
- [17] Bogdanski, D., Köller, M., Müller, D., Muhr, G., Bram, M., Buchkremer, H.P., Stöver, D., Choi, J., Epple, M. Easy assessment of the biocompatibility of Ni–Ti alloys by in vitro cell culture experiments on a functionally graded Ni–NiTi–Ti material. Biomaterials 23 (2002) 4549–4555.
- [18] Trentz, O. A. , Zellweger, R., Amgwerd, M. G. and Uhlschmid, G. K. Testing bone implants on all lines and human osteoblasts. Unfallchirurg (1997) 100:39–43
- [19] Roberta, T., Federico, M., Federica, B., Antonietta, C.M., Sergio, B., Ugo, C. Study of the potential cytotoxicity of dental impression materials Toxicology in Vitro 17 (2003) 657–662
- [20] O’Connor, D.T., Choi, M.G., Kwon, S.Y., Sung, K.L.P. New insight into the mechanism of hip prosthesis loosening: effect of titanium debris size on osteoblast function. Journal of Orthopaedic Research 22 (2004) 229–236
- [21] Pioletti, D.P., Takei, H., Kwon, S.Y., Wood, D., Sung, K.L. The cytotoxic effect of titanium particles phagocytosed by osteoblasts. J Biomed Mater Res 1999;46:399–407.
- [22] Saldan, L., Vilaboa, N., Valle’s, G., Gonza’lez-Cabrero, J., Munuera, L. Osteoblast response to thermally oxidized Ti6Al4V alloy. Journal of Biomedical Materials Research Part A. Volume 73A, Issue 1, Date: 1 April 2005, Pages: 97-107
- [23] <http://www.azom.com/details.asp?ArticleID=1630>
- [24] Goetzel, C.G.. Treatise on Powder Metallurgy, New York. Interscience Publishers, 1949.

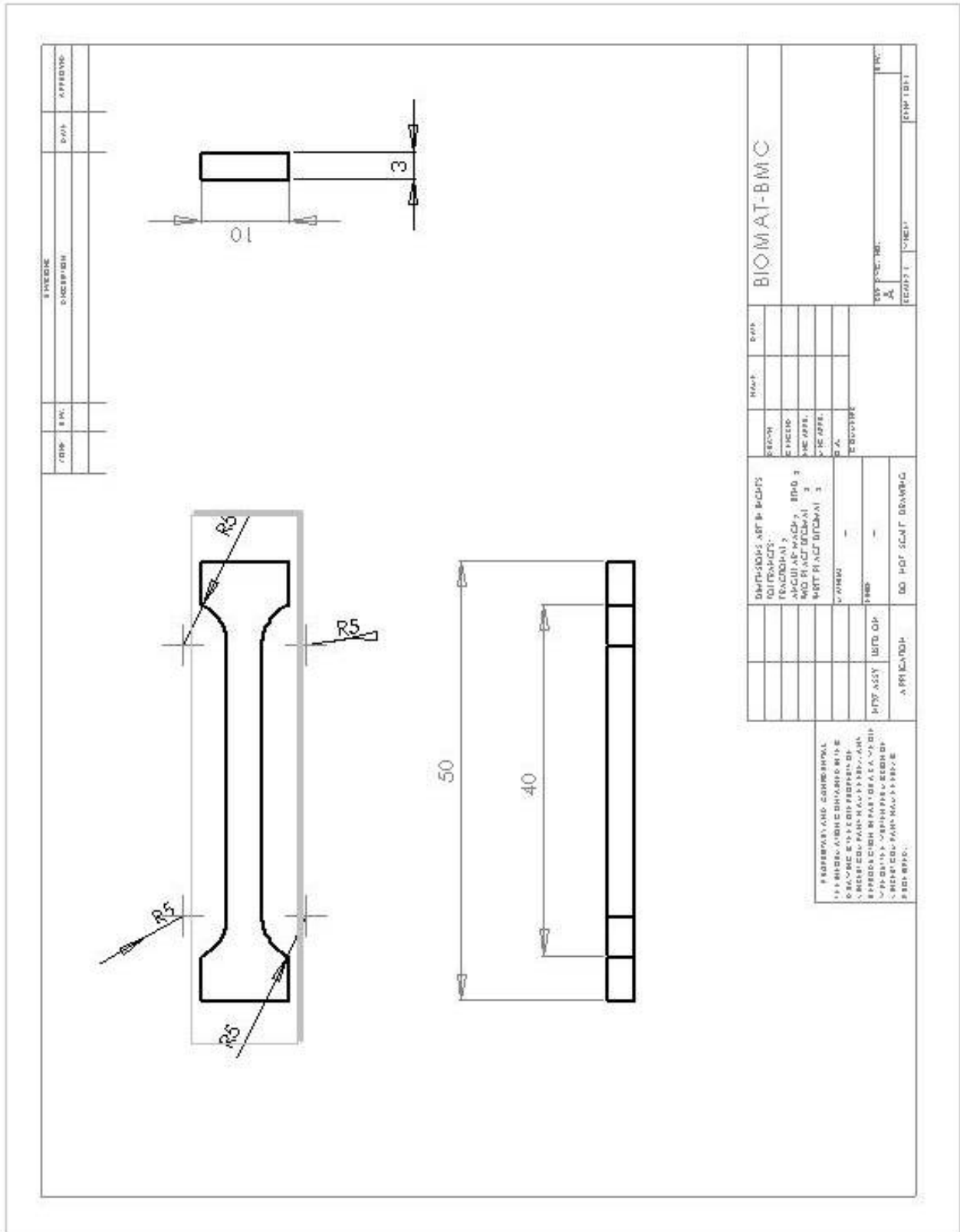
- [25] Harrigan, W.C.. Commercial processing of metal matrix composites. *Materials Science And Engineering A-Structural Materials Properties Microstructure And Processing* 244 (1): 75-79 Mar 31 1998.
- [26] German, R.M. Powder metallurgy science Princeton, N.J. : Metal Powder Industries Federation , c1984.
- [27] Kingery, W.D. and Berg, M. Study of the Initial Stages of Sintering Solids by Viscous Flow, Evaporation-Condensation and Self Diffusion, *J. Appl Phys.*, 26. No. 10. 1955
- [28] Ichinose, H. and Kuczynski, G.C. Role of Grain Boundaries in Sintering. *Acta Metall.*, 10. 1962.
- [29] Shaw, N.B. and Honeycombe, R.W.K. Some Factors Influencing the Sintering Behaviour of Austenitic Stainless Steel Powders. *Powder Met.*, Vol. 20.
- [30] <http://hip.bodycote.com/resources/presenter.pdf>
- [31] <http://hip.bodycote.com/resources/ebody6.pdf>
- [32] [http://www.ahip.com/WebPages/isostatic\\_overview.html](http://www.ahip.com/WebPages/isostatic_overview.html)
- [33] Agarwal S.. The difficult primary hip. *Current Orthopaedics* (2004) 18, 451–460
- [34] Chassot, E., Irigaray, J.L., Terver, S., Vanneuville, G. Contamination by metallic elements released from joint prostheses. *Medical Engineering & Physics* 26 (2004) 193–199.
- [35] <http://arthritis.about.com/cs/hip/a/postopclots.htm>
- [36] <http://orthopedics.about.com/od/hipkneereplacement/a/implants.htm>
- [37] McGee, M.A., Howie, D.W., Costi, K., Haynes, D.R., Wildenauer, C.I., Percy, M.J., McLean, J.D. Implant retrieval studies of the wear and loosening of prosthetic joints: A review. *Wear* 241 2000 158–165
- [38] Bershadsky, A.D., Tint, I.S., Neyfakh, A.A. Jr, Vasiliev, J.M. Focal contacts of normal and RSV-transformed quail cells. Hypothesis of the transformation-induced deficient maturation of focal contacts. *Exp Cell Res* 1985;158:433– 444.
- [39] Geiger, B., Tokuyasu, K.T., Dutton, A.H., Singer, S.J. Vinculin, an intracellular protein localised at specialist sites where micro- filament bundles terminate at cell membranes. *Proc Natl Acad Sci USA* 1980;77:4127– 4131.
- [40] ap Gwynn, I. Cell biology at interfaces. *J Mater Sci Mater Med*1994;5:357–360.

- [41] Helfman, D.M., Levy, E.T., Berthier, C., Shtutman, M., Riveline, D., Grosheva, I., Lachish-Zalait, A., Elbaum, M., Bershadsky, A.D. Caldesmon inhibits non muscle cell contractility and interferes with the formation of focal adhesions. *Mol Biol Cell* 1999;10: 3097–3112.
- [42] Perren, S.M. Titanium as an implant material: clinical performance in new technologies. *Eur Cell Mater* 2001;1:2.
- [43] Woodward, S.C., Salthouse, T.N. The tissue response to implants and its evaluation by light microscopy. In: von Recum AF, editor. *Handbook of biomaterial evaluation*. London: Collier Macmillan; 1986. p 364–378.
- [44] Gristina, A.G. Biomaterial-centered infection: microbial adhesion versus tissue integration. *Science* 1987;237:1588 –1595.
- [45] Ruedi, T.P., Murphy, W.M. *AO principles of fracture management*. Stuttgart: AO Publishing Thieme; 2000.
- [46] Agarwal, S. Osteolysis – basic science, incidence and diagnosis. *Current Orthopaedics* (2004) 18, 220–231
- [47] Eftekhari, N.S., Demarest, R.J. In: *Total hip arthroplasty*, xxxii, 1679, 49. St. Louis: Mosby; 1993. p. 2.
- [48] Engh, C.A., Massin, P., Suthers, K.E. Roentgenographic assessment of the biologic fixation of porous-surfaced femoral components. *Clin Orthop* 1990:107–28.
- [49] Friedman, R.J., Black, J., Galante, J.O., Jacobs, J.J., Skinner, H.B. Current concepts in orthopaedic biomaterials and implant fixation. *Instr Course Lect* 1994;43:233–55.
- [50] Maloney, W.J., Smith, R.L., Castro, F., Schurman, D.J. Fibroblast response to metallic debris in vitro. *J Bone Jt Surg* 1993; 75A:835}44.
- [51] Bruinink, A., Schroeder, A., Francz, G., Hauert, R. In vitro studies on the effect of delaminated a-C:H film fragments on bone marrow cell culture. *Biomaterials* 26 (2005) 3487–3494
- [52] Olivier, V., Duval, J.L., Hindie, M., Nagel, M.D. Comparative particle-induced cytotoxicity towards macrophages and fibroblasts. *Cell Biology and Toxicology*. 2003; 19: 145 – 159.

- [53] Price, R.L., Haberstroh, K.M., Webster, T.J. Improved osteoblast viability in the presence of smaller nanometre dimensioned carbon fibres. *Nanotechnology* 15 (2004) 892–900.
- [54] Elias K.E., Price R.L., and Webster T.J. 2002 Enhanced functions of osteoblasts on nanometre diameter carbon fibers. *Biomaterials*; 23: 3279–87.
- [55] Price R.L., Waid, M.C., Haberstroh, K.M. and Webster, T.J. 2003 Selective bone cell adhesion on formulations containing carbon nanofibers *Biomaterials*; 24: 1877–87
- [56] Blazewicz, M. Carbon materials in the treatment of soft and hard tissue findings *Eur. Cells Mat.* 2 21–9 (2001).
- [57] Harris, W.H. Wear and periprosthetic osteolysis. The problem. *Clin Orthop* 2001;393:66–70.
- [58] Pioletti, D.P., Leoni, L., Genini, D., Takei, H, Du, P., Corbeil, J. Gene expression analysis of osteoblastic cells contacted by orthopedic implant particles. *J Biomed Mater Res* 2002;61:408–420.
- [59] Salvati, E.A., Foster, B., Doty, S.B. Particulate metallic debris in cemented total hip arthroplasty. *Clin Orthop* 1993;293:160–173.
- [60] Bioresource alamarBlue™ Booklet:  
<http://www.biosource.com/content/literatureContent/PDFs/alamarbluebooklet.pdf>
- [61] Ahmed, S.A., Gogal, R.M. and Walsh, J.E. (1994)  
A new rapid and non-radioactive assay to monitor and determine the proliferation of lymphocytes: an alternative to [3H] thymidine incorporation assay. *J. Immunol. Meth.* 170: 211-224.
- [62] <http://www.matweb.com>
- [63] Puleo, D.A. and Huh, W.W. Acute toxicity of metal ions in cultures of osteogenic cells derived from bone marrow stromal cells *J. Appl. Biomater.* 6 109–16(1995)
- [64] Thompson, G.J. and Puleo, D.A. Effects of sublethal metal ion concentrations on osteogenic cells derived from bone marrow stromal cells *J. Appl. Biomater.* 6 249–58 (1995)
- [65] Wang M.L., Nesti, L.J., Tuli, R., Lazatin, J., Danielson, K.G., Sharkey, P.F., Tuan, R.S. Titanium particles suppress expression of osteoblastic phenotype in human mesenchymal stem cells *Journal of Orthopaedic Research* 20 (2002) 1175–1184

- [66] Wang, M.L., Tuli, R., Manner, P.A., Sharkey, P.F., Hall, D.J., Tuan, R.S. Direct and indirect induction of apoptosis in human mesenchymal stem cells in response to titanium particles. *Journal of Orthopaedic Research* 21 (2003) 697–707
- [67] <http://www.skyscan.be/next/downloads.htm>
- [68] Pioletti, D.P., Takei, H., Lin, T., Van Landuyt, P., Ma Q.J., Kwon S.Y., et al. The effects of calcium phosphate cement particles on osteoblast functions. *Biomaterials* 2000;21:1103–14.
- [69] Yang, T.S., Shiu, C.B., Wong, M.S. Structure and hydrophilicity of titanium oxide films prepared by electron beam evaporation.

**Engineering Drawing of Tensile and Fatigue Tests Specimens**



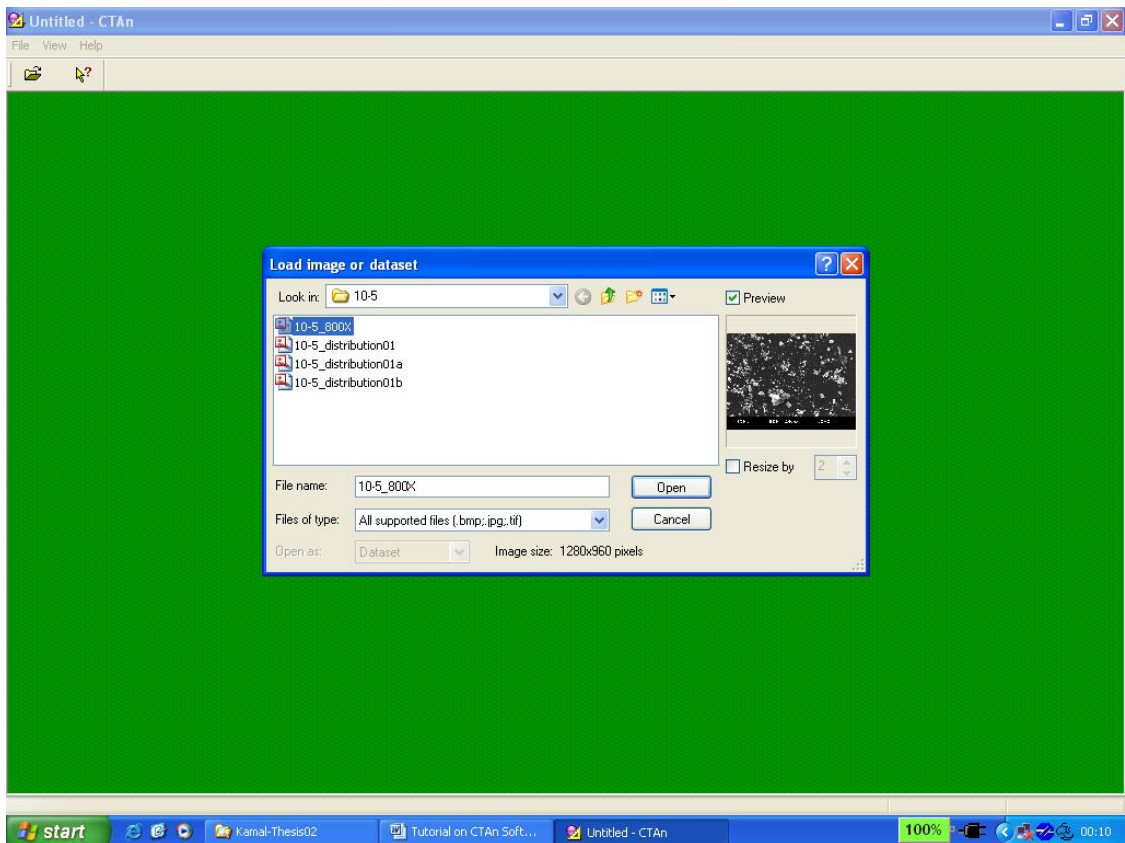




## Appendix 3

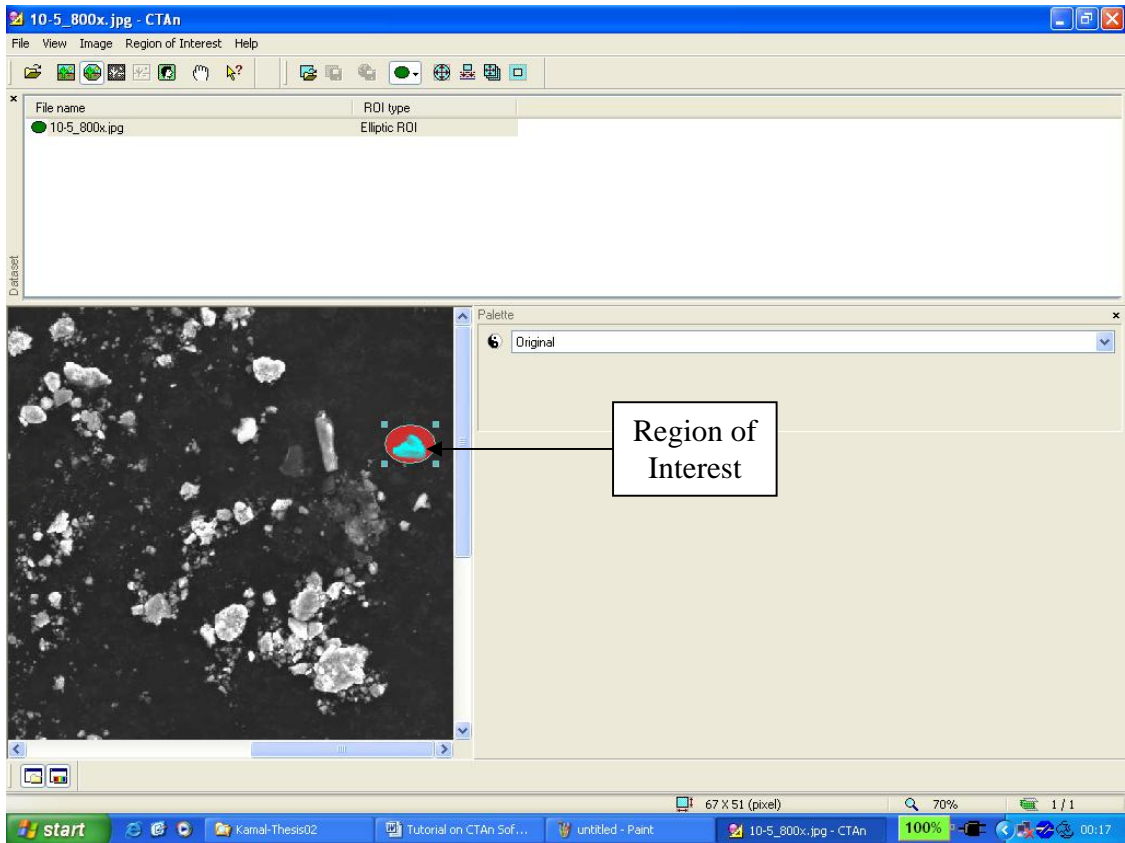
### Tutorial on Using CTAn Software to Determine Particle Size Distribution

- 1) Start the CTAn software.
- 2) Open the image file of the particles to be measured.



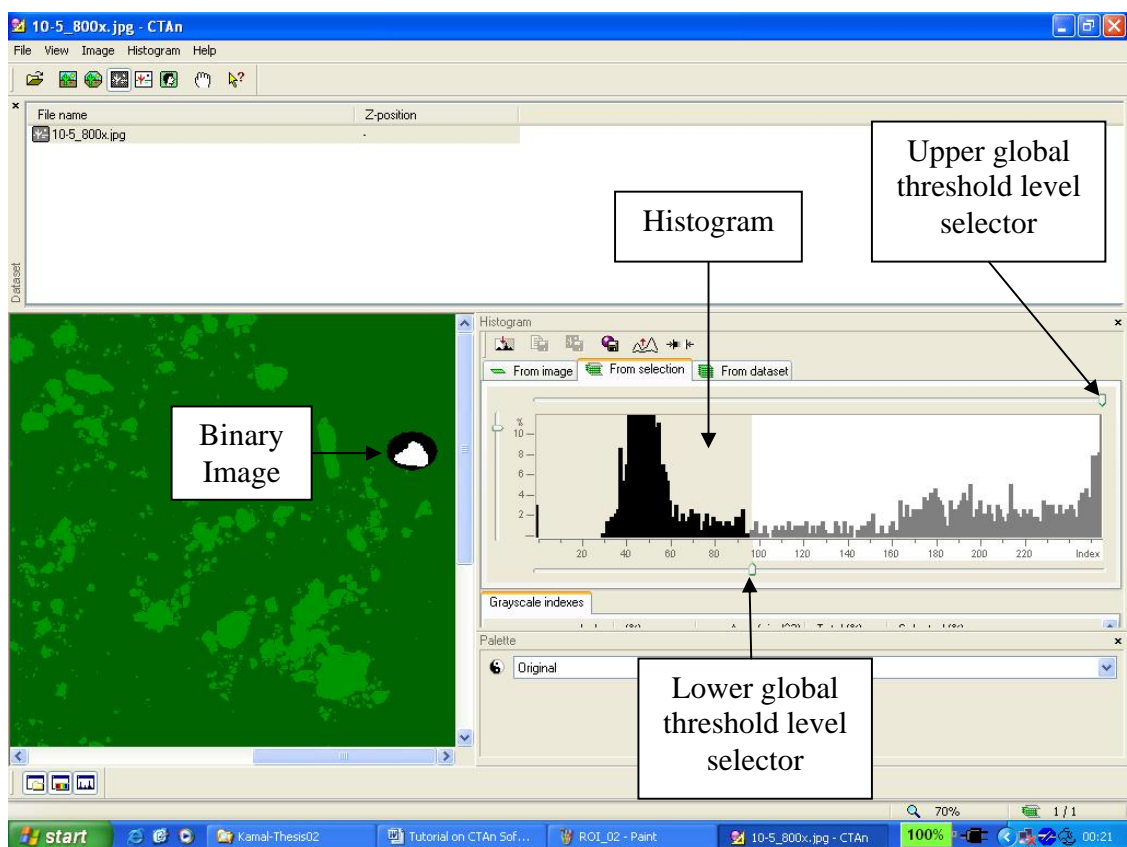
## Appendix 3

- 3) Select region of interest (ROI) on the image file. The region of interest would be highlighted red. To calibrate the pixel count data to linear dimensions of the particles, adjust the ROI such that it would cover only one discrete particle.




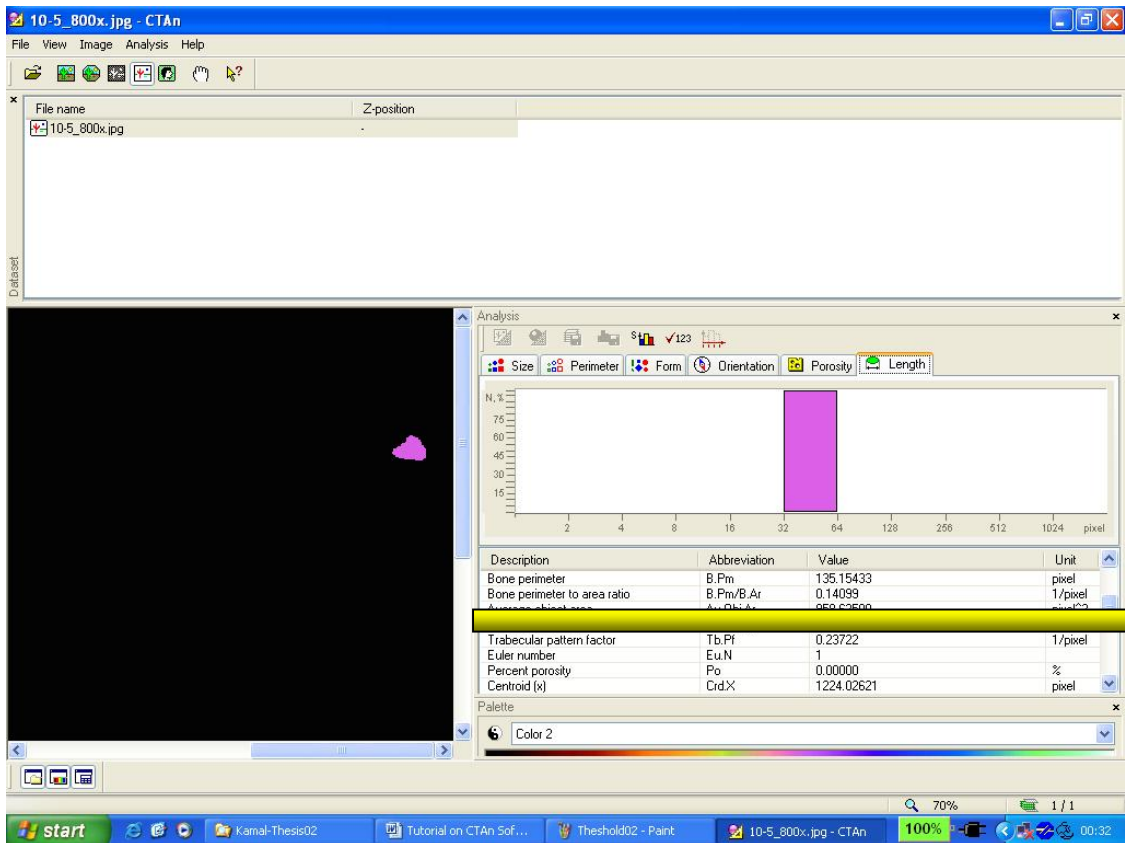
## Appendix 3

- 4) Convert the region of interest to a binary image for analysis. Select the upper and lower global threshold levels by sliders above and under the histogram. Care must be taken to ensure that only the relevant particles are completely selected. The white part of the binary image represents solid objects for the subsequent 2D and 3D analysis.



## Appendix 3

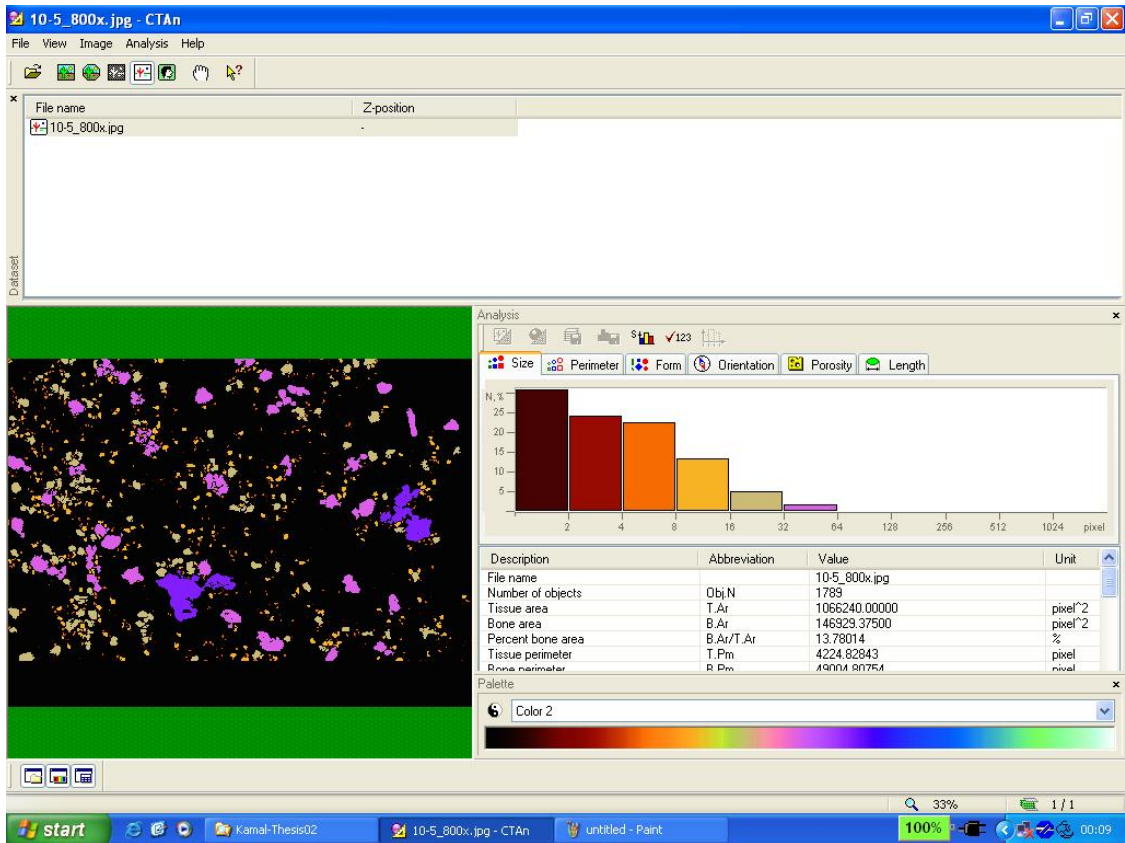
- 5) Click on the “Process Image” button . This function will compute the pixel count for each discrete particle, and display the information on a bar chart. In this example, as shown in the highlighted box below, the average object size is 34.9 pixel.



- 6) Measure the actual particle size from the original image, using the image scale bar. In this example, the size of the particle is 9.8  $\mu\text{m}$ . Hence each micron is represented by 3.6 pixels.
- 7) Repeat Steps 2 to 6 for five other discrete particles on the image, one at a time. Determine the average number of pixels representing one micron.

## Appendix 3

- 8) Now repeat Steps 2 to 6 for all the particles. A particle size distribution bar chart, based on pixel count would be produced. Convert the pixel count to microns, and the particle size distribution of the sample would be obtained.



**Calculations for the Students T-Test on the Cell Proliferation Assay  
Involving Raw Powder**

3T3 Cells	Specimen			
Time: 3 hrs	0-0	$x^2$	10-5	$x^2$
Replicate, $x_1$	0.97	0.94	0.96	0.92
Replicate, $x_2$	0.99	0.97	0.99	0.98
Replicate, $x_3$	0.95	0.90	0.95	0.90
Replicate, $x_4$	0.97	0.93	0.94	0.88
Replicate, $x_5$	0.98	0.96	0.96	0.92
Average ( $\bar{x}$ )	0.97		0.96	
$\Sigma x^2$	4.71		4.61	
$(\Sigma x)^2$	23.52		23.04	
$((\Sigma x)^2)/n$	4.70		4.61	
$\Sigma d^2 = \Sigma x^2 - ((\Sigma x)^2)/n$	7.50E-04		1.40E-03	
$\sigma^2 = \frac{\Sigma d^2}{n-1}$	1.88E-04		3.50E-04	
$\sigma_d^2 = \frac{\sigma_1^2}{n_1} + \frac{\sigma_2^2}{n_2}$	1.08E-04			
$\sigma_d$	1.04E-02			
$t = \frac{\bar{x}_1 - \bar{x}_2}{\sigma_d}$	0.96			

$p > 0.1$

APPENDIX 4

3T3 Cells	Specimen			
	0-0	$x^2$	10-5	$x^2$
Time: 24 hrs				
Replicate, $x_1$	0.95	0.90	0.94	0.88
Replicate, $x_2$	0.99	0.97	0.96	0.92
Replicate, $x_3$	0.94	0.88	0.91	0.83
Replicate, $x_4$	0.94	0.87	0.93	0.86
Replicate, $x_5$	0.94	0.88	0.94	0.88
Average ( $\bar{x}$ )	0.95	0.90	0.94	0.88
$\Sigma x^2$	4.51		4.38	
$(\Sigma x)^2$	22.56		21.90	
$((\Sigma x)^2)/n$	4.51		4.38	
$\Sigma d^2 = \Sigma x^2 - ((\Sigma x)^2)/n$	1.65E-03		1.32E-03	
$\sigma^2 = \frac{\Sigma d^2}{n-1}$	4.12E-04		3.30E-04	
$\sigma_d^2 = \frac{\sigma_1^2}{n_1} + \frac{\sigma_2^2}{n_2}$	1.49E-04			
$\sigma_d$	1.22E-02			
$t = \frac{\bar{x}_1 - \bar{x}_2}{\sigma_d}$	1.15			

p > 0.1



APPENDIX 4

3T3 Cells	Specimen			
	0-0	$x^2$	10-5	$x^2$
Time: 48 hrs				
Replicate, $x_1$	0.98	0.96	0.95	0.90
Replicate, $x_2$	1.00	1.00	0.97	0.93
Replicate, $x_3$	0.95	0.90	0.93	0.86
Replicate, $x_4$	0.97	0.94	0.96	0.92
Replicate, $x_5$	0.99	0.98	0.95	0.90
Average ( $\bar{x}$ )	0.98	0.96	0.95	0.90
$\Sigma x^2$	4.79		4.52	
$(\Sigma x)^2$	23.93		22.61	
$((\Sigma x)^2)/n$	4.79		4.52	
$\Sigma d^2 = \Sigma x^2 - ((\Sigma x)^2)/n$	1.57E-03		7.20E-04	
$\sigma^2 = \frac{\Sigma d^2}{n-1}$	3.93E-04		1.80E-04	
$\sigma_d^2 = \frac{\sigma_1^2}{n_1} + \frac{\sigma_2^2}{n_2}$	1.15E-04			
$\sigma_d$	1.07E-02			
$t = \frac{\bar{x}_1 - \bar{x}_2}{\sigma_d}$	2.56			

p < 0.05

APPENDIX 4

3T3 Cells	Specimen			
	0-0	$x^2$	10-5	$x^2$
Time: 96 hrs				
Replicate, $x_1$	1.00	1.00	0.99	0.98
Replicate, $x_2$	1.03	1.05	0.98	0.96
Replicate, $x_3$	0.98	0.96	1.02	1.04
Replicate, $x_4$	1.01	1.02	1.00	1.00
Replicate, $x_5$	0.99	0.98	0.99	0.98
Average ( $\bar{x}$ )	1.00	1.00	1.00	0.99
$\Sigma x^2$	5.01		4.96	
$(\Sigma x)^2$	25.05		24.80	
$((\Sigma x)^2)/n$	5.01		4.96	
$\Sigma d^2 = \Sigma x^2 - ((\Sigma x)^2)/n$	1.22E-03		9.20E-04	
$\sigma^2 = \frac{\Sigma d^2}{n-1}$	3.05E-04		2.30E-04	
$\sigma_d^2 = \frac{\sigma_1^2}{n_1} + \frac{\sigma_2^2}{n_2}$	1.07E-04			
$\sigma_d$	1.03E-02			
$t = \frac{\bar{x}_1 - \bar{x}_2}{\sigma_d}$	0.48			

p > 0.1

APPENDIX 4

3T3 Cells	Specimen			
	0-0	$x^2$	10-5	$x^2$
Time: 168 hrs				
Replicate, $x_1$	1.01	1.02	0.98	0.96
Replicate, $x_2$	1.04	1.09	1.02	1.04
Replicate, $x_3$	0.97	0.94	0.96	0.92
Replicate, $x_4$	0.99	0.98	1.00	1.00
Replicate, $x_5$	1.02	1.04	0.96	0.92
Average ( $\bar{x}$ )	1.01	1.01	0.98	0.97
$\Sigma x^2$	5.07		4.84	
$(\Sigma x)^2$	25.32		24.21	
$((\Sigma x)^2)/n$	5.06		4.84	
$\Sigma d^2 = \Sigma x^2 - ((\Sigma x)^2)/n$	3.21E-03		2.72E-03	
$\sigma^2 = \frac{\Sigma d^2}{n-1}$	8.01E-04		6.80E-04	
$\sigma_d^2 = \frac{\sigma_1^2}{n_1} + \frac{\sigma_2^2}{n_2}$	2.96E-04			
$\sigma_d$	1.72E-02			
$t = \frac{\bar{x}_1 - \bar{x}_2}{\sigma_d}$	1.30			

p > 0.1

APPENDIX 4

3T3 Cells	Specimen			
	0-0	$x^2$	10-10	$x^2$
Time: 3 hrs				
Replicate, $x_1$	0.97	0.94	0.98	0.96
Replicate, $x_2$	0.99	0.97	0.95	0.90
Replicate, $x_3$	0.95	0.90	1.00	1.00
Replicate, $x_4$	0.97	0.93	0.99	0.98
Replicate, $x_5$	0.98	0.96	0.98	0.96
Average ( $\bar{x}$ )	0.97	0.94	0.98	0.96
$\Sigma x^2$	4.71		4.80	
$(\Sigma x)^2$	23.52		24.01	
$((\Sigma x)^2)/n$	4.70		4.80	
$\Sigma d^2 = \Sigma x^2 - ((\Sigma x)^2)/n$	7.50E-04		1.40E-03	
$\sigma^2 = \frac{\Sigma d^2}{n-1}$	1.88E-04		3.50E-04	
$\sigma_d^2 = \frac{\sigma_1^2}{n_1} + \frac{\sigma_2^2}{n_2}$	1.07E-04			
$\sigma_d$	1.04E-02			
$t = \frac{\bar{x}_1 - \bar{x}_2}{\sigma_d}$	0.96			

$p > 0.1$

APPENDIX 4

3T3 Cells	Specimen			
	0-0	$x^2$	10-10	$x^2$
Time: 24 hrs				
Replicate, $x_1$	0.95	0.90	0.94	0.88
Replicate, $x_2$	0.99	0.97	0.94	0.88
Replicate, $x_3$	0.94	0.88	0.90	0.81
Replicate, $x_4$	0.94	0.87	0.93	0.86
Replicate, $x_5$	0.94	0.88	0.94	0.88
Average ( $\bar{x}$ )	0.95	0.90	0.93	0.87
$\Sigma x^2$	4.51		4.33	
$(\Sigma x)^2$	22.56		21.62	
$((\Sigma x)^2)/n$	4.51		4.32	
$\Sigma d^2 = \Sigma x^2 - ((\Sigma x)^2)/n$	1.65E-03		1.20E-03	
$\sigma^2 = \frac{\Sigma d^2}{n-1}$	4.12E-04		3.00E-04	
$\sigma_d^2 = \frac{\sigma_1^2}{n_1} + \frac{\sigma_2^2}{n_2}$	1.42E-04			
$\sigma_d$	1.19E-02			
$t = \frac{\bar{x}_1 - \bar{x}_2}{\sigma_d}$	1.68			

$p > 0.1$

APPENDIX 4

3T3 Cells	Specimen			
	0-0	$x^2$	10-10	$x^2$
Time: 48 hrs				
Replicate, $x_1$	0.98	0.96	0.96	0.92
Replicate, $x_2$	1.00	1.00	0.94	0.88
Replicate, $x_3$	0.95	0.90	0.98	0.95
Replicate, $x_4$	0.97	0.94	0.97	0.94
Replicate, $x_5$	0.99	0.98	0.96	0.92
Average ( $\bar{x}$ )	0.98	0.96	0.96	0.92
$\Sigma x^2$	4.79		4.62	
$(\Sigma x)^2$	23.93		23.09	
$((\Sigma x)^2)/n$	4.79		4.62	
$\Sigma d^2 = \Sigma x^2 - ((\Sigma x)^2)/n$	1.57E-03		7.20E-04	
$\sigma^2 = \frac{\Sigma d^2}{n-1}$	3.93E-04		1.80E-04	
$\sigma_d^2 = \frac{\sigma_1^2}{n_1} + \frac{\sigma_2^2}{n_2}$	1.15E-04			
$\sigma_d$	1.07E-02			
$t = \frac{\bar{x}_1 - \bar{x}_2}{\sigma_d}$	1.63			

$p > 0.1$

APPENDIX 4

3T3 Cells	Specimen			
	0-0	$x^2$	10-10	$x^2$
Time: 96 hrs				
Replicate, $x_1$	1.00	1.00	0.94	0.88
Replicate, $x_2$	1.03	1.05	0.96	0.92
Replicate, $x_3$	0.98	0.96	0.91	0.83
Replicate, $x_4$	1.01	1.02	0.96	0.92
Replicate, $x_5$	0.99	0.98	0.97	0.94
Average ( $\bar{x}$ )	1.00	1.00	0.95	0.90
$\Sigma x^2$	5.01		4.50	
$(\Sigma x)^2$	25.05		22.47	
$((\Sigma x)^2)/n$	5.01		4.49	
$\Sigma d^2 = \Sigma x^2 - ((\Sigma x)^2)/n$	1.22E-03		2.28E-03	
$\sigma^2 = \frac{\Sigma d^2}{n-1}$	3.05E-04		5.70E-04	
$\sigma_d^2 = \frac{\sigma_1^2}{n_1} + \frac{\sigma_2^2}{n_2}$	1.75E-04			
$\sigma_d$	1.32E-02			
$t = \frac{\bar{x}_1 - \bar{x}_2}{\sigma_d}$	4.01			

$p < 0.01$

APPENDIX 4

3T3 Cells	Specimen			
	0-0	$x^2$	10-10	$x^2$
Time: 168 hrs				
Replicate, $x_1$	1.01	1.02	0.96	0.92
Replicate, $x_2$	1.04	1.09	0.99	0.98
Replicate, $x_3$	0.97	0.94	0.94	0.88
Replicate, $x_4$	0.99	0.98	0.98	0.96
Replicate, $x_5$	1.02	1.04	0.95	0.90
Average ( $\bar{x}$ )	1.01	1.01	0.96	0.93
$\Sigma x^2$	5.07		4.65	
$(\Sigma x)^2$	25.32		23.23	
$((\Sigma x)^2)/n$	5.06		4.65	
$\Sigma d^2 = \Sigma x^2 - ((\Sigma x)^2)/n$	3.21E-03		1.72E-03	
$\sigma^2 = \frac{\Sigma d^2}{n-1}$	8.01E-04		4.30E-04	
$\sigma_d^2 = \frac{\sigma_1^2}{n_1} + \frac{\sigma_2^2}{n_2}$	2.46E-04			
$\sigma_d$	1.57E-02			
$t = \frac{\bar{x}_1 - \bar{x}_2}{\sigma_d}$	2.70			

p < 0.05



APPENDIX 4

3T3 Cells	Specimen			
	0-0	$x^2$	Graphite	$x^2$
Time: 3 hrs				
Replicate, $x_1$	0.97	0.94	0.98	0.96
Replicate, $x_2$	0.99	0.97	0.99	0.98
Replicate, $x_3$	0.95	0.90	0.95	0.90
Replicate, $x_4$	0.97	0.93	0.99	0.98
Replicate, $x_5$	0.98	0.96	0.99	0.98
Average ( $\bar{x}$ )	0.97	0.94	0.98	0.96
$\Sigma x^2$	4.71		4.80	
$(\Sigma x)^2$	23.52		24.01	
$((\Sigma x)^2)/n$	4.70		4.80	
$\Sigma d^2 = \Sigma x^2 - ((\Sigma x)^2)/n$	7.50E-04		1.20E-03	
$\sigma^2 = \frac{\Sigma d^2}{n-1}$	1.88E-04		3.00E-04	
$\sigma_d^2 = \frac{\sigma_1^2}{n_1} + \frac{\sigma_2^2}{n_2}$	9.75E-05			
$\sigma_d$	9.87E-03			
$t = \frac{\bar{x}_1 - \bar{x}_2}{\sigma_d}$	1.01			

p > 0.1

APPENDIX 4

3T3 Cells	Specimen			
	0-0	$x^2$	Graphite	$x^2$
Time: 24 hrs				
Replicate, $x_1$	0.95	0.90	0.94	0.88
Replicate, $x_2$	0.99	0.97	0.96	0.92
Replicate, $x_3$	0.94	0.88	0.91	0.83
Replicate, $x_4$	0.94	0.87	0.95	0.90
Replicate, $x_5$	0.94	0.88	0.94	0.88
Average ( $\bar{x}$ )	0.95	0.90	0.94	0.88
$\Sigma x^2$	4.51		4.42	
$(\Sigma x)^2$	22.56		22.09	
$((\Sigma x)^2)/n$	4.51		4.42	
$\Sigma d^2 = \Sigma x^2 - ((\Sigma x)^2)/n$	1.65E-03		1.40E-03	
$\sigma^2 = \frac{\Sigma d^2}{n-1}$	4.12E-04		3.50E-04	
$\sigma_d^2 = \frac{\sigma_1^2}{n_1} + \frac{\sigma_2^2}{n_2}$	1.53E-04			
$\sigma_d$	1.23E-02			
$t = \frac{\bar{x}_1 - \bar{x}_2}{\sigma_d}$	0.81			

$p > 0.1$

APPENDIX 4

3T3 Cells	Specimen			
	0-0	$x^2$	Graphite	$x^2$
Time: 48 hrs				
Replicate, $x_1$	0.98	0.96	0.93	0.86
Replicate, $x_2$	1.00	1.00	0.96	0.92
Replicate, $x_3$	0.95	0.90	0.92	0.85
Replicate, $x_4$	0.97	0.94	0.92	0.85
Replicate, $x_5$	0.99	0.98	0.96	0.92
Average ( $\bar{x}$ )	0.98	0.96	0.94	0.88
$\Sigma x^2$	4.79		4.40	
$(\Sigma x)^2$	23.93		22.00	
$((\Sigma x)^2)/n$	4.79		4.40	
$\Sigma d^2 = \Sigma x^2 - ((\Sigma x)^2)/n$	1.57E-03		1.68E-03	
$\sigma^2 = \frac{\Sigma d^2}{n-1}$	3.93E-04		4.20E-04	
$\sigma_d^2 = \frac{\sigma_1^2}{n_1} + \frac{\sigma_2^2}{n_2}$	1.63E-04			
$\sigma_d$	1.27E-02			
$t = \frac{\bar{x}_1 - \bar{x}_2}{\sigma_d}$	3.17			

$p < 0.05$

APPENDIX 4

3T3 Cells	Specimen			
	0-0	$x^2$	Graphite	$x^2$
Time: 96 hrs				
Replicate, $x_1$	1.00	1.00	0.93	0.86
Replicate, $x_2$	1.03	1.05	0.89	0.79
Replicate, $x_3$	0.98	0.96	0.90	0.81
Replicate, $x_4$	1.01	1.02	0.89	0.79
Replicate, $x_5$	0.99	0.98	0.92	0.85
Average ( $\bar{x}$ )	1.00	1.00	0.91	0.82
$\Sigma x^2$	5.01		4.11	
$(\Sigma x)^2$	25.05		20.52	
$((\Sigma x)^2)/n$	5.01		4.10	
$\Sigma d^2 = \Sigma x^2 - ((\Sigma x)^2)/n$	1.22E-03		1.32E-03	
$\sigma^2 = \frac{\Sigma d^2}{n-1}$	3.05E-04		3.30E-04	
$\sigma_d^2 = \frac{\sigma_1^2}{n_1} + \frac{\sigma_2^2}{n_2}$	1.27E-04			
$\sigma_d$	1.13E-02			
$t = \frac{\bar{x}_1 - \bar{x}_2}{\sigma_d}$	8.43			

p < 0.001

APPENDIX 4

3T3 Cells	Specimen			
	0-0	$x^2$	Graphite	$x^2$
Time: 168 hrs				
Replicate, $x_1$	1.01	1.02	0.89	0.79
Replicate, $x_2$	1.04	1.09	0.94	0.88
Replicate, $x_3$	0.97	0.94	0.88	0.77
Replicate, $x_4$	0.99	0.98	0.89	0.79
Replicate, $x_5$	1.02	1.04	0.90	0.81
Average ( $\bar{x}$ )	1.01	1.01	0.90	0.81
$\Sigma x^2$	5.07		4.05	
$(\Sigma x)^2$	25.32		20.25	
$((\Sigma x)^2)/n$	5.06		4.05	
$\Sigma d^2 = \Sigma x^2 - ((\Sigma x)^2)/n$	3.21E-03		2.20E-03	
$\sigma^2 = \frac{\Sigma d^2}{n-1}$	8.01E-04		5.50E-04	
$\sigma_d^2 = \frac{\sigma_1^2}{n_1} + \frac{\sigma_2^2}{n_2}$	2.70E-04			
$\sigma_d$	1.64E-02			
$t = \frac{\bar{x}_1 - \bar{x}_2}{\sigma_d}$	6.47			

p < 0.001

APPENDIX 4

Rat Osteoblast	Specimen			
Time: 3 hrs	0-0	$x^2$	10-5	$x^2$
Replicate, $x_1$	0.98	0.96	0.97	0.94
Replicate, $x_2$	1.02	1.04	1.00	1.00
Replicate, $x_3$	0.96	0.92	0.93	0.86
Replicate, $x_4$	0.97	0.93	0.98	0.96
Replicate, $x_5$	0.98	0.96	0.96	0.92
Average ( $\bar{x}$ )	0.98	0.96	0.97	0.94
$\Sigma x^2$	4.81		4.69	
$(\Sigma x)^2$	24.04		23.43	
$((\Sigma x)^2)/n$	4.81		4.69	
$\Sigma d^2 = \Sigma x^2 - ((\Sigma x)^2)/n$	2.09E-03		2.68E-03	
$\sigma^2 = \frac{\Sigma d^2}{n-1}$	5.22E-04		6.70E-04	
$\sigma_d^2 = \frac{\sigma_1^2}{n_1} + \frac{\sigma_2^2}{n_2}$	2.38E-04			
$\sigma_d$	1.54E-02			
$t = \frac{\bar{x}_1 - \bar{x}_2}{\sigma_d}$	0.82			

$p > 0.1$

APPENDIX 4

Rat Osteoblast	Specimen			
Time: 24 hrs	0-0	$x^2$	10-5	$x^2$
Replicate, $x_1$	0.95	0.90	0.94	0.88
Replicate, $x_2$	0.99	0.97	0.96	0.92
Replicate, $x_3$	0.94	0.88	0.91	0.83
Replicate, $x_4$	0.94	0.87	0.93	0.86
Replicate, $x_5$	0.94	0.88	0.94	0.88
Average ( $\bar{x}$ )	0.95	0.90	0.94	0.88
$\Sigma x^2$	4.51		4.38	
$(\Sigma x)^2$	22.56		21.90	
$((\Sigma x)^2)/n$	4.51		4.38	
$\Sigma d^2 = \Sigma x^2 - ((\Sigma x)^2)/n$	1.65E-03		1.32E-03	
$\sigma^2 = \frac{\Sigma d^2}{n-1}$	4.12E-04		3.30E-04	
$\sigma_d^2 = \frac{\sigma_1^2}{n_1} + \frac{\sigma_2^2}{n_2}$	1.49E-04			
$\sigma_d$	1.22E-02			
$t = \frac{\bar{x}_1 - \bar{x}_2}{\sigma_d}$	1.15			

$p > 0.1$

APPENDIX 4

Rat Osteoblast	Specimen			
	0-0	$x^2$	10-5	$x^2$
Time: 48 hrs				
Replicate, $x_1$	0.98	0.96	0.95	0.90
Replicate, $x_2$	1.00	1.00	0.97	0.93
Replicate, $x_3$	0.95	0.90	0.93	0.86
Replicate, $x_4$	0.97	0.94	0.96	0.92
Replicate, $x_5$	0.99	0.98	0.95	0.90
Average ( $\bar{x}$ )	0.98	0.96	0.95	0.90
$\Sigma x^2$	4.79		4.52	
$(\Sigma x)^2$	23.93		22.61	
$((\Sigma x)^2)/n$	4.79		4.52	
$\Sigma d^2 = \Sigma x^2 - ((\Sigma x)^2)/n$	1.57E-03		7.20E-04	
$\sigma^2 = \frac{\Sigma d^2}{n-1}$	3.93E-04		1.80E-04	
$\sigma_d^2 = \frac{\sigma_1^2}{n_1} + \frac{\sigma_2^2}{n_2}$	1.15E-04			
$\sigma_d$	1.07E-02			
$t = \frac{\bar{x}_1 - \bar{x}_2}{\sigma_d}$	2.56			

p < 0.05



APPENDIX 4

Rat Osteoblast	Specimen			
Time: 96 hrs	0-0	$x^2$	10-5	$x^2$
Replicate, $x_1$	1.00	1.00	0.99	0.98
Replicate, $x_2$	1.03	1.05	0.98	0.96
Replicate, $x_3$	0.98	0.96	1.02	1.04
Replicate, $x_4$	1.01	1.02	1.00	1.00
Replicate, $x_5$	0.99	0.98	0.99	0.98
Average ( $\bar{x}$ )	1.00	1.00	1.00	0.99
$\Sigma x^2$	5.01		4.96	
$(\Sigma x)^2$	25.05		24.80	
$((\Sigma x)^2)/n$	5.01		4.96	
$\Sigma d^2 = \Sigma x^2 - ((\Sigma x)^2)/n$	1.22E-03		9.20E-04	
$\sigma^2 = \frac{\Sigma d^2}{n-1}$	3.05E-04		2.30E-04	
$\sigma_d^2 = \frac{\sigma_1^2}{n_1} + \frac{\sigma_2^2}{n_2}$	1.07E-04			
$\sigma_d$	1.03E-02			
$t = \frac{\bar{x}_1 - \bar{x}_2}{\sigma_d}$	0.48			

$p > 0.1$

APPENDIX 4

Rat Osteoblast	Specimen			
	0-0	$x^2$	10-5	$x^2$
Time: 168 hrs				
Replicate, $x_1$	1.01	1.02	0.98	0.96
Replicate, $x_2$	1.04	1.09	1.02	1.04
Replicate, $x_3$	0.97	0.94	0.96	0.92
Replicate, $x_4$	0.99	0.98	1.00	1.00
Replicate, $x_5$	1.02	1.04	0.96	0.92
Average ( $\bar{x}$ )	1.01	1.01	0.98	0.97
$\Sigma x^2$	5.07		4.84	
$(\Sigma x)^2$	25.32		24.21	
$((\Sigma x)^2)/n$	5.06		4.84	
$\Sigma d^2 = \Sigma x^2 - ((\Sigma x)^2)/n$	3.21E-03		2.72E-03	
$\sigma^2 = \frac{\Sigma d^2}{n-1}$	8.01E-04		6.80E-04	
$\sigma_d^2 = \frac{\sigma_1^2}{n_1} + \frac{\sigma_2^2}{n_2}$	2.96E-04			
$\sigma_d$	1.72E-02			
$t = \frac{\bar{x}_1 - \bar{x}_2}{\sigma_d}$	1.30			

p > 0.1

APPENDIX 4

Rat Osteoblast	Specimen			
Time: 3 hrs	0-0	$x^2$	10-10	$x^2$
Replicate, $x_1$	0.98	0.96	0.98	0.96
Replicate, $x_2$	1.02	1.04	0.95	0.90
Replicate, $x_3$	0.96	0.92	1.00	1.00
Replicate, $x_4$	0.97	0.93	0.99	0.98
Replicate, $x_5$	0.98	0.96	0.98	0.96
Average ( $\bar{x}$ )	0.97	0.94	0.98	0.96
$\Sigma x^2$	4.81		4.80	
$(\Sigma x)^2$	24.04		24.01	
$((\Sigma x)^2)/n$	4.81		4.80	
$\Sigma d^2 = \Sigma x^2 - ((\Sigma x)^2)/n$	2.09E-03		1.40E-03	
$\sigma^2 = \frac{\Sigma d^2}{n-1}$	5.22E-04		3.50E-04	
$\sigma_d^2 = \frac{\sigma_1^2}{n_1} + \frac{\sigma_2^2}{n_2}$	1.74E-04			
$\sigma_d$	1.32E-02			
$t = \frac{\bar{x}_1 - \bar{x}_2}{\sigma_d}$	0.76			

$p > 0.1$

APPENDIX 4

Rat Osteoblast	Specimen			
Time: 24 hrs	0-0	$x^2$	10-10	$x^2$
Replicate, $x_1$	0.95	0.90	0.93	0.86
Replicate, $x_2$	0.99	0.97	0.94	0.88
Replicate, $x_3$	0.94	0.88	0.90	0.81
Replicate, $x_4$	0.94	0.87	0.93	0.86
Replicate, $x_5$	0.94	0.88	0.94	0.88
Average ( $\bar{x}$ )	0.95	0.90	0.93	0.86
$\Sigma x^2$	4.51		4.31	
$(\Sigma x)^2$	22.56		21.53	
$((\Sigma x)^2)/n$	4.51		4.31	
$\Sigma d^2 = \Sigma x^2 - ((\Sigma x)^2)/n$	1.65E-03		1.08E-03	
$\sigma^2 = \frac{\Sigma d^2}{n-1}$	4.12E-04		2.70E-04	
$\sigma_d^2 = \frac{\sigma_1^2}{n_1} + \frac{\sigma_2^2}{n_2}$	1.36E-04			
$\sigma_d$	1.17E-02			
$t = \frac{\bar{x}_1 - \bar{x}_2}{\sigma_d}$	1.88			

$p < 0.1$

APPENDIX 4

Rat Osteoblast	Specimen			
	0-0	$x^2$	10-10	$x^2$
Time: 48 hrs				
Replicate, $x_1$	0.98	0.96	0.96	0.92
Replicate, $x_2$	1.00	1.00	0.94	0.88
Replicate, $x_3$	0.95	0.90	0.98	0.95
Replicate, $x_4$	0.97	0.94	0.97	0.94
Replicate, $x_5$	0.99	0.98	0.96	0.92
Average ( $\bar{x}$ )	0.98	0.96	0.96	0.92
$\Sigma x^2$	4.79		4.62	
$(\Sigma x)^2$	23.93		23.09	
$((\Sigma x)^2)/n$	4.79		4.62	
$\Sigma d^2 = \Sigma x^2 - ((\Sigma x)^2)/n$	1.57E-03		7.20E-04	
$\sigma^2 = \frac{\Sigma d^2}{n-1}$	3.93E-04		1.80E-04	
$\sigma_d^2 = \frac{\sigma_1^2}{n_1} + \frac{\sigma_2^2}{n_2}$	1.15E-04			
$\sigma_d$	1.07E-02			
$t = \frac{\bar{x}_1 - \bar{x}_2}{\sigma_d}$	1.63			

p > 0.1

APPENDIX 4

Rat Osteoblast	Specimen			
Time: 96 hrs	0-0	$x^2$	10-10	$x^2$
Replicate, $x_1$	1.00	1.00	0.94	0.88
Replicate, $x_2$	1.03	1.05	0.96	0.92
Replicate, $x_3$	0.98	0.96	0.91	0.83
Replicate, $x_4$	1.01	1.02	0.96	0.92
Replicate, $x_5$	0.99	0.98	0.97	0.94
Average ( $\bar{x}$ )	1.00	1.00	0.95	0.90
$\Sigma x^2$	5.01		4.50	
$(\Sigma x)^2$	25.05		22.47	
$((\Sigma x)^2)/n$	5.01		4.49	
$\Sigma d^2 = \Sigma x^2 - ((\Sigma x)^2)/n$	1.22E-03		2.28E-03	
$\sigma^2 = \frac{\Sigma d^2}{n-1}$	3.05E-04		5.70E-04	
$\sigma_d^2 = \frac{\sigma_1^2}{n_1} + \frac{\sigma_2^2}{n_2}$	1.75E-04			
$\sigma_d$	1.32E-02			
$t = \frac{\bar{x}_1 - \bar{x}_2}{\sigma_d}$	4.01			

$p < 0.01$

APPENDIX 4

Rat Osteoblast	Specimen			
	0-0	$x^2$	10-10	$x^2$
Time: 168 hrs				
Replicate, $x_1$	1.01	1.02	0.96	0.92
Replicate, $x_2$	1.04	1.09	0.99	0.98
Replicate, $x_3$	0.97	0.94	0.94	0.88
Replicate, $x_4$	0.99	0.98	0.98	0.96
Replicate, $x_5$	1.02	1.04	0.95	0.90
Average ( $\bar{x}$ )	1.01	1.01	0.96	0.93
$\Sigma x^2$	5.07		4.65	
$(\Sigma x)^2$	25.32		23.23	
$((\Sigma x)^2)/n$	5.06		4.65	
$\Sigma d^2 = \Sigma x^2 - ((\Sigma x)^2)/n$	3.21E-03		1.72E-03	
$\sigma^2 = \frac{\Sigma d^2}{n-1}$	8.01E-04		4.30E-04	
$\sigma_d^2 = \frac{\sigma_1^2}{n_1} + \frac{\sigma_2^2}{n_2}$	2.46E-04			
$\sigma_d$	1.57E-02			
$t = \frac{\bar{x}_1 - \bar{x}_2}{\sigma_d}$	2.70			

p < 0.05

APPENDIX 4

Rat Osteoblast	Specimen			
	0-0	$x^2$	Graphite	$x^2$
Time: 3 hrs				
Replicate, $x_1$	0.98	0.96	0.98	0.96
Replicate, $x_2$	1.02	1.04	0.99	0.98
Replicate, $x_3$	0.96	0.92	0.95	0.90
Replicate, $x_4$	0.97	0.93	0.99	0.98
Replicate, $x_5$	0.98	0.96	0.99	0.98
Average ( $\bar{x}$ )	0.97	0.94	0.98	0.96
$\Sigma x^2$	4.81		4.80	
$(\Sigma x)^2$	24.04		24.01	
$((\Sigma x)^2)/n$	4.81		4.80	
$\Sigma d^2 = \Sigma x^2 - ((\Sigma x)^2)/n$	2.09E-03		1.20E-03	
$\sigma^2 = \frac{\Sigma d^2}{n-1}$	5.22E-04		3.00E-04	
$\sigma_d^2 = \frac{\sigma_1^2}{n_1} + \frac{\sigma_2^2}{n_2}$	1.64E-04			
$\sigma_d$	1.28E-02			
$t = \frac{\bar{x}_1 - \bar{x}_2}{\sigma_d}$	0.78			

p > 0.1



APPENDIX 4

Rat Osteoblast	Specimen			
	0-0	$x^2$	Graphite	$x^2$
Time: 24 hrs				
Replicate, $x_1$	0.95	0.90	0.94	0.88
Replicate, $x_2$	0.99	0.97	0.96	0.92
Replicate, $x_3$	0.94	0.88	0.91	0.83
Replicate, $x_4$	0.94	0.87	0.95	0.90
Replicate, $x_5$	0.94	0.88	0.94	0.88
Average ( $\bar{x}$ )	0.95	0.90	0.94	0.88
$\Sigma x^2$	4.51		4.42	
$(\Sigma x)^2$	22.56		22.09	
$((\Sigma x)^2)/n$	4.51		4.42	
$\Sigma d^2 = \Sigma x^2 - ((\Sigma x)^2)/n$	1.65E-03		1.40E-03	
$\sigma^2 = \frac{\Sigma d^2}{n-1}$	4.12E-04		3.50E-04	
$\sigma_d^2 = \frac{\sigma_1^2}{n_1} + \frac{\sigma_2^2}{n_2}$	1.53E-04			
$\sigma_d$	1.23E-02			
$t = \frac{\bar{x}_1 - \bar{x}_2}{\sigma_d}$	0.81			

p > 0.1

APPENDIX 4

Rat Osteoblast	Specimen			
Time: 48 hrs	0-0	$x^2$	Graphite	$x^2$
Replicate, $x_1$	0.98	0.96	0.93	0.86
Replicate, $x_2$	1.00	1.00	0.96	0.92
Replicate, $x_3$	0.95	0.90	0.92	0.85
Replicate, $x_4$	0.97	0.94	0.92	0.85
Replicate, $x_5$	0.99	0.98	0.96	0.92
Average ( $\bar{x}$ )	0.98	0.96	0.91	0.83
$\Sigma x^2$	4.79		4.40	
$(\Sigma x)^2$	23.93		22.00	
$((\Sigma x)^2)/n$	4.79		4.40	
$\Sigma d^2 = \Sigma x^2 - ((\Sigma x)^2)/n$	1.57E-03		1.68E-03	
$\sigma^2 = \frac{\Sigma d^2}{n-1}$	3.93E-04		4.20E-04	
$\sigma_d^2 = \frac{\sigma_1^2}{n_1} + \frac{\sigma_2^2}{n_2}$	1.63E-04			
$\sigma_d$	1.27E-02			
$t = \frac{\bar{x}_1 - \bar{x}_2}{\sigma_d}$	5.36			

$p < 0.001$

APPENDIX 4

Rat Osteoblast	Specimen			
Time: 96 hrs	0-0	$x^2$	Graphite	$x^2$
Replicate, $x_1$	1.00	1.00	0.93	0.86
Replicate, $x_2$	1.03	1.05	0.89	0.79
Replicate, $x_3$	0.98	0.96	0.90	0.81
Replicate, $x_4$	1.01	1.02	0.89	0.79
Replicate, $x_5$	0.99	0.98	0.92	0.85
Average ( $\bar{x}$ )	1.00	1.00	0.91	0.82
$\Sigma x^2$	5.01		4.11	
$(\Sigma x)^2$	25.05		20.52	
$((\Sigma x)^2)/n$	5.01		4.10	
$\Sigma d^2 = \Sigma x^2 - ((\Sigma x)^2)/n$	1.22E-03		1.32E-03	
$\sigma^2 = \frac{\Sigma d^2}{n-1}$	3.05E-04		3.30E-04	
$\sigma_d^2 = \frac{\sigma_1^2}{n_1} + \frac{\sigma_2^2}{n_2}$	1.27E-04			
$\sigma_d$	1.13E-02			
$t = \frac{\bar{x}_1 - \bar{x}_2}{\sigma_d}$	8.43			

$p < 0.001$

APPENDIX 4

Rat Osteoblast	Specimen			
	0-0	$x^2$	Graphite	$x^2$
Time: 168 hrs				
Replicate, $x_1$	1.01	1.02	0.89	0.79
Replicate, $x_2$	1.04	1.09	0.94	0.88
Replicate, $x_3$	0.97	0.94	0.88	0.77
Replicate, $x_4$	0.99	0.98	0.89	0.79
Replicate, $x_5$	1.02	1.04	0.90	0.81
Average ( $\bar{x}$ )	1.01	1.01	0.90	0.81
$\Sigma x^2$	5.07		4.05	
$(\Sigma x)^2$	25.32		20.25	
$((\Sigma x)^2)/n$	5.06		4.05	
$\Sigma d^2 = \Sigma x^2 - ((\Sigma x)^2)/n$	3.21E-03		2.20E-03	
$\sigma^2 = \frac{\Sigma d^2}{n-1}$	8.01E-04		5.50E-04	
$\sigma_d^2 = \frac{\sigma_1^2}{n_1} + \frac{\sigma_2^2}{n_2}$	2.70E-04			
$\sigma_d$	1.64E-02			
$t = \frac{\bar{x}_1 - \bar{x}_2}{\sigma_d}$	6.47			

p < 0.001

**Calculations for the Students T-Test on the Cell Proliferation Assay  
Involving Wear Debris**

3T3 Cells	Specimen			
Time: 3 hrs	0-0	$x^2$	10-5	$x^2$
Replicate, $x_1$	0.98	0.96	0.98	0.96
Replicate, $x_2$	0.98	0.97	1.01	1.02
Replicate, $x_3$	0.99	0.98	0.98	0.96
Replicate, $x_4$	0.97	0.93	0.98	0.95
Replicate, $x_5$	0.96	0.92	0.98	0.95
Average ( $\bar{x}$ )	0.98	0.95	0.98	0.97
$\Sigma x^2$	4.76		4.84	
$(\Sigma x)^2$	23.80		24.21	
$((\Sigma x)^2)/n$	4.76		4.84	
$\Sigma d^2 = \Sigma x^2 - ((\Sigma x)^2)/n$	6.46E-04		8.21E-04	
$\sigma^2 = \frac{\Sigma d^2}{n-1}$	1.61E-04		2.05E-04	
$\sigma_d^2 = \frac{\sigma_1^2}{n_1} + \frac{\sigma_2^2}{n_2}$	7.33E-05			
$\sigma_d$	8.56E-03			
$t = \frac{\bar{x}_1 - \bar{x}_2}{\sigma_d}$	0.98			

$p > 0.1$

APPENDIX 5

3T3 Cells	Specimen			
	0-0	$x^2$	10-5	$x^2$
Time: 24 hrs				
Replicate, $x_1$	0.98	0.96	0.98	0.96
Replicate, $x_2$	1.02	1.04	0.99	0.99
Replicate, $x_3$	0.95	0.90	0.96	0.92
Replicate, $x_4$	0.99	0.98	0.97	0.94
Replicate, $x_5$	0.97	0.94	0.98	0.96
Average ( $\bar{x}$ )	0.98	0.96	0.98	0.95
$\Sigma x^2$	4.82		4.77	
$(\Sigma x)^2$	24.10		23.86	
$((\Sigma x)^2)/n$	4.82		4.77	
$\Sigma d^2 = \Sigma x^2 - ((\Sigma x)^2)/n$	2.64E-03		5.76E-04	
$\sigma^2 = \frac{\Sigma d^2}{n-1}$	6.60E-04		1.44E-04	
$\sigma_d^2 = \frac{\sigma_1^2}{n_1} + \frac{\sigma_2^2}{n_2}$	1.61E-04			
$\sigma_d$	1.27E-02			
$t = \frac{\bar{x}_1 - \bar{x}_2}{\sigma_d}$	0.39			

$p > 0.1$

APPENDIX 5

3T3 Cells	Specimen			
	0-0	$x^2$	10-5	$x^2$
Time: 48 hrs				
Replicate, $x_1$	0.97	0.94	0.96	0.92
Replicate, $x_2$	1.01	1.01	0.98	0.96
Replicate, $x_3$	0.94	0.89	0.94	0.88
Replicate, $x_4$	1.00	1.00	0.95	0.90
Replicate, $x_5$	0.95	0.90	0.97	0.94
Average ( $\bar{x}$ )	0.97	0.95	0.96	0.92
$\Sigma x^2$	4.74		4.60	
$(\Sigma x)^2$	23.70		22.98	
$((\Sigma x)^2)/n$	4.74		4.60	
$\Sigma d^2 = \Sigma x^2 - ((\Sigma x)^2)/n$	3.29E-03		1.11E-03	
$\sigma^2 = \frac{\Sigma d^2}{n-1}$	8.22E-04		2.78E-04	
$\sigma_d^2 = \frac{\sigma_1^2}{n_1} + \frac{\sigma_2^2}{n_2}$	2.20E-04			
$\sigma_d$	1.48E-02			
$t = \frac{\bar{x}_1 - \bar{x}_2}{\sigma_d}$	1.01			

p > 0.1

APPENDIX 5

3T3 Cells	Specimen			
	0-0	$x^2$	10-5	$x^2$
Time: 96 hrs				
Replicate, $x_1$	0.99	0.98	0.97	0.94
Replicate, $x_2$	1.03	1.06	0.99	0.98
Replicate, $x_3$	0.97	0.93	0.95	0.89
Replicate, $x_4$	0.98	0.96	0.98	0.96
Replicate, $x_5$	1.00	1.00	0.95	0.90
Average ( $\bar{x}$ )	0.99	0.99	0.97	0.93
$\Sigma x^2$	4.93		4.67	
$(\Sigma x)^2$	24.66		23.36	
$((\Sigma x)^2)/n$	4.93		4.67	
$\Sigma d^2 = \Sigma x^2 - ((\Sigma x)^2)/n$	2.29E-03		1.37E-03	
$\sigma^2 = \frac{\Sigma d^2}{n-1}$	5.74E-04		3.41E-04	
$\sigma_d^2 = \frac{\sigma_1^2}{n_1} + \frac{\sigma_2^2}{n_2}$	1.83E-04			
$\sigma_d$	1.35E-02			
$t = \frac{\bar{x}_1 - \bar{x}_2}{\sigma_d}$	1.96			

p < 0.1



APPENDIX 5

3T3 Cells	Specimen			
	0-0	$x^2$	10-5	$x^2$
Time: 168 hrs				
Replicate, $x_1$	1.01	1.02	0.98	0.96
Replicate, $x_2$	0.99	0.99	1.00	1.00
Replicate, $x_3$	1.03	1.07	0.97	0.94
Replicate, $x_4$	1.00	1.00	0.99	0.98
Replicate, $x_5$	0.99	0.98	0.97	0.94
Average ( $\bar{x}$ )	1.01	1.01	0.98	0.96
$\Sigma x^2$	5.05		4.82	
$(\Sigma x)^2$	25.26		24.08	
$((\Sigma x)^2)/n$	5.05		4.82	
$\Sigma d^2 = \Sigma x^2 - ((\Sigma x)^2)/n$	1.21E-03		7.16E-04	
$\sigma^2 = \frac{\Sigma d^2}{n-1}$	3.03E-04		1.79E-04	
$\sigma_d^2 = \frac{\sigma_1^2}{n_1} + \frac{\sigma_2^2}{n_2}$	9.65E-05			
$\sigma_d$	9.82E-03			
$t = \frac{\bar{x}_1 - \bar{x}_2}{\sigma_d}$	2.42			

$p < 0.05$

APPENDIX 5

3T3 Cells	Specimen			
	0-0	$x^2$	10-10	$x^2$
Time: 3 hrs				
Replicate, $x_1$	0.98	0.96	0.98	0.96
Replicate, $x_2$	0.98	0.97	0.98	0.97
Replicate, $x_3$	0.99	0.98	0.98	0.95
Replicate, $x_4$	0.97	0.93	0.99	0.98
Replicate, $x_5$	0.96	0.92	0.98	0.96
Average ( $\bar{x}$ )	0.98	0.95	0.98	0.96
$\Sigma x^2$	4.76		4.82	
$(\Sigma x)^2$	23.80		24.10	
$((\Sigma x)^2)/n$	4.76		4.82	
$\Sigma d^2 = \Sigma x^2 - ((\Sigma x)^2)/n$	6.46E-04		1.11E-04	
$\sigma^2 = \frac{\Sigma d^2}{n-1}$	1.61E-04		2.78E-05	
$\sigma_d^2 = \frac{\sigma_1^2}{n_1} + \frac{\sigma_2^2}{n_2}$	3.78E-05			
$\sigma_d$	6.15E-03			
$t = \frac{\bar{x}_1 - \bar{x}_2}{\sigma_d}$	0.99			

p > 0.1

APPENDIX 5

3T3 Cells	Specimen			
	0-0	$x^2$	10-10	$x^2$
Time: 24 hrs				
Replicate, $x_1$	0.98	0.96	0.96	0.92
Replicate, $x_2$	1.02	1.04	0.97	0.94
Replicate, $x_3$	0.95	0.90	0.95	0.90
Replicate, $x_4$	0.99	0.98	0.96	0.92
Replicate, $x_5$	0.97	0.94	0.97	0.94
Average ( $\bar{x}$ )	0.98	0.96	0.96	0.92
$\Sigma x^2$	4.82		4.62	
$(\Sigma x)^2$	24.10		23.08	
$((\Sigma x)^2)/n$	4.82		4.62	
$\Sigma d^2 = \Sigma x^2 - ((\Sigma x)^2)/n$	2.64E-03		3.03E-04	
$\sigma^2 = \frac{\Sigma d^2}{n-1}$	6.60E-04		7.57E-05	
$\sigma_d^2 = \frac{\sigma_1^2}{n_1} + \frac{\sigma_2^2}{n_2}$	1.47E-04			
$\sigma_d$	1.21E-02			
$t = \frac{\bar{x}_1 - \bar{x}_2}{\sigma_d}$	1.73			

p > 0.1

APPENDIX 5

3T3 Cells	Specimen			
	0-0	$x^2$	10-10	$x^2$
Time: 48 hrs				
Replicate, $x_1$	0.97	0.94	0.97	0.94
Replicate, $x_2$	1.01	1.01	0.99	0.98
Replicate, $x_3$	0.94	0.89	0.93	0.87
Replicate, $x_4$	1.00	1.00	0.98	0.96
Replicate, $x_5$	0.95	0.90	0.96	0.92
Average ( $\bar{x}$ )	0.97	0.95	0.97	0.93
$\Sigma x^2$	4.74		4.67	
$(\Sigma x)^2$	23.70		23.35	
$((\Sigma x)^2)/n$	4.74		4.67	
$\Sigma d^2 = \Sigma x^2 - ((\Sigma x)^2)/n$	3.29E-03		1.91E-03	
$\sigma^2 = \frac{\Sigma d^2}{n-1}$	8.22E-04		4.78E-04	
$\sigma_d^2 = \frac{\sigma_1^2}{n_1} + \frac{\sigma_2^2}{n_2}$	2.60E-04			
$\sigma_d$	1.61E-02			
$t = \frac{\bar{x}_1 - \bar{x}_2}{\sigma_d}$	0.44			

p > 0.1

APPENDIX 5

3T3 Cells	Specimen			
	0-0	$x^2$	10-10	$x^2$
Time: 96 hrs				
Replicate, $x_1$	0.99	0.98	0.96	0.92
Replicate, $x_2$	1.03	1.06	0.98	0.97
Replicate, $x_3$	0.97	0.93	0.93	0.86
Replicate, $x_4$	0.98	0.96	0.97	0.94
Replicate, $x_5$	1.00	1.00	0.94	0.88
Average ( $\bar{x}$ )	0.99	0.99	0.96	0.91
$\Sigma x^2$	4.93		4.57	
$(\Sigma x)^2$	24.66		22.85	
$((\Sigma x)^2)/n$	4.93		4.57	
$\Sigma d^2 = \Sigma x^2 - ((\Sigma x)^2)/n$	2.29E-03		2.09E-03	
$\sigma^2 = \frac{\Sigma d^2}{n-1}$	5.74E-04		5.23E-04	
$\sigma_d^2 = \frac{\sigma_1^2}{n_1} + \frac{\sigma_2^2}{n_2}$	2.19E-04			
$\sigma_d$	1.48E-02			
$t = \frac{\bar{x}_1 - \bar{x}_2}{\sigma_d}$	2.51			

$p < 0.05$

APPENDIX 5

3T3 Cells	Specimen			
	0-0	$x^2$	10-10	$x^2$
Time: 168 hrs				
Replicate, $x_1$	1.01	1.02	0.96	0.92
Replicate, $x_2$	0.99	0.99	0.98	0.97
Replicate, $x_3$	1.03	1.07	0.93	0.86
Replicate, $x_4$	1.00	1.00	0.97	0.94
Replicate, $x_5$	0.99	0.98	0.95	0.90
Average ( $\bar{x}$ )	1.01	1.01	0.96	0.92
$\Sigma x^2$	5.05		4.59	
$(\Sigma x)^2$	25.26		22.94	
$((\Sigma x)^2)/n$	5.05		4.59	
$\Sigma d^2 = \Sigma x^2 - ((\Sigma x)^2)/n$	1.21E-03		1.85E-03	
$\sigma^2 = \frac{\Sigma d^2}{n-1}$	3.03E-04		4.64E-04	
$\sigma_d^2 = \frac{\sigma_1^2}{n_1} + \frac{\sigma_2^2}{n_2}$	1.53E-04			
$\sigma_d$	1.24E-02			
$t = \frac{\bar{x}_1 - \bar{x}_2}{\sigma_d}$	3.81			

$p < 0.01$

APPENDIX 5

Rat Osteoblast	Specimen			
	0-0	$x^2$	10-5	$x^2$
Time: 3 hrs				
Replicate, $x_1$	0.97	0.94	0.96	0.92
Replicate, $x_2$	0.98	0.95	0.98	0.97
Replicate, $x_3$	0.97	0.93	0.95	0.91
Replicate, $x_4$	0.97	0.93	0.96	0.92
Replicate, $x_5$	0.98	0.96	0.95	0.90
Average ( $\bar{x}$ )	0.97	0.94	0.96	0.93
$\Sigma x^2$	4.72		4.63	
$(\Sigma x)^2$	23.58		23.12	
$((\Sigma x)^2)/n$	4.72		4.62	
$\Sigma d^2 = \Sigma x^2 - ((\Sigma x)^2)/n$	1.65E-04		6.91E-04	
$\sigma^2 = \frac{\Sigma d^2}{n-1}$	4.13E-05		1.73E-04	
$\sigma_d^2 = \frac{\sigma_1^2}{n_1} + \frac{\sigma_2^2}{n_2}$	4.28E-05			
$\sigma_d$	6.55E-03			
$t = \frac{\bar{x}_1 - \bar{x}_2}{\sigma_d}$	1.44			

p > 0.1

APPENDIX 5

Rat Osteoblast	Specimen			
Time: 24 hrs	0-0	$x^2$	10-5	$x^2$
Replicate, $x_1$	0.94	0.88	0.93	0.86
Replicate, $x_2$	0.96	0.92	0.88	0.77
Replicate, $x_3$	0.93	0.86	0.93	0.86
Replicate, $x_4$	0.95	0.90	0.92	0.85
Replicate, $x_5$	0.94	0.88	0.92	0.85
Average ( $\bar{x}$ )	0.94	0.89	0.92	0.84
$\Sigma x^2$	4.46		4.20	
$(\Sigma x)^2$	22.28		20.98	
$((\Sigma x)^2)/n$	4.46		4.20	
$\Sigma d^2 = \Sigma x^2 - ((\Sigma x)^2)/n$	5.20E-04		1.72E-03	
$\sigma^2 = \frac{\Sigma d^2}{n-1}$	1.30E-04		4.30E-04	
$\sigma_d^2 = \frac{\sigma_1^2}{n_1} + \frac{\sigma_2^2}{n_2}$	1.12E-04			
$\sigma_d$	1.06E-02			
$t = \frac{\bar{x}_1 - \bar{x}_2}{\sigma_d}$	2.65			

$p < 0.05$



APPENDIX 5

Rat Osteoblast	Specimen			
	0-0	$x^2$	10-5	$x^2$
Time: 48 hrs				
Replicate, $x_1$	0.93	0.86	0.90	0.81
Replicate, $x_2$	0.94	0.88	0.91	0.83
Replicate, $x_3$	0.91	0.83	0.89	0.79
Replicate, $x_4$	0.92	0.85	0.90	0.81
Replicate, $x_5$	0.93	0.86	0.91	0.83
Average ( $\bar{x}$ )	0.93	0.86	0.90	0.81
$\Sigma x^2$	4.29		4.07	
$(\Sigma x)^2$	21.44		20.34	
$((\Sigma x)^2)/n$	4.29		4.07	
$\Sigma d^2 = \Sigma x^2 - ((\Sigma x)^2)/n$	5.20E-04		2.80E-04	
$\sigma^2 = \frac{\Sigma d^2}{n-1}$	1.30E-04		7.00E-05	
$\sigma_d^2 = \frac{\sigma_1^2}{n_1} + \frac{\sigma_2^2}{n_2}$	4.00E-05			
$\sigma_d$	6.32E-03			
$t = \frac{\bar{x}_1 - \bar{x}_2}{\sigma_d}$	3.79			

p < 0.01

APPENDIX 5

Rat Osteoblast	Specimen			
Time: 96 hrs	0-0	$x^2$	10-5	$x^2$
Replicate, $x_1$	0.95	0.90	0.87	0.76
Replicate, $x_2$	0.91	0.83	0.89	0.79
Replicate, $x_3$	0.88	0.77	0.84	0.71
Replicate, $x_4$	0.92	0.85	0.88	0.77
Replicate, $x_5$	0.90	0.81	0.85	0.72
Average ( $\bar{x}$ )	0.91	0.83	0.87	0.75
$\Sigma x^2$	4.16		3.75	
$(\Sigma x)^2$	20.79		18.75	
$((\Sigma x)^2)/n$	4.16		3.75	
$\Sigma d^2 = \Sigma x^2 - ((\Sigma x)^2)/n$	2.68E-03		1.72E-03	
$\sigma^2 = \frac{\Sigma d^2}{n-1}$	6.70E-04		4.30E-04	
$\sigma_d^2 = \frac{\sigma_1^2}{n_1} + \frac{\sigma_2^2}{n_2}$	2.20E-04			
$\sigma_d$	1.48E-02			
$t = \frac{\bar{x}_1 - \bar{x}_2}{\sigma_d}$	3.10			

$p < 0.05$

APPENDIX 5

Rat Osteoblast	Specimen			
	0-0	$x^2$	10-5	$x^2$
Time: 168 hrs				
Replicate, $x_1$	0.90	0.81	0.86	0.74
Replicate, $x_2$	0.91	0.83	0.88	0.77
Replicate, $x_3$	0.88	0.77	0.85	0.72
Replicate, $x_4$	0.89	0.79	0.87	0.76
Replicate, $x_5$	0.90	0.81	0.86	0.74
Average ( $\bar{x}$ )	0.90	0.80	0.86	0.75
$\Sigma x^2$	4.01		3.73	
$(\Sigma x)^2$	20.07		18.66	
$((\Sigma x)^2)/n$	4.01		3.73	
$\Sigma d^2 = \Sigma x^2 - ((\Sigma x)^2)/n$	5.20E-04		5.20E-04	
$\sigma^2 = \frac{\Sigma d^2}{n-1}$	1.30E-04		1.30E-04	
$\sigma_d^2 = \frac{\sigma_1^2}{n_1} + \frac{\sigma_2^2}{n_2}$	5.20E-05			
$\sigma_d$	7.21E-03			
$t = \frac{\bar{x}_1 - \bar{x}_2}{\sigma_d}$	4.44			

p < 0.01

APPENDIX 5

Rat Osteoblast	Specimen			
	0-0	$x^2$	10-10	$x^2$
Time: 3 hrs				
Replicate, $x_1$	0.97	0.94	0.97	0.94
Replicate, $x_2$	0.98	0.95	0.98	0.96
Replicate, $x_3$	0.97	0.93	0.96	0.92
Replicate, $x_4$	0.97	0.93	0.96	0.92
Replicate, $x_5$	0.98	0.96	0.97	0.94
Average ( $\bar{x}$ )	0.97	0.94	0.97	0.94
$\Sigma x^2$	4.72		4.69	
$(\Sigma x)^2$	23.58		23.43	
$((\Sigma x)^2)/n$	4.72		4.69	
$\Sigma d^2 = \Sigma x^2 - ((\Sigma x)^2)/n$	1.65E-04		2.80E-04	
$\sigma^2 = \frac{\Sigma d^2}{n-1}$	4.13E-05		7.00E-05	
$\sigma_d^2 = \frac{\sigma_1^2}{n_1} + \frac{\sigma_2^2}{n_2}$	2.23E-05			
$\sigma_d$	4.72E-03			
$t = \frac{\bar{x}_1 - \bar{x}_2}{\sigma_d}$	0.66			

p > 0.1

APPENDIX 5

Rat Osteoblast	Specimen			
Time: 24 hrs	0-0	$x^2$	10-10	$x^2$
Replicate, $x_1$	0.94	0.88	0.92	0.85
Replicate, $x_2$	0.96	0.92	0.93	0.86
Replicate, $x_3$	0.93	0.86	0.91	0.83
Replicate, $x_4$	0.95	0.90	0.92	0.85
Replicate, $x_5$	0.94	0.88	0.93	0.86
Average ( $\bar{x}$ )	0.94	0.89	0.92	0.85
$\Sigma x^2$	4.46		4.25	
$(\Sigma x)^2$	22.28		21.25	
$((\Sigma x)^2)/n$	4.46		4.25	
$\Sigma d^2 = \Sigma x^2 - ((\Sigma x)^2)/n$	5.20E-04		2.80E-04	
$\sigma^2 = \frac{\Sigma d^2}{n-1}$	1.30E-04		7.00E-05	
$\sigma_d^2 = \frac{\sigma_1^2}{n_1} + \frac{\sigma_2^2}{n_2}$	4.00E-05			
$\sigma_d$	6.32E-03			
$t = \frac{\bar{x}_1 - \bar{x}_2}{\sigma_d}$	3.48			

p < 0.01

APPENDIX 5

Rat Osteoblast	Specimen			
Time: 48 hrs	0-0	$x^2$	10-10	$x^2$
Replicate, $x_1$	0.93	0.86	0.90	0.81
Replicate, $x_2$	0.94	0.88	0.88	0.77
Replicate, $x_3$	0.91	0.83	0.91	0.83
Replicate, $x_4$	0.92	0.85	0.90	0.81
Replicate, $x_5$	0.93	0.86	0.89	0.79
Average ( $\bar{x}$ )	0.93	0.86	0.90	0.80
$\Sigma x^2$	4.29		4.01	
$(\Sigma x)^2$	21.44		20.07	
$((\Sigma x)^2)/n$	4.29		4.01	
$\Sigma d^2 = \Sigma x^2 - ((\Sigma x)^2)/n$	5.20E-04		5.20E-04	
$\sigma^2 = \frac{\Sigma d^2}{n-1}$	1.30E-04		1.30E-04	
$\sigma_d^2 = \frac{\sigma_1^2}{n_1} + \frac{\sigma_2^2}{n_2}$	5.20E-05			
$\sigma_d$	7.21E-03			
$t = \frac{\bar{x}_1 - \bar{x}_2}{\sigma_d}$	4.16			

$p < 0.01$

APPENDIX 5

Rat Osteoblast	Specimen			
	0-0	$x^2$	10-10	$x^2$
Time: 96 hrs				
Replicate, $x_1$	0.95	0.90	0.86	0.74
Replicate, $x_2$	0.91	0.83	0.87	0.76
Replicate, $x_3$	0.88	0.77	0.82	0.67
Replicate, $x_4$	0.92	0.85	0.86	0.74
Replicate, $x_5$	0.90	0.81	0.87	0.76
Average ( $\bar{x}$ )	0.91	0.83	0.86	0.73
$\Sigma x^2$	4.16		3.67	
$(\Sigma x)^2$	20.79		18.32	
$((\Sigma x)^2)/n$	4.16		3.66	
$\Sigma d^2 = \Sigma x^2 - ((\Sigma x)^2)/n$	2.68E-03		1.72E-03	
$\sigma^2 = \frac{\Sigma d^2}{n-1}$	6.70E-04		4.30E-04	
$\sigma_d^2 = \frac{\sigma_1^2}{n_1} + \frac{\sigma_2^2}{n_2}$	2.20E-04			
$\sigma_d$	1.48E-02			
$t = \frac{\bar{x}_1 - \bar{x}_2}{\sigma_d}$	3.78			

p < 0.01

APPENDIX 5

Rat Osteoblast	Specimen			
	0-0	$x^2$	10-10	$x^2$
Time: 168 hrs				
Replicate, $x_1$	0.90	0.81	0.84	0.71
Replicate, $x_2$	0.91	0.83	0.85	0.72
Replicate, $x_3$	0.88	0.77	0.82	0.67
Replicate, $x_4$	0.89	0.79	0.83	0.69
Replicate, $x_5$	0.90	0.81	0.85	0.72
Average ( $\bar{x}$ )	0.90	0.80	0.84	0.70
$\Sigma x^2$	4.01		3.51	
$(\Sigma x)^2$	20.07		17.56	
$((\Sigma x)^2)/n$	4.01		3.51	
$\Sigma d^2 = \Sigma x^2 - ((\Sigma x)^2)/n$	5.20E-04		6.80E-04	
$\sigma^2 = \frac{\Sigma d^2}{n-1}$	1.30E-04		1.70E-04	
$\sigma_d^2 = \frac{\sigma_1^2}{n_1} + \frac{\sigma_2^2}{n_2}$	6.00E-05			
$\sigma_d$	7.75E-03			
$t = \frac{\bar{x}_1 - \bar{x}_2}{\sigma_d}$	7.49			

p < 0.001



**Calculations for the Students T-Test on the Water Contact Angle Test on Sintered Compacts**

Time: 0 s	Specimen			
	Polished 0-0	$x^2$	Unpolished 0-0	$x^2$
Replicate, $x_1$	64.10	4108.81	62.10	3856.41
Replicate, $x_2$	80.30	6448.09	71.90	5169.61
Replicate, $x_3$	74.20	5505.64	77.00	5929.00
Average ( $\bar{x}$ )	72.87	5354.18	70.33	4985.01
$\Sigma x^2$	16062.54		14955.02	
$(\Sigma x)^2$	47785.96		44521.00	
$((\Sigma x)^2)/n$	15928.65		14840.33	
$\Sigma d^2 = \Sigma x^2 - ((\Sigma x)^2)/n$	133.89		114.69	
$\sigma^2 = \frac{\Sigma d^2}{n-1}$	66.94		57.34	
$\sigma_d^2 = \frac{\sigma_1^2}{n_1} + \frac{\sigma_2^2}{n_2}$	41.43			
$\sigma_d$	6.44			
$t = \frac{\bar{x}_1 - \bar{x}_2}{\sigma_d}$	0.39			

p > 0.1

APPENDIX 6

Time: 10 s	Specimen			
	Polished 0-0	$x^2$	Unpolished 0-0	$x^2$
Replicate, $x_1$	62.50	3906.25	61.40	3769.96
Replicate, $x_2$	76.70	5882.89	68.30	4664.89
Replicate, $x_3$	72.20	5212.84	70.40	4956.16
Average ( $\bar{x}$ )	70.47	5000.66	66.70	4463.67
$\Sigma x^2$	15001.98		13391.01	
$(\Sigma x)^2$	44689.96		40040.01	
$((\Sigma x)^2)/n$	14896.65		13346.67	
$\Sigma d^2 = \Sigma x^2 - ((\Sigma x)^2)/n$	105.33		44.34	
$\sigma^2 = \frac{\Sigma d^2}{n-1}$	52.66		22.17	
$\sigma_d^2 = \frac{\sigma_1^2}{n_1} + \frac{\sigma_2^2}{n_2}$	24.94			
$\sigma_d$	4.99			
$t = \frac{\bar{x}_1 - \bar{x}_2}{\sigma_d}$	0.75			

$p > 0.1$

APPENDIX 6

Time: 20 s	Specimen			
	Polished 0-0	$x^2$	Unpolished 0-0	$x^2$
Replicate, $x_1$	62.20	3868.84	61.10	3733.21
Replicate, $x_2$	76.40	5836.96	65.40	4277.16
Replicate, $x_3$	70.20	4928.04	70.50	4970.25
Average ( $\bar{x}$ )	69.60	4877.95	65.67	4326.87
$\Sigma x^2$	14633.84		12980.62	
$(\Sigma x)^2$	43597.44		38809.00	
$((\Sigma x)^2)/n$	14532.48		12936.33	
$\Sigma d^2 = \Sigma x^2 - ((\Sigma x)^2)/n$	101.36		44.29	
$\sigma^2 = \frac{\Sigma d^2}{n-1}$	50.68		22.14	
$\sigma_d^2 = \frac{\sigma_1^2}{n_1} + \frac{\sigma_2^2}{n_2}$	24.27			
$\sigma_d$	4.93			
$t = \frac{\bar{x}_1 - \bar{x}_2}{\sigma_d}$	0.80			

p > 0.1

APPENDIX 6

Time: 30 s	Specimen			
	Polished 0-0	$x^2$	Unpolished 0-0	$x^2$
Replicate, $x_1$	59.70	3564.09	59.90	3588.01
Replicate, $x_2$	73.30	5372.89	67.00	4489.00
Replicate, $x_3$	68.30	4664.89	66.80	4462.24
Average ( $\bar{x}$ )	67.10	4533.96	64.57	4179.75
$\Sigma x^2$	13601.87		12539.25	
$(\Sigma x)^2$	40521.69		37519.69	
$((\Sigma x)^2)/n$	13507.23		12506.56	
$\Sigma d^2 = \Sigma x^2 - ((\Sigma x)^2)/n$	94.64		32.69	
$\sigma^2 = \frac{\Sigma d^2}{n-1}$	47.32		16.34	
$\sigma_d^2 = \frac{\sigma_1^2}{n_1} + \frac{\sigma_2^2}{n_2}$	21.22			
$\sigma_d$	4.61			
$t = \frac{\bar{x}_1 - \bar{x}_2}{\sigma_d}$	0.55			

$p > 0.1$

APPENDIX 6

Time: 40 s	Specimen			
	Polished 0-0	$x^2$	Unpolished 0-0	$x^2$
Replicate, $x_1$	59.20	3504.64	53.00	2809.00
Replicate, $x_2$	72.20	5212.84	62.40	3893.76
Replicate, $x_3$	67.30	4529.29	66.90	4475.61
Average ( $\bar{x}$ )	66.23	4415.59	60.77	3726.12
$\Sigma x^2$	13246.77		11178.37	
$(\Sigma x)^2$	39481.69		33233.29	
$((\Sigma x)^2)/n$	13160.56		11077.76	
$\Sigma d^2 = \Sigma x^2 - ((\Sigma x)^2)/n$	86.21		100.61	
$\sigma^2 = \frac{\Sigma d^2}{n-1}$	43.10		50.30	
$\sigma_d^2 = \frac{\sigma_1^2}{n_1} + \frac{\sigma_2^2}{n_2}$	31.14			
$\sigma_d$	5.58			
$t = \frac{\bar{x}_1 - \bar{x}_2}{\sigma_d}$	0.98			

$p > 0.1$

APPENDIX 6

Time: 50 s	Specimen			
	Polished 0-0	$x^2$	Unpolished 0-0	$x^2$
Replicate, $x_1$	55.50	3080.25	52.50	2756.25
Replicate, $x_2$	71.70	5140.89	62.70	3931.29
Replicate, $x_3$	66.00	4356.00	65.70	4316.49
Average ( $\bar{x}$ )	64.40	4192.38	60.30	3668.01
$\Sigma x^2$	12577.14		11004.03	
$(\Sigma x)^2$	37326.24		32724.81	
$((\Sigma x)^2)/n$	12442.08		10908.27	
$\Sigma d^2 = \Sigma x^2 - ((\Sigma x)^2)/n$	135.06		95.76	
$\sigma^2 = \frac{\Sigma d^2}{n-1}$	67.53		47.88	
$\sigma_d^2 = \frac{\sigma_1^2}{n_1} + \frac{\sigma_2^2}{n_2}$	38.47			
$\sigma_d$	6.20			
$t = \frac{\bar{x}_1 - \bar{x}_2}{\sigma_d}$	0.66			

$p > 0.1$

APPENDIX 6

Time: 60 s	Specimen			
	Polished 0-0	$x^2$	Unpolished 0-0	$x^2$
Replicate, $x_1$	57.90	3352.41	51.00	2601.00
Replicate, $x_2$	70.00	4900.00	62.30	3881.29
Replicate, $x_3$	63.60	4044.96	65.60	4303.36
Average ( $\bar{x}$ )	63.83	4099.12	59.63	3595.22
$\Sigma x^2$	12297.37		10785.65	
$(\Sigma x)^2$	36672.25		32005.21	
$((\Sigma x)^2)/n$	12224.08		10668.40	
$\Sigma d^2 = \Sigma x^2 - ((\Sigma x)^2)/n$	73.29		117.25	
$\sigma^2 = \frac{\Sigma d^2}{n-1}$	36.64		58.62	
$\sigma_d^2 = \frac{\sigma_1^2}{n_1} + \frac{\sigma_2^2}{n_2}$	31.76			
$\sigma_d$	5.64			
$t = \frac{\bar{x}_1 - \bar{x}_2}{\sigma_d}$	0.75			

$p > 0.1$

APPENDIX 6

Time: 70 s	Specimen			
	Polished 0-0	$x^2$	Unpolished 0-0	$x^2$
Replicate, $x_1$	54.30	2948.49	49.30	2430.49
Replicate, $x_2$	69.20	4788.64	61.10	3733.21
Replicate, $x_3$	62.40	3893.76	65.80	4329.64
Average ( $\bar{x}$ )	61.97	3876.96	58.73	3497.78
$\Sigma x^2$	11630.89		10493.34	
$(\Sigma x)^2$	34558.81		31046.44	
$((\Sigma x)^2)/n$	11519.60		10348.81	
$\Sigma d^2 = \Sigma x^2 - ((\Sigma x)^2)/n$	111.29		144.53	
$\sigma^2 = \frac{\Sigma d^2}{n-1}$	55.64		72.26	
$\sigma_d^2 = \frac{\sigma_1^2}{n_1} + \frac{\sigma_2^2}{n_2}$	42.64			
$\sigma_d$	6.53			
$t = \frac{\bar{x}_1 - \bar{x}_2}{\sigma_d}$	0.50			

$p > 0.1$



APPENDIX 6

Time: 80 s	Specimen			
	Polished 0-0	$x^2$	Unpolished 0-0	$x^2$
Replicate, $x_1$	53.80	2894.44	47.40	2246.76
Replicate, $x_2$	68.80	4733.44	59.20	3504.64
Replicate, $x_3$	61.90	3831.61	63.80	4070.44
Average ( $\bar{x}$ )	61.50	3819.83	56.80	3273.95
$\Sigma x^2$	11459.49		9821.84	
$(\Sigma x)^2$	34040.25		29036.16	
$((\Sigma x)^2)/n$	11346.75		9678.72	
$\Sigma d^2 = \Sigma x^2 - ((\Sigma x)^2)/n$	112.74		143.12	
$\sigma^2 = \frac{\Sigma d^2}{n-1}$	56.37		71.56	
$\sigma_d^2 = \frac{\sigma_1^2}{n_1} + \frac{\sigma_2^2}{n_2}$	42.64			
$\sigma_d$	6.53			
$t = \frac{\bar{x}_1 - \bar{x}_2}{\sigma_d}$	0.72			

$p > 0.1$

APPENDIX 6

Time: 90 s	Specimen			
	Polished 0-0	$x^2$	Unpolished 0-0	$x^2$
Replicate, $x_1$	52.30	2735.29	41.80	1747.24
Replicate, $x_2$	67.00	4489.00	58.30	3398.89
Replicate, $x_3$	61.50	3782.25	60.10	3612.01
Average ( $\bar{x}$ )	60.27	3668.85	53.40	2919.38
$\Sigma x^2$	11006.54		8758.14	
$(\Sigma x)^2$	32688.64		25664.04	
$((\Sigma x)^2)/n$	10896.21		8554.68	
$\Sigma d^2 = \Sigma x^2 - ((\Sigma x)^2)/n$	110.33		203.46	
$\sigma^2 = \frac{\Sigma d^2}{n-1}$	55.16		101.73	
$\sigma_d^2 = \frac{\sigma_1^2}{n_1} + \frac{\sigma_2^2}{n_2}$	52.30			
$\sigma_d$	7.23			
$t = \frac{\bar{x}_1 - \bar{x}_2}{\sigma_d}$	0.95			

$p > 0.1$

APPENDIX 6

Time: 100 s	Specimen			
	Polished 0-0	$x^2$	Unpolished 0-0	$x^2$
Replicate, $x_1$	50.10	2510.01	42.10	1772.41
Replicate, $x_2$	64.30	4134.49	58.50	3422.25
Replicate, $x_3$	58.30	3398.89	60.40	3648.16
Average ( $\bar{x}$ )	57.57	3347.80	53.67	2947.61
$\Sigma x^2$	10043.39		8842.82	
$(\Sigma x)^2$	29825.29		25921.00	
$((\Sigma x)^2)/n$	9941.76		8640.33	
$\Sigma d^2 = \Sigma x^2 - ((\Sigma x)^2)/n$	101.63		202.49	
$\sigma^2 = \frac{\Sigma d^2}{n-1}$	50.81		101.24	
$\sigma_d^2 = \frac{\sigma_1^2}{n_1} + \frac{\sigma_2^2}{n_2}$	50.69			
$\sigma_d$	7.12			
$t = \frac{\bar{x}_1 - \bar{x}_2}{\sigma_d}$	0.55			

$p > 0.1$

APPENDIX 6

Time: 110 s	Specimen			
	Polished 0-0	$x^2$	Unpolished 0-0	$x^2$
Replicate, $x_1$	48.70	2371.69	38.90	1513.21
Replicate, $x_2$	63.50	4032.25	54.50	2970.25
Replicate, $x_3$	56.40	3180.96	58.70	3445.69
Average ( $\bar{x}$ )	56.20	3194.97	50.70	2643.05
$\Sigma x^2$	9584.90		7929.15	
$(\Sigma x)^2$	28425.96		23134.41	
$((\Sigma x)^2)/n$	9475.32		7711.47	
$\Sigma d^2 = \Sigma x^2 - ((\Sigma x)^2)/n$	109.58		217.68	
$\sigma^2 = \frac{\Sigma d^2}{n-1}$	54.79		108.84	
$\sigma_d^2 = \frac{\sigma_1^2}{n_1} + \frac{\sigma_2^2}{n_2}$	54.54			
$\sigma_d$	7.39			
$t = \frac{\bar{x}_1 - \bar{x}_2}{\sigma_d}$	0.74			

$p > 0.1$

APPENDIX 6

Time: 120 s	Specimen			
	Polished 0-0	$x^2$	Unpolished 0-0	$x^2$
Replicate, $x_1$	48.60	2361.96	34.10	1162.81
Replicate, $x_2$	62.20	3868.84	52.50	2756.25
Replicate, $x_3$	55.40	3069.16	55.70	3102.49
Average ( $\bar{x}$ )	55.40	3099.99	47.43	2340.52
$\Sigma x^2$	9299.96		7021.55	
$(\Sigma x)^2$	27622.44		20249.29	
$((\Sigma x)^2)/n$	9207.48		6749.76	
$\Sigma d^2 = \Sigma x^2 - ((\Sigma x)^2)/n$	92.48		271.79	
$\sigma^2 = \frac{\Sigma d^2}{n-1}$	46.24		135.89	
$\sigma_d^2 = \frac{\sigma_1^2}{n_1} + \frac{\sigma_2^2}{n_2}$	60.71			
$\sigma_d$	7.79			
$t = \frac{\bar{x}_1 - \bar{x}_2}{\sigma_d}$	1.02			

$p > 0.1$

APPENDIX 6

Time: 130 s	Specimen			
	Polished 0-0	$x^2$	Unpolished 0-0	$x^2$
Replicate, $x_1$	47.50	2256.25	29.40	864.36
Replicate, $x_2$	61.40	3769.96	51.30	2631.69
Replicate, $x_3$	52.90	2798.41	55.20	3047.04
Average ( $\bar{x}$ )	53.93	2941.54	45.30	2181.03
$\Sigma x^2$	8824.62		6543.09	
$(\Sigma x)^2$	26179.24		18468.81	
$((\Sigma x)^2)/n$	8726.41		6156.27	
$\Sigma d^2 = \Sigma x^2 - ((\Sigma x)^2)/n$	98.21		386.82	
$\sigma^2 = \frac{\Sigma d^2}{n-1}$	49.10		193.41	
$\sigma_d^2 = \frac{\sigma_1^2}{n_1} + \frac{\sigma_2^2}{n_2}$	80.84			
$\sigma_d$	8.99			
$t = \frac{\bar{x}_1 - \bar{x}_2}{\sigma_d}$	0.96			

p > 0.1

APPENDIX 6

Time: 140 s	Specimen			
	Polished 0-0	$x^2$	Unpolished 0-0	$x^2$
Replicate, $x_1$	46.60	2171.56	21.90	479.61
Replicate, $x_2$	58.90	3469.21	50.00	2500.00
Replicate, $x_3$	51.10	2611.21	55.80	3113.64
Average ( $\bar{x}$ )	52.20	2750.66	42.57	2031.08
$\Sigma x^2$	8251.98		6093.25	
$(\Sigma x)^2$	24523.56		16307.29	
$((\Sigma x)^2)/n$	8174.52		5435.76	
$\Sigma d^2 = \Sigma x^2 - ((\Sigma x)^2)/n$	77.46		657.49	
$\sigma^2 = \frac{\Sigma d^2}{n-1}$	38.73		328.74	
$\sigma_d^2 = \frac{\sigma_1^2}{n_1} + \frac{\sigma_2^2}{n_2}$	122.49			
$\sigma_d$	11.07			
$t = \frac{\bar{x}_1 - \bar{x}_2}{\sigma_d}$	0.87			

$p > 0.1$

APPENDIX 6

Time: 150 s	Specimen			
	Polished 0-0	$x^2$	Unpolished 0-0	$x^2$
Replicate, $x_1$	44.50	1980.25	22.30	497.29
Replicate, $x_2$	56.20	3158.44	49.20	2420.64
Replicate, $x_3$	50.60	2560.36	50.90	2590.81
Average ( $\bar{x}$ )	50.43	2566.35	40.80	1836.25
$\Sigma x^2$	7699.05		5508.74	
$(\Sigma x)^2$	22891.69		14981.76	
$((\Sigma x)^2)/n$	7630.56		4993.92	
$\Sigma d^2 = \Sigma x^2 - ((\Sigma x)^2)/n$	68.49		514.82	
$\sigma^2 = \frac{\Sigma d^2}{n-1}$	34.24		257.41	
$\sigma_d^2 = \frac{\sigma_1^2}{n_1} + \frac{\sigma_2^2}{n_2}$	97.22			
$\sigma_d$	9.86			
$t = \frac{\bar{x}_1 - \bar{x}_2}{\sigma_d}$	0.98			

$p > 0.1$



APPENDIX 6

Time: 0 s	Specimen			
	Polished 10-5	$x^2$	Unpolished 10-5	$x^2$
Replicate, $x_1$	70.00	4900.00	64.30	4134.49
Replicate, $x_2$	74.10	5490.81	81.45	6634.10
Replicate, $x_3$	71.60	5126.56	73.30	5372.89
Average ( $\bar{x}$ )	71.90	5172.46	73.02	5380.49
$\Sigma x^2$	15517.37		16141.48	
$(\Sigma x)^2$	46526.49		47982.90	
$((\Sigma x)^2)/n$	15508.83		15994.30	
$\Sigma d^2 = \Sigma x^2 - ((\Sigma x)^2)/n$	8.54		147.18	
$\sigma^2 = \frac{\Sigma d^2}{n-1}$	4.27		73.59	
$\sigma_d^2 = \frac{\sigma_1^2}{n_1} + \frac{\sigma_2^2}{n_2}$	25.95			
$\sigma_d$	5.09			
$t = \frac{\bar{x}_1 - \bar{x}_2}{\sigma_d}$	0.22			

$p > 0.1$

APPENDIX 6

Time: 10 s	Specimen			
	Polished 10-5	$x^2$	Unpolished 10-5	$x^2$
Replicate, $x_1$	62.90	3956.41	57.20	3271.84
Replicate, $x_2$	71.20	5069.44	80.30	6448.09
Replicate, $x_3$	65.60	4303.36	70.10	4914.01
Average ( $\bar{x}$ )	66.57	4443.07	69.20	4877.98
$\Sigma x^2$	13329.21		14633.94	
$(\Sigma x)^2$	39880.09		43097.76	
$((\Sigma x)^2)/n$	13293.36		14365.92	
$\Sigma d^2 = \Sigma x^2 - ((\Sigma x)^2)/n$	35.85		268.02	
$\sigma^2 = \frac{\Sigma d^2}{n-1}$	17.92		134.01	
$\sigma_d^2 = \frac{\sigma_1^2}{n_1} + \frac{\sigma_2^2}{n_2}$	50.64			
$\sigma_d$	7.12			
$t = \frac{\bar{x}_1 - \bar{x}_2}{\sigma_d}$	0.37			

$p > 0.1$

APPENDIX 6

Time: 20 s	Specimen			
	Polished 10-5	$x^2$	Unpolished 10-5	$x^2$
Replicate, $x_1$	61.10	3733.21	56.00	3136.00
Replicate, $x_2$	68.40	4678.56	79.15	6264.72
Replicate, $x_3$	65.20	4251.04	68.40	4678.56
Average ( $\bar{x}$ )	64.90	4220.94	67.85	4693.09
$\Sigma x^2$	12662.81		14079.28	
$(\Sigma x)^2$	37908.09		41432.60	
$((\Sigma x)^2)/n$	12636.03		13810.87	
$\Sigma d^2 = \Sigma x^2 - ((\Sigma x)^2)/n$	26.78		268.41	
$\sigma^2 = \frac{\Sigma d^2}{n-1}$	13.39		134.21	
$\sigma_d^2 = \frac{\sigma_1^2}{n_1} + \frac{\sigma_2^2}{n_2}$	49.20			
$\sigma_d$	7.01			
$t = \frac{\bar{x}_1 - \bar{x}_2}{\sigma_d}$	0.42			

$p > 0.1$

APPENDIX 6

Time: 30 s	Specimen			
	Polished 0-0	$x^2$	Unpolished 0-0	$x^2$
Replicate, $x_1$	60.70	3684.49	55.30	3058.09
Replicate, $x_2$	67.90	4610.41	78.00	6084.00
Replicate, $x_3$	62.90	3956.41	67.00	4489.00
Average ( $\bar{x}$ )	63.83	4083.77	66.77	4543.70
$\Sigma x^2$	12251.31		13631.09	
$(\Sigma x)^2$	36672.25		40120.09	
$((\Sigma x)^2)/n$	12224.08		13373.36	
$\Sigma d^2 = \Sigma x^2 - ((\Sigma x)^2)/n$	27.23		257.73	
$\sigma^2 = \frac{\Sigma d^2}{n-1}$	13.61		128.86	
$\sigma_d^2 = \frac{\sigma_1^2}{n_1} + \frac{\sigma_2^2}{n_2}$	47.49			
$\sigma_d$	6.89			
$t = \frac{\bar{x}_1 - \bar{x}_2}{\sigma_d}$	0.43			

$p > 0.1$

APPENDIX 6

Time: 40 s	Specimen			
	Polished 10-5	$x^2$	Unpolished 10-5	$x^2$
Replicate, $x_1$	58.20	3387.24	53.10	2819.61
Replicate, $x_2$	66.80	4462.24	76.85	5905.92
Replicate, $x_3$	61.00	3721.00	65.30	4264.09
Average ( $\bar{x}$ )	62.00	3856.83	65.08	4329.87
$\Sigma x^2$	11570.48		12989.62	
$(\Sigma x)^2$	34596.00		38122.56	
$((\Sigma x)^2)/n$	11532.00		12707.52	
$\Sigma d^2 = \Sigma x^2 - ((\Sigma x)^2)/n$	38.48		282.10	
$\sigma^2 = \frac{\Sigma d^2}{n-1}$	19.24		141.05	
$\sigma_d^2 = \frac{\sigma_1^2}{n_1} + \frac{\sigma_2^2}{n_2}$	53.43			
$\sigma_d$	7.31			
$t = \frac{\bar{x}_1 - \bar{x}_2}{\sigma_d}$	0.42			

$p > 0.1$

APPENDIX 6

Time: 50 s	Specimen			
	Polished 10-5	$x^2$	Unpolished 10-5	$x^2$
Replicate, $x_1$	57.50	3306.25	52.80	2787.84
Replicate, $x_2$	64.30	4134.49	75.70	5730.49
Replicate, $x_3$	58.90	3469.21	63.90	4083.21
Average ( $\bar{x}$ )	60.23	3636.65	64.13	4200.51
$\Sigma x^2$	10909.95		12601.54	
$(\Sigma x)^2$	32652.49		37017.76	
$((\Sigma x)^2)/n$	10884.16		12339.25	
$\Sigma d^2 = \Sigma x^2 - ((\Sigma x)^2)/n$	25.79		262.29	
$\sigma^2 = \frac{\Sigma d^2}{n-1}$	12.89		131.14	
$\sigma_d^2 = \frac{\sigma_1^2}{n_1} + \frac{\sigma_2^2}{n_2}$	48.01			
$\sigma_d$	6.93			
$t = \frac{\bar{x}_1 - \bar{x}_2}{\sigma_d}$	0.56			

$p > 0.1$

APPENDIX 6

Time: 60 s	Specimen			
	Polished 10-5	$x^2$	Unpolished 10-5	$x^2$
Replicate, $x_1$	55.80	3113.64	48.30	2332.89
Replicate, $x_2$	62.80	3943.84	74.90	5610.01
Replicate, $x_3$	58.00	3364.00	62.10	3856.41
Average ( $\bar{x}$ )	58.87	3473.83	61.77	3933.10
$\Sigma x^2$	10421.48		11799.31	
$(\Sigma x)^2$	31187.56		34336.09	
$((\Sigma x)^2)/n$	10395.85		11445.36	
$\Sigma d^2 = \Sigma x^2 - ((\Sigma x)^2)/n$	25.63		353.95	
$\sigma^2 = \frac{\Sigma d^2}{n-1}$	12.81		176.97	
$\sigma_d^2 = \frac{\sigma_1^2}{n_1} + \frac{\sigma_2^2}{n_2}$	63.26			
$\sigma_d$	7.95			
$t = \frac{\bar{x}_1 - \bar{x}_2}{\sigma_d}$	0.36			

$p > 0.1$

APPENDIX 6

Time: 70 s	Specimen			
	Polished 10-5	$x^2$	Unpolished 10-5	$x^2$
Replicate, $x_1$	54.60	2981.16	48.50	2352.25
Replicate, $x_2$	62.00	3844.00	72.70	5285.29
Replicate, $x_3$	57.00	3249.00	61.00	3721.00
Average ( $\bar{x}$ )	57.87	3358.05	60.73	3786.18
$\Sigma x^2$	10074.16		11358.54	
$(\Sigma x)^2$	30136.96		33196.84	
$((\Sigma x)^2)/n$	10045.65		11065.61	
$\Sigma d^2 = \Sigma x^2 - ((\Sigma x)^2)/n$	28.51		292.93	
$\sigma^2 = \frac{\Sigma d^2}{n-1}$	14.25		146.46	
$\sigma_d^2 = \frac{\sigma_1^2}{n_1} + \frac{\sigma_2^2}{n_2}$	53.57			
$\sigma_d$	7.32			
$t = \frac{\bar{x}_1 - \bar{x}_2}{\sigma_d}$	0.39			

$p > 0.1$



APPENDIX 6

Time: 80 s	Specimen			
	Polished 10-5	$x^2$	Unpolished 10-5	$x^2$
Replicate, $x_1$	54.20	2937.64	47.80	2284.84
Replicate, $x_2$	60.30	3636.09	72.60	5270.76
Replicate, $x_3$	55.70	3102.49	60.10	3612.01
Average ( $\bar{x}$ )	56.73	3225.41	60.17	3722.54
$\Sigma x^2$	9676.22		11167.61	
$(\Sigma x)^2$	28968.04		32580.25	
$((\Sigma x)^2)/n$	9656.01		10860.08	
$\Sigma d^2 = \Sigma x^2 - ((\Sigma x)^2)/n$	20.21		307.53	
$\sigma^2 = \frac{\Sigma d^2}{n-1}$	10.10		153.76	
$\sigma_d^2 = \frac{\sigma_1^2}{n_1} + \frac{\sigma_2^2}{n_2}$	54.62			
$\sigma_d$	7.39			
$t = \frac{\bar{x}_1 - \bar{x}_2}{\sigma_d}$	0.46			

p > 0.1

APPENDIX 6

Time: 90 s	Specimen			
	Polished 10-5	$x^2$	Unpolished 10-5	$x^2$
Replicate, $x_1$	52.70	2777.29	44.60	1989.16
Replicate, $x_2$	59.80	3576.04	71.80	5155.24
Replicate, $x_3$	52.00	2704.00	58.80	3457.44
Average ( $\bar{x}$ )	54.83	3019.11	58.40	3533.95
$\Sigma x^2$	9057.33		10601.84	
$(\Sigma x)^2$	27060.25		30695.04	
$((\Sigma x)^2)/n$	9020.08		10231.68	
$\Sigma d^2 = \Sigma x^2 - ((\Sigma x)^2)/n$	37.25		370.16	
$\sigma^2 = \frac{\Sigma d^2}{n-1}$	18.62		185.08	
$\sigma_d^2 = \frac{\sigma_1^2}{n_1} + \frac{\sigma_2^2}{n_2}$	67.90			
$\sigma_d$	8.24			
$t = \frac{\bar{x}_1 - \bar{x}_2}{\sigma_d}$	0.43			

$p > 0.1$

APPENDIX 6

Time: 100 s	Specimen			
	Polished 10-5	$x^2$	Unpolished 10-5	$x^2$
Replicate, $x_1$	49.30	2430.49	42.00	1764.00
Replicate, $x_2$	57.30	3283.29	70.10	4914.01
Replicate, $x_3$	49.70	2470.09	56.50	3192.25
Average ( $\bar{x}$ )	52.10	2727.96	56.20	3290.09
$\Sigma x^2$	8183.87		9870.26	
$(\Sigma x)^2$	24429.69		28425.96	
$((\Sigma x)^2)/n$	8143.23		9475.32	
$\Sigma d^2 = \Sigma x^2 - ((\Sigma x)^2)/n$	40.64		394.94	
$\sigma^2 = \frac{\Sigma d^2}{n-1}$	20.32		197.47	
$\sigma_d^2 = \frac{\sigma_1^2}{n_1} + \frac{\sigma_2^2}{n_2}$	72.60			
$\sigma_d$	8.52			
$t = \frac{\bar{x}_1 - \bar{x}_2}{\sigma_d}$	0.48			

$p > 0.1$

APPENDIX 6

Time: 110 s	Specimen			
	Polished 10-5	$x^2$	Unpolished 10-5	$x^2$
Replicate, $x_1$	47.00	2209.00	43.10	1857.61
Replicate, $x_2$	56.80	3226.24	69.90	4886.01
Replicate, $x_3$	48.90	2391.21	54.30	2948.49
Average ( $\bar{x}$ )	50.90	2608.82	55.77	3230.70
$\Sigma x^2$	7826.45		9692.11	
$(\Sigma x)^2$	23317.29		27989.29	
$((\Sigma x)^2)/n$	7772.43		9329.76	
$\Sigma d^2 = \Sigma x^2 - ((\Sigma x)^2)/n$	54.02		362.35	
$\sigma^2 = \frac{\Sigma d^2}{n-1}$	27.01		181.17	
$\sigma_d^2 = \frac{\sigma_1^2}{n_1} + \frac{\sigma_2^2}{n_2}$	69.39			
$\sigma_d$	8.33			
$t = \frac{\bar{x}_1 - \bar{x}_2}{\sigma_d}$	0.58			

$p > 0.1$

APPENDIX 6

Time: 120 s	Specimen			
	Polished 10-5	$x^2$	Unpolished 10-5	$x^2$
Replicate, $x_1$	46.90	2199.61	37.80	1428.84
Replicate, $x_2$	55.20	3047.04	67.20	4515.84
Replicate, $x_3$	46.80	2190.24	53.10	2819.61
Average ( $\bar{x}$ )	49.63	2478.96	52.70	2921.43
$\Sigma x^2$	7436.89		8764.29	
$(\Sigma x)^2$	22171.21		24995.61	
$((\Sigma x)^2)/n$	7390.40		8331.87	
$\Sigma d^2 = \Sigma x^2 - ((\Sigma x)^2)/n$	46.49		432.42	
$\sigma^2 = \frac{\Sigma d^2}{n-1}$	23.24		216.21	
$\sigma_d^2 = \frac{\sigma_1^2}{n_1} + \frac{\sigma_2^2}{n_2}$	79.82			
$\sigma_d$	8.93			
$t = \frac{\bar{x}_1 - \bar{x}_2}{\sigma_d}$	0.34			

$p > 0.1$

APPENDIX 6

Time: 130 s	Specimen			
	Polished 10-5	$x^2$	Unpolished 10-5	$x^2$
Replicate, $x_1$	45.10	2034.01	37.50	1406.25
Replicate, $x_2$	52.90	2798.41	65.90	4342.81
Replicate, $x_3$	46.30	2143.69	50.20	2520.04
Average ( $\bar{x}$ )	48.10	2325.37	51.20	2756.37
$\Sigma x^2$	6976.11		8269.10	
$(\Sigma x)^2$	20822.49		23592.96	
$((\Sigma x)^2)/n$	6940.83		7864.32	
$\Sigma d^2 = \Sigma x^2 - ((\Sigma x)^2)/n$	35.28		404.78	
$\sigma^2 = \frac{\Sigma d^2}{n-1}$	17.64		202.39	
$\sigma_d^2 = \frac{\sigma_1^2}{n_1} + \frac{\sigma_2^2}{n_2}$	73.34			
$\sigma_d$	8.56			
$t = \frac{\bar{x}_1 - \bar{x}_2}{\sigma_d}$	0.36			

$p > 0.1$

APPENDIX 6

Time: 140 s	Specimen			
	Polished 10-5	$x^2$	Unpolished 10-5	$x^2$
Replicate, $x_1$	45.00	2025.00	34.80	1211.04
Replicate, $x_2$	52.20	2724.84	61.80	3819.24
Replicate, $x_3$	42.50	1806.25	46.20	2134.44
Average ( $\bar{x}$ )	46.57	2185.36	47.60	2388.24
$\Sigma x^2$	6556.09		7164.72	
$(\Sigma x)^2$	19516.09		20391.84	
$((\Sigma x)^2)/n$	6505.36		6797.28	
$\Sigma d^2 = \Sigma x^2 - ((\Sigma x)^2)/n$	50.73		367.44	
$\sigma^2 = \frac{\Sigma d^2}{n-1}$	25.36		183.72	
$\sigma_d^2 = \frac{\sigma_1^2}{n_1} + \frac{\sigma_2^2}{n_2}$	69.69			
$\sigma_d$	8.35			
$t = \frac{\bar{x}_1 - \bar{x}_2}{\sigma_d}$	0.12			

$p > 0.1$

APPENDIX 6

Time: 150 s	Specimen			
	Polished 10-5	$x^2$	Unpolished 10-5	$x^2$
Replicate, $x_1$	40.20	1616.04	34.70	1204.09
Replicate, $x_2$	52.20	2724.84	60.60	3672.36
Replicate, $x_3$	41.00	1681.00	44.60	1989.16
Average ( $\bar{x}$ )	44.47	2007.29	46.63	2288.54
$\Sigma x^2$	6021.88		6865.61	
$(\Sigma x)^2$	17795.56		19572.01	
$((\Sigma x)^2)/n$	5931.85		6524.00	
$\Sigma d^2 = \Sigma x^2 - ((\Sigma x)^2)/n$	90.03		341.61	
$\sigma^2 = \frac{\Sigma d^2}{n-1}$	45.01		170.80	
$\sigma_d^2 = \frac{\sigma_1^2}{n_1} + \frac{\sigma_2^2}{n_2}$	71.94			
$\sigma_d$	8.48			
$t = \frac{\bar{x}_1 - \bar{x}_2}{\sigma_d}$	0.26			

$p > 0.1$



APPENDIX 6

Time: 0 s	Specimen			
	Polished 10-10	$x^2$	Unpolished 10-10	$x^2$
Replicate, $x_1$	69.60	4844.16	40.80	1664.64
Replicate, $x_2$	59.40	3528.36	54.60	2981.16
Replicate, $x_3$	63.30	4006.89	58.80	3457.44
Average ( $\bar{x}$ )	64.10	4126.47	51.40	2701.08
$\Sigma x^2$	12379.41		8103.24	
$(\Sigma x)^2$	36979.29		23777.64	
$((\Sigma x)^2)/n$	12326.43		7925.88	
$\Sigma d^2 = \Sigma x^2 - ((\Sigma x)^2)/n$	52.98		177.36	
$\sigma^2 = \frac{\Sigma d^2}{n-1}$	26.49		88.68	
$\sigma_d^2 = \frac{\sigma_1^2}{n_1} + \frac{\sigma_2^2}{n_2}$	38.39			
$\sigma_d$	6.20			
$t = \frac{\bar{x}_1 - \bar{x}_2}{\sigma_d}$	2.05			

$p < 0.05$

APPENDIX 6

Time: 10 s	Specimen			
	Polished 10-10	$x^2$	Unpolished 10-10	$x^2$
Replicate, $x_1$	65.30	4264.09	38.70	1497.69
Replicate, $x_2$	56.30	3169.69	49.50	2450.25
Replicate, $x_3$	61.10	3733.21	56.70	3214.89
Average ( $\bar{x}$ )	60.90	3722.33	48.30	2387.61
$\Sigma x^2$	11166.99		7162.83	
$(\Sigma x)^2$	33379.29		20996.01	
$((\Sigma x)^2)/n$	11126.43		6998.67	
$\Sigma d^2 = \Sigma x^2 - ((\Sigma x)^2)/n$	40.56		164.16	
$\sigma^2 = \frac{\Sigma d^2}{n-1}$	20.28		82.08	
$\sigma_d^2 = \frac{\sigma_1^2}{n_1} + \frac{\sigma_2^2}{n_2}$	34.12			
$\sigma_d$	5.84			
$t = \frac{\bar{x}_1 - \bar{x}_2}{\sigma_d}$	2.16			

$p < 0.05$

APPENDIX 6

Time: 20 s	Specimen			
	Polished 10-10	$x^2$	Unpolished 10-10	$x^2$
Replicate, $x_1$	63.80	4070.44	38.00	1444.00
Replicate, $x_2$	52.40	2745.76	48.10	2313.61
Replicate, $x_3$	59.50	3540.25	56.00	3136.00
Average ( $\bar{x}$ )	58.57	3452.15	47.37	2297.87
$\Sigma x^2$	10356.45		6893.61	
$(\Sigma x)^2$	30870.49		20192.41	
$((\Sigma x)^2)/n$	10290.16		6730.80	
$\Sigma d^2 = \Sigma x^2 - ((\Sigma x)^2)/n$	66.29		162.81	
$\sigma^2 = \frac{\Sigma d^2}{n-1}$	33.14		81.40	
$\sigma_d^2 = \frac{\sigma_1^2}{n_1} + \frac{\sigma_2^2}{n_2}$	38.18			
$\sigma_d$	6.18			
$t = \frac{\bar{x}_1 - \bar{x}_2}{\sigma_d}$	1.81			

$p < 0.1$

APPENDIX 6

Time: 30 s	Specimen			
	Polished 10-10	$x^2$	Unpolished 10-10	$x^2$
Replicate, $x_1$	62.60	3918.76	25.10	630.01
Replicate, $x_2$	48.50	2352.25	46.90	2199.61
Replicate, $x_3$	59.50	3540.25	43.10	1857.61
Average ( $\bar{x}$ )	56.87	3270.42	38.37	1562.41
$\Sigma x^2$	9811.26		4687.23	
$(\Sigma x)^2$	29104.36		13248.01	
$((\Sigma x)^2)/n$	9701.45		4416.00	
$\Sigma d^2 = \Sigma x^2 - ((\Sigma x)^2)/n$	109.81		271.23	
$\sigma^2 = \frac{\Sigma d^2}{n-1}$	54.90		135.61	
$\sigma_d^2 = \frac{\sigma_1^2}{n_1} + \frac{\sigma_2^2}{n_2}$	63.51			
$\sigma_d$	7.97			
$t = \frac{\bar{x}_1 - \bar{x}_2}{\sigma_d}$	2.32			

$p < 0.05$

APPENDIX 6

Time: 40 s	Specimen			
	Polished 10-10	$x^2$	Unpolished 10-10	$x^2$
Replicate, $x_1$	61.20	3745.44	19.00	361.00
Replicate, $x_2$	46.50	2162.25	44.00	1936.00
Replicate, $x_3$	56.80	3226.24	37.00	1369.00
Average ( $\bar{x}$ )	54.83	3044.64	33.33	1222.00
$\Sigma x^2$	9133.93		3666.00	
$(\Sigma x)^2$	27060.25		10000.00	
$((\Sigma x)^2)/n$	9020.08		3333.33	
$\Sigma d^2 = \Sigma x^2 - ((\Sigma x)^2)/n$	113.85		332.67	
$\sigma^2 = \frac{\Sigma d^2}{n-1}$	56.92		166.33	
$\sigma_d^2 = \frac{\sigma_1^2}{n_1} + \frac{\sigma_2^2}{n_2}$	74.42			
$\sigma_d$	8.63			
$t = \frac{\bar{x}_1 - \bar{x}_2}{\sigma_d}$	2.49			

$p < 0.05$

APPENDIX 6

Time: 50 s	Specimen			
	Polished 10-10	$x^2$	Unpolished 10-10	$x^2$
Replicate, $x_1$	60.10	3612.01	16.00	256.00
Replicate, $x_2$	44.20	1953.64	43.20	1866.24
Replicate, $x_3$	56.40	3180.96	34.00	1156.00
Average ( $\bar{x}$ )	53.57	2915.54	31.07	1092.75
$\Sigma x^2$	8746.61		3278.24	
$(\Sigma x)^2$	25824.49		8686.24	
$((\Sigma x)^2)/n$	8608.16		2895.41	
$\Sigma d^2 = \Sigma x^2 - ((\Sigma x)^2)/n$	138.45		382.83	
$\sigma^2 = \frac{\Sigma d^2}{n-1}$	69.22		191.41	
$\sigma_d^2 = \frac{\sigma_1^2}{n_1} + \frac{\sigma_2^2}{n_2}$	86.88			
$\sigma_d$	9.32			
$t = \frac{\bar{x}_1 - \bar{x}_2}{\sigma_d}$	2.41			

$p < 0.05$

APPENDIX 6

Time: 60 s	Specimen			
	Polished 10-10	$x^2$	Unpolished 10-10	$x^2$
Replicate, $x_1$	59.40	3528.36	13.10	171.61
Replicate, $x_2$	43.90	1927.21	42.60	1814.76
Replicate, $x_3$	55.20	3047.04	31.10	967.21
Average ( $\bar{x}$ )	52.83	2834.20	28.93	984.53
$\Sigma x^2$	8502.61		2953.58	
$(\Sigma x)^2$	25122.25		7534.24	
$((\Sigma x)^2)/n$	8374.08		2511.41	
$\Sigma d^2 = \Sigma x^2 - ((\Sigma x)^2)/n$	128.53		442.17	
$\sigma^2 = \frac{\Sigma d^2}{n-1}$	64.26		221.08	
$\sigma_d^2 = \frac{\sigma_1^2}{n_1} + \frac{\sigma_2^2}{n_2}$	95.12			
$\sigma_d$	9.75			
$t = \frac{\bar{x}_1 - \bar{x}_2}{\sigma_d}$	2.45			

$p < 0.05$

APPENDIX 6

Time: 70 s	Specimen			
	Polished 10-10	$x^2$	Unpolished 10-10	$x^2$
Replicate, $x_1$	57.80	3340.84	12.80	163.84
Replicate, $x_2$	41.10	1689.21	40.20	1616.04
Replicate, $x_3$	53.10	2819.61	30.80	948.64
Average ( $\bar{x}$ )	50.67	2616.55	27.93	909.51
$\Sigma x^2$	7849.66		2728.52	
$(\Sigma x)^2$	23104.00		7022.44	
$((\Sigma x)^2)/n$	7701.33		2340.81	
$\Sigma d^2 = \Sigma x^2 - ((\Sigma x)^2)/n$	148.33		387.71	
$\sigma^2 = \frac{\Sigma d^2}{n-1}$	74.16		193.85	
$\sigma_d^2 = \frac{\sigma_1^2}{n_1} + \frac{\sigma_2^2}{n_2}$	89.34			
$\sigma_d$	9.45			
$t = \frac{\bar{x}_1 - \bar{x}_2}{\sigma_d}$	2.41			

$p < 0.05$



APPENDIX 6

Time: 80 s	Specimen			
	Polished 10-10	$x^2$	Unpolished 10-10	$x^2$
Replicate, $x_1$	55.80	3113.64	11.40	129.96
Replicate, $x_2$	39.60	1568.16	38.50	1482.25
Replicate, $x_3$	53.60	2872.96	29.40	864.36
Average ( $\bar{x}$ )	49.67	2518.25	26.43	825.52
$\Sigma x^2$	7554.76		2476.57	
$(\Sigma x)^2$	22201.00		6288.49	
$((\Sigma x)^2)/n$	7400.33		2096.16	
$\Sigma d^2 = \Sigma x^2 - ((\Sigma x)^2)/n$	154.43		380.41	
$\sigma^2 = \frac{\Sigma d^2}{n-1}$	77.21		190.20	
$\sigma_d^2 = \frac{\sigma_1^2}{n_1} + \frac{\sigma_2^2}{n_2}$	89.14			
$\sigma_d$	9.44			
$t = \frac{\bar{x}_1 - \bar{x}_2}{\sigma_d}$	2.46			

$p < 0.05$

APPENDIX 6

Time: 90 s	Specimen			
	Polished 10-10	$x^2$	Unpolished 10-10	$x^2$
Replicate, $x_1$	53.30	2840.89	10.20	104.04
Replicate, $x_2$	36.20	1310.44	34.10	1162.81
Replicate, $x_3$	50.70	2570.49	28.20	795.24
Average ( $\bar{x}$ )	46.73	2240.61	24.17	687.36
$\Sigma x^2$	6721.82		2062.09	
$(\Sigma x)^2$	19656.04		5256.25	
$((\Sigma x)^2)/n$	6552.01		1752.08	
$\Sigma d^2 = \Sigma x^2 - ((\Sigma x)^2)/n$	169.81		310.01	
$\sigma^2 = \frac{\Sigma d^2}{n-1}$	84.90		155.00	
$\sigma_d^2 = \frac{\sigma_1^2}{n_1} + \frac{\sigma_2^2}{n_2}$	79.97			
$\sigma_d$	8.94			
$t = \frac{\bar{x}_1 - \bar{x}_2}{\sigma_d}$	2.52			

$p < 0.05$

APPENDIX 6

Time: 100 s	Specimen			
	Polished 10-10	$x^2$	Unpolished 10-10	$x^2$
Replicate, $x_1$	52.40	2745.76	9.80	96.04
Replicate, $x_2$	37.50	1406.25	30.80	948.64
Replicate, $x_3$	50.20	2520.04	27.80	772.84
Average ( $\bar{x}$ )	46.70	2224.02	22.80	605.84
$\Sigma x^2$	6672.05		1817.52	
$(\Sigma x)^2$	19628.01		4678.56	
$((\Sigma x)^2)/n$	6542.67		1559.52	
$\Sigma d^2 = \Sigma x^2 - ((\Sigma x)^2)/n$	129.38		258.00	
$\sigma^2 = \frac{\Sigma d^2}{n-1}$	64.69		129.00	
$\sigma_d^2 = \frac{\sigma_1^2}{n_1} + \frac{\sigma_2^2}{n_2}$	64.56			
$\sigma_d$	8.04			
$t = \frac{\bar{x}_1 - \bar{x}_2}{\sigma_d}$	2.97			

$p < 0.05$

APPENDIX 6

Time: 110 s	Specimen			
	Polished 10-10	$x^2$	Unpolished 10-10	$x^2$
Replicate, $x_1$	50.50	2550.25	7.30	53.29
Replicate, $x_2$	37.80	1428.84	27.20	739.84
Replicate, $x_3$	45.80	2097.64	25.30	640.09
Average ( $\bar{x}$ )	44.70	2025.58	19.93	477.74
$\Sigma x^2$	6076.73		1433.22	
$(\Sigma x)^2$	17982.81		3576.04	
$((\Sigma x)^2)/n$	5994.27		1192.01	
$\Sigma d^2 = \Sigma x^2 - ((\Sigma x)^2)/n$	82.46		241.21	
$\sigma^2 = \frac{\Sigma d^2}{n-1}$	41.23		120.60	
$\sigma_d^2 = \frac{\sigma_1^2}{n_1} + \frac{\sigma_2^2}{n_2}$	53.94			
$\sigma_d$	7.34			
$t = \frac{\bar{x}_1 - \bar{x}_2}{\sigma_d}$	3.37			

$p < 0.01$

APPENDIX 6

Time: 120 s	Specimen			
	Polished 10-10	$x^2$	Unpolished 10-10	$x^2$
Replicate, $x_1$	50.00	2500.00	6.70	44.89
Replicate, $x_2$	32.10	1030.41	25.40	645.16
Replicate, $x_3$	47.00	2209.00	24.70	610.09
Average ( $\bar{x}$ )	43.03	1913.14	18.93	433.38
$\Sigma x^2$	5739.41		1300.14	
$(\Sigma x)^2$	16666.81		3226.24	
$((\Sigma x)^2)/n$	5555.60		1075.41	
$\Sigma d^2 = \Sigma x^2 - ((\Sigma x)^2)/n$	183.81		224.73	
$\sigma^2 = \frac{\Sigma d^2}{n-1}$	91.90		112.36	
$\sigma_d^2 = \frac{\sigma_1^2}{n_1} + \frac{\sigma_2^2}{n_2}$	68.09			
$\sigma_d$	8.25			
$t = \frac{\bar{x}_1 - \bar{x}_2}{\sigma_d}$	2.92			

$p < 0.05$

APPENDIX 6

Time: 130 s	Specimen			
	Polished 10-10	$x^2$	Unpolished 10-10	$x^2$
Replicate, $x_1$	48.70	2371.69	8.90	79.21
Replicate, $x_2$	32.60	1062.76	23.90	571.21
Replicate, $x_3$	47.50	2256.25	26.90	723.61
Average ( $\bar{x}$ )	42.93	1896.90	19.90	458.01
$\Sigma x^2$	5690.70		1374.03	
$(\Sigma x)^2$	16589.44		3564.09	
$((\Sigma x)^2)/n$	5529.81		1188.03	
$\Sigma d^2 = \Sigma x^2 - ((\Sigma x)^2)/n$	160.89		186.00	
$\sigma^2 = \frac{\Sigma d^2}{n-1}$	80.44		93.00	
$\sigma_d^2 = \frac{\sigma_1^2}{n_1} + \frac{\sigma_2^2}{n_2}$	57.81			
$\sigma_d$	7.60			
$t = \frac{\bar{x}_1 - \bar{x}_2}{\sigma_d}$	3.03			

$p < 0.05$

APPENDIX 6

Time: 140 s	Specimen			
	Polished 10-10	$x^2$	Unpolished 10-10	$x^2$
Replicate, $x_1$	46.80	2190.24	6.40	40.96
Replicate, $x_2$	29.70	882.09	22.10	488.41
Replicate, $x_3$	41.50	1722.25	24.40	595.36
Average ( $\bar{x}$ )	39.33	1598.19	17.63	374.91
$\Sigma x^2$	4794.58		1124.73	
$(\Sigma x)^2$	13924.00		2798.41	
$((\Sigma x)^2)/n$	4641.33		932.80	
$\Sigma d^2 = \Sigma x^2 - ((\Sigma x)^2)/n$	153.25		191.93	
$\sigma^2 = \frac{\Sigma d^2}{n-1}$	76.62		95.96	
$\sigma_d^2 = \frac{\sigma_1^2}{n_1} + \frac{\sigma_2^2}{n_2}$	57.53			
$\sigma_d$	7.58			
$t = \frac{\bar{x}_1 - \bar{x}_2}{\sigma_d}$	2.86			

$p < 0.05$

APPENDIX 6

Time: 150 s	Specimen			
	Polished 10-10	$x^2$	Unpolished 10-10	$x^2$
Replicate, $x_1$	44.70	1998.09	6.60	43.56
Replicate, $x_2$	29.40	864.36	20.30	412.09
Replicate, $x_3$	42.70	1823.29	24.60	605.16
Average ( $\bar{x}$ )	38.93	1561.91	17.17	353.60
$\Sigma x^2$	4685.74		1060.81	
$(\Sigma x)^2$	13642.24		2652.25	
$((\Sigma x)^2)/n$	4547.41		884.08	
$\Sigma d^2 = \Sigma x^2 - ((\Sigma x)^2)/n$	138.33		176.73	
$\sigma^2 = \frac{\Sigma d^2}{n-1}$	69.16		88.36	
$\sigma_d^2 = \frac{\sigma_1^2}{n_1} + \frac{\sigma_2^2}{n_2}$	52.51			
$\sigma_d$	7.25			
$t = \frac{\bar{x}_1 - \bar{x}_2}{\sigma_d}$	3.00			

$p < 0.05$



APPENDIX 6

Time: 0 s	Specimen			
	Polished 0-0	$x^2$	Polished 10-5	$x^2$
Replicate, $x_1$	64.10	4108.81	70.00	4900.00
Replicate, $x_2$	80.30	6448.09	74.10	5490.81
Replicate, $x_3$	74.20	5505.64	71.60	5126.56
Average ( $\bar{x}$ )	72.87	5354.18	71.90	5172.46
$\Sigma x^2$	16062.54		15517.37	
$(\Sigma x)^2$	47785.96		46526.49	
$((\Sigma x)^2)/n$	15928.65		15508.83	
$\Sigma d^2 = \Sigma x^2 - ((\Sigma x)^2)/n$	133.89		8.54	
$\sigma^2 = \frac{\Sigma d^2}{n-1}$	66.94		4.27	
$\sigma_d^2 = \frac{\sigma_1^2}{n_1} + \frac{\sigma_2^2}{n_2}$	23.74			
$\sigma_d$	4.87			
$t = \frac{\bar{x}_1 - \bar{x}_2}{\sigma_d}$	0.20			

$p > 0.1$

APPENDIX 6

Time: 10 s	Specimen			
	Polished 0-0	$x^2$	Polished 10-5	$x^2$
Replicate, $x_1$	62.50	3906.25	62.90	3956.41
Replicate, $x_2$	76.70	5882.89	71.20	5069.44
Replicate, $x_3$	72.20	5212.84	65.60	4303.36
Average ( $\bar{x}$ )	70.47	5000.66	66.57	4443.07
$\Sigma x^2$	15001.98		13329.21	
$(\Sigma x)^2$	44689.96		39880.09	
$((\Sigma x)^2)/n$	14896.65		13293.36	
$\Sigma d^2 = \Sigma x^2 - ((\Sigma x)^2)/n$	105.33		35.85	
$\sigma^2 = \frac{\Sigma d^2}{n-1}$	52.66		17.92	
$\sigma_d^2 = \frac{\sigma_1^2}{n_1} + \frac{\sigma_2^2}{n_2}$	23.53			
$\sigma_d$	4.85			
$t = \frac{\bar{x}_1 - \bar{x}_2}{\sigma_d}$	0.80			

$p > 0.1$

APPENDIX 6

Time: 20 s	Specimen			
	Polished 0-0	$x^2$	Polished 10-5	$x^2$
Replicate, $x_1$	62.20	3868.84	61.10	3733.21
Replicate, $x_2$	76.40	5836.96	68.40	4678.56
Replicate, $x_3$	70.20	4928.04	65.20	4251.04
Average ( $\bar{x}$ )	69.60	4877.95	64.90	4220.94
$\Sigma x^2$	14633.84		12662.81	
$(\Sigma x)^2$	43597.44		37908.09	
$((\Sigma x)^2)/n$	14532.48		12636.03	
$\Sigma d^2 = \Sigma x^2 - ((\Sigma x)^2)/n$	101.36		26.78	
$\sigma^2 = \frac{\Sigma d^2}{n-1}$	50.68		13.39	
$\sigma_d^2 = \frac{\sigma_1^2}{n_1} + \frac{\sigma_2^2}{n_2}$	21.36			
$\sigma_d$	4.62			
$t = \frac{\bar{x}_1 - \bar{x}_2}{\sigma_d}$	1.02			

$p > 0.1$

APPENDIX 6

Time: 30 s	Specimen			
	Polished 0-0	$x^2$	Polished 10-5	$x^2$
Replicate, $x_1$	59.70	3564.09	60.70	3684.49
Replicate, $x_2$	73.30	5372.89	67.90	4610.41
Replicate, $x_3$	68.30	4664.89	62.90	3956.41
Average ( $\bar{x}$ )	67.10	4533.96	63.83	4083.77
$\Sigma x^2$	13601.87		12251.31	
$(\Sigma x)^2$	40521.69		36672.25	
$((\Sigma x)^2)/n$	13507.23		12224.08	
$\Sigma d^2 = \Sigma x^2 - ((\Sigma x)^2)/n$	94.64		27.23	
$\sigma^2 = \frac{\Sigma d^2}{n-1}$	47.32		13.61	
$\sigma_d^2 = \frac{\sigma_1^2}{n_1} + \frac{\sigma_2^2}{n_2}$	20.31			
$\sigma_d$	4.51			
$t = \frac{\bar{x}_1 - \bar{x}_2}{\sigma_d}$	0.72			

$p > 0.1$

APPENDIX 6

Time: 40 s	Specimen			
	Polished 0-0	$x^2$	Polished 10-5	$x^2$
Replicate, $x_1$	59.20	3504.64	58.20	3387.24
Replicate, $x_2$	72.20	5212.84	66.80	4462.24
Replicate, $x_3$	67.30	4529.29	61.00	3721.00
Average ( $\bar{x}$ )	66.23	4415.59	62.00	3856.83
$\Sigma x^2$	13246.77		11570.48	
$(\Sigma x)^2$	39481.69		34596.00	
$((\Sigma x)^2)/n$	13160.56		11532.00	
$\Sigma d^2 = \Sigma x^2 - ((\Sigma x)^2)/n$	86.21		38.48	
$\sigma^2 = \frac{\Sigma d^2}{n-1}$	43.10		19.24	
$\sigma_d^2 = \frac{\sigma_1^2}{n_1} + \frac{\sigma_2^2}{n_2}$	20.78			
$\sigma_d$	4.56			
$t = \frac{\bar{x}_1 - \bar{x}_2}{\sigma_d}$	0.93			

$p > 0.1$

APPENDIX 6

Time: 50 s	Specimen			
	Polished 0-0	$x^2$	Polished 10-5	$x^2$
Replicate, $x_1$	55.50	3080.25	57.50	3306.25
Replicate, $x_2$	71.70	5140.89	64.30	4134.49
Replicate, $x_3$	66.00	4356.00	58.90	3469.21
Average ( $\bar{x}$ )	64.40	4192.38	60.23	3636.65
$\Sigma x^2$	12577.14		10909.95	
$(\Sigma x)^2$	37326.24		32652.49	
$((\Sigma x)^2)/n$	12442.08		10884.16	
$\Sigma d^2 = \Sigma x^2 - ((\Sigma x)^2)/n$	135.06		25.79	
$\sigma^2 = \frac{\Sigma d^2}{n-1}$	67.53		12.89	
$\sigma_d^2 = \frac{\sigma_1^2}{n_1} + \frac{\sigma_2^2}{n_2}$	26.81			
$\sigma_d$	5.18			
$t = \frac{\bar{x}_1 - \bar{x}_2}{\sigma_d}$	0.80			

$p > 0.1$

APPENDIX 6

Time: 60 s	Specimen			
	Polished 0-0	$x^2$	Polished 10-5	$x^2$
Replicate, $x_1$	57.90	3352.41	55.80	3113.64
Replicate, $x_2$	70.00	4900.00	62.80	3943.84
Replicate, $x_3$	63.60	4044.96	58.00	3364.00
Average ( $\bar{x}$ )	63.83	4099.12	58.87	3473.83
$\Sigma x^2$	12297.37		10421.48	
$(\Sigma x)^2$	36672.25		31187.56	
$((\Sigma x)^2)/n$	12224.08		10395.85	
$\Sigma d^2 = \Sigma x^2 - ((\Sigma x)^2)/n$	73.29		25.63	
$\sigma^2 = \frac{\Sigma d^2}{n-1}$	36.64		12.81	
$\sigma_d^2 = \frac{\sigma_1^2}{n_1} + \frac{\sigma_2^2}{n_2}$	16.49			
$\sigma_d$	4.06			
$t = \frac{\bar{x}_1 - \bar{x}_2}{\sigma_d}$	1.22			

$p > 0.1$

APPENDIX 6

Time: 70 s	Specimen			
	Polished 0-0	$x^2$	Polished 10-5	$x^2$
Replicate, $x_1$	54.30	2948.49	54.60	2981.16
Replicate, $x_2$	69.20	4788.64	62.00	3844.00
Replicate, $x_3$	62.40	3893.76	57.00	3249.00
Average ( $\bar{x}$ )	61.97	3876.96	57.87	3358.05
$\Sigma x^2$	11630.89		10074.16	
$(\Sigma x)^2$	34558.81		30136.96	
$((\Sigma x)^2)/n$	11519.60		10045.65	
$\Sigma d^2 = \Sigma x^2 - ((\Sigma x)^2)/n$	111.29		28.51	
$\sigma^2 = \frac{\Sigma d^2}{n-1}$	55.64		14.25	
$\sigma_d^2 = \frac{\sigma_1^2}{n_1} + \frac{\sigma_2^2}{n_2}$	23.30			
$\sigma_d$	4.83			
$t = \frac{\bar{x}_1 - \bar{x}_2}{\sigma_d}$	0.85			

$p > 0.1$



APPENDIX 6

Time: 80 s	Specimen			
	Polished 0-0	$x^2$	Polished 10-5	$x^2$
Replicate, $x_1$	53.80	2894.44	54.20	2937.64
Replicate, $x_2$	68.80	4733.44	60.30	3636.09
Replicate, $x_3$	61.90	3831.61	55.70	3102.49
Average ( $\bar{x}$ )	61.50	3819.83	56.73	3225.41
$\Sigma x^2$	11459.49		9676.22	
$(\Sigma x)^2$	34040.25		28968.04	
$((\Sigma x)^2)/n$	11346.75		9656.01	
$\Sigma d^2 = \Sigma x^2 - ((\Sigma x)^2)/n$	112.74		20.21	
$\sigma^2 = \frac{\Sigma d^2}{n-1}$	56.37		10.10	
$\sigma_d^2 = \frac{\sigma_1^2}{n_1} + \frac{\sigma_2^2}{n_2}$	22.16			
$\sigma_d$	4.71			
$t = \frac{\bar{x}_1 - \bar{x}_2}{\sigma_d}$	1.01			

$p > 0.1$

APPENDIX 6

Time: 90 s	Specimen			
	Polished 0-0	$x^2$	Polished 10-5	$x^2$
Replicate, $x_1$	52.30	2735.29	52.70	2777.29
Replicate, $x_2$	67.00	4489.00	59.80	3576.04
Replicate, $x_3$	61.50	3782.25	52.00	2704.00
Average ( $\bar{x}$ )	60.27	3668.85	54.83	3019.11
$\Sigma x^2$	11006.54		9057.33	
$(\Sigma x)^2$	32688.64		27060.25	
$((\Sigma x)^2)/n$	10896.21		9020.08	
$\Sigma d^2 = \Sigma x^2 - ((\Sigma x)^2)/n$	110.33		37.25	
$\sigma^2 = \frac{\Sigma d^2}{n-1}$	55.16		18.62	
$\sigma_d^2 = \frac{\sigma_1^2}{n_1} + \frac{\sigma_2^2}{n_2}$	24.60			
$\sigma_d$	4.96			
$t = \frac{\bar{x}_1 - \bar{x}_2}{\sigma_d}$	1.10			

$p > 0.1$

APPENDIX 6

Time: 100 s	Specimen			
	Polished 0-0	$x^2$	Polished 10-5	$x^2$
Replicate, $x_1$	50.10	2510.01	49.30	2430.49
Replicate, $x_2$	64.30	4134.49	57.30	3283.29
Replicate, $x_3$	58.30	3398.89	49.70	2470.09
Average ( $\bar{x}$ )	57.57	3347.80	52.10	2727.96
$\Sigma x^2$	10043.39		8183.87	
$(\Sigma x)^2$	29825.29		24429.69	
$((\Sigma x)^2)/n$	9941.76		8143.23	
$\Sigma d^2 = \Sigma x^2 - ((\Sigma x)^2)/n$	101.63		40.64	
$\sigma^2 = \frac{\Sigma d^2}{n-1}$	50.81		20.32	
$\sigma_d^2 = \frac{\sigma_1^2}{n_1} + \frac{\sigma_2^2}{n_2}$	23.71			
$\sigma_d$	4.87			
$t = \frac{\bar{x}_1 - \bar{x}_2}{\sigma_d}$	1.12			

$p > 0.1$

APPENDIX 6

Time: 110 s	Specimen			
	Polished 0-0	$x^2$	Polished 10-5	$x^2$
Replicate, $x_1$	48.70	2371.69	47.00	2209.00
Replicate, $x_2$	63.50	4032.25	56.80	3226.24
Replicate, $x_3$	56.40	3180.96	48.90	2391.21
Average ( $\bar{x}$ )	56.20	3194.97	50.90	2608.82
$\Sigma x^2$	9584.90		7826.45	
$(\Sigma x)^2$	28425.96		23317.29	
$((\Sigma x)^2)/n$	9475.32		7772.43	
$\Sigma d^2 = \Sigma x^2 - ((\Sigma x)^2)/n$	109.58		54.02	
$\sigma^2 = \frac{\Sigma d^2}{n-1}$	54.79		27.01	
$\sigma_d^2 = \frac{\sigma_1^2}{n_1} + \frac{\sigma_2^2}{n_2}$	27.27			
$\sigma_d$	5.22			
$t = \frac{\bar{x}_1 - \bar{x}_2}{\sigma_d}$	1.01			

p > 0.1

APPENDIX 6

Time: 120 s	Specimen			
	Polished 0-0	$x^2$	Polished 10-5	$x^2$
Replicate, $x_1$	48.60	2361.96	46.90	2199.61
Replicate, $x_2$	62.20	3868.84	55.20	3047.04
Replicate, $x_3$	55.40	3069.16	46.80	2190.24
Average ( $\bar{x}$ )	55.40	3099.99	49.63	2478.96
$\Sigma x^2$	9299.96		7436.89	
$(\Sigma x)^2$	27622.44		22171.21	
$((\Sigma x)^2)/n$	9207.48		7390.40	
$\Sigma d^2 = \Sigma x^2 - ((\Sigma x)^2)/n$	92.48		46.49	
$\sigma^2 = \frac{\Sigma d^2}{n-1}$	46.24		23.24	
$\sigma_d^2 = \frac{\sigma_1^2}{n_1} + \frac{\sigma_2^2}{n_2}$	23.16			
$\sigma_d$	4.81			
$t = \frac{\bar{x}_1 - \bar{x}_2}{\sigma_d}$	1.20			

p > 0.1

APPENDIX 6

Time: 130 s	Specimen			
	Polished 0-0	$x^2$	Polished 10-5	$x^2$
Replicate, $x_1$	47.50	2256.25	45.10	2034.01
Replicate, $x_2$	61.40	3769.96	52.90	2798.41
Replicate, $x_3$	52.90	2798.41	46.30	2143.69
Average ( $\bar{x}$ )	53.93	2941.54	48.10	2325.37
$\Sigma x^2$	8824.62		6976.11	
$(\Sigma x)^2$	26179.24		20822.49	
$((\Sigma x)^2)/n$	8726.41		6940.83	
$\Sigma d^2 = \Sigma x^2 - ((\Sigma x)^2)/n$	98.21		35.28	
$\sigma^2 = \frac{\Sigma d^2}{n-1}$	49.10		17.64	
$\sigma_d^2 = \frac{\sigma_1^2}{n_1} + \frac{\sigma_2^2}{n_2}$	22.25			
$\sigma_d$	4.72			
$t = \frac{\bar{x}_1 - \bar{x}_2}{\sigma_d}$	1.24			

$p > 0.1$

APPENDIX 6

Time: 140 s	Specimen			
	Polished 0-0	$x^2$	Polished 10-5	$x^2$
Replicate, $x_1$	46.60	2171.56	45.00	2025.00
Replicate, $x_2$	58.90	3469.21	52.20	2724.84
Replicate, $x_3$	51.10	2611.21	42.50	1806.25
Average ( $\bar{x}$ )	52.20	2750.66	46.57	2185.36
$\Sigma x^2$	8251.98		6556.09	
$(\Sigma x)^2$	24523.56		19516.09	
$((\Sigma x)^2)/n$	8174.52		6505.36	
$\Sigma d^2 = \Sigma x^2 - ((\Sigma x)^2)/n$	77.46		50.73	
$\sigma^2 = \frac{\Sigma d^2}{n-1}$	38.73		25.36	
$\sigma_d^2 = \frac{\sigma_1^2}{n_1} + \frac{\sigma_2^2}{n_2}$	21.36			
$\sigma_d$	4.62			
$t = \frac{\bar{x}_1 - \bar{x}_2}{\sigma_d}$	1.22			

$p > 0.1$

APPENDIX 6

Time: 150 s	Specimen			
	Polished 0-0	$x^2$	Polished 10-5	$x^2$
Replicate, $x_1$	44.50	1980.25	40.20	1616.04
Replicate, $x_2$	56.20	3158.44	52.20	2724.84
Replicate, $x_3$	50.60	2560.36	41.00	1681.00
Average ( $\bar{x}$ )	50.43	2566.35	44.47	2007.29
$\Sigma x^2$	7699.05		6021.88	
$(\Sigma x)^2$	22891.69		17795.56	
$((\Sigma x)^2)/n$	7630.56		5931.85	
$\Sigma d^2 = \Sigma x^2 - ((\Sigma x)^2)/n$	68.49		90.03	
$\sigma^2 = \frac{\Sigma d^2}{n-1}$	34.24		45.01	
$\sigma_d^2 = \frac{\sigma_1^2}{n_1} + \frac{\sigma_2^2}{n_2}$	26.42			
$\sigma_d$	5.14			
$t = \frac{\bar{x}_1 - \bar{x}_2}{\sigma_d}$	1.16			

$p > 0.1$



APPENDIX 6

Time: 0 s	Specimen			
	Polished 0-0	$x^2$	Polished 10-10	$x^2$
Replicate, $x_1$	64.10	4108.81	69.60	4844.16
Replicate, $x_2$	80.30	6448.09	59.40	3528.36
Replicate, $x_3$	74.20	5505.64	63.30	4006.89
Average ( $\bar{x}$ )	72.87	5354.18	64.10	4126.47
$\Sigma x^2$	16062.54		12379.41	
$(\Sigma x)^2$	47785.96		36979.29	
$((\Sigma x)^2)/n$	15928.65		12326.43	
$\Sigma d^2 = \Sigma x^2 - ((\Sigma x)^2)/n$	133.89		52.98	
$\sigma^2 = \frac{\Sigma d^2}{n-1}$	66.94		26.49	
$\sigma_d^2 = \frac{\sigma_1^2}{n_1} + \frac{\sigma_2^2}{n_2}$	31.14			
$\sigma_d$	5.58			
$t = \frac{\bar{x}_1 - \bar{x}_2}{\sigma_d}$	1.57			

p > 0.1

APPENDIX 6

Time: 10 s	Specimen			
	Polished 0-0	$x^2$	Polished 10-10	$x^2$
Replicate, $x_1$	62.50	3906.25	65.30	4264.09
Replicate, $x_2$	76.70	5882.89	56.30	3169.69
Replicate, $x_3$	72.20	5212.84	61.10	3733.21
Average ( $\bar{x}$ )	70.47	5000.66	60.90	3722.33
$\Sigma x^2$	15001.98		11166.99	
$(\Sigma x)^2$	44689.96		33379.29	
$((\Sigma x)^2)/n$	14896.65		11126.43	
$\Sigma d^2 = \Sigma x^2 - ((\Sigma x)^2)/n$	105.33		40.56	
$\sigma^2 = \frac{\Sigma d^2}{n-1}$	52.66		20.28	
$\sigma_d^2 = \frac{\sigma_1^2}{n_1} + \frac{\sigma_2^2}{n_2}$	24.31			
$\sigma_d$	4.93			
$t = \frac{\bar{x}_1 - \bar{x}_2}{\sigma_d}$	1.94			

$p < 0.1$

APPENDIX 6

Time: 20 s	Specimen			
	Polished 0-0	$x^2$	Polished 10-10	$x^2$
Replicate, $x_1$	62.20	3868.84	63.80	4070.44
Replicate, $x_2$	76.40	5836.96	52.40	2745.76
Replicate, $x_3$	70.20	4928.04	59.50	3540.25
Average ( $\bar{x}$ )	69.60	4877.95	58.57	3452.15
$\Sigma x^2$	14633.84		10356.45	
$(\Sigma x)^2$	43597.44		30870.49	
$((\Sigma x)^2)/n$	14532.48		10290.16	
$\Sigma d^2 = \Sigma x^2 - ((\Sigma x)^2)/n$	101.36		66.29	
$\sigma^2 = \frac{\Sigma d^2}{n-1}$	50.68		33.14	
$\sigma_d^2 = \frac{\sigma_1^2}{n_1} + \frac{\sigma_2^2}{n_2}$	27.94			
$\sigma_d$	5.29			
$t = \frac{\bar{x}_1 - \bar{x}_2}{\sigma_d}$	2.09			

$p < 0.1$

APPENDIX 6

Time: 30 s	Specimen			
	Polished 0-0	$x^2$	Polished 10-10	$x^2$
Replicate, $x_1$	59.70	3564.09	62.60	3918.76
Replicate, $x_2$	73.30	5372.89	48.50	2352.25
Replicate, $x_3$	68.30	4664.89	59.50	3540.25
Average ( $\bar{x}$ )	67.10	4533.96	56.87	3270.42
$\Sigma x^2$	13601.87		9811.26	
$(\Sigma x)^2$	40521.69		29104.36	
$((\Sigma x)^2)/n$	13507.23		9701.45	
$\Sigma d^2 = \Sigma x^2 - ((\Sigma x)^2)/n$	94.64		109.81	
$\sigma^2 = \frac{\Sigma d^2}{n-1}$	47.32		54.90	
$\sigma_d^2 = \frac{\sigma_1^2}{n_1} + \frac{\sigma_2^2}{n_2}$	34.07			
$\sigma_d$	5.84			
$t = \frac{\bar{x}_1 - \bar{x}_2}{\sigma_d}$	1.75			

p > 0.1

APPENDIX 6

Time: 40 s	Specimen			
	Polished 0-0	$x^2$	Polished 10-10	$x^2$
Replicate, $x_1$	59.20	3504.64	61.20	3745.44
Replicate, $x_2$	72.20	5212.84	46.50	2162.25
Replicate, $x_3$	67.30	4529.29	56.80	3226.24
Average ( $\bar{x}$ )	66.23	4415.59	54.83	3044.64
$\Sigma x^2$	13246.77		9133.93	
$(\Sigma x)^2$	39481.69		27060.25	
$((\Sigma x)^2)/n$	13160.56		9020.08	
$\Sigma d^2 = \Sigma x^2 - ((\Sigma x)^2)/n$	86.21		113.85	
$\sigma^2 = \frac{\Sigma d^2}{n-1}$	43.10		56.92	
$\sigma_d^2 = \frac{\sigma_1^2}{n_1} + \frac{\sigma_2^2}{n_2}$	33.34			
$\sigma_d$	5.77			
$t = \frac{\bar{x}_1 - \bar{x}_2}{\sigma_d}$	1.97			

p < 0.1

APPENDIX 6

Time: 50 s	Specimen			
	Polished 0-0	$x^2$	Polished 10-10	$x^2$
Replicate, $x_1$	55.50	3080.25	60.10	3612.01
Replicate, $x_2$	71.70	5140.89	44.20	1953.64
Replicate, $x_3$	66.00	4356.00	56.40	3180.96
Average ( $\bar{x}$ )	64.40	4192.38	53.57	2915.54
$\Sigma x^2$	12577.14		8746.61	
$(\Sigma x)^2$	37326.24		25824.49	
$((\Sigma x)^2)/n$	12442.08		8608.16	
$\Sigma d^2 = \Sigma x^2 - ((\Sigma x)^2)/n$	135.06		138.45	
$\sigma^2 = \frac{\Sigma d^2}{n-1}$	67.53		69.22	
$\sigma_d^2 = \frac{\sigma_1^2}{n_1} + \frac{\sigma_2^2}{n_2}$	45.58			
$\sigma_d$	6.75			
$t = \frac{\bar{x}_1 - \bar{x}_2}{\sigma_d}$	1.60			

p > 0.1

APPENDIX 6

Time: 60 s	Specimen			
	Polished 0-0	$x^2$	Polished 10-10	$x^2$
Replicate, $x_1$	57.90	3352.41	59.40	3528.36
Replicate, $x_2$	70.00	4900.00	43.90	1927.21
Replicate, $x_3$	63.60	4044.96	55.20	3047.04
Average ( $\bar{x}$ )	63.83	4099.12	52.83	2834.20
$\Sigma x^2$	12297.37		8502.61	
$(\Sigma x)^2$	36672.25		25122.25	
$((\Sigma x)^2)/n$	12224.08		8374.08	
$\Sigma d^2 = \Sigma x^2 - ((\Sigma x)^2)/n$	73.29		128.53	
$\sigma^2 = \frac{\Sigma d^2}{n-1}$	36.64		64.26	
$\sigma_d^2 = \frac{\sigma_1^2}{n_1} + \frac{\sigma_2^2}{n_2}$	33.64			
$\sigma_d$	5.80			
$t = \frac{\bar{x}_1 - \bar{x}_2}{\sigma_d}$	1.90			

$p < 0.1$

APPENDIX 6

Time: 70 s	Specimen			
	Polished 0-0	$x^2$	Polished 10-10	$x^2$
Replicate, $x_1$	54.30	2948.49	57.80	3340.84
Replicate, $x_2$	69.20	4788.64	41.10	1689.21
Replicate, $x_3$	62.40	3893.76	53.10	2819.61
Average ( $\bar{x}$ )	61.97	3876.96	50.67	2616.55
$\Sigma x^2$	11630.89		7849.66	
$(\Sigma x)^2$	34558.81		23104.00	
$((\Sigma x)^2)/n$	11519.60		7701.33	
$\Sigma d^2 = \Sigma x^2 - ((\Sigma x)^2)/n$	111.29		148.33	
$\sigma^2 = \frac{\Sigma d^2}{n-1}$	55.64		74.16	
$\sigma_d^2 = \frac{\sigma_1^2}{n_1} + \frac{\sigma_2^2}{n_2}$	43.27			
$\sigma_d$	6.58			
$t = \frac{\bar{x}_1 - \bar{x}_2}{\sigma_d}$	1.72			

p > 0.1



APPENDIX 6

Time: 80 s	Specimen			
	Polished 0-0	$x^2$	Polished 10-10	$x^2$
Replicate, $x_1$	53.80	2894.44	55.80	3113.64
Replicate, $x_2$	68.80	4733.44	39.60	1568.16
Replicate, $x_3$	61.90	3831.61	53.60	2872.96
Average ( $\bar{x}$ )	61.50	3819.83	49.67	2518.25
$\Sigma x^2$	11459.49		7554.76	
$(\Sigma x)^2$	34040.25		22201.00	
$((\Sigma x)^2)/n$	11346.75		7400.33	
$\Sigma d^2 = \Sigma x^2 - ((\Sigma x)^2)/n$	112.74		154.43	
$\sigma^2 = \frac{\Sigma d^2}{n-1}$	56.37		77.21	
$\sigma_d^2 = \frac{\sigma_1^2}{n_1} + \frac{\sigma_2^2}{n_2}$	44.53			
$\sigma_d$	6.67			
$t = \frac{\bar{x}_1 - \bar{x}_2}{\sigma_d}$	1.77			

p > 0.1

APPENDIX 6

Time: 90 s	Specimen			
	Polished 0-0	$x^2$	Polished 10-10	$x^2$
Replicate, $x_1$	52.30	2735.29	53.30	2840.89
Replicate, $x_2$	67.00	4489.00	36.20	1310.44
Replicate, $x_3$	61.50	3782.25	50.70	2570.49
Average ( $\bar{x}$ )	60.27	3668.85	46.73	2240.61
$\Sigma x^2$	11006.54		6721.82	
$(\Sigma x)^2$	32688.64		19656.04	
$((\Sigma x)^2)/n$	10896.21		6552.01	
$\Sigma d^2 = \Sigma x^2 - ((\Sigma x)^2)/n$	110.33		169.81	
$\sigma^2 = \frac{\Sigma d^2}{n-1}$	55.16		84.90	
$\sigma_d^2 = \frac{\sigma_1^2}{n_1} + \frac{\sigma_2^2}{n_2}$	46.69			
$\sigma_d$	6.83			
$t = \frac{\bar{x}_1 - \bar{x}_2}{\sigma_d}$	1.98			

$p < 0.1$

APPENDIX 6

Time: 100 s	Specimen			
	Polished 0-0	$x^2$	Polished 10-10	$x^2$
Replicate, $x_1$	50.10	2510.01	52.40	2745.76
Replicate, $x_2$	64.30	4134.49	37.50	1406.25
Replicate, $x_3$	58.30	3398.89	50.20	2520.04
Average ( $\bar{x}$ )	57.57	3347.80	46.70	2224.02
$\Sigma x^2$	10043.39		6672.05	
$(\Sigma x)^2$	29825.29		19628.01	
$((\Sigma x)^2)/n$	9941.76		6542.67	
$\Sigma d^2 = \Sigma x^2 - ((\Sigma x)^2)/n$	101.63		129.38	
$\sigma^2 = \frac{\Sigma d^2}{n-1}$	50.81		64.69	
$\sigma_d^2 = \frac{\sigma_1^2}{n_1} + \frac{\sigma_2^2}{n_2}$	38.50			
$\sigma_d$	6.20			
$t = \frac{\bar{x}_1 - \bar{x}_2}{\sigma_d}$	1.75			

p > 0.1

APPENDIX 6

Time: 110 s	Specimen			
	Polished 0-0	$x^2$	Polished 10-10	$x^2$
Replicate, $x_1$	48.70	2371.69	50.50	2550.25
Replicate, $x_2$	63.50	4032.25	37.80	1428.84
Replicate, $x_3$	56.40	3180.96	45.80	2097.64
Average ( $\bar{x}$ )	56.20	3194.97	44.70	2025.58
$\Sigma x^2$	9584.90		6076.73	
$(\Sigma x)^2$	28425.96		17982.81	
$((\Sigma x)^2)/n$	9475.32		5994.27	
$\Sigma d^2 = \Sigma x^2 - ((\Sigma x)^2)/n$	109.58		82.46	
$\sigma^2 = \frac{\Sigma d^2}{n-1}$	54.79		41.23	
$\sigma_d^2 = \frac{\sigma_1^2}{n_1} + \frac{\sigma_2^2}{n_2}$	32.01			
$\sigma_d$	5.66			
$t = \frac{\bar{x}_1 - \bar{x}_2}{\sigma_d}$	2.03			

$p < 0.1$

APPENDIX 6

Time: 120 s	Specimen			
	Polished 0-0	$x^2$	Polished 10-10	$x^2$
Replicate, $x_1$	48.60	2361.96	50.00	2500.00
Replicate, $x_2$	62.20	3868.84	32.10	1030.41
Replicate, $x_3$	55.40	3069.16	47.00	2209.00
Average ( $\bar{x}$ )	55.40	3099.99	43.03	1913.14
$\Sigma x^2$	9299.96		5739.41	
$(\Sigma x)^2$	27622.44		16666.81	
$((\Sigma x)^2)/n$	9207.48		5555.60	
$\Sigma d^2 = \Sigma x^2 - ((\Sigma x)^2)/n$	92.48		183.81	
$\sigma^2 = \frac{\Sigma d^2}{n-1}$	46.24		91.90	
$\sigma_d^2 = \frac{\sigma_1^2}{n_1} + \frac{\sigma_2^2}{n_2}$	46.05			
$\sigma_d$	6.79			
$t = \frac{\bar{x}_1 - \bar{x}_2}{\sigma_d}$	1.82			

p > 0.1

APPENDIX 6

Time: 130 s	Specimen			
	Polished 0-0	$x^2$	Polished 10-10	$x^2$
Replicate, $x_1$	47.50	2256.25	48.70	2371.69
Replicate, $x_2$	61.40	3769.96	32.60	1062.76
Replicate, $x_3$	52.90	2798.41	47.50	2256.25
Average ( $\bar{x}$ )	53.93	2941.54	42.93	1896.90
$\Sigma x^2$	8824.62		5690.70	
$(\Sigma x)^2$	26179.24		16589.44	
$((\Sigma x)^2)/n$	8726.41		5529.81	
$\Sigma d^2 = \Sigma x^2 - ((\Sigma x)^2)/n$	98.21		160.89	
$\sigma^2 = \frac{\Sigma d^2}{n-1}$	49.10		80.44	
$\sigma_d^2 = \frac{\sigma_1^2}{n_1} + \frac{\sigma_2^2}{n_2}$	43.18			
$\sigma_d$	6.57			
$t = \frac{\bar{x}_1 - \bar{x}_2}{\sigma_d}$	1.67			

$p > 0.1$

APPENDIX 6

Time: 140 s	Specimen			
	Polished 0-0	$x^2$	Polished 10-10	$x^2$
Replicate, $x_1$	46.60	2171.56	46.80	2190.24
Replicate, $x_2$	58.90	3469.21	29.70	882.09
Replicate, $x_3$	51.10	2611.21	41.50	1722.25
Average ( $\bar{x}$ )	52.20	2750.66	39.33	1598.19
$\Sigma x^2$	8251.98		4794.58	
$(\Sigma x)^2$	24523.56		13924.00	
$((\Sigma x)^2)/n$	8174.52		4641.33	
$\Sigma d^2 = \Sigma x^2 - ((\Sigma x)^2)/n$	77.46		153.25	
$\sigma^2 = \frac{\Sigma d^2}{n-1}$	38.73		76.62	
$\sigma_d^2 = \frac{\sigma_1^2}{n_1} + \frac{\sigma_2^2}{n_2}$	38.45			
$\sigma_d$	6.20			
$t = \frac{\bar{x}_1 - \bar{x}_2}{\sigma_d}$	2.07			

$p < 0.1$

APPENDIX 6

Time: 150 s	Specimen			
	Polished 0-0	$x^2$	Polished 10-10	$x^2$
Replicate, $x_1$	44.50	1980.25	44.70	1998.09
Replicate, $x_2$	56.20	3158.44	29.40	864.36
Replicate, $x_3$	50.60	2560.36	42.70	1823.29
Average ( $\bar{x}$ )	50.43	2566.35	38.93	1561.91
$\Sigma x^2$	7699.05		4685.74	
$(\Sigma x)^2$	22891.69		13642.24	
$((\Sigma x)^2)/n$	7630.56		4547.41	
$\Sigma d^2 = \Sigma x^2 - ((\Sigma x)^2)/n$	68.49		138.33	
$\sigma^2 = \frac{\Sigma d^2}{n-1}$	34.24		69.16	
$\sigma_d^2 = \frac{\sigma_1^2}{n_1} + \frac{\sigma_2^2}{n_2}$	34.47			
$\sigma_d$	5.87			
$t = \frac{\bar{x}_1 - \bar{x}_2}{\sigma_d}$	1.96			

$p < 0.1$



APPENDIX 6

Time: 0 s	Specimen			
	Unpolished 0-0	$x^2$	Unpolished 10-5	$x^2$
Replicate, $x_1$	62.10	3856.41	64.30	4134.49
Replicate, $x_2$	71.90	5169.61	81.45	6634.10
Replicate, $x_3$	77.00	5929.00	73.30	5372.89
Average ( $\bar{x}$ )	70.33	4985.01	73.02	5380.49
$\Sigma x^2$	14955.02		16141.48	
$(\Sigma x)^2$	44521.00		47982.90	
$((\Sigma x)^2)/n$	14840.33		15994.30	
$\Sigma d^2 = \Sigma x^2 - ((\Sigma x)^2)/n$	114.69		147.18	
$\sigma^2 = \frac{\Sigma d^2}{n-1}$	57.34		73.59	
$\sigma_d^2 = \frac{\sigma_1^2}{n_1} + \frac{\sigma_2^2}{n_2}$	43.64			
$\sigma_d$	6.61			
$t = \frac{\bar{x}_1 - \bar{x}_2}{\sigma_d}$	0.41			

$p > 0.1$

APPENDIX 6

Time: 10 s	Specimen			
	Unpolished 0-0	$x^2$	Unpolished 10-5	$x^2$
Replicate, $x_1$	61.40	3769.96	57.20	3271.84
Replicate, $x_2$	68.30	4664.89	80.30	6448.09
Replicate, $x_3$	70.40	4956.16	70.10	4914.01
Average ( $\bar{x}$ )	66.70	4463.67	69.20	4877.98
$\Sigma x^2$	13391.01		14633.94	
$(\Sigma x)^2$	40040.01		43097.76	
$((\Sigma x)^2)/n$	13346.67		14365.92	
$\Sigma d^2 = \Sigma x^2 - ((\Sigma x)^2)/n$	44.34		268.02	
$\sigma^2 = \frac{\Sigma d^2}{n-1}$	22.17		134.01	
$\sigma_d^2 = \frac{\sigma_1^2}{n_1} + \frac{\sigma_2^2}{n_2}$	52.06			
$\sigma_d$	7.22			
$t = \frac{\bar{x}_1 - \bar{x}_2}{\sigma_d}$	0.35			

$p > 0.1$

APPENDIX 6

Time: 20 s	Specimen			
	Unpolished 0-0	$x^2$	Unpolished 10-5	$x^2$
Replicate, $x_1$	61.10	3733.21	56.00	3136.00
Replicate, $x_2$	65.40	4277.16	79.15	6264.72
Replicate, $x_3$	70.50	4970.25	68.40	4678.56
Average ( $\bar{x}$ )	65.67	4326.87	67.85	4693.09
$\Sigma x^2$	12980.62		14079.28	
$(\Sigma x)^2$	38809.00		41432.60	
$((\Sigma x)^2)/n$	12936.33		13810.87	
$\Sigma d^2 = \Sigma x^2 - ((\Sigma x)^2)/n$	44.29		268.41	
$\sigma^2 = \frac{\Sigma d^2}{n-1}$	22.14		134.21	
$\sigma_d^2 = \frac{\sigma_1^2}{n_1} + \frac{\sigma_2^2}{n_2}$	52.12			
$\sigma_d$	7.22			
$t = \frac{\bar{x}_1 - \bar{x}_2}{\sigma_d}$	0.30			

$p > 0.1$

APPENDIX 6

Time: 30 s	Specimen			
	Unpolished 0-0	$x^2$	Unpolished 10-5	$x^2$
Replicate, $x_1$	59.90	3588.01	55.30	3058.09
Replicate, $x_2$	67.00	4489.00	78.00	6084.00
Replicate, $x_3$	66.80	4462.24	67.00	4489.00
Average ( $\bar{x}$ )	64.57	4179.75	66.77	4543.70
$\Sigma x^2$	12539.25		13631.09	
$(\Sigma x)^2$	37519.69		40120.09	
$((\Sigma x)^2)/n$	12506.56		13373.36	
$\Sigma d^2 = \Sigma x^2 - ((\Sigma x)^2)/n$	32.69		257.73	
$\sigma^2 = \frac{\Sigma d^2}{n-1}$	16.34		128.86	
$\sigma_d^2 = \frac{\sigma_1^2}{n_1} + \frac{\sigma_2^2}{n_2}$	48.40			
$\sigma_d$	6.96			
$t = \frac{\bar{x}_1 - \bar{x}_2}{\sigma_d}$	0.32			

$p > 0.1$

APPENDIX 6

Time: 40 s	Specimen			
	Unpolished 0-0	$x^2$	Unpolished 10-5	$x^2$
Replicate, $x_1$	53.00	2809.00	53.10	2819.61
Replicate, $x_2$	62.40	3893.76	76.85	5905.92
Replicate, $x_3$	66.90	4475.61	65.30	4264.09
Average ( $\bar{x}$ )	60.77	3726.12	65.08	4329.87
$\Sigma x^2$	11178.37		12989.62	
$(\Sigma x)^2$	33233.29		38122.56	
$((\Sigma x)^2)/n$	11077.76		12707.52	
$\Sigma d^2 = \Sigma x^2 - ((\Sigma x)^2)/n$	100.61		282.10	
$\sigma^2 = \frac{\Sigma d^2}{n-1}$	50.30		141.05	
$\sigma_d^2 = \frac{\sigma_1^2}{n_1} + \frac{\sigma_2^2}{n_2}$	63.78			
$\sigma_d$	7.99			
$t = \frac{\bar{x}_1 - \bar{x}_2}{\sigma_d}$	0.54			

$p > 0.1$

APPENDIX 6

Time: 50 s	Specimen			
	Unpolished 0-0	$x^2$	Unpolished 10-5	$x^2$
Replicate, $x_1$	52.50	2756.25	52.80	2787.84
Replicate, $x_2$	62.70	3931.29	75.70	5730.49
Replicate, $x_3$	65.70	4316.49	63.90	4083.21
Average ( $\bar{x}$ )	60.30	3668.01	64.13	4200.51
$\Sigma x^2$	11004.03		12601.54	
$(\Sigma x)^2$	32724.81		37017.76	
$((\Sigma x)^2)/n$	10908.27		12339.25	
$\Sigma d^2 = \Sigma x^2 - ((\Sigma x)^2)/n$	95.76		262.29	
$\sigma^2 = \frac{\Sigma d^2}{n-1}$	47.88		131.14	
$\sigma_d^2 = \frac{\sigma_1^2}{n_1} + \frac{\sigma_2^2}{n_2}$	59.67			
$\sigma_d$	7.72			
$t = \frac{\bar{x}_1 - \bar{x}_2}{\sigma_d}$	0.50			

$p > 0.1$

APPENDIX 6

Time: 60 s	Specimen			
	Unpolished 0-0	$x^2$	Unpolished 10-5	$x^2$
Replicate, $x_1$	51.00	2601.00	48.30	2332.89
Replicate, $x_2$	62.30	3881.29	74.90	5610.01
Replicate, $x_3$	65.60	4303.36	62.10	3856.41
Average ( $\bar{x}$ )	59.63	3595.22	61.77	3933.10
$\Sigma x^2$	10785.65		11799.31	
$(\Sigma x)^2$	32005.21		34336.09	
$((\Sigma x)^2)/n$	10668.40		11445.36	
$\Sigma d^2 = \Sigma x^2 - ((\Sigma x)^2)/n$	117.25		353.95	
$\sigma^2 = \frac{\Sigma d^2}{n-1}$	58.62		176.97	
$\sigma_d^2 = \frac{\sigma_1^2}{n_1} + \frac{\sigma_2^2}{n_2}$	78.53			
$\sigma_d$	8.86			
$t = \frac{\bar{x}_1 - \bar{x}_2}{\sigma_d}$	0.24			

p > 0.1

APPENDIX 6

Time: 70 s	Specimen			
	Unpolished 0-0	$x^2$	Unpolished 10-5	$x^2$
Replicate, $x_1$	49.30	2430.49	48.50	2352.25
Replicate, $x_2$	61.10	3733.21	72.70	5285.29
Replicate, $x_3$	65.80	4329.64	61.00	3721.00
Average ( $\bar{x}$ )	58.73	3497.78	60.73	3786.18
$\Sigma x^2$	10493.34		11358.54	
$(\Sigma x)^2$	31046.44		33196.84	
$((\Sigma x)^2)/n$	10348.81		11065.61	
$\Sigma d^2 = \Sigma x^2 - ((\Sigma x)^2)/n$	144.53		292.93	
$\sigma^2 = \frac{\Sigma d^2}{n-1}$	72.26		146.46	
$\sigma_d^2 = \frac{\sigma_1^2}{n_1} + \frac{\sigma_2^2}{n_2}$	72.91			
$\sigma_d$	8.54			
$t = \frac{\bar{x}_1 - \bar{x}_2}{\sigma_d}$	0.23			

$p > 0.1$



APPENDIX 6

Time: 80 s	Specimen			
	Unpolished 0-0	$x^2$	Unpolished 10-5	$x^2$
Replicate, $x_1$	47.40	2246.76	47.80	2284.84
Replicate, $x_2$	59.20	3504.64	72.60	5270.76
Replicate, $x_3$	63.80	4070.44	60.10	3612.01
Average ( $\bar{x}$ )	56.80	3273.95	60.17	3722.54
$\Sigma x^2$	9821.84		11167.61	
$(\Sigma x)^2$	29036.16		32580.25	
$((\Sigma x)^2)/n$	9678.72		10860.08	
$\Sigma d^2 = \Sigma x^2 - ((\Sigma x)^2)/n$	143.12		307.53	
$\sigma^2 = \frac{\Sigma d^2}{n-1}$	71.56		153.76	
$\sigma_d^2 = \frac{\sigma_1^2}{n_1} + \frac{\sigma_2^2}{n_2}$	75.11			
$\sigma_d$	8.67			
$t = \frac{\bar{x}_1 - \bar{x}_2}{\sigma_d}$	0.39			

p > 0.1

APPENDIX 6

Time: 90 s	Specimen			
	Unpolished 0-0	$x^2$	Unpolished 10-5	$x^2$
Replicate, $x_1$	41.80	1747.24	44.60	1989.16
Replicate, $x_2$	58.30	3398.89	71.80	5155.24
Replicate, $x_3$	60.10	3612.01	58.80	3457.44
Average ( $\bar{x}$ )	53.40	2919.38	58.40	3533.95
$\Sigma x^2$	8758.14		10601.84	
$(\Sigma x)^2$	25664.04		30695.04	
$((\Sigma x)^2)/n$	8554.68		10231.68	
$\Sigma d^2 = \Sigma x^2 - ((\Sigma x)^2)/n$	203.46		370.16	
$\sigma^2 = \frac{\Sigma d^2}{n-1}$	101.73		185.08	
$\sigma_d^2 = \frac{\sigma_1^2}{n_1} + \frac{\sigma_2^2}{n_2}$	95.60			
$\sigma_d$	9.78			
$t = \frac{\bar{x}_1 - \bar{x}_2}{\sigma_d}$	0.51			

p > 0.1

APPENDIX 6

Time: 100 s	Specimen			
	Unpolished 0-0	$x^2$	Unpolished 10-5	$x^2$
Replicate, $x_1$	42.10	1772.41	42.00	1764.00
Replicate, $x_2$	58.50	3422.25	70.10	4914.01
Replicate, $x_3$	60.40	3648.16	56.50	3192.25
Average ( $\bar{x}$ )	53.67	2947.61	56.20	3290.09
$\Sigma x^2$	8842.82		9870.26	
$(\Sigma x)^2$	25921.00		28425.96	
$((\Sigma x)^2)/n$	8640.33		9475.32	
$\Sigma d^2 = \Sigma x^2 - ((\Sigma x)^2)/n$	202.49		394.94	
$\sigma^2 = \frac{\Sigma d^2}{n-1}$	101.24		197.47	
$\sigma_d^2 = \frac{\sigma_1^2}{n_1} + \frac{\sigma_2^2}{n_2}$	99.57			
$\sigma_d$	9.98			
$t = \frac{\bar{x}_1 - \bar{x}_2}{\sigma_d}$	0.25			

$p > 0.1$

APPENDIX 6

Time: 110 s	Specimen			
	Unpolished 0-0	$x^2$	Unpolished 10-5	$x^2$
Replicate, $x_1$	38.90	1513.21	43.10	1857.61
Replicate, $x_2$	54.50	2970.25	69.90	4886.01
Replicate, $x_3$	58.70	3445.69	54.30	2948.49
Average ( $\bar{x}$ )	50.70	2643.05	55.77	3230.70
$\Sigma x^2$	7929.15		9692.11	
$(\Sigma x)^2$	23134.41		27989.29	
$((\Sigma x)^2)/n$	7711.47		9329.76	
$\Sigma d^2 = \Sigma x^2 - ((\Sigma x)^2)/n$	217.68		362.35	
$\sigma^2 = \frac{\Sigma d^2}{n-1}$	108.84		181.17	
$\sigma_d^2 = \frac{\sigma_1^2}{n_1} + \frac{\sigma_2^2}{n_2}$	96.67			
$\sigma_d$	9.83			
$t = \frac{\bar{x}_1 - \bar{x}_2}{\sigma_d}$	0.52			

$p > 0.1$

APPENDIX 6

Time: 120 s	Specimen			
	Unpolished 0-0	$x^2$	Unpolished 10-5	$x^2$
Replicate, $x_1$	34.10	1162.81	37.80	1428.84
Replicate, $x_2$	52.50	2756.25	67.20	4515.84
Replicate, $x_3$	55.70	3102.49	53.10	2819.61
Average ( $\bar{x}$ )	47.43	2340.52	52.70	2921.43
$\Sigma x^2$	7021.55		8764.29	
$(\Sigma x)^2$	20249.29		24995.61	
$((\Sigma x)^2)/n$	6749.76		8331.87	
$\Sigma d^2 = \Sigma x^2 - ((\Sigma x)^2)/n$	271.79		432.42	
$\sigma^2 = \frac{\Sigma d^2}{n-1}$	135.89		216.21	
$\sigma_d^2 = \frac{\sigma_1^2}{n_1} + \frac{\sigma_2^2}{n_2}$	117.37			
$\sigma_d$	10.83			
$t = \frac{\bar{x}_1 - \bar{x}_2}{\sigma_d}$	0.49			

p > 0.1

APPENDIX 6

Time: 130 s	Specimen			
	Unpolished 0-0	$x^2$	Unpolished 10-5	$x^2$
Replicate, $x_1$	29.40	864.36	37.50	1406.25
Replicate, $x_2$	51.30	2631.69	65.90	4342.81
Replicate, $x_3$	55.20	3047.04	50.20	2520.04
Average ( $\bar{x}$ )	45.30	2181.03	51.20	2756.37
$\Sigma x^2$	6543.09		8269.10	
$(\Sigma x)^2$	18468.81		23592.96	
$((\Sigma x)^2)/n$	6156.27		7864.32	
$\Sigma d^2 = \Sigma x^2 - ((\Sigma x)^2)/n$	386.82		404.78	
$\sigma^2 = \frac{\Sigma d^2}{n-1}$	193.41		202.39	
$\sigma_d^2 = \frac{\sigma_1^2}{n_1} + \frac{\sigma_2^2}{n_2}$	131.93			
$\sigma_d$	11.49			
$t = \frac{\bar{x}_1 - \bar{x}_2}{\sigma_d}$	0.51			

$p > 0.1$

APPENDIX 6

Time: 140 s	Specimen			
	Unpolished 0-0	$x^2$	Unpolished 10-5	$x^2$
Replicate, $x_1$	21.90	479.61	34.80	1211.04
Replicate, $x_2$	50.00	2500.00	61.80	3819.24
Replicate, $x_3$	55.80	3113.64	46.20	2134.44
Average ( $\bar{x}$ )	42.57	2031.08	47.60	2388.24
$\Sigma x^2$	6093.25		7164.72	
$(\Sigma x)^2$	16307.29		20391.84	
$((\Sigma x)^2)/n$	5435.76		6797.28	
$\Sigma d^2 = \Sigma x^2 - ((\Sigma x)^2)/n$	657.49		367.44	
$\sigma^2 = \frac{\Sigma d^2}{n-1}$	328.74		183.72	
$\sigma_d^2 = \frac{\sigma_1^2}{n_1} + \frac{\sigma_2^2}{n_2}$	170.82			
$\sigma_d$	13.07			
$t = \frac{\bar{x}_1 - \bar{x}_2}{\sigma_d}$	0.39			

$p > 0.1$

APPENDIX 6

Time: 150 s	Specimen			
	Unpolished 0-0	$x^2$	Unpolished 10-5	$x^2$
Replicate, $x_1$	22.30	497.29	34.70	1204.09
Replicate, $x_2$	49.20	2420.64	60.60	3672.36
Replicate, $x_3$	50.90	2590.81	44.60	1989.16
Average ( $\bar{x}$ )	40.80	1836.25	46.63	2288.54
$\Sigma x^2$	5508.74		6865.61	
$(\Sigma x)^2$	14981.76		19572.01	
$((\Sigma x)^2)/n$	4993.92		6524.00	
$\Sigma d^2 = \Sigma x^2 - ((\Sigma x)^2)/n$	514.82		341.61	
$\sigma^2 = \frac{\Sigma d^2}{n-1}$	257.41		170.80	
$\sigma_d^2 = \frac{\sigma_1^2}{n_1} + \frac{\sigma_2^2}{n_2}$	142.74			
$\sigma_d$	11.95			
$t = \frac{\bar{x}_1 - \bar{x}_2}{\sigma_d}$	0.49			

$p > 0.1$



APPENDIX 6

Time: 0 s	Specimen			
	Unpolished 0-0	$x^2$	Unpolished 10-10	$x^2$
Replicate, $x_1$	62.10	3856.41	40.80	1664.64
Replicate, $x_2$	71.90	5169.61	54.60	2981.16
Replicate, $x_3$	77.00	5929.00	58.80	3457.44
Average ( $\bar{x}$ )	70.33	4985.01	51.40	2701.08
$\Sigma x^2$	14955.02		8103.24	
$(\Sigma x)^2$	44521.00		23777.64	
$((\Sigma x)^2)/n$	14840.33		7925.88	
$\Sigma d^2 = \Sigma x^2 - ((\Sigma x)^2)/n$	114.69		177.36	
$\sigma^2 = \frac{\Sigma d^2}{n-1}$	57.34		88.68	
$\sigma_d^2 = \frac{\sigma_1^2}{n_1} + \frac{\sigma_2^2}{n_2}$	48.67			
$\sigma_d$	6.98			
$t = \frac{\bar{x}_1 - \bar{x}_2}{\sigma_d}$	2.71			

$p < 0.05$

APPENDIX 6

Time: 10 s	Specimen			
	Unpolished 0-0	$x^2$	Unpolished 10-10	$x^2$
Replicate, $x_1$	61.40	3769.96	38.70	1497.69
Replicate, $x_2$	68.30	4664.89	49.50	2450.25
Replicate, $x_3$	70.40	4956.16	56.70	3214.89
Average ( $\bar{x}$ )	66.70	4463.67	48.30	2387.61
$\Sigma x^2$	13391.01		7162.83	
$(\Sigma x)^2$	40040.01		20996.01	
$((\Sigma x)^2)/n$	13346.67		6998.67	
$\Sigma d^2 = \Sigma x^2 - ((\Sigma x)^2)/n$	44.34		164.16	
$\sigma^2 = \frac{\Sigma d^2}{n-1}$	22.17		82.08	
$\sigma_d^2 = \frac{\sigma_1^2}{n_1} + \frac{\sigma_2^2}{n_2}$	34.75			
$\sigma_d$	5.89			
$t = \frac{\bar{x}_1 - \bar{x}_2}{\sigma_d}$	3.12			

$p < 0.05$

APPENDIX 6

Time: 20 s	Specimen			
	Unpolished 0-0	$x^2$	Unpolished 10-10	$x^2$
Replicate, $x_1$	61.10	3733.21	38.00	1444.00
Replicate, $x_2$	65.40	4277.16	48.10	2313.61
Replicate, $x_3$	70.50	4970.25	56.00	3136.00
Average ( $\bar{x}$ )	65.67	4326.87	47.37	2297.87
$\Sigma x^2$	12980.62		6893.61	
$(\Sigma x)^2$	38809.00		20192.41	
$((\Sigma x)^2)/n$	12936.33		6730.80	
$\Sigma d^2 = \Sigma x^2 - ((\Sigma x)^2)/n$	44.29		162.81	
$\sigma^2 = \frac{\Sigma d^2}{n-1}$	22.14		81.40	
$\sigma_d^2 = \frac{\sigma_1^2}{n_1} + \frac{\sigma_2^2}{n_2}$	34.52			
$\sigma_d$	5.87			
$t = \frac{\bar{x}_1 - \bar{x}_2}{\sigma_d}$	3.11			

$p < 0.05$

APPENDIX 6

Time: 30 s	Specimen			
	Unpolished 0-0	$x^2$	Unpolished 10-10	$x^2$
Replicate, $x_1$	59.90	3588.01	25.10	630.01
Replicate, $x_2$	67.00	4489.00	46.90	2199.61
Replicate, $x_3$	66.80	4462.24	43.10	1857.61
Average ( $\bar{x}$ )	64.57	4179.75	38.37	1562.41
$\Sigma x^2$	12539.25		4687.23	
$(\Sigma x)^2$	37519.69		13248.01	
$((\Sigma x)^2)/n$	12506.56		4416.00	
$\Sigma d^2 = \Sigma x^2 - ((\Sigma x)^2)/n$	32.69		271.23	
$\sigma^2 = \frac{\Sigma d^2}{n-1}$	16.34		135.61	
$\sigma_d^2 = \frac{\sigma_1^2}{n_1} + \frac{\sigma_2^2}{n_2}$	50.65			
$\sigma_d$	7.12			
$t = \frac{\bar{x}_1 - \bar{x}_2}{\sigma_d}$	3.68			

$p < 0.01$

APPENDIX 6

Time: 40 s	Specimen			
	Unpolished 0-0	$x^2$	Unpolished 10-10	$x^2$
Replicate, $x_1$	53.00	2809.00	19.00	361.00
Replicate, $x_2$	62.40	3893.76	44.00	1936.00
Replicate, $x_3$	66.90	4475.61	37.00	1369.00
Average ( $\bar{x}$ )	60.77	3726.12	33.33	1222.00
$\Sigma x^2$	11178.37		3666.00	
$(\Sigma x)^2$	33233.29		10000.00	
$((\Sigma x)^2)/n$	11077.76		3333.33	
$\Sigma d^2 = \Sigma x^2 - ((\Sigma x)^2)/n$	100.61		332.67	
$\sigma^2 = \frac{\Sigma d^2}{n-1}$	50.30		166.33	
$\sigma_d^2 = \frac{\sigma_1^2}{n_1} + \frac{\sigma_2^2}{n_2}$	72.21			
$\sigma_d$	8.50			
$t = \frac{\bar{x}_1 - \bar{x}_2}{\sigma_d}$	3.23			

$p < 0.05$

APPENDIX 6

Time: 50 s	Specimen			
	Unpolished 0-0	$x^2$	Unpolished 10-10	$x^2$
Replicate, $x_1$	52.50	2756.25	16.00	256.00
Replicate, $x_2$	62.70	3931.29	43.20	1866.24
Replicate, $x_3$	65.70	4316.49	34.00	1156.00
Average ( $\bar{x}$ )	60.30	3668.01	31.07	1092.75
$\Sigma x^2$	11004.03		3278.24	
$(\Sigma x)^2$	32724.81		8686.24	
$((\Sigma x)^2)/n$	10908.27		2895.41	
$\Sigma d^2 = \Sigma x^2 - ((\Sigma x)^2)/n$	95.76		382.83	
$\sigma^2 = \frac{\Sigma d^2}{n-1}$	47.88		191.41	
$\sigma_d^2 = \frac{\sigma_1^2}{n_1} + \frac{\sigma_2^2}{n_2}$	79.76			
$\sigma_d$	8.93			
$t = \frac{\bar{x}_1 - \bar{x}_2}{\sigma_d}$	3.27			

$p < 0.05$

APPENDIX 6

Time: 60 s	Specimen			
	Unpolished 0-0	$x^2$	Unpolished 10-10	$x^2$
Replicate, $x_1$	51.00	2601.00	13.10	171.61
Replicate, $x_2$	62.30	3881.29	42.60	1814.76
Replicate, $x_3$	65.60	4303.36	31.10	967.21
Average ( $\bar{x}$ )	59.63	3595.22	28.93	984.53
$\Sigma x^2$	10785.65		2953.58	
$(\Sigma x)^2$	32005.21		7534.24	
$((\Sigma x)^2)/n$	10668.40		2511.41	
$\Sigma d^2 = \Sigma x^2 - ((\Sigma x)^2)/n$	117.25		442.17	
$\sigma^2 = \frac{\Sigma d^2}{n-1}$	58.62		221.08	
$\sigma_d^2 = \frac{\sigma_1^2}{n_1} + \frac{\sigma_2^2}{n_2}$	93.24			
$\sigma_d$	9.66			
$t = \frac{\bar{x}_1 - \bar{x}_2}{\sigma_d}$	3.18			

$p < 0.05$

APPENDIX 6

Time: 70 s	Specimen			
	Unpolished 0-0	$x^2$	Unpolished 10-10	$x^2$
Replicate, $x_1$	49.30	2430.49	12.80	163.84
Replicate, $x_2$	61.10	3733.21	40.20	1616.04
Replicate, $x_3$	65.80	4329.64	30.80	948.64
Average ( $\bar{x}$ )	58.73	3497.78	27.93	909.51
$\Sigma x^2$	10493.34		2728.52	
$(\Sigma x)^2$	31046.44		7022.44	
$((\Sigma x)^2)/n$	10348.81		2340.81	
$\Sigma d^2 = \Sigma x^2 - ((\Sigma x)^2)/n$	144.53		387.71	
$\sigma^2 = \frac{\Sigma d^2}{n-1}$	72.26		193.85	
$\sigma_d^2 = \frac{\sigma_1^2}{n_1} + \frac{\sigma_2^2}{n_2}$	88.71			
$\sigma_d$	9.42			
$t = \frac{\bar{x}_1 - \bar{x}_2}{\sigma_d}$	3.27			

$p < 0.05$



APPENDIX 6

Time: 80 s	Specimen			
	Unpolished 0-0	$x^2$	Unpolished 10-10	$x^2$
Replicate, $x_1$	47.40	2246.76	11.40	129.96
Replicate, $x_2$	59.20	3504.64	38.50	1482.25
Replicate, $x_3$	63.80	4070.44	29.40	864.36
Average ( $\bar{x}$ )	56.80	3273.95	26.43	825.52
$\Sigma x^2$	9821.84		2476.57	
$(\Sigma x)^2$	29036.16		6288.49	
$((\Sigma x)^2)/n$	9678.72		2096.16	
$\Sigma d^2 = \Sigma x^2 - ((\Sigma x)^2)/n$	143.12		380.41	
$\sigma^2 = \frac{\Sigma d^2}{n-1}$	71.56		190.20	
$\sigma_d^2 = \frac{\sigma_1^2}{n_1} + \frac{\sigma_2^2}{n_2}$	87.25			
$\sigma_d$	9.34			
$t = \frac{\bar{x}_1 - \bar{x}_2}{\sigma_d}$	3.25			

$p < 0.05$

APPENDIX 6

Time: 90 s	Specimen			
	Unpolished 0-0	$x^2$	Unpolished 10-10	$x^2$
Replicate, $x_1$	41.80	1747.24	10.20	104.04
Replicate, $x_2$	58.30	3398.89	34.10	1162.81
Replicate, $x_3$	60.10	3612.01	28.20	795.24
Average ( $\bar{x}$ )	53.40	2919.38	24.17	687.36
$\Sigma x^2$	8758.14		2062.09	
$(\Sigma x)^2$	25664.04		5256.25	
$((\Sigma x)^2)/n$	8554.68		1752.08	
$\Sigma d^2 = \Sigma x^2 - ((\Sigma x)^2)/n$	203.46		310.01	
$\sigma^2 = \frac{\Sigma d^2}{n-1}$	101.73		155.00	
$\sigma_d^2 = \frac{\sigma_1^2}{n_1} + \frac{\sigma_2^2}{n_2}$	85.58			
$\sigma_d$	9.25			
$t = \frac{\bar{x}_1 - \bar{x}_2}{\sigma_d}$	3.16			

$p < 0.05$

APPENDIX 6

Time: 100 s	Specimen			
	Unpolished 0-0	$x^2$	Unpolished 10-10	$x^2$
Replicate, $x_1$	42.10	1772.41	9.80	96.04
Replicate, $x_2$	58.50	3422.25	30.80	948.64
Replicate, $x_3$	60.40	3648.16	27.80	772.84
Average ( $\bar{x}$ )	53.67	2947.61	22.80	605.84
$\Sigma x^2$	8842.82		1817.52	
$(\Sigma x)^2$	25921.00		4678.56	
$((\Sigma x)^2)/n$	8640.33		1559.52	
$\Sigma d^2 = \Sigma x^2 - ((\Sigma x)^2)/n$	202.49		258.00	
$\sigma^2 = \frac{\Sigma d^2}{n-1}$	101.24		129.00	
$\sigma_d^2 = \frac{\sigma_1^2}{n_1} + \frac{\sigma_2^2}{n_2}$	76.75			
$\sigma_d$	8.76			
$t = \frac{\bar{x}_1 - \bar{x}_2}{\sigma_d}$	3.52			

$p < 0.01$

APPENDIX 6

Time: 110 s	Specimen			
	Unpolished 0-0	$x^2$	Unpolished 10-10	$x^2$
Replicate, $x_1$	38.90	1513.21	7.30	53.29
Replicate, $x_2$	54.50	2970.25	27.20	739.84
Replicate, $x_3$	58.70	3445.69	25.30	640.09
Average ( $\bar{x}$ )	50.70	2643.05	19.93	477.74
$\Sigma x^2$	7929.15		1433.22	
$(\Sigma x)^2$	23134.41		3576.04	
$((\Sigma x)^2)/n$	7711.47		1192.01	
$\Sigma d^2 = \Sigma x^2 - ((\Sigma x)^2)/n$	217.68		241.21	
$\sigma^2 = \frac{\Sigma d^2}{n-1}$	108.84		120.60	
$\sigma_d^2 = \frac{\sigma_1^2}{n_1} + \frac{\sigma_2^2}{n_2}$	76.48			
$\sigma_d$	8.75			
$t = \frac{\bar{x}_1 - \bar{x}_2}{\sigma_d}$	3.52			

$p < 0.01$

APPENDIX 6

Time: 120 s	Specimen			
	Unpolished 0-0	$x^2$	Unpolished 10-10	$x^2$
Replicate, $x_1$	34.10	1162.81	6.70	44.89
Replicate, $x_2$	52.50	2756.25	25.40	645.16
Replicate, $x_3$	55.70	3102.49	24.70	610.09
Average ( $\bar{x}$ )	47.43	2340.52	18.93	433.38
$\Sigma x^2$	7021.55		1300.14	
$(\Sigma x)^2$	20249.29		3226.24	
$((\Sigma x)^2)/n$	6749.76		1075.41	
$\Sigma d^2 = \Sigma x^2 - ((\Sigma x)^2)/n$	271.79		224.73	
$\sigma^2 = \frac{\Sigma d^2}{n-1}$	135.89		112.36	
$\sigma_d^2 = \frac{\sigma_1^2}{n_1} + \frac{\sigma_2^2}{n_2}$	82.75			
$\sigma_d$	9.10			
$t = \frac{\bar{x}_1 - \bar{x}_2}{\sigma_d}$	3.13			

$p < 0.05$

APPENDIX 6

Time: 130 s	Specimen			
	Unpolished 0-0	$x^2$	Unpolished 10-10	$x^2$
Replicate, $x_1$	29.40	864.36	8.90	79.21
Replicate, $x_2$	51.30	2631.69	23.90	571.21
Replicate, $x_3$	55.20	3047.04	26.90	723.61
Average ( $\bar{x}$ )	45.30	2181.03	19.90	458.01
$\Sigma x^2$	6543.09		1374.03	
$(\Sigma x)^2$	18468.81		3564.09	
$((\Sigma x)^2)/n$	6156.27		1188.03	
$\Sigma d^2 = \Sigma x^2 - ((\Sigma x)^2)/n$	386.82		186.00	
$\sigma^2 = \frac{\Sigma d^2}{n-1}$	193.41		93.00	
$\sigma_d^2 = \frac{\sigma_1^2}{n_1} + \frac{\sigma_2^2}{n_2}$	95.47			
$\sigma_d$	9.77			
$t = \frac{\bar{x}_1 - \bar{x}_2}{\sigma_d}$	2.60			

$p < 0.05$

APPENDIX 6

Time: 140 s	Specimen			
	Unpolished 0-0	$x^2$	Unpolished 10-10	$x^2$
Replicate, $x_1$	21.90	479.61	6.40	40.96
Replicate, $x_2$	50.00	2500.00	22.10	488.41
Replicate, $x_3$	55.80	3113.64	24.40	595.36
Average ( $\bar{x}$ )	42.57	2031.08	17.63	374.91
$\Sigma x^2$	6093.25		1124.73	
$(\Sigma x)^2$	16307.29		2798.41	
$((\Sigma x)^2)/n$	5435.76		932.80	
$\Sigma d^2 = \Sigma x^2 - ((\Sigma x)^2)/n$	657.49		191.93	
$\sigma^2 = \frac{\Sigma d^2}{n-1}$	328.74		95.96	
$\sigma_d^2 = \frac{\sigma_1^2}{n_1} + \frac{\sigma_2^2}{n_2}$	141.57			
$\sigma_d$	11.90			
$t = \frac{\bar{x}_1 - \bar{x}_2}{\sigma_d}$	2.10			

$p < 0.1$

APPENDIX 6

Time: 150 s	Specimen			
	Unpolished 0-0	$x^2$	Unpolished 10-10	$x^2$
Replicate, $x_1$	22.30	497.29	6.60	43.56
Replicate, $x_2$	49.20	2420.64	20.30	412.09
Replicate, $x_3$	50.90	2590.81	24.60	605.16
Average ( $\bar{x}$ )	40.80	1836.25	17.17	353.60
$\Sigma x^2$	5508.74		1060.81	
$(\Sigma x)^2$	14981.76		2652.25	
$((\Sigma x)^2)/n$	4993.92		884.08	
$\Sigma d^2 = \Sigma x^2 - ((\Sigma x)^2)/n$	514.82		176.73	
$\sigma^2 = \frac{\Sigma d^2}{n-1}$	257.41		88.36	
$\sigma_d^2 = \frac{\sigma_1^2}{n_1} + \frac{\sigma_2^2}{n_2}$	115.26			
$\sigma_d$	10.74			
$t = \frac{\bar{x}_1 - \bar{x}_2}{\sigma_d}$	2.20			

$p < 0.1$



**Calculations for the Students T-Test on the Cell Proliferation Assay Involving Sintered Compacts**

3T3 Cells	Specimen			
Time: 3 hrs	0-0	$x^2$	10-5	$x^2$
Replicate, $x_1$	0.97	0.93	0.94	0.89
Replicate, $x_2$	0.97	0.94	0.96	0.93
Replicate, $x_3$	0.96	0.92	0.93	0.87
Replicate, $x_4$	0.96	0.92	0.95	0.90
Replicate, $x_5$	0.97	0.94	0.93	0.86
Average ( $\bar{x}$ )	0.97	0.93	0.94	0.89
$\Sigma x^2$	4.66		4.46	
$(\Sigma x)^2$	23.29		22.31	
$((\Sigma x)^2)/n$	4.66		4.46	
$\Sigma d^2 = \Sigma x^2 - ((\Sigma x)^2)/n$	9.79E-05		7.19E-04	
$\sigma^2 = \frac{\Sigma d^2}{n-1}$	2.45E-05		1.80E-04	
$\sigma_d^2 = \frac{\sigma_1^2}{n_1} + \frac{\sigma_2^2}{n_2}$	4.09E-05			
$\sigma_d$	6.39E-03			
$t = \frac{\bar{x}_1 - \bar{x}_2}{\sigma_d}$	3.22			

$p < 0.05$

APPENDIX 7

3T3 Cells	Specimen			
	0-0	$x^2$	10-5	$x^2$
Time: 24 hrs				
Replicate, $x_1$	1.00	1.00	0.87	0.76
Replicate, $x_2$	1.05	1.09	0.89	0.78
Replicate, $x_3$	0.95	0.90	0.85	0.73
Replicate, $x_4$	0.99	0.98	0.87	0.76
Replicate, $x_5$	1.01	1.02	0.88	0.77
Average ( $\bar{x}$ )	1.00	1.00	0.87	0.76
$\Sigma x^2$	5.00		3.81	
$(\Sigma x)^2$	24.98		19.04	
$((\Sigma x)^2)/n$	5.00		3.81	
$\Sigma d^2 = \Sigma x^2 - ((\Sigma x)^2)/n$	4.89E-03		5.95E-04	
$\sigma^2 = \frac{\Sigma d^2}{n-1}$	1.22E-03		1.49E-04	
$\sigma_d^2 = \frac{\sigma_1^2}{n_1} + \frac{\sigma_2^2}{n_2}$	2.74E-04			
$\sigma_d$	1.66E-02			
$t = \frac{\bar{x}_1 - \bar{x}_2}{\sigma_d}$	7.67			

p < 0.001

APPENDIX 7

3T3 Cells	Specimen			
	0-0	$x^2$	10-5	$x^2$
Time: 48 hrs				
Replicate, $x_1$	0.98	0.95	0.88	0.77
Replicate, $x_2$	1.04	1.07	0.91	0.83
Replicate, $x_3$	0.92	0.85	0.84	0.71
Replicate, $x_4$	0.97	0.94	0.88	0.77
Replicate, $x_5$	0.98	0.96	0.87	0.76
Average ( $\bar{x}$ )	0.98	0.96	0.88	0.77
$\Sigma x^2$	4.78		3.84	
$(\Sigma x)^2$	23.87		19.19	
$((\Sigma x)^2)/n$	4.77		3.84	
$\Sigma d^2 = \Sigma x^2 - ((\Sigma x)^2)/n$	6.50E-03		2.24E-03	
$\sigma^2 = \frac{\Sigma d^2}{n-1}$	1.62E-03		5.60E-04	
$\sigma_d^2 = \frac{\sigma_1^2}{n_1} + \frac{\sigma_2^2}{n_2}$	4.37E-04			
$\sigma_d$	2.09E-02			
$t = \frac{\bar{x}_1 - \bar{x}_2}{\sigma_d}$	4.83			

p < 0.01

APPENDIX 7

3T3 Cells	Specimen			
	0-0	$x^2$	10-5	$x^2$
Time: 96 hrs				
Replicate, $x_1$	1.08	1.17	0.99	0.98
Replicate, $x_2$	1.10	1.22	1.06	1.13
Replicate, $x_3$	1.04	1.08	0.97	0.94
Replicate, $x_4$	1.09	1.19	1.02	1.04
Replicate, $x_5$	1.10	1.21	1.01	1.02
Average ( $\bar{x}$ )	1.08	1.17	1.01	1.02
$\Sigma x^2$	5.86		5.11	
$(\Sigma x)^2$	29.29		25.53	
$((\Sigma x)^2)/n$	5.86		5.11	
$\Sigma d^2 = \Sigma x^2 - ((\Sigma x)^2)/n$	2.74E-03		5.04E-03	
$\sigma^2 = \frac{\Sigma d^2}{n-1}$	6.86E-04		1.26E-03	
$\sigma_d^2 = \frac{\sigma_1^2}{n_1} + \frac{\sigma_2^2}{n_2}$	3.89E-04			
$\sigma_d$	1.97E-02			
$t = \frac{\bar{x}_1 - \bar{x}_2}{\sigma_d}$	3.64			

p < 0.01

APPENDIX 7

3T3 Cells	Specimen			
	0-0	$x^2$	10-5	$x^2$
Time: 168 hrs				
Replicate, $x_1$	1.15	1.32	1.05	1.10
Replicate, $x_2$	1.24	1.54	1.12	1.26
Replicate, $x_3$	1.05	1.11	0.98	0.97
Replicate, $x_4$	1.12	1.25	1.08	1.17
Replicate, $x_5$	1.20	1.44	1.02	1.04
Average ( $\bar{x}$ )	1.15	1.33	1.05	1.11
$\Sigma x^2$	6.67		5.54	
$(\Sigma x)^2$	33.22		27.64	
$((\Sigma x)^2)/n$	6.64		5.53	
$\Sigma d^2 = \Sigma x^2 - ((\Sigma x)^2)/n$	2.08E-02		1.14E-02	
$\sigma^2 = \frac{\Sigma d^2}{n-1}$	5.20E-03		2.84E-03	
$\sigma_d^2 = \frac{\sigma_1^2}{n_1} + \frac{\sigma_2^2}{n_2}$	1.61E-03			
$\sigma_d$	4.01E-02			
$t = \frac{\bar{x}_1 - \bar{x}_2}{\sigma_d}$	2.53			

$p < 0.05$

APPENDIX 7

3T3 Cells	Specimen			
Time: 3 hrs	0-0	$x^2$	10-10	$x^2$
Replicate, $x_1$	0.97	0.93	0.92	0.85
Replicate, $x_2$	0.97	0.94	0.92	0.85
Replicate, $x_3$	0.96	0.92	0.92	0.84
Replicate, $x_4$	0.96	0.92	0.92	0.85
Replicate, $x_5$	0.97	0.94	0.92	0.85
Average ( $\bar{x}$ )	0.97	0.93	0.92	0.85
$\Sigma x^2$	4.66		4.24	
$(\Sigma x)^2$	23.29		21.19	
$((\Sigma x)^2)/n$	4.66		4.24	
$\Sigma d^2 = \Sigma x^2 - ((\Sigma x)^2)/n$	9.79E-05		2.85E-05	
$\sigma^2 = \frac{\Sigma d^2}{n-1}$	2.45E-05		7.13E-06	
$\sigma_d^2 = \frac{\sigma_1^2}{n_1} + \frac{\sigma_2^2}{n_2}$	6.32E-06			
$\sigma_d$	2.51E-03			
$t = \frac{\bar{x}_1 - \bar{x}_2}{\sigma_d}$	17.74			

p < 0.001

APPENDIX 7

3T3 Cells	Specimen			
Time: 24 hrs	0-0	$x^2$	10-10	$x^2$
Replicate, $x_1$	1.00	1.00	0.89	0.79
Replicate, $x_2$	1.05	1.09	0.90	0.80
Replicate, $x_3$	0.95	0.90	0.88	0.77
Replicate, $x_4$	0.99	0.98	0.88	0.77
Replicate, $x_5$	1.01	1.02	0.90	0.81
Average ( $\bar{x}$ )	1.00	1.00	0.89	0.79
$\Sigma x^2$	5.00		3.95	
$(\Sigma x)^2$	24.98		19.75	
$((\Sigma x)^2)/n$	5.00		3.95	
$\Sigma d^2 = \Sigma x^2 - ((\Sigma x)^2)/n$	4.89E-03		4.01E-04	
$\sigma^2 = \frac{\Sigma d^2}{n-1}$	1.22E-03		1.00E-04	
$\sigma_d^2 = \frac{\sigma_1^2}{n_1} + \frac{\sigma_2^2}{n_2}$	2.65E-04			
$\sigma_d$	1.63E-02			
$t = \frac{\bar{x}_1 - \bar{x}_2}{\sigma_d}$	6.81			

p < 0.001

APPENDIX 7

3T3 Cells	Specimen			
Time: 48 hrs	0-0	$x^2$	10-10	$x^2$
Replicate, $x_1$	0.98	0.95	0.90	0.81
Replicate, $x_2$	1.04	1.07	0.91	0.82
Replicate, $x_3$	0.92	0.85	0.89	0.80
Replicate, $x_4$	0.97	0.94	0.89	0.79
Replicate, $x_5$	0.98	0.96	0.91	0.83
Average ( $\bar{x}$ )	0.98	0.96	0.90	0.81
$\Sigma x^2$	4.78		4.05	
$(\Sigma x)^2$	23.87		20.23	
$((\Sigma x)^2)/n$	4.77		4.05	
$\Sigma d^2 = \Sigma x^2 - ((\Sigma x)^2)/n$	6.50E-03		3.16E-04	
$\sigma^2 = \frac{\Sigma d^2}{n-1}$	1.62E-03		7.90E-05	
$\sigma_d^2 = \frac{\sigma_1^2}{n_1} + \frac{\sigma_2^2}{n_2}$	3.41E-04			
$\sigma_d$	1.85E-02			
$t = \frac{\bar{x}_1 - \bar{x}_2}{\sigma_d}$	4.20			

p < 0.01



APPENDIX 7

3T3 Cells	Specimen			
Time: 96 hrs	0-0	$x^2$	10-10	$x^2$
Replicate, $x_1$	1.08	1.17	0.95	0.90
Replicate, $x_2$	1.10	1.22	0.98	0.95
Replicate, $x_3$	1.04	1.08	0.92	0.85
Replicate, $x_4$	1.09	1.19	0.96	0.92
Replicate, $x_5$	1.10	1.21	0.94	0.88
Average ( $\bar{x}$ )	1.08	1.17	0.95	0.90
$\Sigma x^2$	5.86		4.52	
$(\Sigma x)^2$	29.29		22.57	
$((\Sigma x)^2)/n$	5.86		4.51	
$\Sigma d^2 = \Sigma x^2 - ((\Sigma x)^2)/n$	2.74E-03		1.59E-03	
$\sigma^2 = \frac{\Sigma d^2}{n-1}$	6.86E-04		3.97E-04	
$\sigma_d^2 = \frac{\sigma_1^2}{n_1} + \frac{\sigma_2^2}{n_2}$	2.17E-04			
$\sigma_d$	1.47E-02			
$t = \frac{\bar{x}_1 - \bar{x}_2}{\sigma_d}$	8.99			

p < 0.001

APPENDIX 7

3T3 Cells	Specimen			
Time: 168 hrs	0-0	$x^2$	10-10	$x^2$
Replicate, $x_1$	1.15	1.32	1.01	1.02
Replicate, $x_2$	1.24	1.54	1.05	1.10
Replicate, $x_3$	1.05	1.11	0.92	0.85
Replicate, $x_4$	1.12	1.25	1.01	1.02
Replicate, $x_5$	1.20	1.44	1.02	1.04
Average ( $\bar{x}$ )	1.15	1.33	1.00	1.01
$\Sigma x^2$	6.67		5.03	
$(\Sigma x)^2$	33.22		25.10	
$((\Sigma x)^2)/n$	6.64		5.02	
$\Sigma d^2 = \Sigma x^2 - ((\Sigma x)^2)/n$	2.08E-02		8.70E-03	
$\sigma^2 = \frac{\Sigma d^2}{n-1}$	5.20E-03		2.18E-03	
$\sigma_d^2 = \frac{\sigma_1^2}{n_1} + \frac{\sigma_2^2}{n_2}$	1.48E-03			
$\sigma_d$	3.84E-02			
$t = \frac{\bar{x}_1 - \bar{x}_2}{\sigma_d}$	3.93			

p < 0.01

APPENDIX 7

Rat Osteoblast	Specimen			
	0-0	$x^2$	10-5	$x^2$
Time: 3 hrs				
Replicate, $x_1$	0.90	0.81	0.86	0.74
Replicate, $x_2$	0.91	0.82	0.88	0.78
Replicate, $x_3$	0.90	0.80	0.85	0.73
Replicate, $x_4$	0.90	0.81	0.87	0.76
Replicate, $x_5$	0.90	0.81	0.85	0.72
Average ( $\bar{x}$ )	0.90	0.81	0.86	0.74
$\Sigma x^2$	4.06		3.72	
$(\Sigma x)^2$	20.28		18.60	
$((\Sigma x)^2)/n$	4.06		3.72	
$\Sigma d^2 = \Sigma x^2 - ((\Sigma x)^2)/n$	4.96E-05		6.80E-04	
$\sigma^2 = \frac{\Sigma d^2}{n-1}$	1.24E-05		1.70E-04	
$\sigma_d^2 = \frac{\sigma_1^2}{n_1} + \frac{\sigma_2^2}{n_2}$	3.65E-05			
$\sigma_d$	6.04E-03			
$t = \frac{\bar{x}_1 - \bar{x}_2}{\sigma_d}$	6.33			

p < 0.001

APPENDIX 7

Rat Osteoblast	Specimen			
	0-0	$x^2$	10-5	$x^2$
Time: 24 hrs				
Replicate, $x_1$	0.92	0.85	0.88	0.77
Replicate, $x_2$	0.97	0.93	0.89	0.80
Replicate, $x_3$	0.87	0.76	0.86	0.74
Replicate, $x_4$	0.94	0.87	0.87	0.76
Replicate, $x_5$	0.91	0.83	0.88	0.77
Average ( $\bar{x}$ )	0.92	0.85	0.88	0.77
$\Sigma x^2$	4.24		3.85	
$(\Sigma x)^2$	21.17		19.23	
$((\Sigma x)^2)/n$	4.23		3.85	
$\Sigma d^2 = \Sigma x^2 - ((\Sigma x)^2)/n$	5.02E-03		5.76E-04	
$\sigma^2 = \frac{\Sigma d^2}{n-1}$	1.25E-03		1.44E-04	
$\sigma_d^2 = \frac{\sigma_1^2}{n_1} + \frac{\sigma_2^2}{n_2}$	2.80E-04			
$\sigma_d$	1.67E-02			
$t = \frac{\bar{x}_1 - \bar{x}_2}{\sigma_d}$	2.59			

p < 0.05

APPENDIX 7

Rat Osteoblast	Specimen			
	0-0	$x^2$	10-5	$x^2$
Time: 48 hrs				
Replicate, $x_1$	0.96	0.92	0.93	0.86
Replicate, $x_2$	0.99	0.97	0.94	0.88
Replicate, $x_3$	0.93	0.86	0.92	0.84
Replicate, $x_4$	0.97	0.94	0.94	0.88
Replicate, $x_5$	0.95	0.90	0.93	0.86
Average ( $\bar{x}$ )	0.96	0.92	0.93	0.87
$\Sigma x^2$	4.60		4.33	
$(\Sigma x)^2$	22.97		21.66	
$((\Sigma x)^2)/n$	4.59		4.33	
$\Sigma d^2 = \Sigma x^2 - ((\Sigma x)^2)/n$	1.95E-03		3.21E-04	
$\sigma^2 = \frac{\Sigma d^2}{n-1}$	4.86E-04		8.01E-05	
$\sigma_d^2 = \frac{\sigma_1^2}{n_1} + \frac{\sigma_2^2}{n_2}$	1.13E-04			
$\sigma_d$	1.06E-02			
$t = \frac{\bar{x}_1 - \bar{x}_2}{\sigma_d}$	2.60			

p < 0.05

APPENDIX 7

Rat Osteoblast	Specimen			
	0-0	$x^2$	10-5	$x^2$
Time: 96 hrs				
Replicate, $x_1$	0.97	0.94	0.95	0.90
Replicate, $x_2$	1.03	1.07	0.99	0.98
Replicate, $x_3$	0.93	0.86	0.93	0.86
Replicate, $x_4$	0.97	0.94	0.97	0.94
Replicate, $x_5$	0.94	0.88	0.94	0.88
Average ( $\bar{x}$ )	0.97	0.94	0.95	0.91
$\Sigma x^2$	4.69		4.56	
$(\Sigma x)^2$	23.40		22.79	
$((\Sigma x)^2)/n$	4.68		4.56	
$\Sigma d^2 = \Sigma x^2 - ((\Sigma x)^2)/n$	6.64E-03		2.36E-03	
$\sigma^2 = \frac{\Sigma d^2}{n-1}$	1.66E-03		5.91E-04	
$\sigma_d^2 = \frac{\sigma_1^2}{n_1} + \frac{\sigma_2^2}{n_2}$	4.50E-04			
$\sigma_d$	2.12E-02			
$t = \frac{\bar{x}_1 - \bar{x}_2}{\sigma_d}$	0.60			

p > 0.1

APPENDIX 7

Rat Osteoblast	Specimen			
	0-0	$x^2$	10-5	$x^2$
Time: 168 hrs				
Replicate, $x_1$	1.01	1.02	0.97	0.94
Replicate, $x_2$	1.04	1.09	1.01	1.03
Replicate, $x_3$	0.97	0.94	0.92	0.84
Replicate, $x_4$	0.99	0.98	1.00	1.00
Replicate, $x_5$	1.02	1.04	0.96	0.92
Average ( $\bar{x}$ )	1.01	1.01	0.97	0.95
$\Sigma x^2$	5.07		4.73	
$(\Sigma x)^2$	25.32		23.64	
$((\Sigma x)^2)/n$	5.06		4.73	
$\Sigma d^2 = \Sigma x^2 - ((\Sigma x)^2)/n$	3.21E-03		5.74E-03	
$\sigma^2 = \frac{\Sigma d^2}{n-1}$	8.01E-04		1.43E-03	
$\sigma_d^2 = \frac{\sigma_1^2}{n_1} + \frac{\sigma_2^2}{n_2}$	4.47E-04			
$\sigma_d$	2.11E-02			
$t = \frac{\bar{x}_1 - \bar{x}_2}{\sigma_d}$	1.61			

p > 0.1

APPENDIX 7

Rat Osteoblast	Specimen			
	0-0	$x^2$	10-10	$x^2$
Time: 3 hrs				
Replicate, $x_1$	0.90	0.81	0.88	0.77
Replicate, $x_2$	0.91	0.82	0.88	0.78
Replicate, $x_3$	0.90	0.80	0.88	0.77
Replicate, $x_4$	0.90	0.81	0.88	0.77
Replicate, $x_5$	0.90	0.81	0.88	0.77
Average ( $\bar{x}$ )	0.90	0.81	0.88	0.78
$\Sigma x^2$	4.06		3.88	
$(\Sigma x)^2$	20.28		19.38	
$((\Sigma x)^2)/n$	4.06		3.88	
$\Sigma d^2 = \Sigma x^2 - ((\Sigma x)^2)/n$	4.96E-05		2.80E-05	
$\sigma^2 = \frac{\Sigma d^2}{n-1}$	1.24E-05		7.00E-06	
$\sigma_d^2 = \frac{\sigma_1^2}{n_1} + \frac{\sigma_2^2}{n_2}$	3.88E-06			
$\sigma_d$	1.97E-03			
$t = \frac{\bar{x}_1 - \bar{x}_2}{\sigma_d}$	10.35			

p < 0.001



APPENDIX 7

Rat Osteoblast	Specimen			
	0-0	$x^2$	10-10	$x^2$
Time: 24 hrs				
Replicate, $x_1$	0.92	0.85	0.91	0.83
Replicate, $x_2$	0.97	0.93	0.92	0.84
Replicate, $x_3$	0.87	0.76	0.90	0.81
Replicate, $x_4$	0.94	0.87	0.90	0.81
Replicate, $x_5$	0.91	0.83	0.92	0.85
Average ( $\bar{x}$ )	0.92	0.85	0.91	0.83
$\Sigma x^2$	4.24		4.13	
$(\Sigma x)^2$	21.17		20.65	
$((\Sigma x)^2)/n$	4.23		4.13	
$\Sigma d^2 = \Sigma x^2 - ((\Sigma x)^2)/n$	5.02E-03		4.01E-04	
$\sigma^2 = \frac{\Sigma d^2}{n-1}$	1.25E-03		1.00E-04	
$\sigma_d^2 = \frac{\sigma_1^2}{n_1} + \frac{\sigma_2^2}{n_2}$	2.71E-04			
$\sigma_d$	1.65E-02			
$t = \frac{\bar{x}_1 - \bar{x}_2}{\sigma_d}$	0.69			

p > 0.1

APPENDIX 7

Rat Osteoblast	Specimen			
	0-0	$x^2$	10-10	$x^2$
Time: 48 hrs				
Replicate, $x_1$	0.96	0.92	0.94	0.88
Replicate, $x_2$	0.99	0.97	0.97	0.94
Replicate, $x_3$	0.93	0.86	0.92	0.85
Replicate, $x_4$	0.97	0.94	0.95	0.90
Replicate, $x_5$	0.95	0.90	0.93	0.86
Average ( $\bar{x}$ )	0.96	0.92	0.94	0.89
$\Sigma x^2$	4.60		4.44	
$(\Sigma x)^2$	22.97		22.19	
$((\Sigma x)^2)/n$	4.59		4.44	
$\Sigma d^2 = \Sigma x^2 - ((\Sigma x)^2)/n$	1.95E-03		1.50E-03	
$\sigma^2 = \frac{\Sigma d^2}{n-1}$	4.86E-04		3.75E-04	
$\sigma_d^2 = \frac{\sigma_1^2}{n_1} + \frac{\sigma_2^2}{n_2}$	1.72E-04			
$\sigma_d$	1.31E-02			
$t = \frac{\bar{x}_1 - \bar{x}_2}{\sigma_d}$	1.24			

p > 0.1

APPENDIX 7

Rat Osteoblast	Specimen			
	0-0	$x^2$	10-10	$x^2$
Time: 96 hrs				
Replicate, $x_1$	0.97	0.94	0.98	0.96
Replicate, $x_2$	1.03	1.07	1.01	1.02
Replicate, $x_3$	0.93	0.86	0.94	0.88
Replicate, $x_4$	0.97	0.94	1.00	1.00
Replicate, $x_5$	0.94	0.88	0.97	0.94
Average ( $\bar{x}$ )	0.97	0.94	0.98	0.96
$\Sigma x^2$	4.69		4.80	
$(\Sigma x)^2$	23.40		23.97	
$((\Sigma x)^2)/n$	4.68		4.79	
$\Sigma d^2 = \Sigma x^2 - ((\Sigma x)^2)/n$	6.64E-03		3.32E-03	
$\sigma^2 = \frac{\Sigma d^2}{n-1}$	1.66E-03		8.30E-04	
$\sigma_d^2 = \frac{\sigma_1^2}{n_1} + \frac{\sigma_2^2}{n_2}$	4.98E-04			
$\sigma_d$	2.23E-02			
$t = \frac{\bar{x}_1 - \bar{x}_2}{\sigma_d}$	0.52			

p > 0.1

APPENDIX 7

Rat Osteoblast	Specimen			
	0-0	$x^2$	10-10	$x^2$
Time: 168 hrs				
Replicate, $x_1$	1.01	1.02	0.99	0.98
Replicate, $x_2$	1.04	1.09	1.01	1.02
Replicate, $x_3$	0.97	0.94	0.97	0.94
Replicate, $x_4$	0.99	0.98	0.98	0.96
Replicate, $x_5$	1.02	1.04	1.00	1.00
Average ( $\bar{x}$ )	1.01	1.01	0.99	0.98
$\Sigma x^2$	5.07		4.90	
$(\Sigma x)^2$	25.32		24.48	
$((\Sigma x)^2)/n$	5.06		4.90	
$\Sigma d^2 = \Sigma x^2 - ((\Sigma x)^2)/n$	3.21E-03		8.97E-04	
$\sigma^2 = \frac{\Sigma d^2}{n-1}$	8.01E-04		2.24E-04	
$\sigma_d^2 = \frac{\sigma_1^2}{n_1} + \frac{\sigma_2^2}{n_2}$	2.05E-04			
$\sigma_d$	1.43E-02			
$t = \frac{\bar{x}_1 - \bar{x}_2}{\sigma_d}$	1.17			

p > 0.1